



HAL
open science

Behavior of bonded anchors in concrete under fire

Omar Al-Mansouri

► **To cite this version:**

Omar Al-Mansouri. Behavior of bonded anchors in concrete under fire. Civil Engineering. Ecole nationale supérieure Mines-Télécom Lille Douai, 2020. English. NNT : 2020MTLD0011 . tel-03139839

HAL Id: tel-03139839

<https://theses.hal.science/tel-03139839>

Submitted on 12 Feb 2021

HAL is a multi-disciplinary open access archive for the deposit and dissemination of scientific research documents, whether they are published or not. The documents may come from teaching and research institutions in France or abroad, or from public or private research centers.

L'archive ouverte pluridisciplinaire **HAL**, est destinée au dépôt et à la diffusion de documents scientifiques de niveau recherche, publiés ou non, émanant des établissements d'enseignement et de recherche français ou étrangers, des laboratoires publics ou privés.

Institut Mines-Télécom Lille Douai

Ecole doctorale Sciences Pour l'ingénieur Université de Lille Nord-de-France

THESIS

Submitted for the degree of

DOCTORATE IN PHILOSOPHY

In

Specialty: Civil and Environmental Engineering

By

Omar Al-Mansouri

Title of the thesis:

Behavior of bonded anchors in concrete under fire

Defended on the 09/12/2020 in front of the jury composed of:

Reviewer	Hélène Carré, Maître de conférence. Université de Pau
Reviewer	Jean-François Caron, Pr. Ecole des ponts et chaussées
President	Dashnor Hoxha, Pr. Université d'Orléans
Supervisor	Romain Mège, Dr. Centre Scientifique et Technique du Bâtiment
Supervisor	Roberto Piccinin, Dr. Hilti corp
Thesis director	Sébastien Rémond, Pr. Université d'Orléans

Host laboratory: Security, Structures and Fire department at the Scientific and Technical Center for Building (Centre Scientifique et Technique du Bâtiment/CSTB) and Laboratory of Civil Engineering and Geo-Environment (Laboratoire de Génie Civil et Géo-Environnement/LGCgE)

Remerciements/Acknowledgement

Je remercie H el ene Carr e et Jean-Fran ois Caron d’avoir accept e de rapporter ce travail de recherche ainsi que Dashnor Hoxha de m’avoir fait l’honneur de pr esider mon jury. Merci  galement   Roberto Piccinin, Romain M ege et S ebastien R emond d’avoir particip e   ce jury.

Les travaux de ma th ese ont  t e r ealis es au CSTB de Marne-la-Vall ee au sein de la Direction S ecurit e, Structures et Feu dans la division Structures (DSSF), Ma onnerie Partition (SMP). Je tiens donc   remercier l’ensemble des personnes ayant pu intervenir de pr es ou de loin dans la r ealisation de mes travaux de recherche durant ces trois derni eres ann ees.

Je souhaite remercier dans un premier temps Fran ois Jallot et sa pr ed ecessure Anne Voeltzel, chefs de la Direction S ecurit e, Structures et Feu, de m’avoir permis d’ evoluer au sein de leur service avec une grande libert e.

Je tiens   exprimer ma gratitude   l’ensemble des divisions Etudes et Essais M ecaniques (EEM), Etudes et Essais Feu (EEF), Expertise, Avis R eglementaire et Recherche (EA2R) et Structures, Ma onnerie, Partition (SMP) commen ant par les responsables Philippe Rivillon, Martial Bonhomme, Romain M ege et son pr ed ecessur S ephane Hameury et Anca Cronopol pour leur encadrement technique et scientifique tout au long de ces trois ann ees. Je remercie particuli erement les laboratoires Feu et Fixations, commen ant par leurs responsables S ephane Charuel et son pr ed ecessur Romuald Avenel et Killian Regnier et son pr ed ecessur Christophe Canezin ainsi que tous les membres de leurs  quipes (Francis Diafuanana Luntala, Paulo Pangia Ngani, Jean-Fran ois Moller, Florian Demoulin, L eo Gontier, Miguel Cruz, Anthony Malara et Jos e Pestana du laboratoire Feu, et Julie Skorupka, Aurore Lenjalley, Richard Lenoir, Wissem Lassadi, Fabien Perrault du laboratoire fixations). J’ mets un remerciement sp ecial   Thierry Guillet pour son expertise et de m’avoir introduit aux mondes des fixations,  valuation technique et normalisation. Je remercie  galement les chercheurs de l’ equipe EA2R pour leur support en mod elisation et analytique (Paul Lardet, Amine Lahouar, Mehdi ElKoutaiba, Duc Toan Pham, Yahia Msaad, Seddik Sakji et Quentin Jullien). Je remercie mes coll egues th esards et stagiaires que j’ai eus pendant la th ese pour avoir cr e une ambiance de dynamisme et enthousiasme.

Je remercie mon directeur de th ese S ebastien R emond pour son encadrement scientifique et sa disponibilit e et r eactivit e exceptionnelles. Je suis tr es reconnaissant pour son aide et ses conseils de qualit e toujours apport es de mani ere claire et dans les plus brefs d elais.

Une partie de la th ese a  t e co-financ ee par Hilti corp, Schaan, Lichtenstein. I therefore thank Ulrich Bourground, Roberto Piccinin, Kenton McBrdie, Marco Abate and Gregor Giessmann for their help and support. Having worked with you on my PhD among other topics will remain a game changer and a very rich experience for me.

Avant de finir, je remercie ma famille commen ant par mon  pouse Safaa et ma fille Zeina (qui est n ee pendant la th ese), ainsi que ma m ere, mon p ere et ma s eur pour leur soutien moral le long de cette exp erience.

Je souhaite pour finir remercier une derni ere fois mes principaux encadrants de th ese : S ebastien R emond, Romain M ege, Thierry Guillet et Nicolas Pinoteau pour leur accompagnement, expertise et support scientifique et technique.

RESUME

La technique des ancrages par scellement chimique consiste à sceller une tige filetée dans un trou foré dans le béton durci grâce à une résine polymère. Les principaux avantages de cette technique sont la facilité d'installation et les propriétés mécaniques élevées de la résine à température ambiante. Grâce à l'adhérence de la résine, ce type d'ancrage peut être dimensionné pour avoir des performances similaires voire supérieures à celles des autres systèmes d'ancrages (mécaniques et coulés en place). En revanche, à hautes températures, e.g. incendie, l'adhérence de la résine se dégrade rapidement menaçant la capacité de l'ancrage à supporter les charges appliquées. Cela crée un risque sur les vies et les biens dans le bâtiment. Plusieurs accidents se sont produits comme l'effondrement du Big Dig Tunnel aux USA (2006) et le tunnel Sasago au Japon (2012) qui ont montré l'importance d'avoir des méthodes d'évaluation fiables de ce type d'ancrages. L'objectif de cette thèse est d'établir une méthode d'évaluation et une méthode de dimensionnement afin d'assurer la tenue structurale des ancrages par scellement chimique en situation d'incendie. L'étude est structurée en quatre parties :

i. Protocoles expérimentaux pour les essais au feu des chevilles chimiques. Des essais d'arrachements au feu ont été réalisés sur des chevilles chimiques (résine époxy). Les profils de températures le long de l'ancrage ont été déterminés expérimentalement pour différentes configurations d'essais. Ensuite, ces profils thermiques ont été exploités comme donnée d'entrée pour calculer la résistance des chevilles par la méthode Pinoteau (intégration des résistances). Cette étude a permis de préciser les conditions expérimentales à utiliser pour l'évaluation des chevilles chimiques au feu.

ii. Proposition d'un modèle de dimensionnement basé sur des calculs thermiques en utilisant la méthode des éléments finis en 3D. Les profils de température correspondants aux différentes configurations d'un ancrage dans le bâtiment ont été calculés à l'aide des propriétés thermophysiques des matériaux Eurocode pour le béton et l'acier. La modélisation en 3D a été comparée à la modélisation en 2D plane utilisée communément dans la littérature. Les deux approches ont été comparées aux mesures expérimentales et couplées avec la méthode Pinoteau pour évaluer l'influence de la méthode de modélisation sur le résultat de l'intégration des résistances. Suite à la validation du modèle 3D, des investigations thermiques ont été conduites sur d'autres paramètres pouvant influencer les essais au feu des chevilles chimiques. Cette étude a permis de valider la méthode de calcul en 3D comme la méthode la plus représentative du problème d'une cheville chimique au feu.

iii. Validation de la méthode Pinoteau pour le dimensionnement des chevilles chimiques au feu en utilisant le modèle de dimensionnement proposé précédemment. Les calculs de la résistance au feu de trois chevilles chimiques différentes ont été comparés à des essais d'arrachement au feu. Cette étude menée sur une large gamme de tailles de chevilles a permis de valider l'utilisation de l'intégration des résistances pour le dimensionnement.

iv. Etude du comportement des chevilles chimiques dans le béton fissuré à hautes températures. Une méthode d'évaluation a été développée afin de déterminer la réduction de la résistance d'adhérence liée à la fissuration du béton, à hautes températures (chauffage électrique). Des essais ont été faits sur des chevilles chimiques (résine époxy) dans le béton fissuré et non-fissuré à température ambiante et à hautes températures. La réduction de la résistance avec l'augmentation de la température a été investiguée. Cette étude a permis d'obtenir une bonne répétabilité des résultats grâce à l'augmentation du nombre d'essais et le bon contrôle du scénario thermique appliqué.

Mots clés : chevilles chimiques, résistance au feu, béton, résine, époxy, contrainte d'adhérence, fissure.

ABSTRACT

The technique of bonded anchors consists of fastening a threaded rod in a drilled hole in hardened concrete by polymer adhesives. The main advantages of this technique are ease of installation and the high mechanical properties of the adhesive at ambient temperature. Due to the adherence of the adhesive resin, this type of anchors can be designed to ensure similar or even higher performances compared to other anchor systems (mechanical and cast-in). However, at high temperatures, e.g. fire situation, the adherence of the adhesive degrades rapidly. Fire decreases the adherence of the adhesive and leads to the inability of the anchor to support the fixed objects. This creates a risk on the lives and goods inside the building. Several accidents occurred like the collapse of the Big Dig Tunnel in the USA (2006) and the Sasago tunnel in Japan (2012) and highlighted the importance of having reliable evaluation methods of this type of anchors. The objective of this thesis is to establish an assessment and a design method to ensure the structural resistance of bonded anchors in fire situations. This project is structured into four main parts:

i. Experimental protocols for fire tests on bonded anchors. Pull-out fire tests were conducted on bonded anchors (epoxy adhesive). Temperature profiles along the embedment depth of anchors were determined experimentally for different test configurations. Then, these temperature profiles were used as entry data to calculate the fire resistance of anchors using Pinoteau's method (Resistance Integration Method). This study allowed to precise the experimental conditions to be adopted for fire evaluation tests of bonded anchors.

ii. Proposition of a design model based on transient thermal calculations using finite element method in 3D. Temperature profiles were calculated using the thermophysical material properties of concrete and steel in the Eurocodes. 3D modelling was compared to 2D plane modelling commonly used in the literature. Both approaches were compared to measurements during fire tests and coupled with Pinoteau's method to assess their impact on the calculation of fire resistance of anchors. Following the validation of the 3D model, thermal investigations were conducted on other parameters that could influence fire tests of bonded anchors. This study allowed to validate the 3D modelling approach as the most representative of the problem of bonded anchors exposed to fire.

iii. Validation of Pinoteau's method for the design of bonded anchors under fire by using the previously proposed design model. Calculations of fire resistance of three different bonded anchor products were compared to pull-out tests under. This study conducted on a wide range of anchor sizes lead to the validation of the Pinoteau's Method for the design of bonded anchors.

iv. Study of the behavior of bonded anchors in cracked concrete at high temperatures. An assessment method was developed to determine the reduction of bond strength due to cracked concrete, at high temperatures (electrical heating). Tests were conducted on bonded anchors (epoxy adhesive) in cracked and uncracked concrete, at ambient and high temperatures. The evolution of the reduction with temperature increase was investigated. This study ensured a good repeatability of test results due to the increased testing potential and the good control of the applied heating scenario.

Key words: Bonded anchor, fire resistance, concrete, adhesive, epoxy, bond strength, bond resistance, crack.

Table of contents

Remerciements/Acknowledgement.....	2
Résumé.....	3
Abstract	4
General introduction.....	7
Chapter I: Literature study on the behavior of post-installed adhesive anchor systems and material properties.....	11
1. Description of bonded anchors.....	11
1.1. Implementation method of bonded anchors	11
1.2. Application fields of bonded anchors.....	12
2. Thermal transfer in fire situations and its standardized conditions.....	13
3. Mechanical behavior of studied materials at high temperature	14
3.1. Concrete.....	14
3.2. Steel.....	20
3.3. Adhesive resin	24
4. Guidelines and standards.....	30
4.1. Assessment of anchors in concrete at ambient temperature	30
4.2. Fire assessment of anchors in concrete.....	35
4.3. Fire resistance tests according to NF EN 1363-1	38
4.4. European Assessment document for post-installed rebars (EAD 330087-00-0601)	39
5. Design models for bonded anchors under fire.....	42
5.1. Pinoteau’s Resistance Integration Method	42
5.2. Lahouar’s non-linear shear-lag model.....	44
Conclusion of the literature study	45
Chapter II: Experimental protocols for fire tests on bonded anchors.....	46
Objectives.....	46
Paper: Influence of testing conditions on thermal distribution and resulting load-bearing capacity of bonded anchors under fire	48
Discussion and analysis.....	73
Chapter III: Development of a 3D numerical model for the design of bonded anchors in uncracked concrete under ISO 834 fire	75
Objectives.....	75
Paper: Numerical investigation of parameters influencing fire evaluation tests of chemically bonded anchors in uncracked concrete.....	76
Analysis and discussion.....	95
Chapter IV: Validation of Pinoteau’s method (Resistance Integration Method) for the evaluation and design of bonded anchors in uncracked concrete under ISO 834 fire	101
Objectives.....	101

Paper: design recommendations for bonded anchors under fire conditions using the resistance integration method..... 102

Analysis and discussion..... 118

Chapter V: Behavior of bonded anchors in cracked concrete at high temperature using electrical heating 122

Objectives..... 122

Paper: Behavior of bonded anchors in cracked concrete at high temperatures 123

Analysis and discussion..... 130

General conclusion and perspectives..... 131

Annex A: Principles of fire safety engineering 134

References 137

General introduction

Context

Bonded anchors in hardened concrete is a technique that exists since decades. The anchor, a steel threaded rod, is installed in a concrete bearing element by an adhesive material ensuring the adhesion between both materials. The advantage of this technique is that it allows a rapid installation of anchors and offers high flexibility in construction works. The properties of these anchors have developed significantly since their first appearance (technical feasibility in the 1940s, first use in the 1960s, first European Technical Approvals in 1997 following the issuing of the first European Technical Approval Guidelines/ETAGs). Since then, the resistances of bonded anchors have been enhanced from similar to higher than the resistance of cast-in place or mechanical systems at ambient temperature. However, the resistance of bonded anchors decreases rapidly with temperature increase. This is due to the loss of adhesion because of the sensitivity of adhesives to temperature. This increases the vulnerability of this type of anchors in fire situations, putting lives and goods inside the building at risk.

The vulnerability of bonded anchors in concrete to certain environmental or accidental actions (earthquakes, service temperature, time, freeze/thaw, humidity, sulphorus atmosphere and high alkalinity, fire) has been investigated in several studies to design anchors safely. The use of polymeric adhesives has raised questions on the durability of bonded anchor systems and their resistance in such situations. Three accidents linked to the use of adhesive resins occurred. In 2006, the collapse of concrete ceiling panels in the Big Dig tunnel in Boston led to the death of 2 people. In 2011, the Atlanta Botanical Garden Canopy walkway collapsed. In 2012, another collapse of concrete ceiling panels happened in the Sasago tunnel in Japan leading to 9 deaths. The reason of the Big Dig tunnel and the Canopy walkway accidents was the pull-out of bonded anchors following poor installation conditions and the creep behavior of the adhesive leading to high deformations. Whereas, the reason for the collapse of the Sasago tunnel was the aging and deterioration of the bond due to the long-term exposure, of bonded anchors holding the ceiling panels, to high temperatures inside the tunnel under sustained load. In terms of existing assessment and design criteria for similar anchorage systems, Post-Installed Rebars (PIRs) and mechanical anchors are well covered by the guidelines. Indeed, the European Organization for Technical Assessment (EOTA) has extended the European Assessment Document (EAD 330087-00-0601) for the assessment of PIRs to evaluate their pull-out strength at high temperatures in the last decade. Also, assessment and testing of mechanical anchors under fire can be conducted according to EAD 330232-01-0601 and their design according to Eurocode 2 – Part 4. However, no guidelines exist for the assessment, testing and design of bonded anchors under fire.

Recently, research has been conducted on bonded anchors under fire by the technical university of Kaiserslautern (TU Kaiserslautern) and university of Stuttgart (Stuttgart Universität). These research projects show a potential in the adaptation of the work done on PIRs at high temperature for the problem of bonded anchors under fire. In these projects, experimental and numerical investigations have been carried out on the behavior of bonded anchors according to the existing guidelines for the evaluation of mechanical anchors under fire. However, the testing conditions for the evaluation of bonded anchors under fire are still to be specified and the design models need to be developed further in order to be representative of bonded anchors exposed to fire. These tests served as reference for the validation of numerical design models for the prediction of the pull-out capacity of bonded anchors under fire. The results of the models in the literature sometimes yielded very conservative or non-conservative results raising questions on the sensitivity of these models to entry data and boundary conditions. Also, these projects have focused on the behavior of bonded anchors in uncracked concrete. The assessment and design of anchors in fire conditions must be done also in cracked concrete according to the provisions of European Assessment Documents and Eurocode 2-4, Annex D. Indeed, concrete is generally assumed to be cracked in a fire situation. However, the behavior of bonded anchors in cracked concrete remains under-investigated. Therefore, it is essential to consider the thermal and mechanical effects of cracks on the resistance of bonded anchors under fire.

Objective

This thesis aims to extend the existing knowledge on the influence of temperature on the mechanical resistance of bonded anchors in order to evaluate and design bonded anchors under fire safely in uncracked and cracked concrete.

The study of parameters influencing the outcome of fire tests is necessary to ensure the representativity of these tests regarding bonded anchor in a building.

First, experimental fire tests were conducted to characterize the pull-out resistance of bonded anchors installed in concrete elements with fire exposure. Then, these tests served as a reference to develop a numerical model to predict a thermal distribution along the anchor that is closest to the one measured in fire tests (using finite element modelling to solve the transient heat transfer along the anchors). This also allowed to define the most penalizing (conservative) cases/parameters and potentially limit the number of tested configurations.

Furthermore, bonded anchors in cracked concrete are known to have a decrease on the bond strength at ambient temperature. Generally, cracked concrete is assumed for the design of anchors under fire. Therefore, it is necessary to study the influence of cracks on the load-bearing capacity under fire.

Work process and thesis structure

This dissertation is divided into 5 chapters corresponding to several publications. Chapters II to V are the subject of journal or conference papers. At the beginning of each chapter, a brief introduction is presented, followed by the plan of the paper, the paper and finally a discussion and analysis. Table 1 summarizes the objectives, the content and the links between these 5 chapters. The process is described hereafter.

1. Chapter I aims to identify the research conducted in the literature on the topic. **The objective** is to determine the testing methods for the assessment of the resistance of bonded anchors at ambient temperature, the load transfer mechanisms from the rod to concrete, and to identify the parameters that could influence the mechanical behavior of a bonded anchor under fire. **Therefore**, this literature study is conducted to identify: the existing assessment and design methods (for bonded anchors at ambient and high temperatures), the existing mechanical models for the description of the load transfer mechanisms, and the influence of temperature on the properties of the three studied materials.
2. Chapter II highlights the influence of testing conditions as they are described for mechanical anchors in the guidelines on the thermal distribution along bonded anchors, hence on the behavior of the adhesive. **The objective** is to observe the variation of temperature profiles along the embedment depth of the anchors depending on the adopted configuration of the anchor in fire tests. Then, it aims to quantify the influence of this temperature variation on the prediction of the load-bearing capacity using Pinoteau's method (the Resistance Integration Method) applied previously on PIRs. **Therefore**, the influence of anchor diameter, thickness of the concrete bearing element, existence of a metallic fixture on the anchor and insulation of fixtures, on temperature profiles along the anchor was conducted by means of ISO 834-1 fire tests on an epoxy based bonded anchor. The influence of the previously mentioned parameters as well as adopting concrete temperature instead of the temperature of steel/adhesive interface on the outcome of the Pinoteau's method was investigated. This study allowed to determine the most and least-penalizing configurations of bonded anchors in a building under fire, hence, to recommend it for evaluation and design purposes.
3. Chapter III proposes a 3D Numerical model to represent the problem of bonded anchors in concrete under ISO 834-1 fire. **The objective** is to propose a model for the design of bonded anchors using thermal calculations and Pinoteau's method. First, the model describes how the finite element software solves the heat equation in 3D. The equation is described for transient heat transfer through radiation and convection at the boundaries and conduction inside the exposed elements. Eurocode material properties of concrete and steel are used to account for the variation of thermal and physical properties of the studied materials with temperature increase. The representation of the problem of anchors in concrete in 3D is compared to 2D plane simulations commonly used in the literature. The errors of considering 2D plane modelling are presented and discussed compared to the consideration of 3D modelling and measured results from fire tests. **Therefore**, the output of the model uses previous characterization of the adhesive at high temperature as input data. After validation of the model, a parametric study is conducted to study other parameters influencing fire tests on bonded anchors that were not investigated experimentally in chapter II.
4. Chapter IV aims to validate Pinoteau's method (Resistance Integration Method) for the design of bonded anchors under fire. **The objective** is to validate the method by integrating the resistances (presented in the literature study in chapter I). **Therefore**, calculation results based on the proposed model in chapter III are compared to test results conducted in the thesis as well as in research project "Verbunddübel im Brandfall-DIBt" of TU Kaiserslautern and DIBt. Tests on bonded anchors exposed to ISO 834-1 fire under constant load to pull-out failure were conducted on three different types of adhesives for configurations varying from M8 to M30 anchor sizes. Then, these configurations are modelled in 3D and calculated temperature profiles are used as entry data along with previous characterization of the adhesive at high temperature to calculate the bond resistance of the anchor with fire exposure time.

- Chapter V aims to investigate the influence of crack existence on the resistance of bonded anchors at high temperatures. Indeed, anchors can be situated in crack plane on the tension side of reinforced concrete elements and their evaluation procedure at ambient temperature requires the assessment of cracks on the load-bearing capacity. Unlike PIRs which can be influenced locally by perpendicular cracks (flexural cracks), anchors behave as “crack magnets” due to the stress concentration in the area in which they are installed and are significantly influenced by cracks forming along the whole embedment depth. **The objective** is to determine the reduction of the load-bearing capacity of bonded anchors due to crack existence at high temperatures, compared to the reduction at ambient temperature. **Therefore**, tests are conducted on epoxy based bonded anchors heated with radiant panels to temperatures ensuring their thermal degradation (beyond glass transition). Then, pull-out tests are conducted on anchors in cracked and uncracked concrete immediately after heating to capture the load reduction due to crack existence at high temperatures. The variation of this reduction is observed at different heating times, hence different temperature profiles. Finally, the obtained ratio of resistance of anchors in cracked concrete to the resistance of anchors in uncracked concrete at high temperatures is compared to the ratio at ambient temperature.

Table 1: Process, objectives and content of the thesis

Chapter I	Chapter II	Chapter III	Chapter IV	Chapter V
Literature study	Influence of testing conditions under fire	Numerical modelling	Validation tests in uncracked concrete under fire	Influence of crack existence at high temperatures
Objectives				
<ol style="list-style-type: none"> Determination of the effect of temperature on mechanical properties of the 3 materials. Identification of the existing theoretical models for design. Identification of the existing evaluation methods of bonded anchors at ambient and high temperatures. 	<ol style="list-style-type: none"> Highlight of the impact of using testing conditions as described for mechanical anchors on bonded anchors. Variation of tested configurations of anchors to represent an anchor in a building. Assessment of the influence of each parameter on thermal distribution and the resulting load-bearing capacity. 	<ol style="list-style-type: none"> Propose a 3D FE model for design simply applicable by engineers. Compare the results of common 2D plane modelling to 3D modelling. Numerical investigation of other parameters influencing thermal distribution by means of numerical simulations. 	<ol style="list-style-type: none"> Validation of Pinoteau's method for design of bonded anchors under fire using tests and FE simulations. Comparison of design results to test results in this thesis and in the literature. 	<ol style="list-style-type: none"> Development of testing method in cracked concrete at high temperatures. Evaluate the influence of crack existence at ambient temperature and its evolution at high temperatures.
Content				
<ol style="list-style-type: none"> Research on the behavior of concrete, steel and adhesive at high temperatures. Presentation of theoretical models and a design method at high temperatures. Classification of tests at ambient temperature and under fire. 	<ol style="list-style-type: none"> Pull-out fire tests on epoxy based bonded anchors. Measurement of thermal distribution along the anchor during tests and comparison between different configurations. Application of Pinoteau's method to assess the mechanical influence of different thermal distribution. 	<ol style="list-style-type: none"> Description of the resolution of heat equation in 3D on an anchor exposed to fire. Prediction of failure load by 2D plane and 3D modelling with Pinoteau's method compared to calculation based on experimental measurements. Highlight of errors obtained by 2D modelling. Numerical investigation of other influencing parameters. 	<ol style="list-style-type: none"> Presentation of Pinoteau's method taking account of temperature profiles during fire. Tests on bonded anchors in concrete slabs under ISO 834-1 fire on 1 epoxy adhesive and comparison with results of the literature on 2 other adhesives (epoxy and cementitious based). 	<ol style="list-style-type: none"> Pull-out tests on epoxy based bonded anchors in cracked and uncracked concrete at ambient temperature. Tests in cracked and uncracked concrete at high temperatures heated with radiant panels followed by pull-out tests.

Chapter I: Literature study on the behavior of post-installed adhesive anchor systems and material properties

1. Description of bonded anchors

The technique of bonded anchors consists in using adhesive resins to glue a metallic threaded anchor-rod in a drilled hole in hardened concrete. The adhesive resin must ensure sufficient adherence between steel and concrete to transmit the loads applied on the anchor between both assembled structural elements.

The advantage of bonded anchors resides in their ease and rapidity of installation compared to cast-in anchors (steel/concrete connections). The first utilizations of this technique appeared in the 1960s (*Shaw, 1985*) following a validation of its technical feasibility in the 1940s (*ACI committee 503, 1973*). Since then, this technique has significantly developed in the field of reinforced concrete constructions because of the enhancement in the mechanical properties of the used adhesive resins and because of the many advantages that they present, especially in the renovation field.

1.1. Implementation method of bonded anchors

The manufacturer of the adhesive resin generally provides instructions for the implementation of the anchor. The installation of a bonded anchor is done using simple equipments provided often by the manufacturer and following several steps (Fig. 1):

- Drilling of the hole inside the concrete bearing element at a depth called “embedment depth of the anchor” (h_{ef}). The drilling diameter is defined as a function of the steel insert diameter and is generally taken greater than the steel insert diameter from 2 to 5 mm. The installation method of the manufacturer has to be followed.
- Cleaning of the hole to eliminate the dust, caused by drilling, using a specific brush and compressed air or a manual air pump. The cleaning process defines the mechanical performances of chemically bonded anchors (*Meszáros & Eligehausen, 1998*). The instructions (number of brushing and blowing) are also defined by the manufacturer of the adhesive resin and mentioned in the technical assessment of the product, for example: an ETA (European Technical Assessment) or an ESR (Evaluation Summary Report).
- Injection of the adhesive resin beginning from the bottom of the hole with the help of a dispenser and a cartridge equipped with a mixing nozzle allowing to mix the two components of the adhesive resin. The first injections have to be thrown away until a homogeneous color of the adhesive resin is obtained.
- Insertion of the metallic element by spinning it to allow air bubbles to exit and ensuring that the metallic insert is centered inside the hole to have a homogeneous adhesive thickness around the insert. This step must be done before the end of the work time (t_{work}) defined by the manufacturer. The extra adhesive resin outside of the mouth of the hole should be removed.

Once the implementation is done, the anchor can be loaded after a sufficient curing time (t_{cure}) to obtain the optimal hardening of the adhesive resin. The hardening is normally reached before 24h of cure. Finally, a maximal tightening torque defined by the manufacturer has to be applied on the nut. The loading of the anchor is then possible.

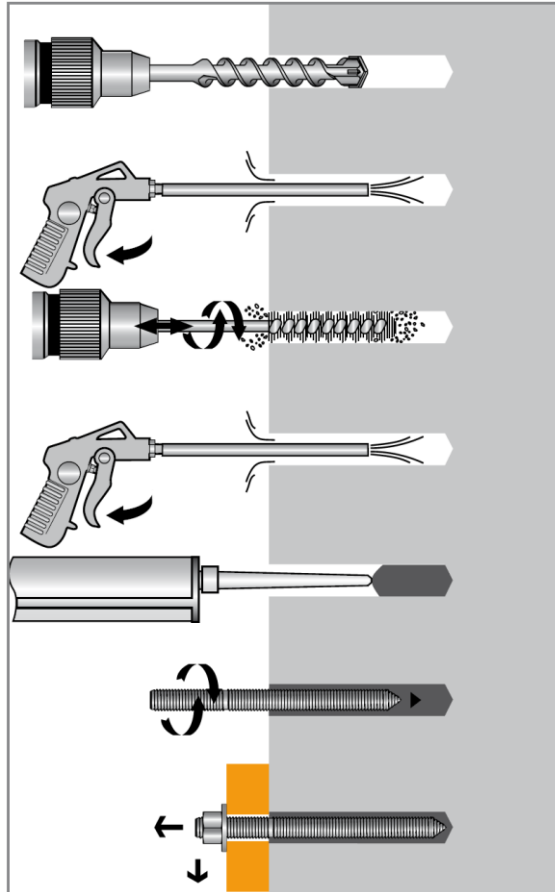


Fig. 1: Steps for implementing bonded anchors

1.2. Application fields of bonded anchors

The use of bonded anchors has developed significantly recently. Indeed, this technique was first applied for the renovation and reinforcement of concrete structures to allow for the junction between two existing structures (Sato *et al.*, 2004). Bonded anchors were also integrated in the field of bridges, tunnels and underground parkings. In this case, they were used with reinforcement bars instead of threaded rods.

In order to detail the fields of application of bonded anchors, it is important to distinguish the different frequently used types of anchors:

a. Bonded anchors

Bonded anchors can be implemented in a wall or a reinforced concrete slab. They consist generally in threaded rods (Fig. 2) which ensure load transfer by adherence of the adhesive resin, unlike mechanical anchors which bulge or expand inside the hole in concrete (Fig. 3) and ensure the steel/concrete load transfer by friction at the interface between both elements.

Bonded anchors are meant for several applications: domestic (fasten an object against a wall or a slab, fix a suspended ceiling...) or on construction sites (fasten ventilation systems for tunnels or façade elements).

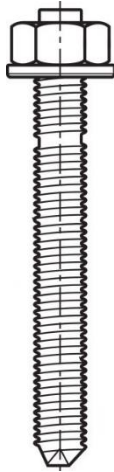


Fig. 2: Sketch of a threaded rod

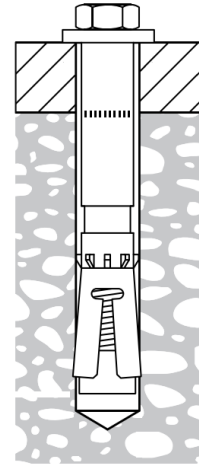


Fig. 3: Example of mechanical expansion anchors

Also, there are composite anchors identical to the previous systems. However, they are different compared to chemically bonded anchors. In the case of composite anchors, a cement-based mortar is used instead of an adhesive resin or a combination of both (hybrid resins).

The mechanical properties of adhesive resins change considerably with temperature increase and their adherence decreases. This has an impact on the load-bearing capacity of the anchor. This research project is concentrated on the study of this type of bonded anchors in concrete.

b. Post-installed rebars in concrete (PIRs)

In this type of anchors, the metallic element is a reinforcement steel bar (rebar) which transmits tension loads in reinforced concrete structures. Two types of bars can be used:

- Smooth steel rods: with a diameter between 5 and 50 mm.
- High adherence reinforcement bars (HA): with a diameter between 6 and 50 mm.

c. Glued-in rods

This type of anchors is used in concrete or timber and is more recent than the previous. It appeared thirty years ago thanks to its mechanical performances and esthetic aspect (Lahouar *et al.*, 2018). It allows to fasten one timber structure to another or with other types of concrete or steel structures.

Behavior at high temperature

When a sudden temperature increase occurs, such as in the case of a fire, bonded anchors show a significant degradation in resistance that progresses with temperature increase. The used adhesive resins to ensure load transfer between steel and concrete suffer a degradation leading to excessive creep of the anchor and sometimes to its failure when its resistance becomes less than the applied load. Until this day, the available knowledge does not allow to efficiently and precisely assess the load-bearing capacity of bonded anchors in fire situations.

The qualification of bonded anchors under fire is treated inadequately until today. Indeed, the Technical Report (EOTA TR 020, 2009) describes the assessment method of anchor systems under fire conditions, where the testing procedure and the failure modes are not well described. Moreover, the current European Assessment Document (EAD) dealing with bonded anchors (EAD 330499-01-0601, 2019) is the only document that allows to deliver European Technical Assessments (ETAs) and does not cover the assessment of bonded anchors under fire conditions. However, the European Assessment document dealing with mechanical anchors (EAD 330232-01-0601, 2019) has integrated the fire assessment method described in the Technical Report in its guidelines.

2. Thermal transfer in fire situations and its standardized conditions

Simulation of fire inside a furnace:

A fire inside a residential building is conditioned by the temperature-time curve of the international standard (ISO 834-1, 1999). The curve is defined by [Eq. 1] and plotted in Fig. 4:

$$T = 20 + 345 \cdot \log_{10}(8t + 1) \dots [\text{Eq. 1}]$$

Where: T is the average temperature inside the furnace in °C, and t is fire exposure time in min.

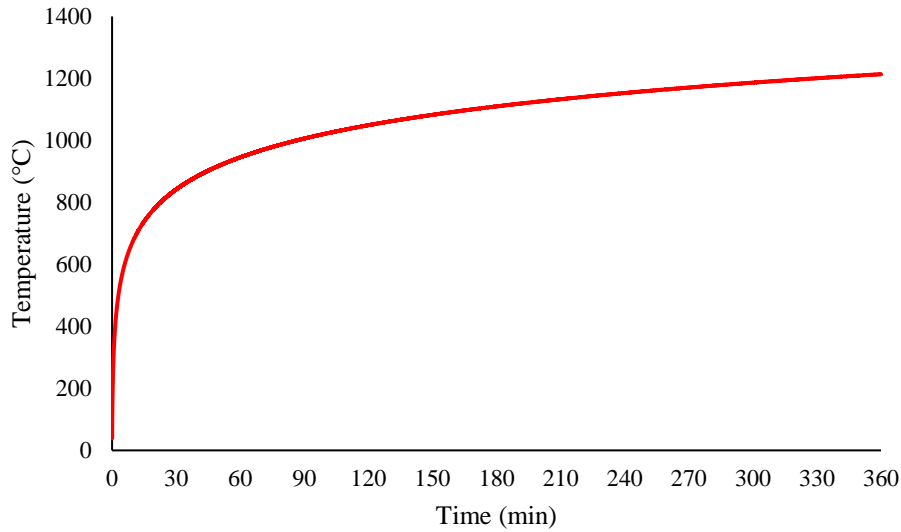


Fig. 4: Standard temperature-time curve of the ISO 834 fire (ISO 834-1, 1999)

The temperature inside the furnace is measured by plate thermometers specified in section 4.3. The temperature must be supervised and controlled to respect [Eq. 2].

- 1) $d_e \leq 15\%$ for $5 < t \leq 10$;
- 2) $d_e = (15 - 0.5(t - 10)) \%$ for $10 < t \leq 30$;
- 3) $d_e = (5 - 0.083(t - 30)) \%$ for $30 < t \leq 60$;
- 4) $d_e = 2.5\%$ for $t > 60$.

$$d_e = \frac{A - A_s}{A_s} \dots [\text{Eq. 2}]$$

Where: A is the surface under the real curve of average temperature as a function of fire exposure time;

A_s is the surface under the normalized temperature-time curve.

t is the fire exposure time in min.

After the first 10 minutes of the fire test, the measured temperature by any thermocouple must stay within 100°C of the temperature corresponding to the normalized ISO 834 curve, except in the case of combustible materials where the difference can exceed 100°C during 10 min under the condition that this difference can be associated to the sudden inflammation of large quantities of combustible materials increasing the average temperature of the furnace.

An average pressure gradient of 8 kPa by meter of height exists on the height of the furnace. This value must be supervised and must respect a maximal difference of 5 Pa during the first 10 min of the test and 3 Pa after the first 10 min.

3. Mechanical behavior of studied materials at high temperature

The goal of this section is to assess the mechanical behavior of the materials constituting the study under an accidental temperature increase especially in fire situations.

3.1. Concrete

Concrete is a heterogeneous material, obtained from a mix of cement, water and aggregates (coarse and fine), with or without adding adjuvants and additives. The possibilities of parameter variation within this mix are practically unlimited. Temperature increase causes complicated phenomena inside hardened concrete. A simple consideration of thermal properties (thermal conductivity and specific heat) is not sufficient to describe the behavior of this material.

The first apparition of concrete goes back to the first century, at the time of Romans. In France, natural cements with fast setting times were subjected to many researches (*Durand-Claye, 1885*), (*Debauve, 1886*), (*Leduc, 1902*), (*Wagner et al., 1903*), (*Candlot, 1906*) et (*Fritsch, 1911*) since their discovery in 1796, and their operation until the end of the 19th century. The discovery of artificial cements (Portland) was patented in 1824 by Aspdin. This emergence was issued from the progress in mineral chemistry and the fear of exhausting natural cement deposits. Artificial cements became performant after 1850 following scientific publications that showed the importance of their resistance and hardening compared to natural cements.

The composition of *Portland cement*, commonly used in civil engineering, is controlled by the following standards (*ASTM International, 2007*) and (*CEN NF 197-1,2012*). It contains:

- Clinker: which results from heating up to 1450°C followed by soaking, limestone (80%) and aluminosilicate materials (20%).
- Calcium sulfate (Gypsum, anhydrate or hemihydrate): which is a rock. It plays the role of regulating mass hardening by reacting with tricalcium aluminate and water to form Ettringite crystals which delay mass hardening until the operation.
- Mineral additions: limestone and siliceous additions, fly ash, silica fume, and blast furnace slag that can have, depending on the case, hydraulic or pozzolanic properties.

Table 2 summarizes the principal components of Portland clinker (*Mindeguia, 2009*).

Designation	Exact chemical formula	Specified chemical formula	Proportion in ordinary cement
Tricalcium silica	3 CaO, SiO ₂	C ₃ S	60-65%
Bicalcium silica	2 CaO, SiO ₂	C ₂ S	20-25%
Tricalcium aluminate	3 CaO, Al ₂ O ₃	C ₃ A	8-25%
Tricalcium Aluminoferrite	4 CaO, Al ₂ O ₃ , Fe ₂ O ₃	C ₄ AF	8-10%

Table 2: Principal components of ordinary Portland cement (Mindeguia, 2009)

Aggregates are particles ranging from about 100 µm up to several centimeters that can be either of natural (mostly), artificial or recycled origine. Natural aggregates come from silicious or limestone sedimentary rocks, methamorphic rocks (quartz and quartzite) or eruptive rocks (basalt, granite or porphyry). Their dimensions are between 0 and 125 mm, going from 0 to 4 mm for sand, from 4 to 32 mm for gravel and greater than 32 mm for chippings. Aggregates constitute the skeleton of concrete representing between 50% and 80% of its total volume. They are generally less deformable than the cement matrix. They oppose to the propagation of micro-cracks caused in the cement mix by shrinkage. The mechanical resistances of concrete are mainly conditioned by the properties of the Interfacial Transition Zone (ITZ) which is a thin layer of cement paste surrounding aggregates possessing a larger W/C ratio than the bulk paste.

The choice of concrete composition is always studied as a function of the expected performances, especially in terms of durability.

Water in concrete plays two roles:

- Granting the cement-sand-gravel mix a certain fluidity (workability).
- Allowing the hydration reactions of cement to form, after hardening, the solid matrix “gluing” all the components together.

Water is then the component that transforms powder into a solid element. It exists inside concrete in 3 forms: Chemically bound water in hydrates, absorbed water and free water. The relation between water and cement inside concrete plays an important role in its behavior at fresh state, its mechanical behavior and durability, and the larger the W/C ratio, the larger the workability is. On the other hand, the mechanical resistance of concrete decreases with the increase of the W/C ratio, which increases the porosity of the matrix.

The hydration reactions occur after mixing water and cement. It leads to the formation of hydrates. Concrete presents a good fire resistance thanks to its incombustibility and weak thermal diffusivity. However, at high temperature, the properties of concrete change (permeability, expansion, tensile and compressive resistance...) and several phenomena occur (spalling, cracking...).

Physico-chemical modifications:

Temperature increase in concrete leads to the departure of free water, even for temperature less than 105°C (Bazant et Kaplan, 2008). The amount of evaporable water depends on the maturity and the quantity of cement mix inside the concrete and also the relative humidity of ambient air (Msaad et al. 2005).

When a concrete made from Portland or blended cement is subjected to heat, different transformations and reactions occur (Msaad et al. 2005), (Ehm et al., 1981), (Alonso et al., 2004) & (Mendes, 2010). These modifications are:

- Decomposition of some hydrates (especially ettringite) from 70°C, the temperature at which evaporable water is already evacuated if the heating rate is slow. On the other hand, if the heating rate is fast, the evaporation process could be extended up to 200°C (Heinfling, 1998).
- Continuation of dehydration of C-S-H progressively up to temperatures near 900°C.
- Decomposition of the C-S-H gel to fine particles from 100°C to 200°C (Feldman & Sereda, 1968).
- Decomposition of Portlandite to calcium oxide from 450°C.
- Transformation of quartz α to quartz β at 570°C (this transformation concerns concrete containing silicious aggregates).
- Cracking of C-S-H and formation of dicalcium silicates β C₂S during the second phase of dehydration between 600°C and 700°C.
- Decomposition and decarbonization of aggregates by forming quicklime between 700°C and 900°C.
- Total melting of aggregates and cement mix around 1300°C.

Concrete undergoes a significant mass loss at high temperature. This loss is low below 150°C (essentially linked to the departure of free water inside concrete) and begins to increase rapidly from 150°C because of the departure of water contained initially in the hydrates and because of the decomposition of gypsum. Above 300°C, this loss is low and corresponds to the dehydroxylation of Portlandite between 450°C and 550°C, the decomposition of silanols (SiOH) and the decarbonation of limestone (CaCO₃) between 600°C and 800°C (Xing, 2011), (Pliya, 2010), (Kanema, 2007), (Xiao et al., 2006), (Hager, 2004), (Phan et al., 2001), (Noumowé, 1995), (Khoury, 1992). Fig. 5 shows mass loss of different components of concrete as a function of temperature according to (Hager, 2004).

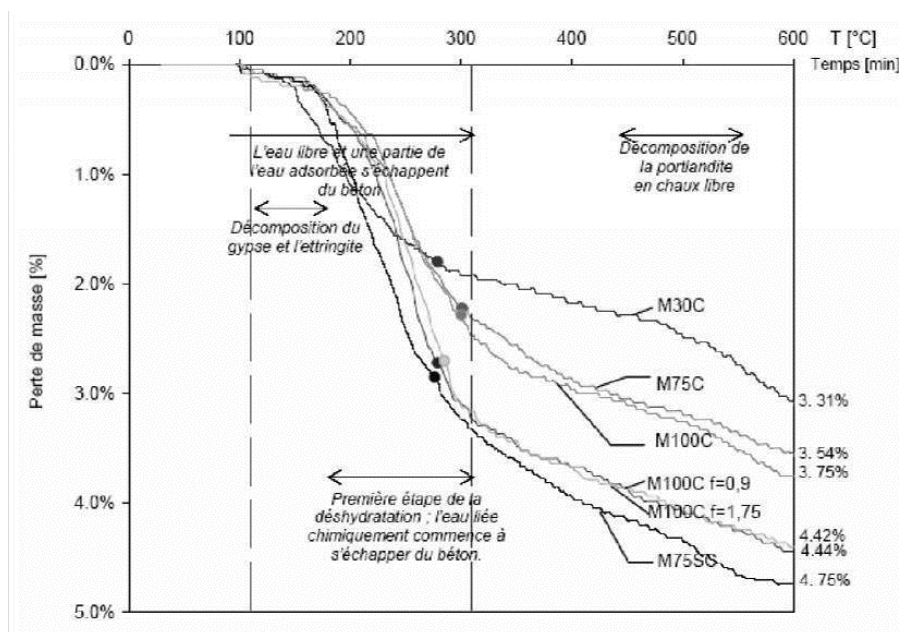


Fig. 5: Evolution of mass loss as a function of temperature for different components of concrete (Hager, 2004)

A high-performance concrete (HPC) undergoes less mass loss at high temperature than ordinary concrete (OC). Nevertheless, because HPC has a denser structure, its water content is less and the volume of non-hydrated cement particles is larger, the kinetic and the extent of its diverse microstructural and chemical modifications present certain particularities (Pimienta *et al.*, 2017).

Increase of permeability:

The previously discussed modifications also provoke changes in physical properties for concrete, especially its permeability. This phenomenon is significant especially for high performance concrete (HPC). The increase of permeability is significant between 200°C and 400°C because it is linked to the increase of the radius of capillary pores up to 300°C and to micro-cracking above 300°C.

(Tsimbrovska 98) studied the evolution of gas permeability (nitrogen) on mortars and ordinary concretes subjected beforehand to a thermal treatment until reaching constant mass at temperatures between 105°C and 400°C. All mortar samples (cylinders with a diameter of 54 mm and a height of 30 mm) and concrete samples (cylinders with a diameter of 150 mm and a height of 50 mm) were subjected to a temperature increase at 0.2°C/min. Fig. 6 shows the evolution of gas permeability measured after cooling for mortars and concretes. Mortar and concrete gas permeability at high temperature increases between 200°C and 400°C. This is attributed to the apparition of micro-cracks and volume increase of connected capillary pores. Indeed, the permeability, which is strongly influenced by the morphology of pores, is extremely sensitive to the increase of the size of pores and the creation of interconnected micro-cracks. As a result, permeability of mortars and concretes increases with temperature.

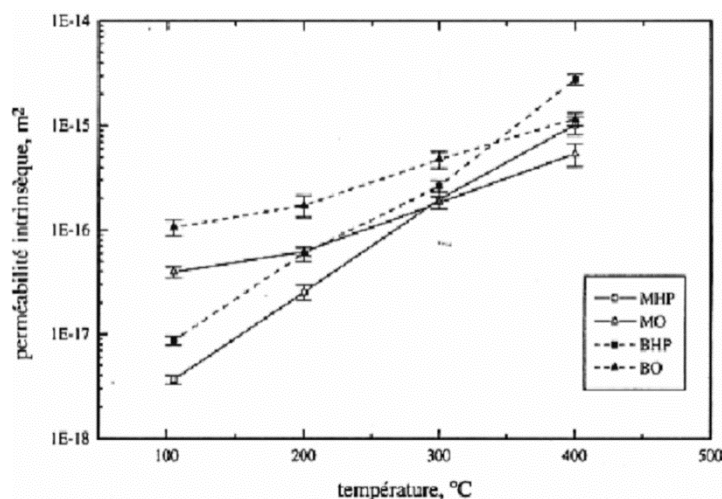


Fig. 6: Evolution of intrinsic permeability in mortars, ordinary, and high-performance concretes as a function of temperature (Tsimbrovska, 98)

Thermal expansion of concrete:

Thermal expansion of concrete at high temperature is linked to several combined phenomena: at high temperature, aggregates undergo a continuous thermal expansion. On the other hand, the cement matrix is subjected to expansion from 30°C to 150°C and shrinkage above 150°C. Micro-cracks occur because of these two opposite thermal strains. Also, concrete components undergo physic-chemical modifications amplifying thermal expansion, it is considered isotropic and depends on temperature increase. (Diederichs *et al.*, 1989) compared thermal expansion of an ordinary concrete to three high performance concretes (HPCs) (Fig. 7). The studied samples had a diameter of 80 mm and a length of 300 mm. Heating rate was 2 K/min. The slope corresponding to thermal expansion at 1×10^{-5} in Fig. 7 is represented with a dashed line. Expansion coefficients of aggregates for each concrete were studied because they represent most of the volume in concrete (between 50% and 80%). Consequently, their thermal expansion significantly influences the thermal expansion of concrete. The studied ordinary concrete contained silicious aggregates with a thermal expansion coefficient of $1.6 \times 10^{-5} / \text{K}$ when the studied HPCs contained crushed diabases and granitic sands with a thermal expansion coefficient of $0.8 \times 10^{-5} / \text{K}$. The studied HPCs showed a lower thermal expansion coefficient than ordinary concrete (0.8×10^{-5} for 1.1×10^{-5}). This could be linked to the fact that the studied HPCs had a lower aggregate content and that their aggregates had a lower thermal expansion coefficient.

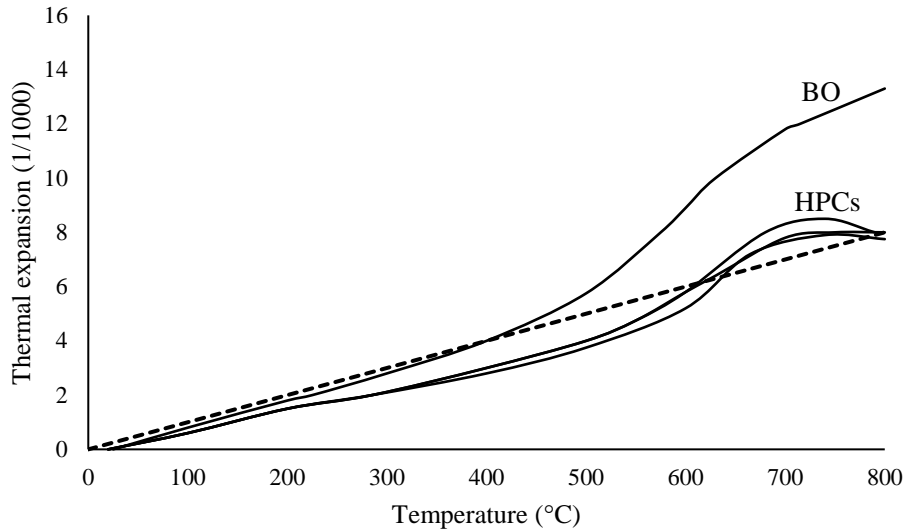


Fig. 7: Comparison of thermal expansion coefficients between three HPCs and ordinary concrete (Diederisch et al., 1989)

Concrete cracking:

Concrete cracking during heating is the result of differential expansion between cement matrix and aggregates. This is linked to the fact that they both undergo thermal expansion up to 150°C, but above this value, aggregates continue to expand whereas the cement matrix shrinks. This phenomenon creates constrained stresses and provokes thermal cracking. (Bazant et Kaplan, 1996) studied the expansion of concrete at high temperature and explained that aggregates dominate the thermal behavior by cracking the cement matrix because they are more resistant.

Decrease of compressive strength:

The decrease of compressive strength has been extensively studied by several researchers (Diederisch et al., 1989), (Khoury, 1992) and (Noumowé, 1996). Their studies showed that the decrease of compressive resistance of concrete is linked to the dehydration which causes the evolution of the microstructure. A concrete heated at 120°C then left to cool down can recover its mechanical properties at ambient temperature. However, above 120°C, the dehydration and microcracking are irreversible. Fig. 8 shows the evolution of the compressive resistance of concrete according to Eurocode 2.

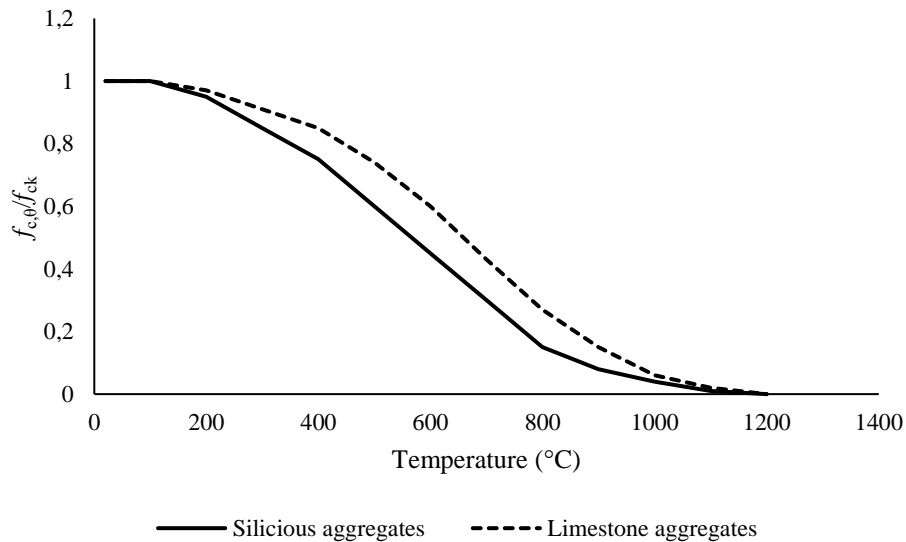


Fig. 8: Evolution of relative compressive resistance of concrete as a function of temperature according to Eurocode 2

Decrease of tensile strength:

The decrease of tensile strength is quasi-linear and plays a decisive role in the cracking mechanism. Very few researchers took an interest in this property and neglect it mostly for security purposes, especially at high temperature. (*Noumowé, 1996*) studied this property by conducting axial tension and splitting tests on an ordinary concrete (OC) and a high-performance concrete (HPC).

Unlike compressive resistance (Fig. 8), moderate heating (1 to 10°C/min) decreases the residual tensile resistance (after cooling). Fig. 9 shows the evolution of concrete tensile resistance as a function of temperature according to Eurocode 2.

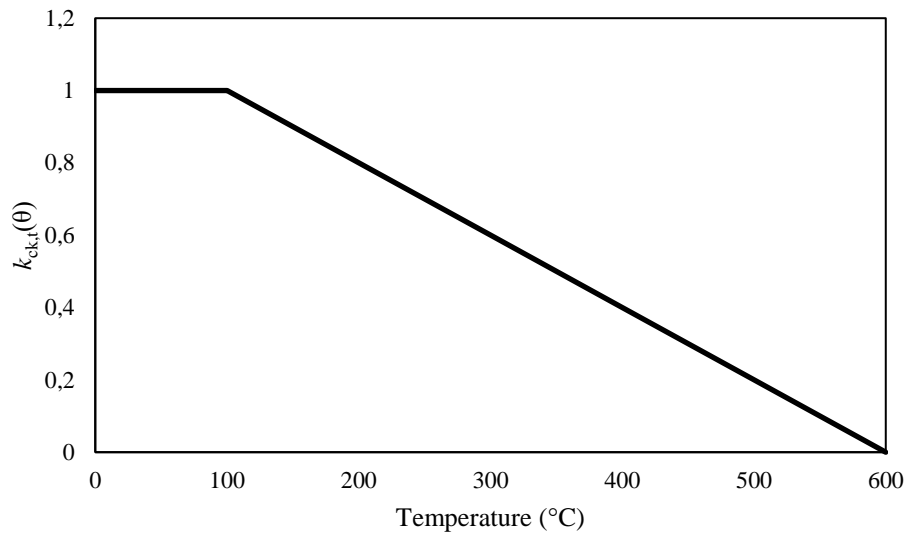


Fig. 9: Factor $k_{ck,t}(\theta)$ applicable for concrete tensile strength $f_{ck,t}$ reduction at high temperature

Concrete spalling:

This phenomenon occurs especially for HPCs. Humidity and water vapour migrate because of temperature increase and this migration is restrained by the low permeability of concrete. (*Msaad et al., 2005*) proposed two explanations for this phenomenon :

- Hydraulic spalling by pressure: here spalling is explained by the presence of a zone which is rich in water (plug) provoquing gas pressure increase on the hot side of the saturated face.
- Spalling by restrained thermal expansion: on one hand the thermal expansion caused by heating leads (when it is restrained) to compressive stresses parallel to the fire exposed surface.

According to (*Khoury, 2000*) there are four different forms of spalling: aggregates spalling, explosive spalling, surface spalling and edge spalling. This phenomenon is linked to several factors depending on the material properties (permeability, size and mineralogical nature of aggregate). According to (*Khoury, 1992*), elevated heating rate, low concrete permeability, pore saturation corresponding to water content above 2-3%, the presence of reinforcement and the applied force are the principal factors which generate concrete spalling.

According to (*Mindeguia et al., 2015*), spalling cannot be expressed solely by the development of an elevated interstitial gas pressure. During ISO 834 fire tests, spalling was observed on slabs despite their low interstitial gas pressure. For tests on small samples at a slow heating rate, an elevated interstitial gas pressure was observed without spalling. Concrete spalling can be linked to the apparition of a “critical zone”, an interpretation proposed by (*Jansson et al., 2013*) and confirmed by (*Mindeguia et al., 2015*) consisting of a water saturated zone. It can be localized at a few centimeters from the fire exposed surface. If this water succeeds in escaping rapidly and easily from the first exposed centimeters, there will be a low risk of spalling. Concrete spalling under fire near the critical zone can be caused by a deterioration of the mechanical properties of water saturated concrete (*Jansson et al., 2013*) and (*Lankard et al., 1971*). According to the critical zone hypothesis, no spalling can be observed when the creation of the water saturated zone is avoided. A more pronounced spalling can be observed for fast fires (more

aggressive temperature-time curves), for example: spalling is more occurent for hydrocarbon fire which is more aggressive compared to ISO 834 fire (*Pimienta et al., 2010*).

3.2. Steel

Steel used in the world of anchors varies between reinforcement and fastening applications.

Reinforcement bars:

The European standard (*NF EN 10080, 2005*) defines the term “steel” for reinforced concrete: a steel product with a circular or practically circular cross-section which is suitable for the reinforcement of concrete. The geometry and adherence of reinforced bars covered by the previous European standard vary depending on the product (ribbed and indented reinforcement steel). The product is characterized by its geometry, by means of which bond with concrete is achieved.

Ribbed steel bars have different configurations of transverse and longitudinal ribs. The product must have at least two rows of transverse ribs uniformly distributed around the perimeter with uniform spacing between the ribs within each row. Fig. 10 gives an example of a ribbed steel with two rows of transverse ribs (*NF EN 10080, 2005*).

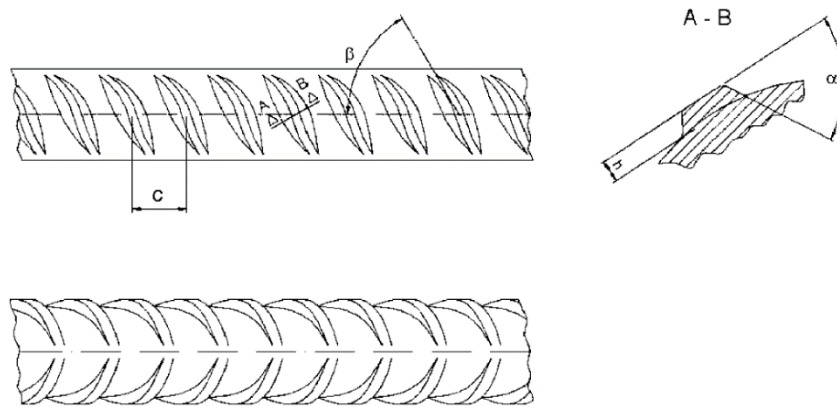


Fig. 10: Geometry of two rows transverse ribs (*NF EN 10080, 2005*)

Indented steel bars have different configurations of indents. The product must have at least two equally distributed rows of indentations. The indentations form an angle of inclination with the bar axis. Fig. 11 gives an example of an indented bar with three rows of indentations.

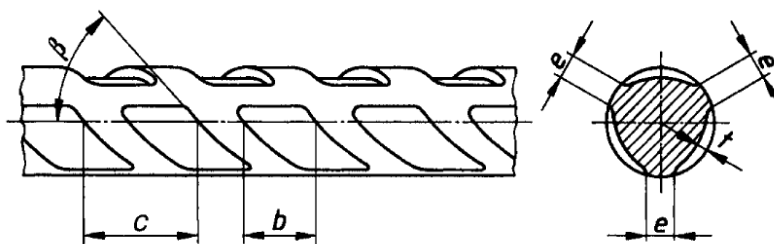


Fig. 11: Geometry of three rows of indentations (*NF EN 10080, 2005*)

Reinforcement can also exist under the form of smooth rods for a diameter varying from 5 to 50 mm. In reinforced concrete structures, reinforcement bars are generally implemented to support the tensile forces in the section.

Annexe D of the standard (*NF EN 10080, 2005*) specifies the evaluation method for assessing bond resistance of ribbed and indented bars used for reinforcement in concrete. The tension test is called “pull-out test” and gives a basis for comparison between bars for reinforced concrete which present approximatively the same diameter but have different surface configurations.

The principle of the pull-out test consists in loading the bar with a tensile force. The bar must be incorporated in a concrete cube with a defined embedment length. No stresses are applied on the other end of the bar. The relation between the tensile force and the slip (relative displacement between steel and concrete) is measured up to failure.

The force continues to increase until the failure of the bond or the steel itself fails. Fig. 12 illustrates the principle of the test.

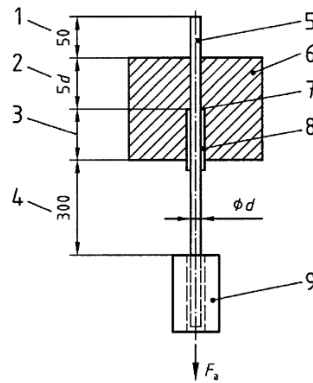


Fig. 12: Illustration of the principle of a pull-out test (NF EN 10080, 2005)

Where: 1 is the part of the bar up to the point of the application of the displacement measuring device, 2 is the bond length, 3 is the free part pre-length, 4 is the part of the bar up to the point of application of the tension force, 5 is the reinforcing bar, 6 is concrete, 7 is a plugging, 8 is a plastic sleeve and 9 is the grip of the testing machine.

The bar is located in the center of the cube with an effective bond length of $5d$ corresponding only to a part of the specimen. Bond is prevented on the other end of the bar. The bar extends beyond the two sides of the cube. The tension force is applied to the longer end and the slip measurement device is set on the shorter end. The sleeves must fit about 1 mm tolerance around the bar and their thickness must not exceed 2 mm.

Threaded rods:

Part 1 of the standard (NF EN ISO 898, 2013) specifies the mechanical and physical characteristics of bolts, screws and studs in carbon steel and alloy steel at ambient temperature. The standard (NF EN 10269, 2013) describes the specifications for anchors in steels and nickel alloy at high temperatures. Fig. 13 shows the geometry of a threaded studs and rods according to the international standard (NF EN ISO 888, 2018).

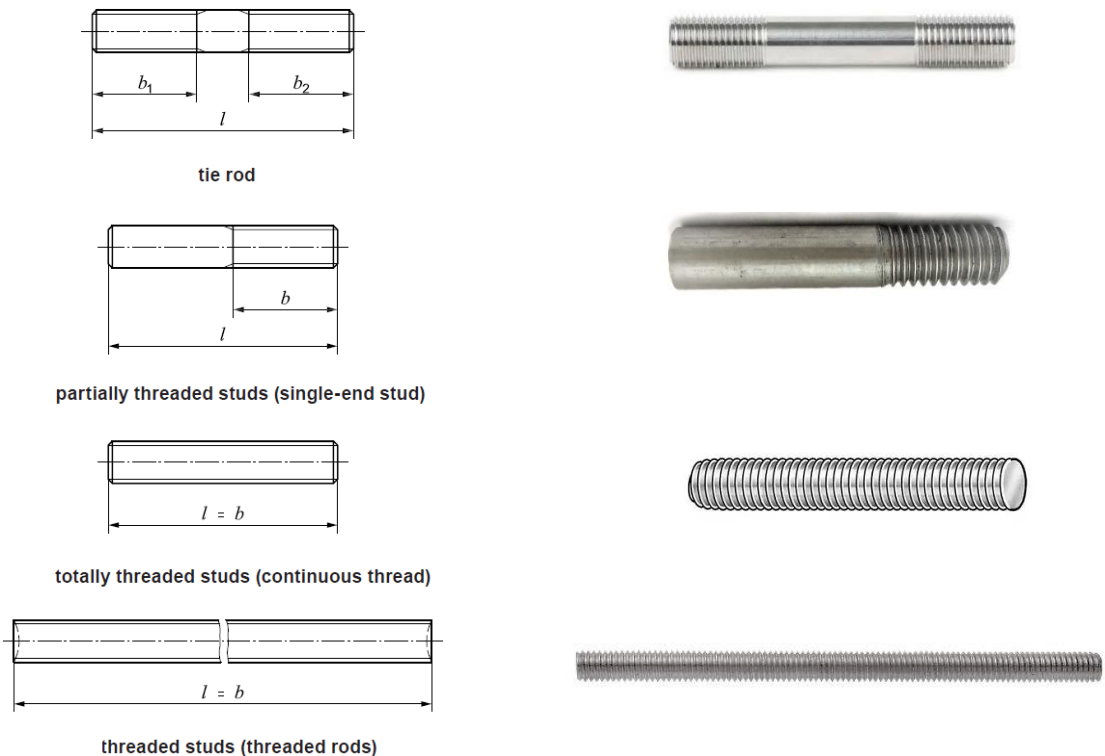


Fig. 13: Threaded stud (NF EN ISO 888, 2018)

The symbols and descriptions of geometrical dimensions in the figure above, according to the standards (*NF EN ISO 4753, 2012*) and (*NF EN ISO 888, 2018*), are:

d : nominal diameter of the thread (mm).

b_1 : thread length of one end for double end studs (mm).

b_2 : thread length for the other end for double end studs.

l : nominal length.

The steel of the anchor is designed depending on the type, diameter, steel grade, yield strength and ductility class of the anchor.

The tensile strength of anchors with an embedment depth $\geq 2.5d$ shall be determined according to the international standards (*NF EN ISO 6892, 2016*) and (*NF EN ISO 898, 2013*). A minimal threaded length equal to at least the nominal diameter of the thread is subjected to tension. The failure shall occur inside the free threaded length l_{th} or the unthreaded shank (Fig. 14). The failure must be avoided in the head of the anchor and in the transition section between the head and the threaded length. An exception is made for this case when failure originates in the threaded length.

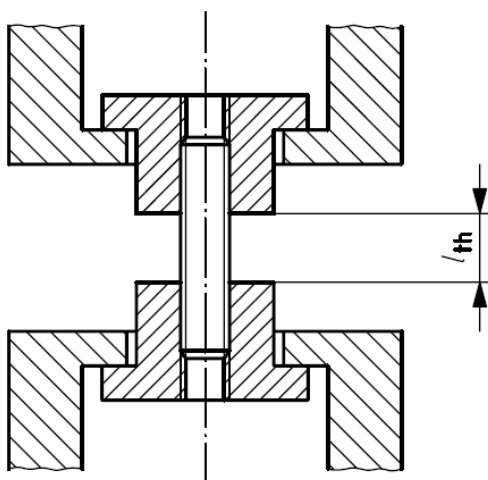


Fig. 14: Example of testing device for tensile test on full-size threaded rods (*NF EN ISO 898, 2013*)

Steel has an elastic modulus equal to 210 GPa at ambient temperature (20°C). Fig. 15 shows the simplified stress-strain diagram for steel according to Eurocode 2, Part 1-1 (*NF EN 1992-1-1, 2005*), with:

- f_{yk} : yield strength (MPa).
- $k \cdot f_{yk}$: tensile resistance for steel (MPa).
- ϵ_{uk} : steel elongation at failure.

k and ϵ_{uk} depend on steel ductility.

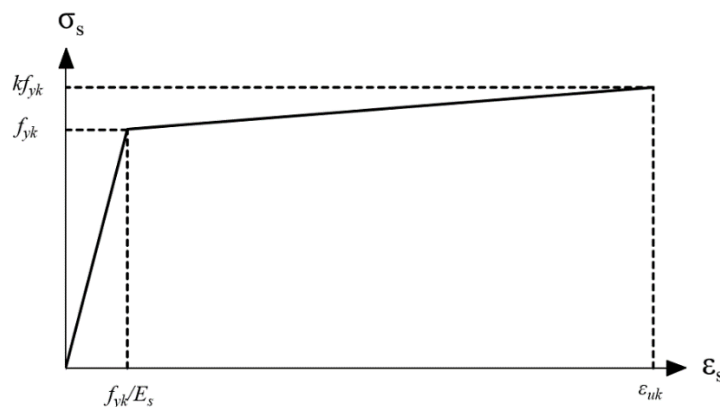


Fig. 15: Simplified stress-strain diagram for steel according to Eurocode 2, part 1-1 (*NF EN 1992-1-1, 2005*)

Density:

Steel density can be considered temperature independent (*NF EN 1993-1-2, 2005*). A value of 7850 kg/m³ can be adopted.

Thermal expansion:

Thermal expansion of steel is temperature dependent and given in Fig. 16 according to Eurocode 3, Part 1-2 (*NF EN 1993-1-2, 2005*).

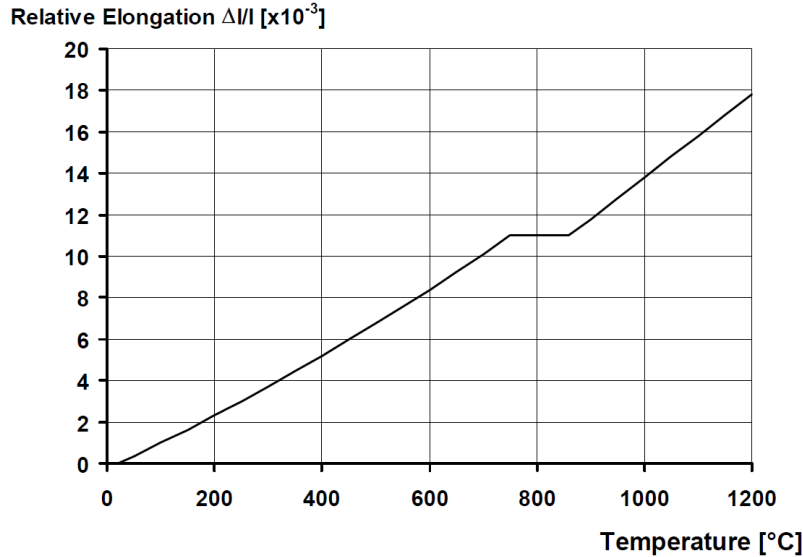


Fig. 16: Relative elongation of carbon steel as a function of temperature (*NF EN 1993-1-2, 2005*)

Specific heat:

The variation of the specific heat for steel as a function of temperature is illustrated in Fig. 17 according to Eurocode 3, Part 1-2 (*NF EN 1993-1-2, 2005*).

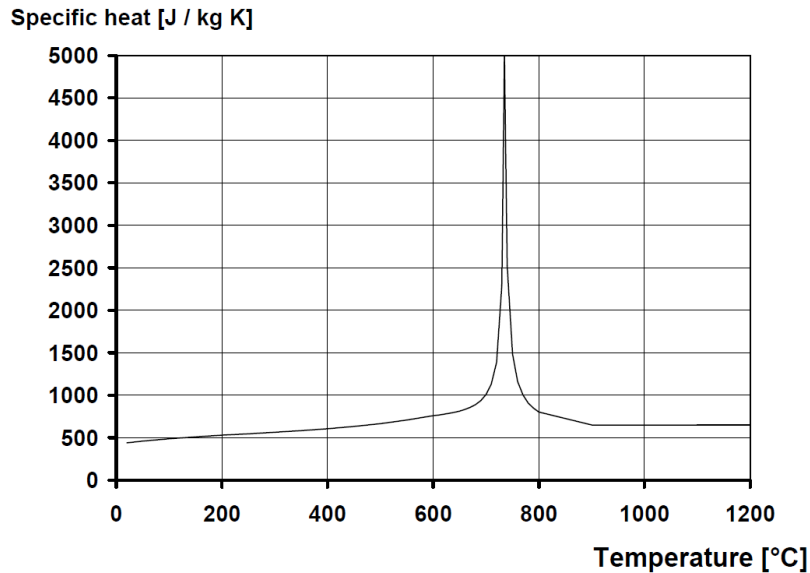


Fig. 17: Specific heat of carbon steel as a function of temperature (*NF EN 1993-1-2, 2005*)

Thermal conductivity:

The variation of thermal conductivity for steel as a function of temperature is illustrated in Fig. 18 according to Eurocode 3, Part 1-2 (*NF EN 1993-1-2, 2005*).

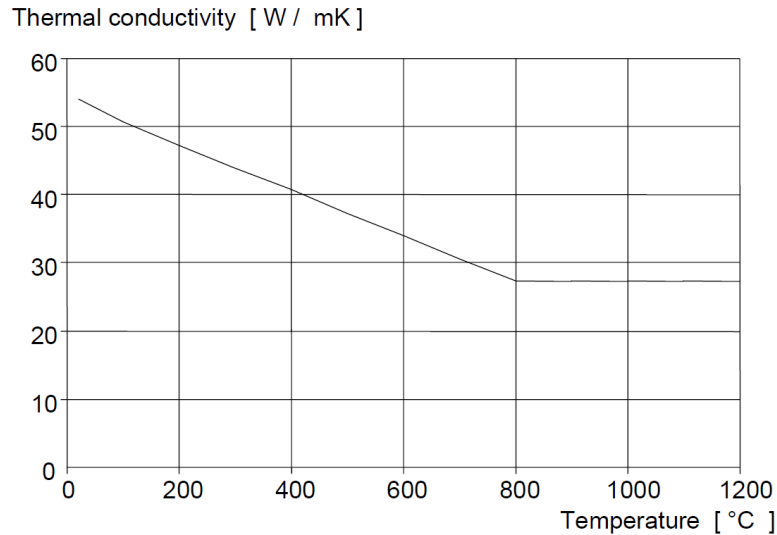


Fig. 18: Thermal conductivity of carbon steel as a function of temperature (NF EN 1993-1-2, 2005)

3.3. Adhesive resin

Components of adhesive resins:

The used adhesive resins in the field of construction are generally polymer based (for example: epoxy) to which other adjuvants are added to enhance their mechanical properties, durability, chemical stability, conservation, ease of implementation and product appearance (Pinoteau, 2013).

Polymer, from a chemical point of view, is a macromolecule composed of carbon and other elements such as hydrogen, nitrogen, chlorine and fluorine. According to (Pinoteau, 2013), adhesive resins used in anchors belong to the family of thermosetting polymers. A thermosetting polymer is composed of cross-linked linear chains. The chains are linked in space with strong covalent bonds. Thus, they present a three-dimensional insoluble and infusible (can not be melted) network.

Structural adhesive resins are composed of three principal families (Lahouar, 2018):

1. Methacrylic: based on acrylic and methacrylic esters. They are formed by mixing Methyl methacrylate with peroxide.
2. Polyurethane: thermosetting bicomponents formed by mixing polyols with an isocyanate hardener.
3. Vinyl ester and epoxide: thermosetting bi-components formed by esterification of an epoxide pre-polymer with an insaturated carboxylic acid such as acrylic acid or methacrylic acid in the case of vinyl ester adhesive resins, and with an acid anhydrite or amine in the case of epoxy adhesive resins (M. Allenbach Patrick, 2014).

The cohesion of the adhesive resin is ensured by two type of bonds:

1. Inter-atomic bonds that ensure the cohesion between the atoms of the same molecule.
2. Inter-molecular bonds that ensure the junction between different molecules.

Fillers:

They represent up to 60-65% of the final mass of the adhesive resin. They are generally mineral substances (silica, alumina and graphite). The price of silica and its mechanical performances makes it the most used component. Silica procures the best mechanical performances and it is very economical which explains why it is found in most of the applications. Alumina gives a certain self-extinguishing property (the capacity of a substance to burn in a flame and automatically extinguish itself after removing the flame) and a better resistance to tracking index (the capacity of an insulating material to resist to an electric field beyond its capacity). All the fillers contribute not only to the decrease of the price, but they are also essential on the technical plan. They allow to reinforce the material by increasing the mechanical properties of composites (tensile, compressive and bending strength). They also decrease the stresses linked to the shrinkage of the polymerization and compensate for the elevated thermal expansion coefficient of the matrix phase.

Flexibilizers and plasticisers:

The aim of these products is to enhance the resilience of the adhesive resin (shock resistance) by slightly decreasing its viscosity. Flexibilizers are present at a proportion that should not exceed 25% in a bisphenol resin to avoid significantly decreasing the mechanical resistance at high temperatures. For epoxy adhesive resins, flexibilizers integrate the three-dimensional molecular network of the cross-linked polymer because of the presence of an epoxy group. The latter is not present in the plasticisers, making it incapable to integrate the molecular network, leading to their migration and causing a premature aging of the adhesive resin.

Reactive thinners:

These components aim to increase the fluidity of the product. In general, the used quantity depends on the wanted thermal properties. The bigger the dosage is, the lesser the glass transition temperature. This is why they are not used for fixing ceilings to avoid leakage of the adhesive resin. If the thinners exceed 10% of the product, the drop of the properties is significant.

Dyes:

They can be composed of mineral or organic pigments. Certain colors are difficult to obtain, like light colors for epoxy adhesive resins with a heavy dose of silica (*Bardonnet, 1992a*).

Solvents:

They are added to the formula to delay the cross-linking reaction of the resin/hardener mixture. They extend the expiration date of resin pot and allow to adjust the viscosity of the mixture. The most known solvents are ketones, alcohols and aromatic compounds.

Exothermicity of the reaction:

The installation of the adhesive resin requires to mix the mother resin with the hardener, creating a chemical reaction called "cross-linking". This reaction releases heat (exothermic). It increases the temperature of the adhesive resin during its cure. (*Bardonnet, 1992a*) explains that the mass entering the reaction plays an essential role. Indeed, the molecules that started to cross-link give away their heat from the reaction to the neighboring molecules. He also explains that a poorly controlled reaction between the mother resin and the hardener can lead to thermal peaks that can reach up to 250-300°C.

It is then important that the heat dissipates sufficiently with time to avoid the apparition of exothermic peaks that can generate internal stresses and cracks. (*Bardonnet, 1992a*) listed several parameters that have to be taken into account to avoid high exothermicity:

- The presence or absence of metal inerts capable of evacuating heat.
- The presence or absence of a mineral filler capable of increasing the conductivity of the adhesive resin towards the wall of the mold.
- The mass concentration: a concentrated mass is more difficult to treat than the hollow body of the same thin-walled mass.

The influence of hardening time on the temperature of the mother resin/hardener mix for the same mixture in two different configurations is shown in Fig. 19. In case I, the initial temperature of the stove was 120°C and in case II it was 160°C. In the first case, there is a slight exothermic peak (slight increase of temperature compared to that of the stove), whereas for the second case the higher temperature of the stove caused a violent exothermic reaction with a peak of 280°C (160°C stove + 120°C increase). Naturally, the amount of heat released does not depend on the reached temperature but on the surface under the curve. The hatched surface under both curves of Fig. 19 is the same. This means that for the same sample of a given mixture, the heat quantity released by the reaction must be the same.

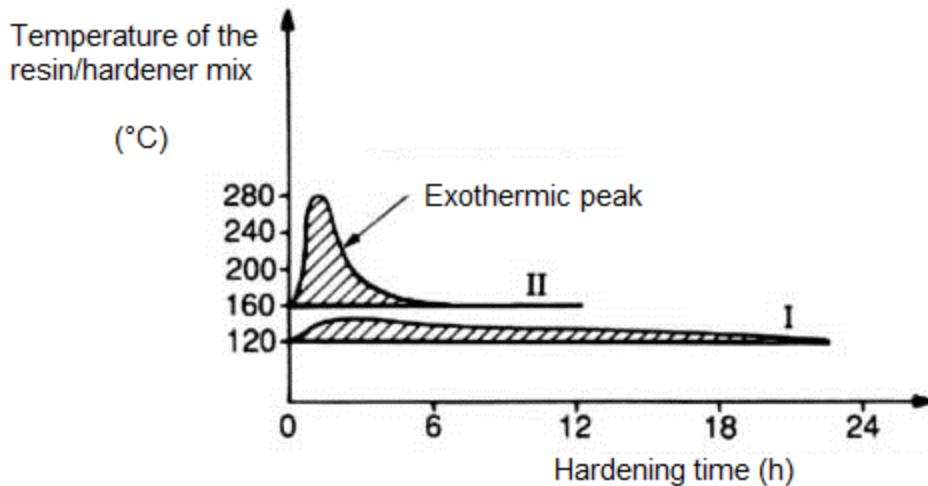


Fig. 19: Thermal analysis of the hardening of an epoxy resin (Bardonnnet, 1992a)

Thermosetting adhesive resins are subjected to shrinkage (decrease in volume) during their cooling-down from the cure temperature to ambient temperature. This shrinkage is a consequence of the overheating due to the cure. The intensity of the shrinkage depends on the chemical structure of the adhesive material and on the type of attraction forces appearing during the cure (Marques, 2014).

(Coppendale, 1977) showed by using a two-dimensional finite element model analysis, that for failure loads between 10 and 20 kN for a uniform adhesive joint, the contribution of shrinkage is not significant in the deformation (around 0.5%). This means that for adhesive joints it is not necessary to take shrinkage into account. Other research works focused on compression with thermally induced stresses.

(Mallik, 1989) studied the stresses inside a unique adhesive joint fastening a carbon fibre reinforced polymer (CFRP) to aluminium. The shrinkage had very little influence on the total state of stresses inside the adhesive joint. (Yu, 1999) investigated an adhesive layer-lined metallic strip and showed that the stress caused by the difference in the thermal expansion coefficients of the materials were much greater than shrinkage stress. In order to properly design an adhesive joint, it is important to reduce the thermal expansion stresses of the adhesive material.

Thermal post-cure:

During the installation of the adhesive resin, the mother resin and the hardener blend by doing a cross-linking reaction which progresses at certain speed. The speed of cross-linking is directly proportional to the number of chemical groups that have not yet reacted.

The freezing time is the moment at which the reactive mixture between the mother resin and the hardener begins to set. Shortly after the freezing point, the mixture increases its volume, but generally it is far from complete hardening and there is only about half of the molecules that are cross-linked (Bardonnnet, 1992a). Once the freezing point is reached, the structure freezes because of the weak mobility of the chains preventing the continuation of the reaction.

Any subsequent increase in the temperature of the mixture leads to a mobility of the unreacted chains. This leads to the resumption of the progression of the reaction and consequently to the further densification of the three-dimensional network and the modification of the mechanical properties of the mixture. For the case of polymers formed at ambient temperature, this phenomenon occurs when a large number of molecules has not yet cross-linked after freezing.

In Fig. 20 (Rekik Medhioub, 2009) has brought together the different stages leading to the formation of an epoxide polymer:

- Stage A: reaction between the mother resin and the hardener has not yet begun (low viscosity).
- Stage B: beginning of the polymerization between the components of the mixture (mother resin + hardener).
- Stage C: cross-linking of the adhesive resin (insolubility and total infusibility).

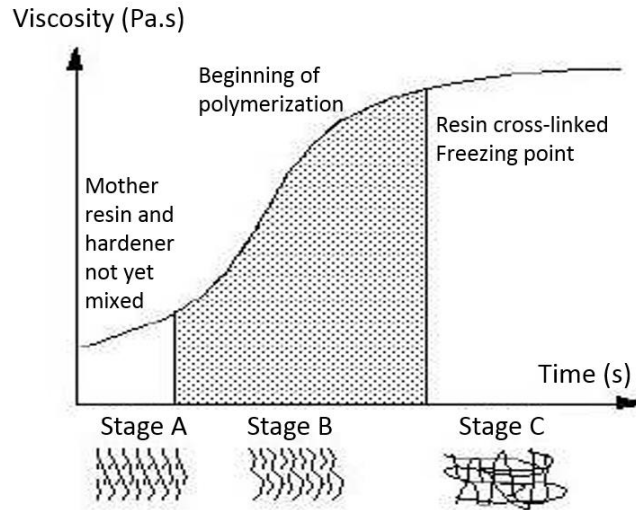


Fig. 20: Evolution of viscosity with time showing the different stages leading to the formation of an epoxide polymer (Rekik Medhioub, 1992)

Epoxy adhesive resins:

There are many types of epoxy adhesive resins in the market. The most used is diglycidylether of bisphenol A (DGEBA). It accounts for 95% of the world's tonnage (Barrère et Dal Maso, 1997). Its structure is presented in Fig. 21.

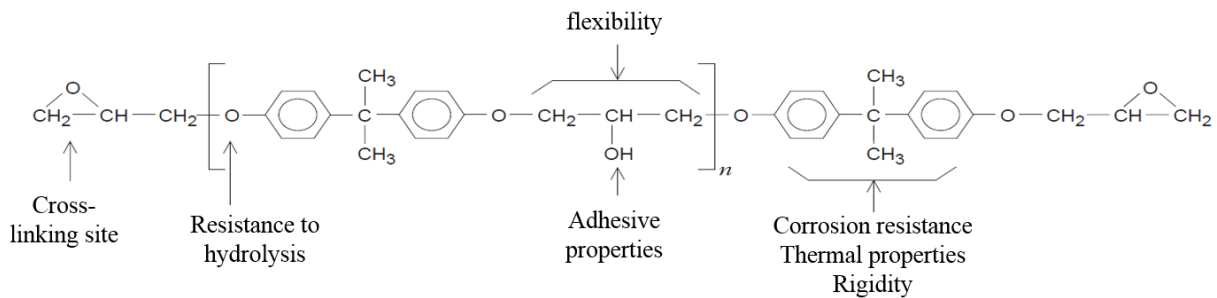


Fig. 21: Structural formula of diglycidylether of bisphenol A (DGEBA)

Where: n is the degree of polymerization.

Diglycidylether contains a certain quantity of diphenylpropane (bisphenol A) which reacts with epichlorohydrin in the presence of sodium hydroxide. The degree of polymerization n depends on the molar ratio between epichlorohydrin and bisphenol A. The viscosity of the product depends on the degree of polymerization. For a value of n between 0 and 1, the polymer is liquid. Beyond this, the polymer becomes solid at ambient temperature (Dessertenne, 2012).

Epoxy adhesive resins are heavily used in the field of civil engineering because of their following advantages:

- Good fatigue resistance.
- Long service life.
- Good adherence and high shear modulus.
- Good thermal insulation.
- Good water and chemical agent resistance.

But they present certain disadvantages:

- Low fire resistance (creep, loss of adhesion).
- Toxicity.
- Low adaptability to installation at low temperatures and high humidity.

- Sensitivity to ultraviolet radiation.
- High influence of the installation quality, forcing certain countries to impose a qualification for installers.

Glass transition:

It is the passage of the polymer, during heating, from the glass state to the liquid melted state (rubbery) (*Teysède et Lacabanne, 1997*). During the passage of polymers by the glass transition temperature (T_g), they are subjected to a drop of mechanical properties (Young and Coulomb modulus). This consists of a thermodynamic transition of the second endothermic order requiring energy supply.

According to (*Tamulevich et Moore, 1980*), the postcure (after hardening of the adhesive resin) influences the glass transition. Glass transition depends therefore of the advancement degree of the crosslinking reaction between the mother resin and the hardener.

For rigorous measurements, it is necessary to specify not only the determination method of T_g , but also the temperature sweep degree and, more generally the thermomechanical history of the sample (*Rekik Medhioub, 2009*). There are three main methods for the determination of T_g :

1. Differential scanning calorimetry (DSC):

It depends in the energetic effect. T_g is determined by the variation of the specific heat of the polymer during heating compared to a reference sample.

Thermosetting resins form a solid material under heat action. This crosslinking procedure is exothermic. Therefore, DSC is a well adapted method for the study of the polymerization-crosslinking parameters of this type of adhesive resins. DSC allows to study not only the temperatures and heats of the reactions, but also the kinetics of these reactions because the heat flux is proportional to the reaction speed (*Gernet et Légendre, 2010*).

2. Thermomechanical analysis (TMA):

It depends on a physical effect. T_g is determined by the change in the expansion coefficient during heating. Indeed, the thermal expansion coefficient increases significantly at the glass transition temperature T_g .

Likewise, the physical aging can be characterized by these techniques (*Struik, 1978*). It is also possible to determine Young's modulus in tension as a function of temperature by knowing the deformation component linked to the expansion (*Teysède et Lacabanne, 1997*). This type of measurements is found in mechanical tests on materials (*François, 1984*) et (*Pabiot, 1991*).

3. Dynamic mechanical thermal analysis (DMTA):

It consists of recording the response of the tested material under a dynamic mechanical load of sinusoidal form as a function of time and temperature. The complex variations of Young's modulus and damping factor allow to determine the transitions of the polymer as a function of temperature (for example: glass transition) (*Isselmou Mohamed Habib, 2013*). DMTA is heavily used for the aging characterization of polymer materials (*Aref-Azar et al., 1996*), (*Berthumeyrie et al., 2013*) and (*Larché et al., 2011*).

(*Lahouar et al., 2018*) performed tests at the material scale on bonded anchors. They focused on the influence of temperature on the studied adhesive resins. Stabilised temperature and constant load tests were performed (procedure detailed in chapter 3 section 4). They noticed that when the glass transition temperature (T_g) is reached, a significant decrease in the stiffness of the anchor occurs, along with a change in the failure mode. It was demonstrated that:

- When $T_{\text{resin}} < T_g$: failure of bonded anchors occurs at the steel/adhesive resin interface.
- When $T_{\text{resin}} \approx T_g$: a mixed failure mode is observed (beginning of the glass transition).
- When $T_{\text{resin}} > T_g$: failure of bonded anchors occurs at the adhesive resin/concrete interface.

Water resistance:

Water is likely to diffuse inside a polymer adhesive resin. Exposure to water causes a loss of bond adherence and can cause corrosion of the metallic rod (*Nguyen et al., 1996*). The physical properties of polymers depend on

several factors such as their absorption capacity of little molecules (for example: water). Absorbed water molecules change freezing and glass transition temperatures (*Wu et al., 2003*).

According to (*Apicella et al., 1985*) polymer adhesive resins absorb moisture from surrounding environment. According to these authors, there are three sorption modes:

- Mass dissolution of water in the polymer network.
- Absorption of moisture at the surface of vacuoles (central cells), because of an excess of free volume in the glassy structure.
- Formation of bonds between the hydrophilic groups of the polymer and water.

The plastification of the adhesive resin by water occurs, according to (*Verdu, 2000*), when water molecules integrate the macromolecular network and break the secondary bonds between polar groups carried by neighbouring chains to establish preferential links with water (Fig. 22).

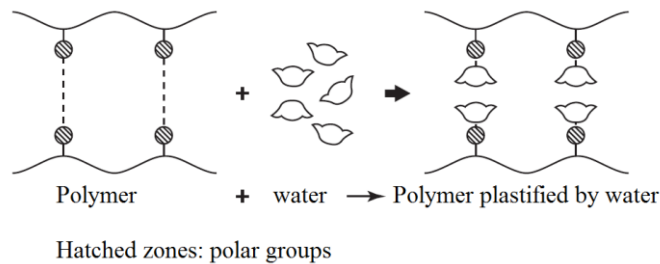


Fig. 22: Plastification effect in a macromolecule of a polymer resin due to water exposure (*Verdu, 2000*)

One of the consequences of the plastification of the adhesive resin is the destruction of the mechanical cohesion of the network and the increase of molecular mobility. A characteristic study was conducted by (*Verdu, 2000*) on the same polymer adhesive resin presented in Fig. 22. After conditioning of samples at different humidities, tension tests were conducted.

Flow stress and modulus of elasticity decrease significantly with increasing humidity (Fig. 23).

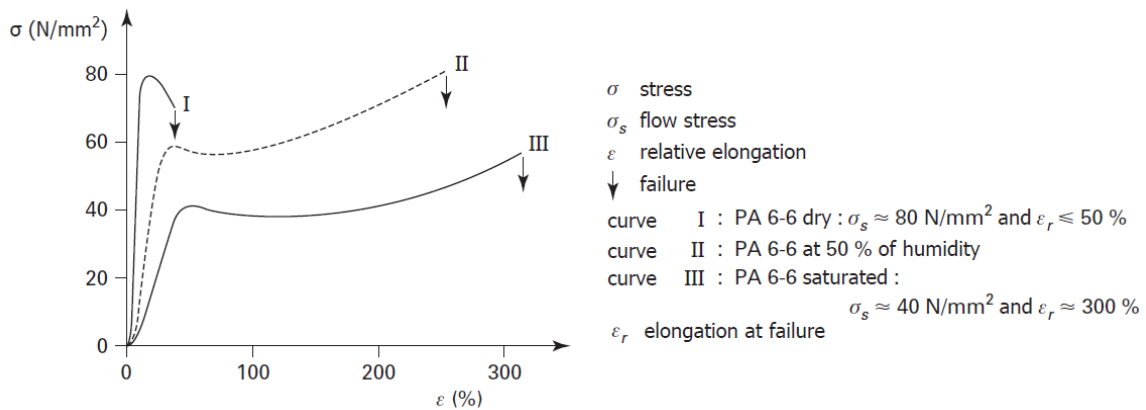


Fig. 23: Tension curves of a 6-6 polyamide for different water saturation states (*Verdu, 2000*)

Creep behavior:

Creep is the irreversible long-term deformation of a material subjected to a constant stress below its yield strength for a sufficient time. The creep of the adhesive resin may occur, like in the case of the Boston Big Dig Tunnel (*National Transportation Safety Board, 2006*), the Sasago tunnel in Japan (*Umehara et al., 2014*) and the bridge barrier in Atlanta (*Canopy Failure Investigation, 2011*). The expertises carried out after these disasters have shown that the failure mechanism corresponds to a long-term slip of the bonded anchor.

(*Chin et al., 2010*) conducted a study on the creep behavior of two epoxy adhesive resins. They proposed an experimental method capable of predicting the long-term creep behavior in service conditions from short-term tests, by using the time-temperature superposition principle. Two adhesive materials were made by the same

manufacturer and had a similar chemical form. One of them contained accelerators to obtain a faster curing time. (Chin *et al.* 2010) conducted DSC tests (Differential Scanning Calorimetry), TGA (Thermogravimetric Analysis) and sorption moisture analysis. The time-temperature superposition principle is based on the hypothesis that for certain polymer materials, the mechanical behavior at high temperatures is the same at ambient temperature for long-term. This hypothesis allows to determine the long-term creep behavior by varying the temperature or the excitation frequency during a dynamic test, by applying a “shift factor” as proposed by (Hunston *et al.*, 1981).

(Lahouar, 2018) adopted this method for an experimental study on a polymer adhesive resin, by combining the portions of the curves, obtained from tests at different temperatures or different frequencies (Fig. 24). He highlighted the fact that the creep behavior of polymer adhesive resins can be the second most important factor for the determination of their behavior after the glass transition temperature T_g . He demonstrated the existence of a relationship between temperature and delayed displacement of polymer adhesive resins. Fig. 24 shows that creep increases non-linearly with temperature increase. This proves the importance and risk of the association of temperature and creep to the durability and the mechanical resistance of bonded anchors.

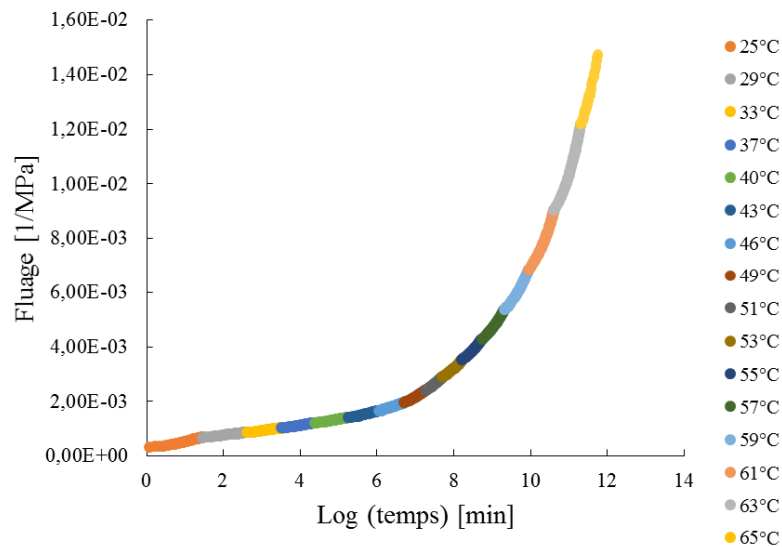


Fig. 24: Prediction of the creep behavior of a polymer adhesive resin with temperature increase (Lahouar, 2018)

Poisson’s coefficient increases with temperature (Theocaris, 1979) and (Pandini and Pegoretti, 2008). (Chin *et al.*, 2010) showed that a glass transition (T_g) below 60°C may occur for certain structural adhesive resins and consequently it is concluded that the governing material for the design of bonded anchors under fire is the adhesive resin.

4. Guidelines and standards

4.1. Assessment of anchors in concrete at ambient temperature

Generally, the requirements of the assessment of anchors in concrete at ambient temperature are described in Eurocode 2 – Part 4 (EN 1992-4, 2018).

Anchors can be loaded in tension, shear and combined tension and shear situations, or shear load by lever arm (Fig. 25).

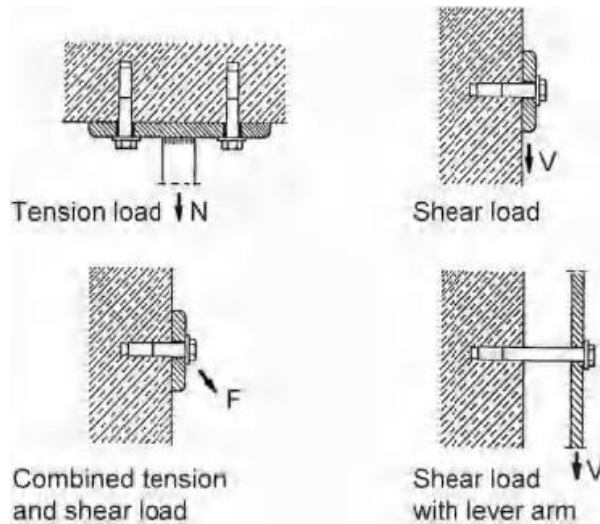


Fig. 25: Actions on anchors

For an anchor loaded in tension, four failure modes can be distinguished (Eligehausen, 2006) (NF EN 1992-4, 2018):

1. Concrete failure (characteristic cone failure or concrete splitting failure).
2. Bond failure (loss of adhesion).
3. Steel failure.
4. Mixed failure, only for bonded anchors (partial concrete cone + loss of adhesion at the concrete/ adhesive resin interface + potential bond failure by tension at the end of the embedment depth)

These failure modes are presented in Fig. 26.

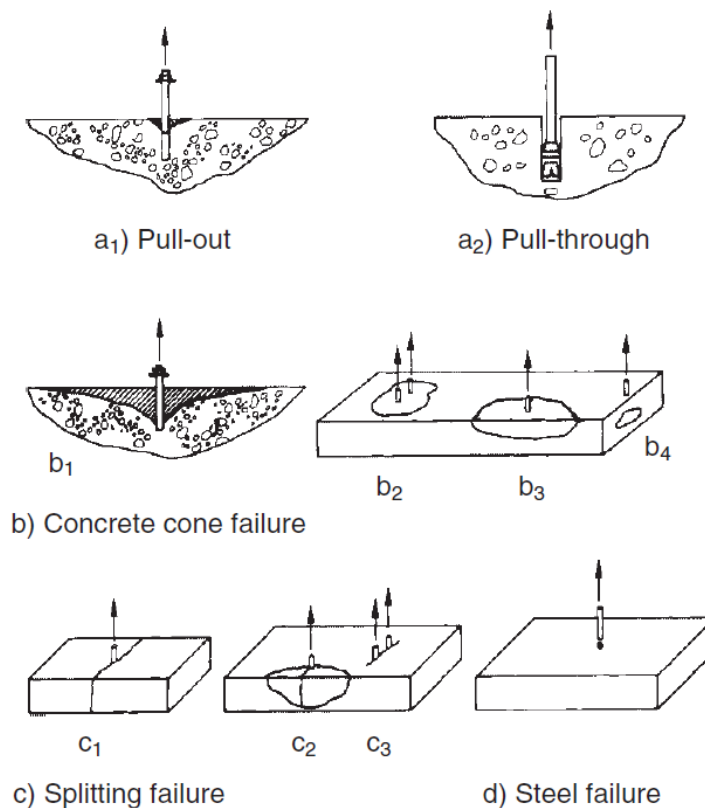


Fig. 26: Failure modes associated to an anchor loaded in tension (Eligehausen et al., 2006)

Pull-out or pull-through failure of the anchor consists of the anchor being pulled out of the hole, this failure can also cause the damage of the surrounding concrete (Fig. 26a₁,a₂). This failure mode can occur for expansion anchors and plastic anchors when the expansion force is insufficient to hold the anchor at the installed embedment depth for the load corresponding to concrete cone failure. This failure mode can also occur for screws, studs and threaded rods if the resisting area is insufficient, and also for bonded anchors.

In addition to the failure modes cited above, the following distinctions are observed for the case of bonded anchors: failure at the steel/ adhesive resin interface (Fig. 27a), failure at the adhesive resin/concrete interface (Fig. 27b) or mixed failure (Fig. 27c). In all of these cases, a concrete cone with a depth of $2d$ to $3d$ (d = diameter of the threaded rod) is formed around the adhesive layer and the failure by loss of adhesion of the adhesive resin occurs for the rest of the embedment depth.

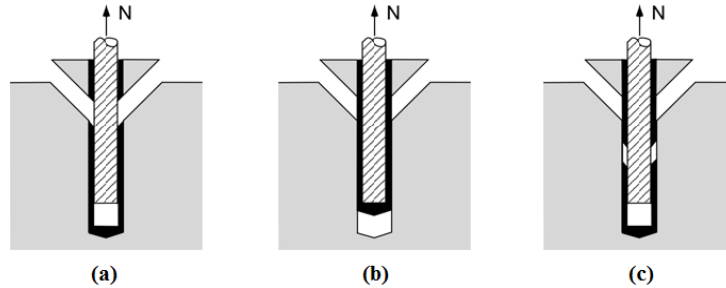


Fig. 27: Pull-out failure modes for bonded anchors (Cook et al. 1998)

Fig. 28 shows schematic load-displacement curves for non-prestressed bonded anchors loaded in tension exhibiting pull-out failure (Meszaros, 1999). The load-displacement behavior depends on the stiffness and adhesive properties of the adhesive resin. For good adhesive properties, bonded anchors present a good elastic behavior nearly up to failure (Fig. 28a). Post-peak behavior depends on the interface at which the failure occurs. If bond is lost at the concrete/ adhesive resin interface (Fig. 28b), the anchor rod and adhesive layer of resin are pulled out of the non-uniform surface of the drilled hole and frictional resistance is generated. If the frictional resistance is lower than the adhesion strength, then the resisted load shows steady decline with displacement increase (Fig. 28a). If the adhesion strength is lower than the frictional resistance between the adhesive resin and the surface of the hole, the ultimate load is reached at relatively large displacements. The ratio of adhesion resistance to ultimate load can be relatively high (Fig. 28b) or for low robust systems quite low (Fig. 28c). If bond failure occurs at the steel/ adhesive resin interface (Fig. 28c), the resistance will drop rapidly with displacement increase (Fig. 28d) due to the shearing of the adhesive resin projections into the threads of the rod at the small displacements followed by the pull-out of the anchor. After the shearing off of the adhesive resin between the threads, the surface of the adhesive resin is relatively smooth, and the frictional resistance tends to be small. The load-displacement behavior in Fig. 28 is clearly more favorable than that of Fig. 28d because it allows load redistribution.

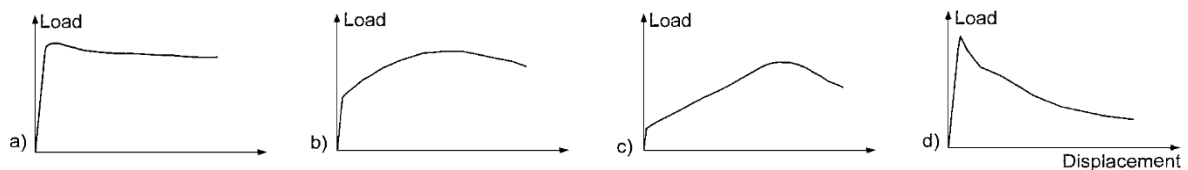


Fig. 28: Schematic load-displacement curves of single loaded bonded anchors for pull-out failure (Meszaros, 1999)

Concrete splitting failure occurs typically when the dimensions of the concrete element are limited (Fig. 26b₁), when the anchor is situated very close to an edge (Fig. 26b₂), or when several anchors are installed close from one to another (Fig. 26b₃).

Concrete cone failure is characterized by the splitting of a cone-shaped concrete chunk from the deepest part of the anchor (Fig. 26c₁). Individual concrete cones for a group of anchors can overlap (Fig. 26c₂). The cone may be truncated if the anchor is situated near the edge of the concrete element (Fig. 26c₃). Anchors situated very close to an edge which generate a high load-bearing capacity can cause a local splitting of the concrete element near the head of the anchor (blow-out). Unconfined tests with a minimal embedment depth ($4d$ to $5d$) can lead to concrete cone failure. If these tests are used to characterize the load-bearing capacity of the bonded anchor, the approach is

conservative (*EAD 330499-01-0601, 2019*). More precise results can be obtained if the embedment depth is chosen in a way to ensure a mixed failure mode (pull-out + concrete cone).

Anchors with a sufficient edge distance and embedment depth, loaded in shear exhibit steel failure, whereas a small conical spalling of concrete at the surface could occur before steel failure (Fig. 29a). If the anchor is loaded in shear toward a proximate free edge (Fig. 29b₁,b₂), or a corner (Fig. 29b₃), failure occurs by the development of a surface fracture in the concrete originating at the point of loading oriented to the free surface. This failure mode is similar to concrete mode under tension. For concrete elements with limited thickness (Fig. 29b₄) or limited width (Fig. 29b₅), splitting of concrete can be truncated.

Anchors with a relatively shallow embedment depth can reach concrete cone failure on the side of the anchor opposite to the direction of the applied shear load (pry-out) (Fig. 29c₁,c₂).

Mechanical expansion anchors loaded in shear can exhibit pull-out failure if the expansion force ensured by the anchor is insufficient to resist the tension forces induced by shear loading (Fig. 29d).

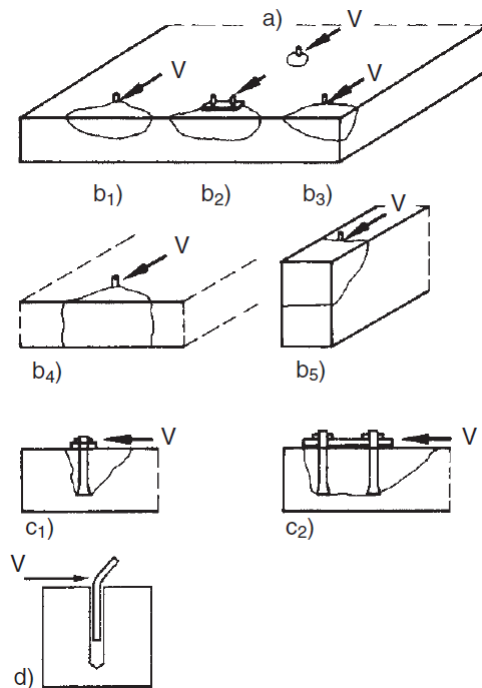


Fig. 29: Failure modes associated to an anchor loaded in shear (*Eligehausen et al., 2006*)

Reinforced concrete structures are generally subjected to cracks under service load due to the tensile stresses on the tension side caused by loads or by the restraint of the imposed deformations. Therefore, in general, the design of anchors should be based on the assumption that concrete is cracked (*Eligehausen, 2006*). Several studies showed that the behavior of mechanical anchors in uncracked concrete can be different compared to anchors in cracked concrete (*Cannon, 1981*), (*Eligehausen & Balogh, 1995*). The behavior difference can manifest by a change in rigidity, ultimate load-bearing capacity and the potential failure mode of the anchor (Fig. 30).

Post Installed Reinforcement bars (PIRs) are only influenced locally by flexural cracks perpendicular to the embedment depth causing an insignificant impact on the load-bearing behavior. Unlike PIRs, the load-bearing behavior of anchors is significantly influenced by cracks depending on the type and design of the anchor. Furthermore, very little information exists on the behavior of anchors in cracked concrete at high temperatures. The only available data lead to the development of the empirical criteria for the design of anchor in cracked concrete under fire in Eurocode 2 - Part 4. Most of the research done on the behavior of anchors in cracked concrete was carried at ambient temperature. Therefore, the general requirement for evaluating anchors in cracked concrete needs to be further investigated for the case of high temperatures (i.e. in case of fire exposure).

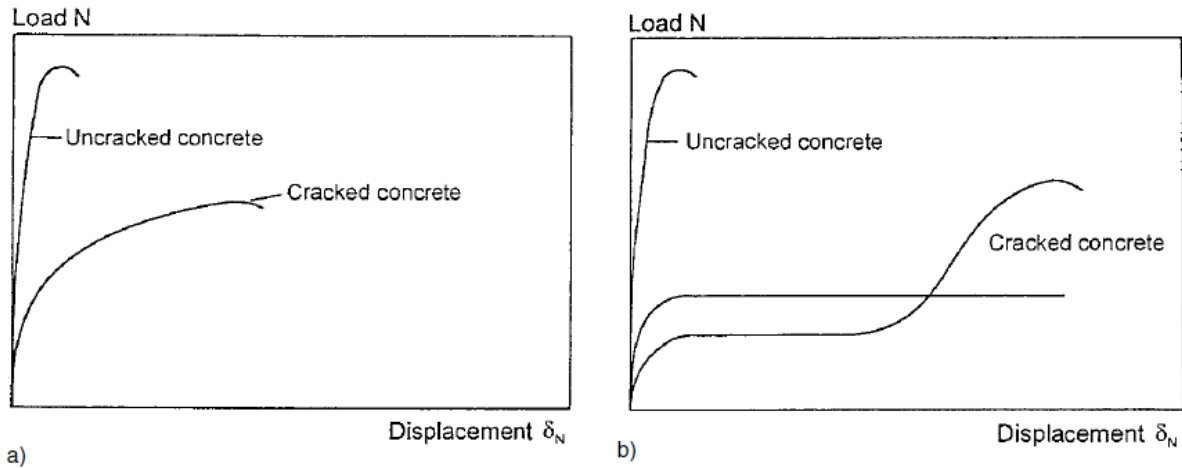


Fig. 30: Schematic load-displacement curves of mechanical anchors tested in tension in cracked and uncracked concrete (Rehm, Lehmann, 1982): a) anchors suitable for use in cracked concrete and b) Anchors not suitable for use in cracked concrete (inadequate or non-existing follow-up expansion)

A large number of anchors designed for use in uncracked concrete is not adapted for use in cracked concrete. The criteria for the determination of the influence of crack existence are: anchor type and design, anchor position inside the crack, load applied on the anchor and crack width.

Tests on several types of anchors under tension with static cracks (non-cyclic loading) showed a reduction in the load-bearing capacity up to 30% or more in relatively small crack widths ($w = 0.3 \text{ mm}$). Fig. 31 shows the ratios of the load-bearing capacity in cracked and uncracked concrete obtained by experimental tests, and the tendencies of the reduction due to crack existence for three typical anchor types.

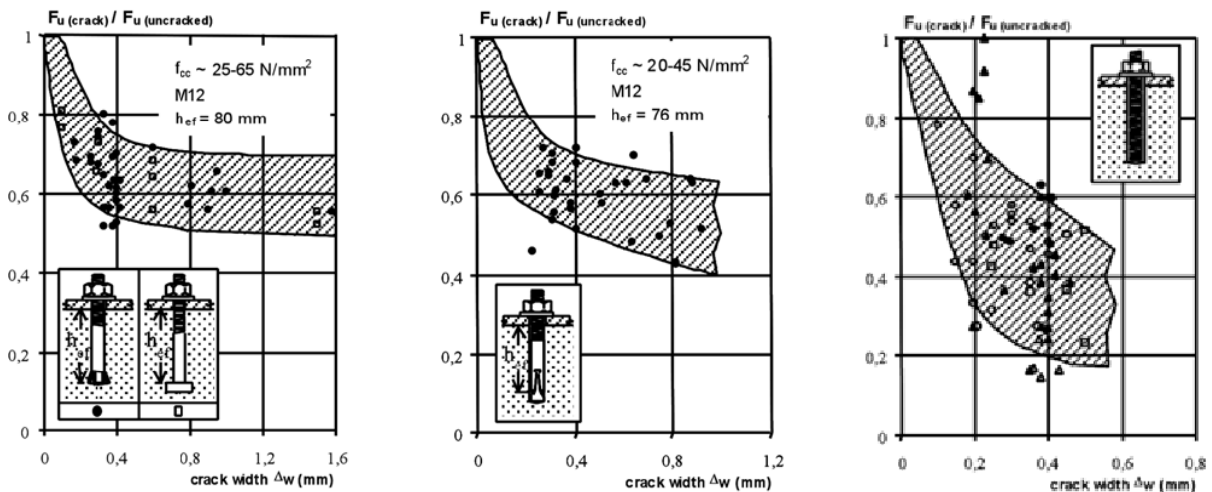


Fig. 31: Ultimate load-bearing capacity of anchors loaded in tension in cracked concrete: a) expansion anchors and threaded rods; b) Torque controlled expansion anchors; c) bonded anchors (Eligehausen & Balogh, 1995)

Fig. 32 compares load-displacement curves for bonded anchors in cracked and uncracked concrete. As with other anchor types, anchor stiffness is lower in cracked concrete. Inadequate hole cleaning may lead to further reductions in the ultimate tension capacity (Eligehausen, Mallée, Rehm, 1997).

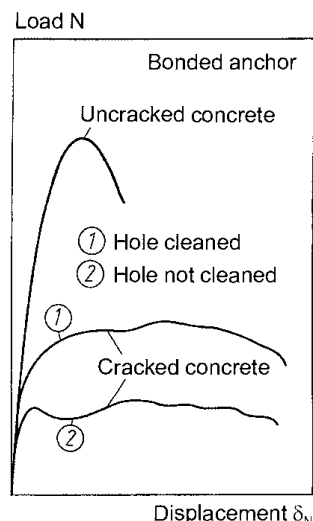


Fig. 32: Schematic load-displacement curves of bonded anchors loaded in tension in cracked and uncracked concrete (Eligehausen, Mallée, Rehm, 1997)

The assessment of the load-bearing capacity of bonded anchors in cracked and uncracked concrete without fire is described in the European Assessment document (EAD 330499-01-0601, 2019).

European Assessment Document for bonded anchors (EAD 330499-01-0601)

The EAD (European Assessment Document) 330499-01-0601 “Bonded fasteners for use in concrete” defines the rules for the technical assessment of bonded anchors in concrete without fire. It covers a variety of bonded anchors for fastening applications and describes the guidelines to be followed by the Technical Assessment Body (TAB) to control the assessed product from its manufacturing phase to its utilization in the structure. This EAD assesses the performance of bonded anchors for all failure modes indicated here-above, in uncracked concrete and cracked concrete with controlled crack width. In general, it covers concrete strength class from C20/25 (low strength concrete) to C50/60 (high strength concrete).

Technical assessment according to this EAD must respect certain criteria according to the associated failure mode and testing configuration: confined test setup for bond failure (characterization of bond strength), unconfined to favorize concrete failure...etc. In cracked concrete, a reduction coefficient is applied to determine the relationship between the resistance in uncracked and cracked concrete. However, this document does not cover the assessment of bonded anchors under fire.

4.2. Fire assessment of anchors in concrete

Until this day, tests on anchors in concrete under fire follow the guidelines of the Technical Report (EOTA TR 020, 2009) which is integrated today as annex in the European Assessment Document for mechanical anchors in concrete (EAD 330232-01-0601, 2019). The current state of the technical report is suitable for the evaluation of mechanical anchors (i.e. with mechanical interlock or expansion) but does not allow proper evaluation of bonded anchors under fire especially for the pull-out failure mode (loss of adhesion). Indeed, bonded anchors use adhesives that are significantly influenced by temperature increase. Therefore, the thermal influence of the current testing conditions on the load-bearing behavior of bonded anchors under fire should be assessed, and more precise provisions and guidelines should be provided before integrating them in the European Assessment Document for bonded fasteners in concrete (EAD 330499-01-0601, 2019). Meanwhile, the technical report gives two different methods for the determination of the load-bearing capacity under fire:

Simplified design method in cracked and uncracked concrete:

This method deals with failure modes under tension (steel failure, bond failure and concrete failure in cracked and uncracked concrete), under shear (steel and bond failure modes) and combined tension and shear loading. The duration of the fire resistance is calculated as a function of the reference values at ambient temperature and no fire tests are required.

Steel failure values were determined by conducting a large number of tests on steel mechanical anchors. Table 3 contains the values for anchors made of carbon steel according to (*NF EN 10025-1, 2005*). Table 4 contains the values for anchors made of stainless steel of at least grade A4, according to (*NF EN ISO 3506-1, 2010*).

Anchor diameter [mm]	Embedment depth of the anchor [mm]	Characteristic tension strength of an unprotected anchor made of C-steel in case of fire exposure in the time up to:			
		$\sigma_{Rk,s,fi}$ [N/mm ²]			
		30 min	60 min	90 min	120 min
$\phi 6 / M6$	≥ 30	10	9	7	5
$\phi 8 / M8$	≥ 30	10	9	7	5
$\phi 10 / M10$	≥ 40	15	13	10	8
$\phi 12 / M12$ and greater	≥ 50	20	15	13	10

Table 3: Characteristic tension strength of an anchor made of carbon steel under fire exposure

Anchor diameter [mm]	Embedment depth of the anchor [mm]	Characteristic tension strength of an unprotected anchor made of stainless steel in case of fire exposure in the time up to:			
		$\sigma_{Rk,s,fi}$ [N/mm ²]			
		30 min	60 min	90 min	120 min
$\phi 6 / M6$	≥ 30	10	9	7	5
$\phi 8 / M8$	≥ 30	20	16	12	10
$\phi 10 / M10$	≥ 40	25	20	16	14
$\phi 12 / M12$ and greater	≥ 50	30	25	20	16

Table 4: Characteristic tension strength of an anchor made of stainless steel under fire exposure

For special anchors such as bonded anchors and bonded undercut anchors, the determination of fire resistance with the simplified method is not possible. Therefore, the second method has to be applied. For these anchors (principle shown in Fig. 33), the resistance of the anchor is obtained by the “friction force” and the adhesion of the bond. Likewise, the resistance of bonded anchors is highly product dependent and changes from one product to another depending on the used adhesive, type of steel and concrete strength class. These parameters change differently with temperature increase. Therefore, Eurocode 2 – Part 4 (*NF EN 1992-4, 2018*) states clearly that the fire resistance of these products should be determined experimentally from fire tests.

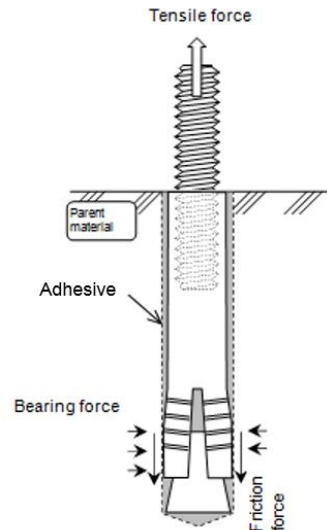


Fig. 33: Principle of a bonded undercut anchor

The experimental method:

There are many existing methods today for the determination of the load-bearing capacity of bonded anchors under fire. Some of these methods use mixed methods (fire tests + numerical simulations). This paragraph only describes the pure experimental method detailed in (*EOTA TR 020, 2009*). The anchor is tested experimentally under fire. Then, the values of the duration of fire resistance for the tested failure modes and/or loading directions can be taken into account in the homologation. A carbon-steel fixture has to be installed according to the dimensions of the guide as a function of the load category. The load must be transferred to the anchor similarly to Fig. 34.

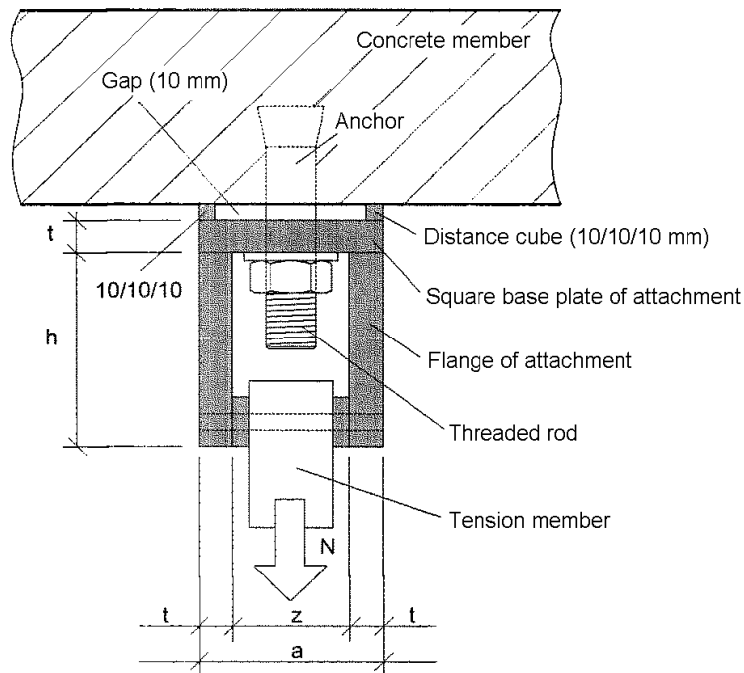


Fig. 34: Test setup for the determination of failure under tension according to (*EOTA TR 020, 2009*)

Table 5 presents the details of the metallic fixture (adapter) transferring the applied load to the anchor according to (*EOTA TR 020, 2009*).

Type of adapter	Load categories	Length of the square base plate	Flange height/width	Profile thickness	Distance between the flanges
	$N_{Rk,s,fi}$ [kN]	a [mm]	h/b [mm]	t [mm]	z [mm]
I	$> 1 \leq 3$	90	100/90	15	60
	$> 3 \leq 5$	90	100/90	15	60
II	$> 5 \leq 7$	110	120/110	20	70
	$> 7 \leq 9$	110	120/110	20	70
III	$> 9 \leq 11$	120	120/120	25	70
	$> 11 \leq 13$	120	120/120	25	70

Table 5: Dimensions of the load-transfer fixture for fire tests on anchors according to (EOTA TR 020, 2009)

The lower side of the test setup (anchor + fixture + concrete element) are then exposed to the combustion curve of the fire depending on the fire type. Usually, the (ISO 834-1, 1999) fire time-temperature curve is adopted. The results of fire tests are a resisting duration for a constant applied load. Fire tests must respect the guidelines in (NF EN 1363-1, 2020). More details are provided in (EOTA TR 020, 2009).

In order to have a good representation of the fire resistance vs. fire exposure time relationship, five tests must be conducted for the smallest and medium diameter of the tested anchors. At least four of these tests have to report a fire resistance duration above 60 min. Then, the applied loads on anchors are converted to steel stress values σ_s and plotted as a function of the corresponding failure time t_u . The results are then described by the following relationship [Eq. 3]:

$$\sigma_{s1} = c_1 + c_2/t_u \dots \text{ [Eq. 3]}$$

The tendency curve must be shifted with a factor c_3 (lower than 1) at the lowest point of the experimental results. By replacing time in the equation of the obtained tendency curve, the fire resistance values are obtained for fire exposure times of 60, 90 and 120 min. On a secant of this curve passing by the values at 60 and 90 min, the fire resistance value for 30 min is obtained. Fig. 35 shows an example of the procedure.

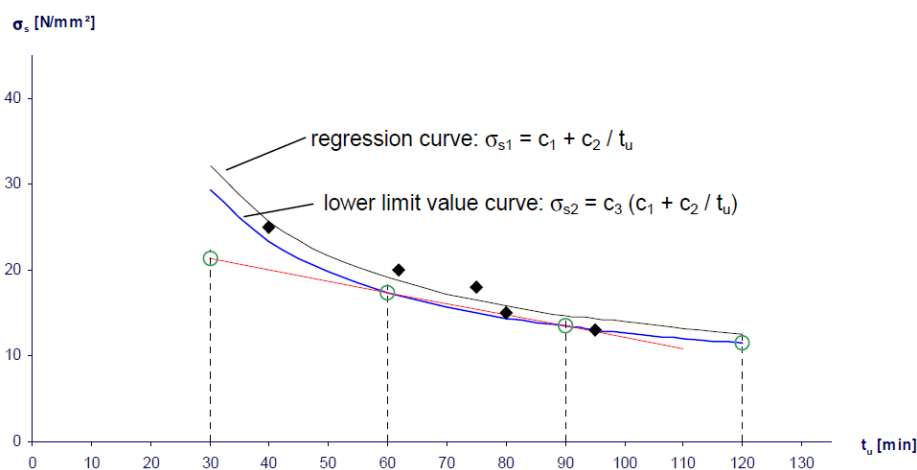


Fig. 35: Determination of the characteristic steel stress according to (EOTA TR 020, 2009)

4.3. Fire resistance tests according to NF EN 1363-1

The conduction of fire resistance tests in Europe is governed by the standard (NF EN 1363-1, 2020). Part 1 of this standard describes the general requirements, especially the heating curve. In general, the temperature of the furnace is regulated as a function of the time-temperature curve of the ISO 834 fire.

The temperature of the furnace must be measured and controlled by at least one plate thermometer by burner. The plate thermometers must be in accordance with the structure illustrated in Fig. 36.

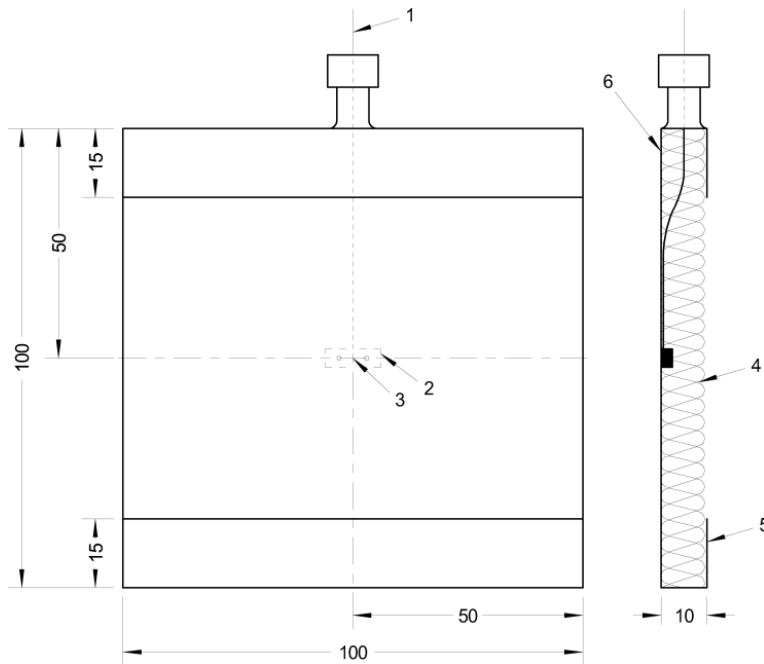


Fig. 36: Illustration of a plate thermometer in front of a burner to control the furnace (ISO 834-1, 1999)

Where: 1) sheathed thermocouple with insulated hot junction, 2) spots welded or screwed steel strip, 3) hot junction of thermocouple, 4) insulation material, 5) nickel alloy strip (0.7 ± 0.1) mm thick, 6) face A. The dimensions of Fig. 36 are in mm.

The internal pressure inside the furnace is also controlled during the fire test. Therefore, we can suppose a pressure gradient of 8.5 kPa by meter of height of the furnace.

4.4. European Assessment document for post-installed rebars (EAD 330087-00-0601)

The EAD n° 330087-00-0601 “Systems for post-installed rebar connections with mortar” handles the assessment of post-installed rebars at ambient temperature and at high temperatures. Post-installed rebars (PIRs) are not directly exposed to fire in fire situations. These elements are subjected to heat via the concrete element (if no spalling occurs). In order to qualify a PIR for use in concrete, it must ensure a performance equal or greater than cast-in rebars.

The resistance of post-installed rebars decreases with temperature increase due to the degradation of the mechanical properties of the bond. This EAD gives a reduction factor of the bond strength as a function of temperature. This reduction is obtained from pull-out tests on PIRs at high temperatures. This guide describes tests on PIRs installed in cylindrical concrete specimens heated on the lateral side. The test setup is illustrated in Fig. 37.

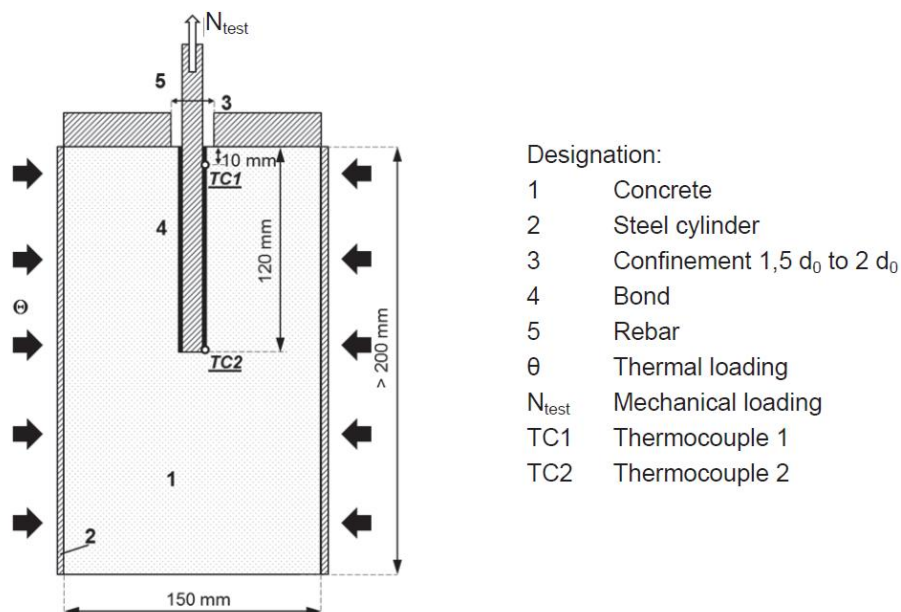


Fig. 37: Test setup of PIRs at high temperature according to (EAD 330087-00-0601)

Where: 1) concrete, 2) steel cylinder, 3) confinement from $1.5d_0$ to $2d_0$, 4) bond, 5) rebar, θ thermal loading, N mechanical loading, TC1 thermocouple 1 at 10 mm from the head of the anchor, TC2 thermocouple 2 at the end of the anchor.

In this test, a PIR consisting of an adhesive resin and a steel rebar, is installed in the middle of the cylinder (according to the manufacturer's instructions). Two thermocouples are placed near the head and at the end of the anchor. The thermocouple near the head is placed at 10 mm from the confined surface (from the exterior of the cylinder). The second thermocouple is placed at the deepest part of the embedment depth of the anchor. A constant tensile load N is applied. A steel confinement plate is placed at the extended part of the anchor (outside of the cylinder), with a hole in the middle slightly larger than the diameter of the rebar (hole diameter from $1.5d_0$ to $2d_0$, with d_0 the diameter of the hole of the anchor). The thermal loading θ is applied on the external lateral sides of the cylinder at a minimum heating rate of $5^\circ\text{C}/\text{min}$.

The temperature inside the embedded part of the anchor at the moment of failure is determined by a weighted average between the measures of the two thermocouples. The weighted average is calculated at $1/3$ of the highest temperature and $2/3$ of the lowest temperature between TC1 and TC2. A maximum temperature difference between TC1 and TC2 of 10°C is accepted up to 50°C . This criterion is not mandatory above 50°C due to the phenomenon of water vaporization at the outer layers of the concrete specimen which unsettles temperature measurement.

A minimum of 20 tests with different load levels has to be carried out. The average temperature and bond strength (corresponding to the applied constant load) at failure are plotted. In addition, the following rules must be respected:

1. A maximum interval of 1 N/mm^2 between two neighbouring data points on the f_{bm} (N/mm^2) axis.
2. A maximum interval of 50°C between two neighbouring data points on the temperature axis.
3. A maximum test duration of 3 hours.

Furthermore, three tests must be conducted for a bond stress of 0.5 N/mm^2 . The diagram below (Fig. 38) shows an example of a series of tests results and the associated tendency curve. According to the tendency curve, a reduction factor is then deducted as a function of temperature (Fig. 39).

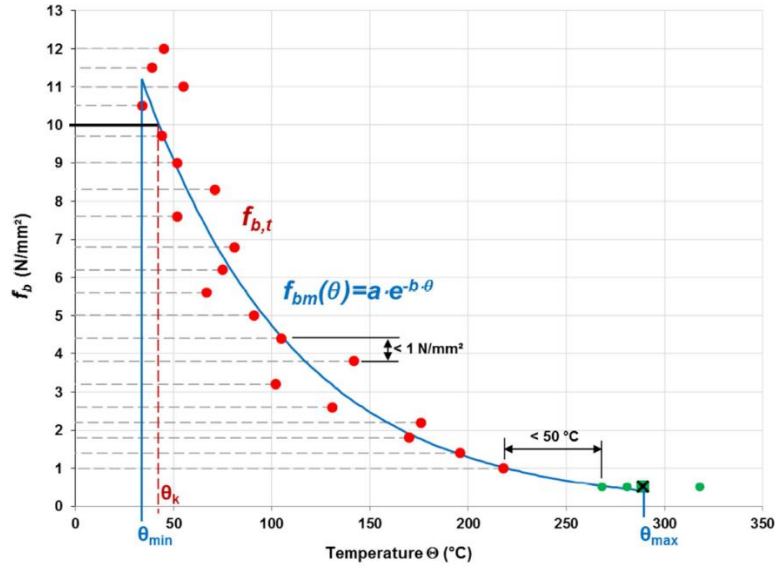


Fig. 38: Example for the determination of bond strength f_{bm} as a function of temperature θ

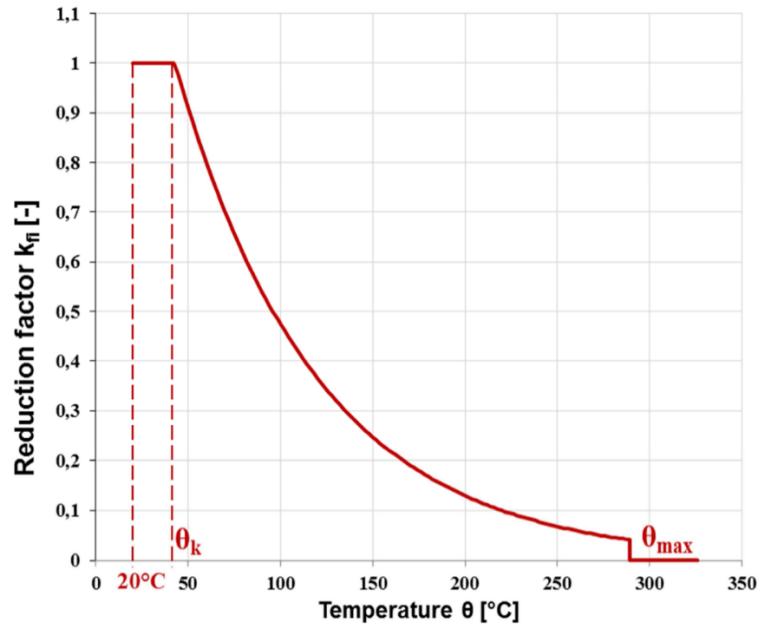


Fig. 39: Reduction factor $k_{fi}(\theta)$ for concrete strength class C20/25 for good bond conditions

The reduction factor k_{fi} must be determined from the following [Eq. 4,5]:

$$k_{fi}(\theta) = \frac{f_{bm}(\theta)}{f_{bm,rqd,d}} \leq 1 \quad \text{for} \quad 21 \text{ °C} \leq \theta \leq \theta_{max} \quad \dots \text{ [Eq. 4]}$$

$$k_{fi}(\theta) = 0 \quad \text{for} \quad \theta > \theta_{max} \quad \dots \text{ [Eq. 5]}$$

No extrapolation of test temperature is authorised. For temperatures higher than the highest measured temperature in the tests (θ_{max}), the reduction factor k_{fi} is zero.

In the research of (Pinoteau, 2013), different heating types (gas furnace and electrical heating) and different heating rates were tested and compared. The conclusion was that electrical heating using a constant mechanical load gives the most consistent results (repeatable with more controllable testing conditions from one test to another). Therefore, it was authorized to use electrical heating for the characterization of bond strength at high temperatures.

It should be noted that in the framework of this EAD, CSTB has provided experimental data showing that test results are independent from rebar diameter and rebar geometry (i.e. as well as from heating rates $> 5^\circ\text{C}/\text{min}$). This work was done on several adhesives to also eliminate the effect of different types of adhesive resins. Hence, these tests can serve for design of all PIR geometries.

5. Design models for bonded anchors under fire

5.1. Pinoteau's Resistance Integration Method

This method was initially developed by (Pinoteau, 2013) at CSTB for the design of post-installed reinforcement (PIR) under fire conditions. For simplicity purposes, this method does not account for the strain distribution (described by the term “shear-lag”). Its principle is the same as its name; the pull-out resistance of the anchor is designed by integrating the resistances along the embedment depth. The design method takes into account the thermal gradient along the embedment depth of the anchor to modify the bond strength. This method is analogous to the design method of piles embedded in different soil layers (DTU 13.2, 1992), where the resistance is calculated by the sum of the shear stresses taken by the different geological layers in which the pile is embedded.

The pull-out capacity of the anchor under fire conditions is then calculated based on the resistance profiles along the embedment depth of the anchor. In order to determine the resistance profile, two entry data are required:

1. The thermal distribution along the embedment depth of the anchor at any time of exposure to fire conditions: this can be determined by thermal calculations using numerical methods.
2. The relationship between the temperature and the bond strength: determined by pull-out tests at high temperature (see §4.4).

By knowing the thermal distribution along the anchor at any time of exposure to fire conditions, it is then possible to convert the temperature profiles to resistance profiles. This is done by dividing the anchor into relatively little segments (allowing to assume uniform temperature along the segment). Then, the temperature dependant bond strength associated to each segment of the anchor (using the bond strength vs. temperature relationship obtained from §4.4), allows to convert the temperatures to resistances. (Pinoteau, 2013) illustrated in Fig. 40 how the resistance at a certain depth x_i is determined at a time t_i from the thermal distribution.

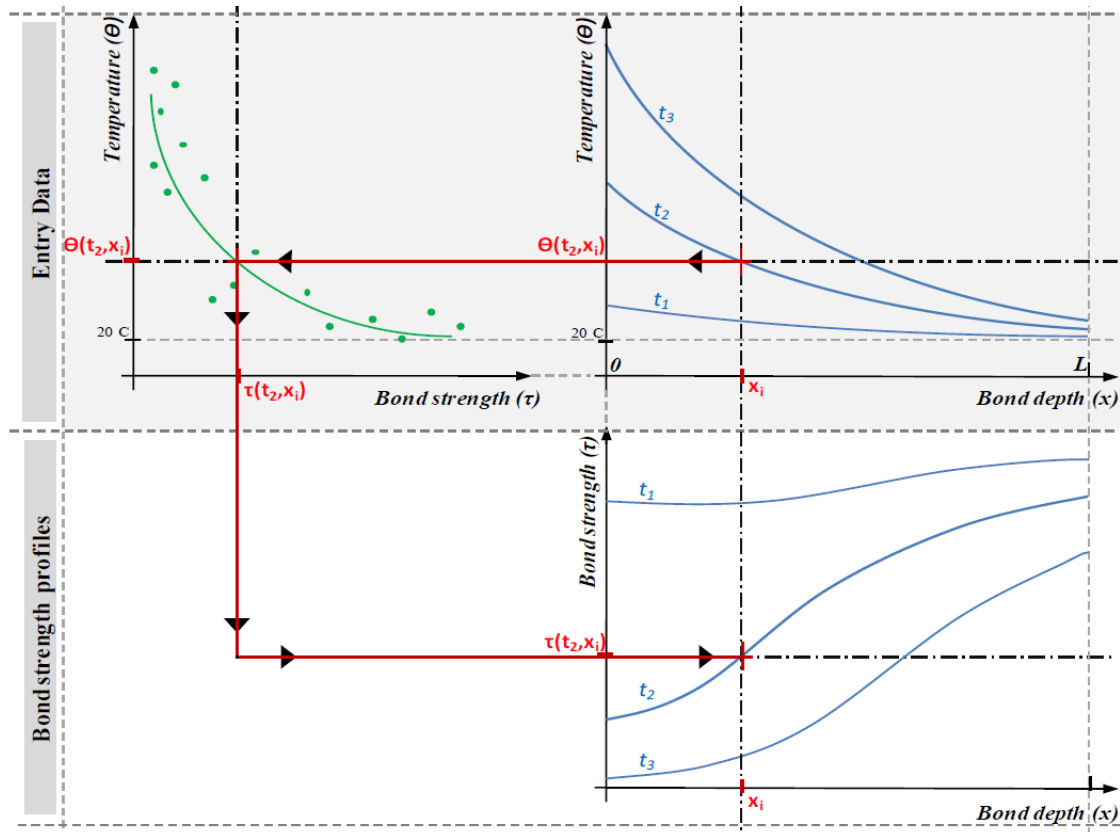


Fig. 40: Schematic representation of Pinoteau's Resistance Integration Method

5.2. Lahouar's non-linear shear-lag model

(Lahouar, 2017) developed a model capable of describing the distribution of bond stresses along the embedment depth of bonded anchors at high temperature, called the non-linear shear-lag model. The model was based on the work of Volkersen (1938) applicable to the adherence of reinforcement or threaded rods embedded in a bearing material (concrete, timber, mortar). The calculation of the stress distribution can be conducted based on either the properties of the material components of the anchor (general adhesion models) or based on the overall properties of the anchor (bond strength models).

Two methods can be considered to take into account the influence of temperature increase on mechanical behavior of the bonded anchor. The first method comes from the family of general adhesion models and consists in injecting the variation of the shear modulus of the adhesive as a function of temperature in the constitutive equations of the model, passing by Hooke's law. The variation of the shear modulus of the adhesive can be obtained from Dynamic Mechanical Analysis (DMA) tests. However, the use of Hooke's law is only valid in the elastic phase. Consequently, the use of such a law implicates that the model is not capable of describing the behavior of bonded anchors beyond the elastic phase. Such a model does not allow to predict the failure of the anchor and therefore does not allow to describe the stress profiles at the moment of pull-out failure. This method was then excluded from the study.

The second method comes from the family of bond strength models and is based on solving equations describing the overall mechanical behavior of the anchor as a function of temperature. The overall behavior of the anchor is described based on the variation curves of the bond stress as a function of the slip of the anchor, obtained from pull-out tests at stabilized temperature (similar to the approach in §4.4, but with stabilization of the temperature along the anchor and increased displacements at the desired time/temperature of characterization), see (Lahouar, 2017). In order to facilitate the mathematical resolution of such curves, adhesion models are used.

(Lahouar et al., 2018) have investigated the validity of the shear-lag model by comparing the outcome of the method to a large-scale test on a cantilever wall-slab connection using adhesive post-installed rebars (Fig. 42). To further investigate the validity of the model, the Resistance Integration Method was introduced to the comparison. The final conclusion was that both methods were reliable for the prediction of the pull-out failure of the PIRs in wall-slab connection.

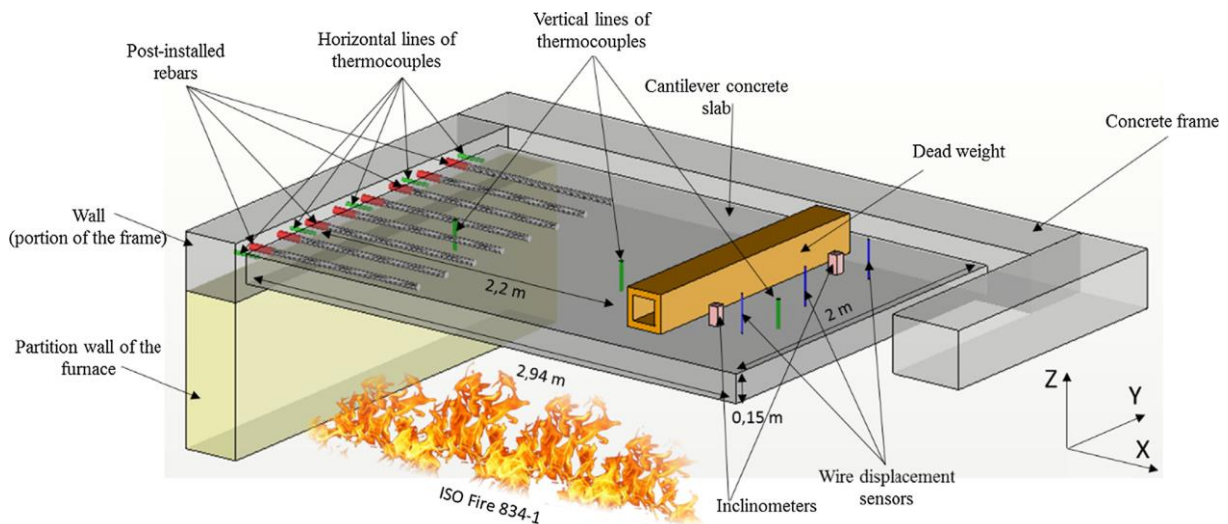


Fig. 42: Large-scale cantilever wall-slab adhesive PIR connection at Vulcain furnace at CSTB

The main differences between Lahouar's shear-lag (Lahouar et al., 2018) model and Pinoteau's Resistance Integration Method (Pinoteau et al., 2013) are the main entry data and the test method used to produce this entry data. In the Resistance Integration Method, the bond stress vs. temperature curve is obtained using a constant load-increased temperature method, whereas in the shear-lag model the load-displacement curves are obtained using a stabilized temperature-increased displacement method (see (Lahouar et al., 2017) for the comparison between both methods).

Conclusion of the literature study

The literature study highlights the different evaluation methods for assessing the load-bearing behavior of bonded anchors under fire: i) by studying the mechanical properties of the adhesive based on characterization tests of the used materials separately (concrete, steel and adhesive), and ii) by studying the behavior of the assembly of all materials (fixing system/i.e. the bonded anchor product) by fire tests.

Anchor elements in concrete are not regulated by NF or EN standards. Consequently, these non-regulated elements have to be qualified by a European Technical Assessment (ETA). There is a variety of European Assessment Documents (EADs) covering all types of anchors. These standards are completed by Technical Reports which specify their particular rules of application.

Fire evaluation of mechanical anchors (functioning by mechanical interlock or expansion in the embedment part) is governed by the European Assessment Document (*EAD 330232-01-0601, 2019*). However, the assessment of bonded anchors under fire is not covered by any EAD and is treated inadequately in the Technical Report (*EOTA TR 020, 2009*). The current situation does not allow the publication of ETAs for bonded anchors under fire. This research project aims to develop an evaluation and design method for bonded anchors in fire situations.

Based on the current state of the literature, the following scientific plan was adopted for the research conducted in this thesis to provide a better understanding of the behavior of bonded anchors under fire:

1. On the fire test method: The current testing method was developed almost two decades ago and adapted to the case of mechanical anchors. In order to understand the influence of the current method and if it needs to be reviewed/adapted for testing bonded anchors under fire, a thorough study must be conducted to investigate the influence of each parameter of the testing apparatus (Anchor size and embedment, loading system, concrete bearing element...).
2. On the design method: the current design method for PIRs consists a good basis and yields reasonably precise predictions of their behavior under fire. The method must be reviewed and adapted to the case of bonded anchors under fire. This method should be validated against experimental data (fire tests). Comparison of test results to other existing models for the design of bonded anchors under fire must also be conducted to verify their suitability. The scope of the design method should also allow design of different anchors sizes and embedments, therefore a wide check against fire test results should be carried out. In order for this method to be considered satisfactory, its representativeness of temperature profiles along the embedment depth of bonded anchors under fire, and the conservativeness of the design values should be compared to fire tests.
3. Finally, the case of bonded anchors in cracked concrete should be investigated at high temperature in terms of mechanical and thermal influence of crack existence. The general assumption of cracked concrete on the tension side of reinforced concrete elements imposes the evaluation of the load-bearing behavior of anchors in cracked concrete.

Chapter II: Experimental protocols for fire tests on bonded anchors

Chapter II resumes the paper entitled “**Influence of testing conditions on the behavior of bonded anchors under ISO 834 fire**” published on April 30, 2019 in the Journal of Engineering Structures. This paper focuses on the parameters influencing the behavior of bonded anchors during fire tests.

Objectives

This chapter focuses on the current experimental protocol for testing anchors under fire. EOTA Technical Report 020. The testing method allows suitable characterization of the fire resistance of mechanical anchors under sustained load. However, its suitability for the case of bonded anchors under fire has never been investigated. Indeed, many parameters of the tested configuration can influence the outcome of test results. The influence of any element acting as an obstacle to the external thermal exposure in the furnace (base plate of the loading adapter possibly protecting the anchor from direct exposure to fire) should be studied. Furthermore, the boundary conditions of the concrete bearing element might influence the thermal diffusion and must be accounted for.

This chapter has two main objectives:

1. Identify the test parameters influencing the thermal distribution along the anchors used in Pinoteau’s method (Resistance Integration Method):

The testing procedure was developed in principle for the assessment of mechanical anchors under fire (*EOTA TR 020, 2005*). The procedure in the context of TR 020 covers bonded anchors. However, its influence on bonded anchors is still uninvestigated, especially when certain testing configurations allow insulation of the fixture and anchor (i.e. tests in cracked concrete). However, the latter was only investigated in uncracked concrete.

2. Fill the gap in the literature on the influence of the configuration of fire tests on their outcome and their representativity of different configurations of an anchor in fire tests:

Three different configurations were identified: anchors directly exposed to fire, anchors with metallic fixtures and anchors with insulated fixtures. The first configuration can be encountered for cases similar to drop ceilings and hangers installed using long wires and anchors (Fig. 43). The second configuration is more common and can be encountered for anchors with steel plates like the configuration shown in EOTA TR 029 or Eurocode 2 – Part 4. The last configuration can be encountered when insulating materials are used as fire solutions or retardants (foam spray, fire resistant paint, rock wool...). Fig. 44 shows examples of thermal insulation of concrete. In the case where an anchor is installed in such configurations, it penetrates the insulating material to reach the fixed object. It is less common in buildings but in this study, it has proven to be an efficient solution to enhance the resistance of bonded anchors under fire by delaying the thermal degradation of the adhesive.



Fig. 43: Example of anchors that can be directly exposed to fire

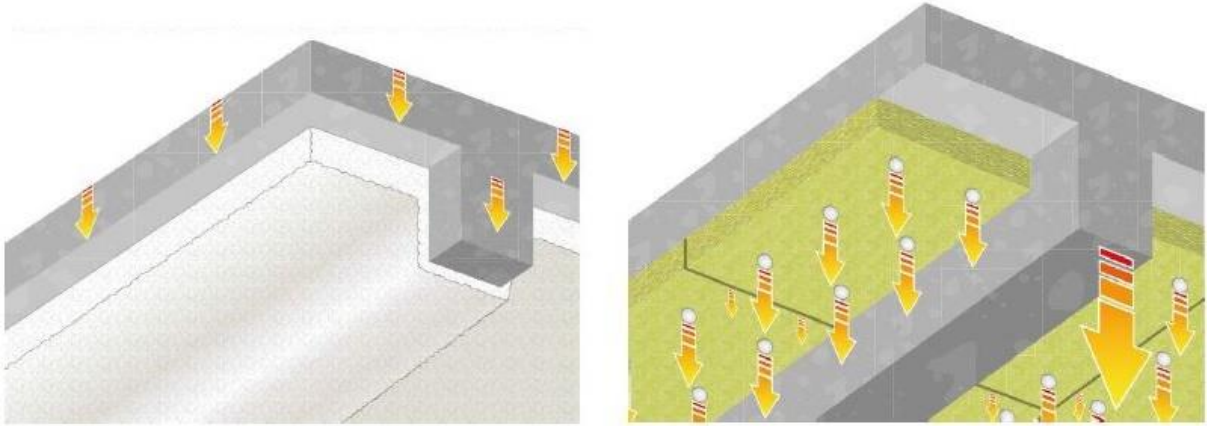


Fig. 44: Examples of thermal insulating solutions of concrete using spray-on coating (left) and rock wool panels (right)

Paper reference:

Al-Mansouri O, Mege R, Pinoteau N, Guillet T, Rémond S. Influence of testing conditions on thermal distribution and resulting load-bearing capacity of bonded anchors under fire. *Eng Struct J* 2019;192:190-204.

INFLUENCE OF TESTING CONDITIONS ON THERMAL DISTRIBUTION AND RESULTING LOAD-BEARING CAPACITY OF BONDED ANCHORS UNDER FIRE

Omar Al-Mansouri^{a,b}, Romain Mège^a, Nicolas Pinoteau^a, Thierry Guillet^a, Sébastien Rémond^b

^a Université Paris-Est, Centre Scientifique et Technique du Bâtiment (CSTB), 84 avenue Jean Jaurès, Champs-sur-Marne, 77447 Marne-la-Vallée Cedex 2, France

^b IMT Lille-Douai, Univ. Lille, EA 4515 – LGCgE, Département Génie Civil & Environnemental, F-59000 Lille, France.

Abstract

This paper aims to experimentally apply the existing method for evaluating the pull-out capacity of mechanical anchors under fire, to bonded anchors. Due to the absence of sufficient guidelines for evaluating bonded anchors directly exposed to fire, this experimental work studies the influence of the existing evaluation method on the prediction of the bond resistance and failure time. Different testing conditions and possible configurations for anchors in buildings are explored. The studied influencing parameters are: presence of fixtures, insulation of fixtures, thickness of the concrete bearing element, diameter of the anchor, concrete/steel temperature. The influence of each parameter on the predicted bond resistance and failure time, determined with a design method based on resistance integration is studied. Results show that parameters such as concrete element thickness and attaching metallic fixtures on anchors have a negligible influence on the predicted load-bearing capacity and failure time. However, adopting concrete temperature instead of anchor steel temperature in the resistance integration method, and putting insulation around fixtures may lead to a false estimation of the load-bearing capacity and failure time.

Keywords: bond, resin adhesive, bonded anchor, pull-out, fire tests, thermal distribution.

1. Introduction

One of the techniques used in the field of construction consists in anchoring steel elements in concrete by using adhesive resins for structural purposes. This technique allows for an easy and rapid installation of anchors in pre-existing structural elements. Installed anchors can be loaded in tension and/or in shear situations. Chemically bonded anchors can either ensure a junction between two structural elements such as post-installed rebars, in this case they are not directly exposed to fire due to concrete cover, or they can be directly exposed to fire such as chemically bonded threaded rods which are studied in the work presented in this paper. The advantages of these bonded anchors are their ease of implantation and their high load-bearing capacity at ambient temperature for deep embedment depths. However, when exposed to an accidental increase of temperature such as a fire, these structural elements show a rapid decrease in bond resistance.

Chemically bonded anchors can be bonded using polyester, vinylester and epoxy resins [1]. Research studies on the influence of temperature on the elastic modulus and flexural strength of polymer mortars using a thermostatic chamber have shown that the deformation and strength decrease of mortars are temperature dependent [2]. These studies have also shown that for a temperature range from room temperature up to 60°C, temperature effect is limited. However, for temperatures above 60°C, the decrease of mortar strength becomes drastic. Other research studies on adhesive-joints for a temperature range from -60°C up to 200°C have shown that stress/strain properties of polymer adhesives change a lot with temperature. Many studies have focused on the contrast of structural performance of connectors at ambient and elevated temperatures [3]. At high temperatures, the strain capability of these adhesives is high whereas their load capacity is low [4]. It was also shown that epoxy mortars are more sensitive to temperature than polyester mortars [5]. Moreover, mechanical properties of resins have been found to be highly susceptible to resin type and reinforcement employed as well as their quantities in the bearing structural element [2]. Glass transition is considered as the limiting factor of the state of a polymer and as an indicator of durability [6].

The design and assessment of the structural integrity of anchors under fire are defined in EOTA TR 020 [7]. This document defines the guidelines to perform fire tests on anchors in order to establish the bond resistance vs. exposure time relationship. This relationship gives the duration of fire-resistance for a certain applied load. However, pull-out assessment of bonded anchors under fire is not mentioned in this technical report [8]. Bonded anchors are only covered for steel failure, whereas steel resistance could be greater than bond resistance under fire.

Furthermore, no guideline exists for the design of bonded anchors under fire while a reliable method exists for the design of bonded rebars at high temperature.

The resistance integration method is based on the good knowledge of temperature profiles along the embedment depth of the anchor. The obtained temperature profiles are used then to establish the relationship between bond resistance and temperature by dividing the anchor into little segments. Each segment gives a certain resistance as a function of temperature using tests described in EAD 330087-00-0601 [9]. This finally allows plotting the relationship between bond resistance and exposure time. The resistance integration method presented promising results for pull-out failure under fire of chemically bonded post-installed rebars indirectly exposed to fire in the works of Pinoteau et al. [10] and Lahouar et al. [11], [12]. Furthermore, this method was also adopted in the numerical work of Lakhani and Hofmann [13] to determine the pull-out strength of bonded anchors directly exposed to fire.

Experimental parametric studies on different types of resins have shown that a maximum adhesive shear strength is reached for a resin thickness of 2 mm around the rod. Beyond this value the shear strength decreases until a certain value which remains constant. Moreover, increasing the embedment depth leads to an increase in the tension capacity of the anchor until a certain point beyond which the capacity remains constant [14].

Studies conducted by means of pull-out tests on adhesive joints [15] and on cast-in and post-installed rebars [16], have shown that the performances of chemical bonds and steel/concrete connections are comparable at ambient temperature. Studies have shown that the mechanical behavior is very similar with a slight advantage for bond resistance over cast-in rebars. However, at high temperature, such as in a building fire scenario, mechanical properties of adhesive resins assuring the connection between steel and concrete decrease rapidly due to temperature gradients and the increase of temperature along the member. This capacity reduction is faster in the case of bonded anchor systems using polymeric mortars, which can cause safety issues [13]. Thus, a good design of these bonded anchors under fire is needed to ensure the safety of lives and properties in burning buildings.

The European technical report EOTA TR 020 [7] covers the evaluation of mechanical anchors under fire for different failure modes. Possible failure mechanisms for bonded anchors under tensile loads are: a) concrete cone failure (manifested either as the characteristic cone failure or concrete splitting), b) steel failure, c) combined failure (concrete cone failure + bond failure at the adhesive-concrete interface + possibly tensile failure at the lower part of the adhesive) and d) bond failure of the anchor [17]. However, the European technical report EOTA TR 020 [7] covers the evaluation of bonded anchors under fire only for steel failure mode. Failure of bonded anchors may occur for pull-out more frequently than other failure modes during fire exposure due to the rapid degradation of mechanical properties of the resin. Thus, for safety reasons, it is the most decisive failure mode for bonded anchors under fire. Therefore, it is most interesting to evaluate bonded anchors by performing pull-out tests under fire to predict bond capacity in accidental situations such as a building under fire [18].

The required testing method to determine the fire-resistance of bonded anchors under fire and the obtained data must allow subsequent classification. This classification must be based on fire-resistance duration of tested bonded anchors. For this duration, the performances of tested anchors for a standard fire exposure scenario need to satisfy specific criteria. Thus, the method described in Part 1 of ISO 834 [19] was adopted in the work presented in this paper.

Studies on anchor rods and polyester base adhesives were conducted by Paterson [20] with 10 mm diameter rods and 75 mm effective depth. These studies have shown that pull-out failure of anchors exposed to standard fire is within 10-15 min of fire and the anchor temperature is between 330-440°C, for temperatures measured near the fixture (between bolts assuring the connection between the fixture and the rod). Paterson also alerted that under fire the adhesive anchor may reach failure earlier than the structural element in which it is installed and thus creating a major issue putting the life of occupants at risk.

The mechanical properties of adhesive resins at high temperature were investigated by Pinoteau [21]. His work highlighted that the glass transition temperatures (T_g) of the used epoxy products ranged between 80°C and 130°C and their tension capacity became lower than 2.5 MPa above 140°C. Furthermore, Lahouar et al. [22] showed that temperature profiles of bonded anchors vary depending on the adopted test procedure for evaluating their pull-out capacity at high temperature. Indeed, Lahouar et al. studied two approaches: by applying a constant tensile load to the anchor before heating and keeping it while progressively heating the specimen until failure (constant load tests), and by stabilizing bond temperature then applying pull-out (stabilized temperature test). Their theoretical

work allowed obtaining stress profiles for a thermal distribution along the embedment depth of the anchor using experimental entry data from the characterization of the anchor. Researchers have shown that the stress distribution along the embedment depth of adhesive anchors cannot be considered uniform for long embedment depths (larger than $7.5d$) [23-25].

In order to get a better understanding of the load-bearing behavior of chemical anchor systems under fire, the research project “Bonded anchors in case of fire” conducted by Reichert & Thiele [8] studied a combination of different types of fire tests and simulations. This project demonstrated that the existing guidelines of fire tests on bonded anchors are not clear till today. The Technical report TR 020 [7] contains no regulation for the evaluation of chemical anchor systems. Test execution and evaluation have to be determined thereby.

Similar testing conditions in EOTA TR 020 [7] were studied by Lakhani and Hofmann [13] by means of finite element numerical modeling. These conditions were applied on an anchor rod with 12 mm of diameter and 110 mm of embedment depth. The differences between the thermal distribution of the configuration where the anchor in itself was exposed to fire (acting as heat transfer path) and the configuration where the anchor was insulated (along with a fixture) were large. The pull-out capacity obtained from the thermal distribution highlighted a drastic reduction in case of unprotected anchors (without fixture and insulation). This large difference may lead to a pull-out failure for non-insulated anchors which would occur faster than the failure for insulated anchors.

The influence of existing testing conditions in EOTA TR 020 [7] for bonded anchors under fire on the precision of failure prediction using the resistance integration method is highlighted in the work presented in this paper. Pull-out fire tests were carried out on several possible configurations of bonded anchors in concrete beams submitted to elevated temperatures. Temperature profiles along the embedment depth of bonded anchor during fire were thus measured. These profiles are the thermal data needed for the resistance integration method in order to predict bond strength vs. exposure time of anchors. EAD 330087-00-0601 [9] allows predicting bond resistance vs. temperature relationship for bonded rebars at high temperature. In this paper, tested bonded anchors were threaded rods installed with an epoxy resin. Fasteners were installed according to the manufacturer’s indications (hole diameter, cleaning method, injection system...etc.). The rods were directly exposed to fire. In order to obtain a good prediction of the resistance of these bonded anchors under fire, the integration method requires a good knowledge of temperature profiles along the embedment depth of the anchor during fire. Knowing precisely the temperature profiles allows a precise prediction of failure time for an applied load. Due to the lack of European guidelines to perform pull-out fire tests for bonded anchors, the only applicable evaluation method for non-uniform temperature profiles along the embedment depth is the one for mechanical anchors cast-in concrete without resin [7].

Many parameters of testing conditions may influence temperature profiles. Hence, it is difficult to precisely calculate the bond resistance vs. fire exposure time relationship which affects the precision of the predicted failure time for a given load. The influence of the following parameters was explored by conducting fire tests under a standard ISO 834 fire:

- Anchor’s diameter and adopting concrete temperature instead of steel temperature in the resistance integration method.
- Thickness of the concrete beam in which the anchor was installed.
- Existence of a fixture on the anchor.
- Insulation of fixtures.

In this paper first, the existing testing method for the evaluation of pull-out strength of mechanical anchors is presented. Then, pull-out fire tests were conducted using the same method on chemically bonded anchors. Furthermore, a parametric study was conducted to determine the influence of each parameter on the predicted bond strength and failure time by conducting fire tests without pull-out.

2. Testing procedure and design method

This section describes the existing experimental method for the determination of pull-out resistance duration under fire for bonded anchors in uncracked concrete. It also recalls a design method (the resistance integration method), for the determination of bond strength of these anchors under fire. Furthermore, it presents a first application of this method on experimental data exploited from pull-out fire tests. This application is based on thermal profiles along the embedment depth of the anchor as entry data for the resistance integration method.

2.1. Existing procedure for assessing the structural integrity of anchors under fire

According to EOTA TR 020, part 4 [7], tests have to be carried out according to the general rules for structural fire design in [26]. For fire tests on bonded anchors, pull-out failure is more decisive in general conditions than other failure modes such as concrete cone and steel failure [13]. In order to favor pull-out and avoid other failure modes, the degree of reinforcement and the concrete element thickness must respect certain precautions [7].

According to EOTA TR 020 (Fig. 45), a fixture has to be attached to the anchor to transfer the tensile load from a tension member. The fixture must ensure a steel stress of 2-4 N/mm² in the flanges of the fixtures. This is due to the fact that the loading system is connected to the fixtures via the flanges. Fixture dimensions have to be chosen depending on load categories. However, the tension member linked to the fixture is not described in this technical report. Fire tests have to be carried out according to the general requirements of the determination of fire-resistance of different structural elements in EN 1363-1:1999-10 [27]. In order to perform pull-out fire tests, EOTA TR 020 [7] requires insulation around the fixture. Only details in Fig. 46 are presented in the technical report. This insulation in the case of bonded anchors may hugely influence thermal distribution leading to lower temperature profiles and a significant delay in failure time.

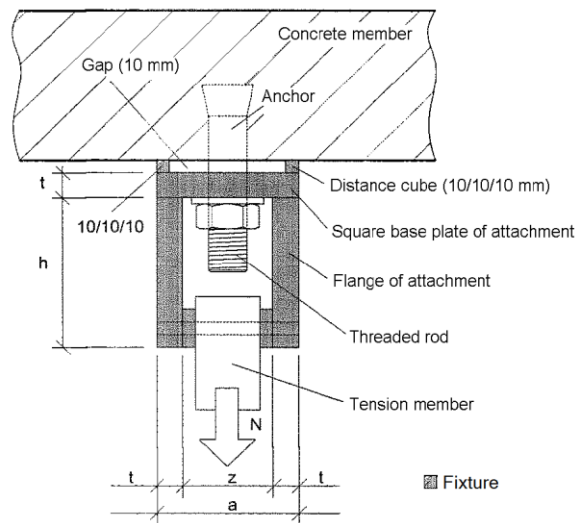
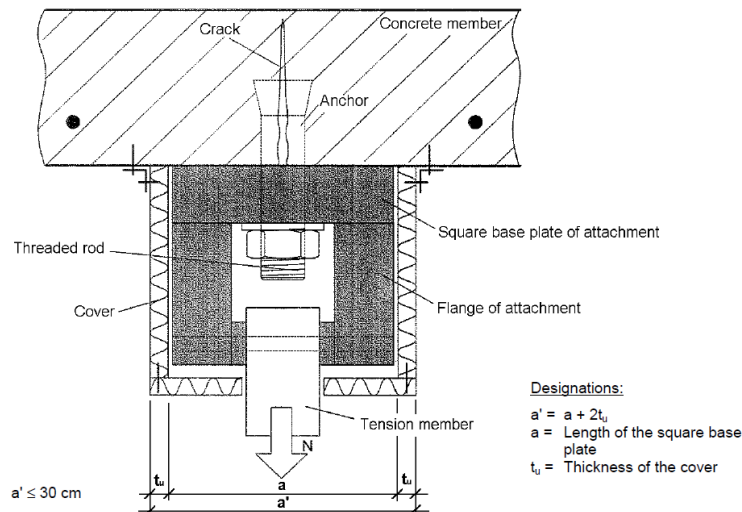


Fig. 45: Test set-up for the determination of steel failure test under fire in EOTA TR 020



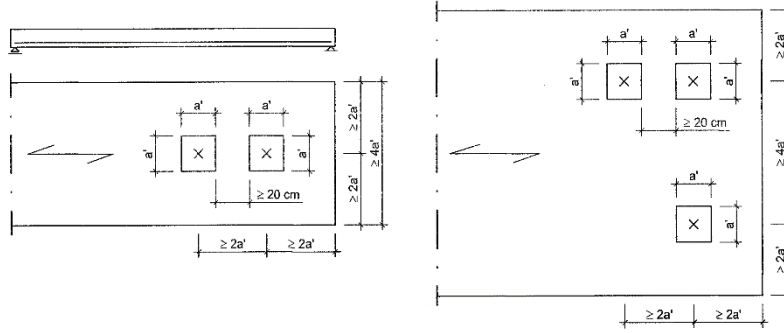


Fig. 46: Test set-up for the determination of the characteristic resistance under fire exposure to pull-out failure [7]

2.2. Design method for the determination of the pull-out resistance of bonded anchors under fire

Pinoteau [21] [10], Lahouar [12] [28] and Reichert & Thiele [8] proposed a method for the determination of the load capacity of anchors at a given time during fire exposure. The resistance integration method was used to determine the pull-out capacity of bonded anchors under fire. The thermal data necessary for the resistance integration method was obtained using various methods, one of which was experimental pull-out fire tests at constant load on bonded anchors installed in cylindrical concrete specimens according to EAD 330087-00-061 [9]. The cylindrical tested specimens were heated laterally. Concrete surface and extended parts of anchors were not heated directly, thus obtaining an acceptable uniform temperature profile along the embedment depth. In these works, bond resistance vs. temperature relationship was obtained by pull-out tests according to [9]. This relationship served later to predict the bond resistance vs. fire exposure time for non-uniform temperature profiles during fire tests. This was obtained by dividing the anchor into discrete elements (Fig. 47). By making the hypothesis that every discrete element has a uniform temperature, the bond resistance of each element is obtained from the bond resistance vs. temperature relationship. By integrating the bond resistance of the discrete elements, the total load resistance is obtained for a given time (Eq. 7 in Fig. 47).

This prediction method works very well for post-installed rebars in concrete, while an anchor directly exposed to fire has a more aggressive thermal diffusion. However, it is reasonable to say that the non-uniform temperature profiles of anchors directly exposed to fire can be used to calculate the bond resistance vs. fire exposure time. Hence, to predict failure time as long as the resin is not subjected to fire directly. This confirms that temperature profiles must be well known at every time during fire test in order to obtain good failure prediction.

The resistance of the anchor is calculated according to Eq. 7:

$$N_{Rd,fire} = \pi \cdot d \cdot \int_0^{l_v} f_{bd,0} \cdot k(\theta(x)) \cdot dx \quad \dots \text{ [Eq. 7].}$$

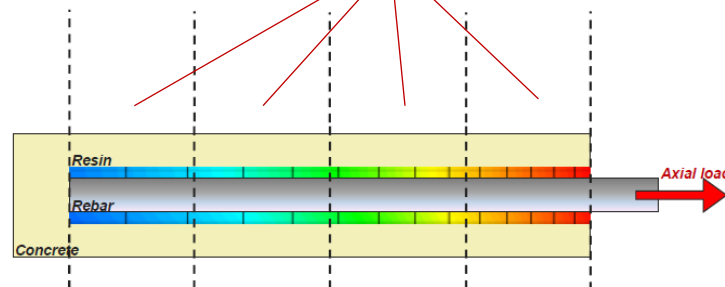


Fig. 47: Principle of the resistance integration method

Where: $N_{Rd,fire}$ is the fire design load resistance (kN).

d is the diameter of the anchor (mm).

$f_{bd,0}$ is the design bond resistance at ambient temperature (N/mm²).

$k(\theta)$ is a reduction factor that depends on temperature.

l_v is the length of the anchor (mm).

The advantage of this design method is that it can be applied on different configurations of pull-out fire tests which provide the thermal data of the bond. The configurations presented in EOTA TR 020 [7] do not cover pull-out for bonded anchors without insulation. Whereas, in the event of a real fire inside a building or on a building site, an anchor may be subjected directly to the thermal exposure while being subjected to tensile loads. This could cause failure more rapidly than for insulated cases [13]. Moreover, anchors could exist in thinner concrete elements. Boundary conditions of this problem influence temperature profiles along the anchor. Many shapes of fixtures could be applied on anchors where some may cover completely the anchor insulating it from a direct thermal exposure to fire.

The design method was experimentally validated in this paper. This was done using failure time obtained from loaded tests and the predicted time obtained from the resistance integration method.

2.3. Details of the experimental application for validating the design method

Fire tests were carried out on concrete beams of 230 mm of width and 1500 mm of length and different beam thicknesses (150 mm, 180 mm and 300 mm). Concrete beams were carved from slabs reinforced with HA10 rebars. The obtained beam sections were reinforced with different degrees of reinforcement according to the number of rebars in each section. The carving procedure ensured at least two rebars in the section of each beam so that the surface exposed to fire could resist to cracking and thermal expansion. A typical cross section of one of the concrete beams is shown in Fig. 48. In these beams, some bonded anchors were equipped with coax thermocouples to measure temperature profiles along the embedment depth. ISO 834 fire was applied using a gas furnace at CSTB with the following dimensions: 1.4 m length, 1 m width and 1.05 m height. A loading system was put in place for the three loaded tests (Fig. 49). The loading system used hydraulic jacks powered by hydraulic pumps, applying a downward mechanical load on a system of tubes surrounding the concrete beam. Metallic tubes transferred the applied load to fixtures connected to the anchor facing the inside of the furnace. Tube dimensions were 40 mm × 40 mm × 400 mm. Dimensions described in EOTA TR 020 [7] were adopted for the fixtures.

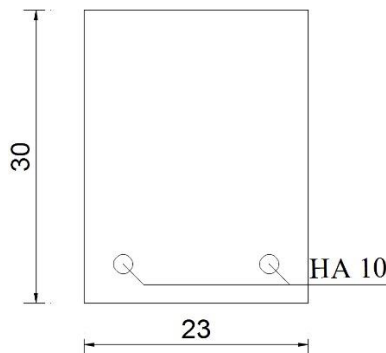


Fig. 48: Typical cross section of one of the concrete beams

In order to ensure a one-dimensional heat-transfer inside the beams and along the bond, the lateral faces of the beams were insulated using a glass wool-based material (50 mm thickness). The bonded anchors were fastened using a polymer-based resin. In order not to influence the bond surface between adhesive resin and steel of the rod, no thermocouples were positioned on the mechanically loaded anchors. This would result in a decrease of adherence between resin and steel leading to a false measurement of bond resistance. In order to measure temperature profile along the embedment depth without influencing the bond of the anchor, another unloaded anchor rod was instrumented with at least 4 thermocouples and installed in the same beam as the loaded one (Fig. 50 and Fig. 51). This aimed to emulate the same temperature profile in the loaded anchor. The instrumented anchor did not interact mechanically with the loaded one, because it was not loaded. Thus, choice of 150 mm distance was taken between the loaded anchor (centered above the furnace) and the unloaded anchor.

As recommended in EOTA TR 020 [7] and in order to reuse the metallic parts transferring the load to the fixture and the tension member, insulating material was put in place to protect the steel of the loading system from reaching failure before pull-out.

It is required to take a minimum of 2 mm of resin around the anchor diameter. Fire tests were performed on 2 beams at a time. The furnace was left at least one day to cool before performing the next test.

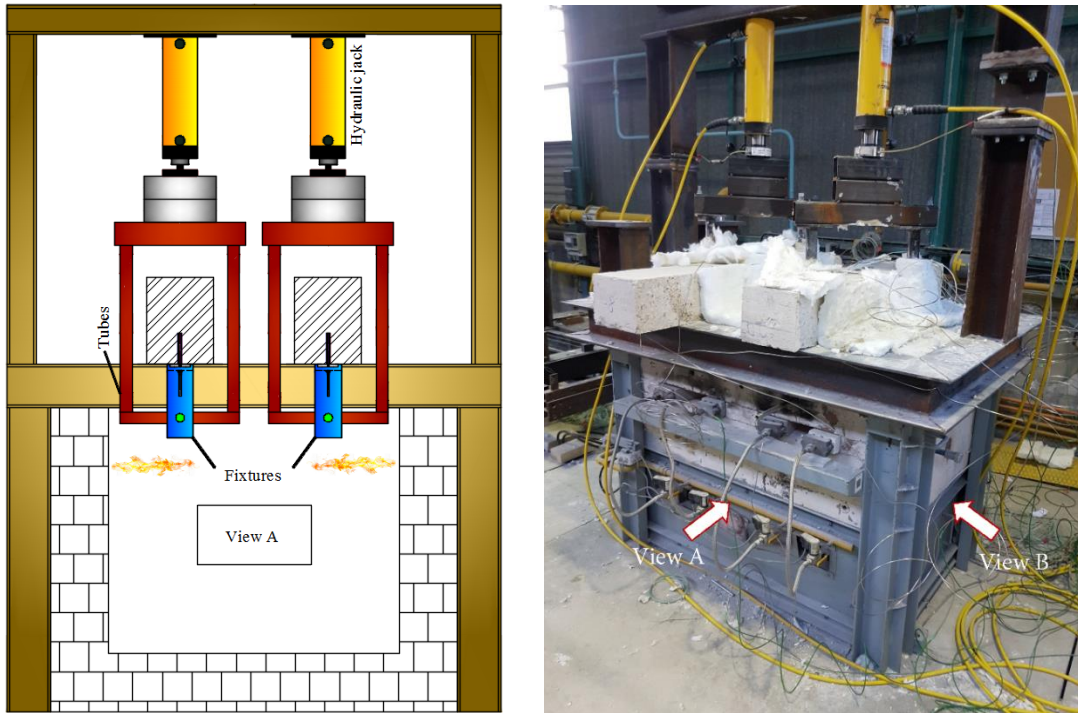


Fig. 49: View A (left) and photo (right) showing the gas furnace and the loading system

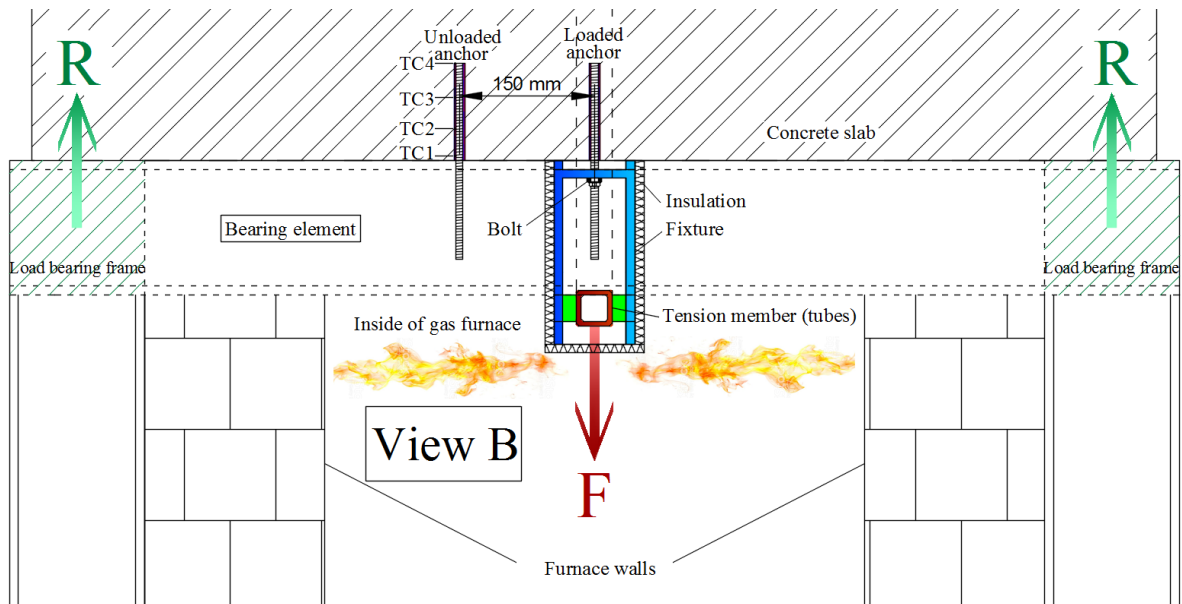


Fig. 50: View B of the gas furnace and the loading system

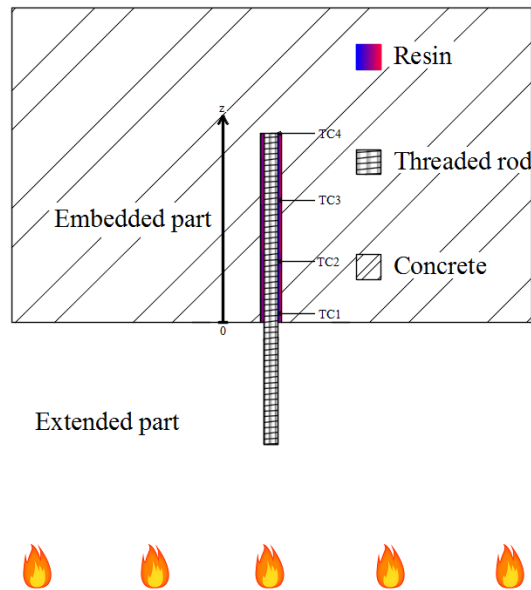


Fig. 51: Positioning of thermocouples along the embedment depth of unloaded anchors.

The composition of the C20/25 concrete used for the manufacture of beams is presented in Table 6.

Designation	Origin	Quantities (kg/m ³)
G 0/8 Sand Siliceous-Limestone	Bouaffles (27) (Morillon-Corvol factory)	880
G4/14 Gravel RC Labrosse	Labrosse (77) (Sablières de la Seine factory)	792
G4/20 Gravel RC Labrosse		88
CEM II/B-LL 32.5R CE CP2 NF	Calcia (Couvrot factory)	320
Water	-	227

Table 6: Composition of concrete used for the manufacture of beams

Threaded rods of grade-8.8 were used. The details of the threaded rods are presented in Table 7.

Major diameter (mm)	Minor diameter (mm)	Pitch diameter (mm)	Pitch (mm)	Thread angle	Helix angle	Tensile strength (MPa)
8	7.188	6.647	1.25	60°	3.17°	800-980
12	10.863	10.106	1.75	60°	2.93°	

Table 7: Details of threaded rods provided by the manufacturer of the resin

In order to reach a maximum bond strength for the three different rod diameters (8 mm, 12 mm and 16 mm), the adopted thickness for the adhesive material was 2 mm as recommended by the manufacturer of the resin.

The adhesive resin presents a bond stress up to 25 MPa at ambient temperature for threaded rods with diameters below 16 mm. Resin properties at high temperatures according to EAD 330087-00-0601 [9] are presented in Fig. 52.

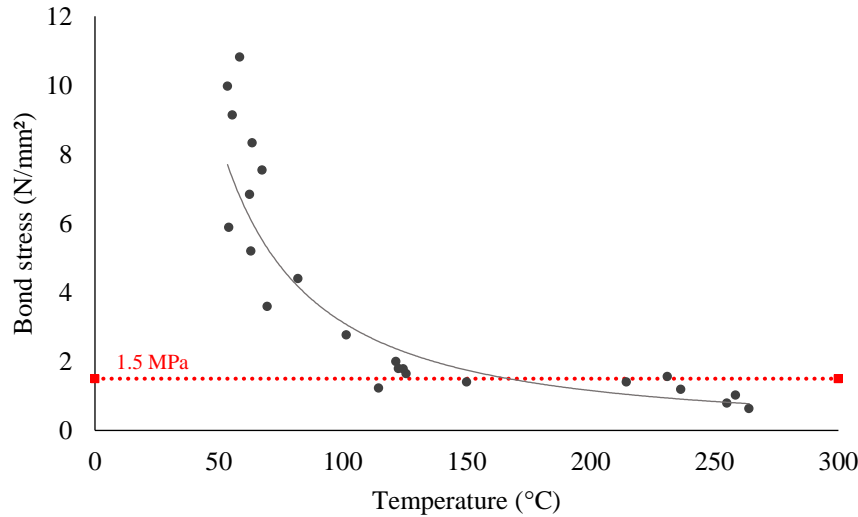
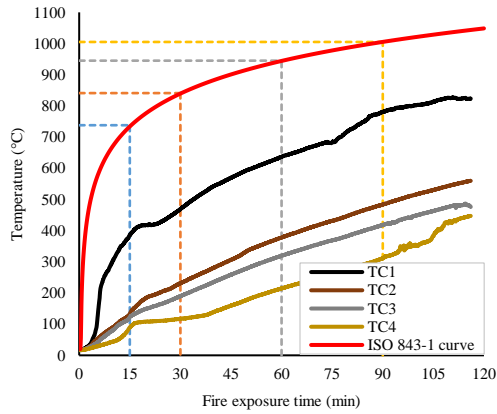


Fig. 52: Bond stress vs. Temperature relationship of the used polymer resin

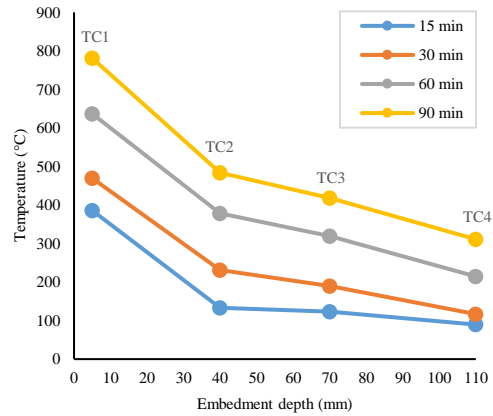
The furnace satisfies the requirements for fire resistance studies in the international standard ISO 834 [19]. Therefore, thermal exposures are uniform on all samples. Temperature profiles were used as entry data to calculate the bond stress vs. temperature and bond stress vs. fire exposure time curves in order to predict the same failure time. Pre-existing data was available on the tested resin by performing pull-out tests according to EAD 330087-00-0601 [9] for the characterization of the mechanical properties of adhesives at high temperature (Fig. 52).

The resistance integration method used to calculate bond failure and failure time is based on temperature profiles measured experimentally. In this paper, load application was only used to validate the prediction obtained from the resistance integration method. The parametric study of the influence of the loading system did not need load application but only temperature profiles to compare failure between different test configurations.

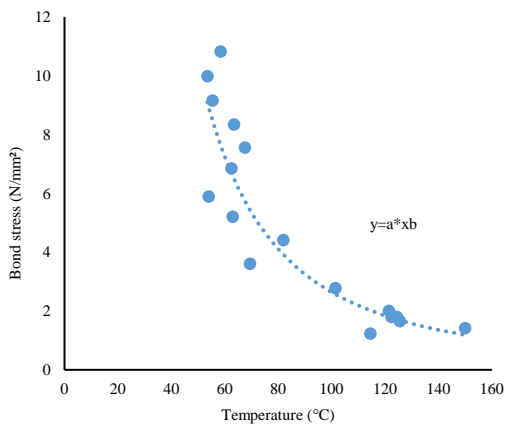
The work on loaded tests went as following: First, temperature profiles at all times of fire exposure are obtained by performing fire tests. Then, bond stress vs. temperature relationship is plotted allowing, thanks to the discretization of the anchor, to attribute a resistance as a function of temperature to each discrete element. Finally, the load-bearing capacity of the anchor is obtained by integrating the resistances of all the discrete elements obtaining the resistance of the anchor at all times of fire exposure. The bond resistance vs. fire exposure time curve can be plotted and a comparison can be done between the applied load and load-bearing capacity of the anchor (Fig. 53).



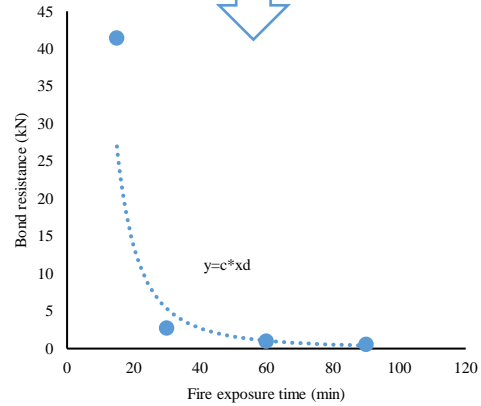
Furnace average Temperature vs. Exposure time



Experimental results – Resin Temperature vs. Embedment depth



Fire test (acc. EAD) – Bond strength vs. Temperature



Bond resistance vs. Time of exposure to ISO fire

Fig. 53: Steps of the Resistance Integration Method

The conducted loaded fire tests are summarized in Table 8.

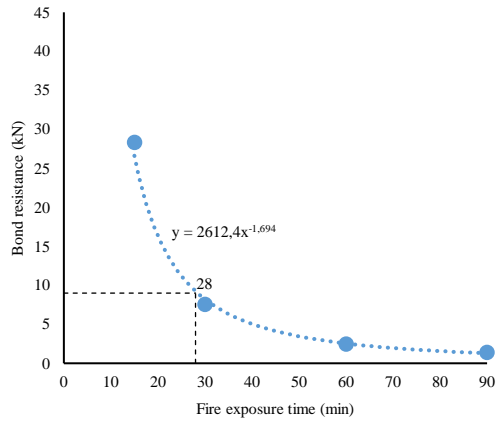
Fire type	Test n°	Bond geometry			Beam dimensions (m)	Load (kN)	Experimental failure time (min)	Predicted failure time (min)
		Ø (mm)	h _{ef} (mm)	N° of TC	Length × width × thickness			
ISO 834	1	12	110	8	1.5 × 0.23 × 0.18	9	29	28
	2	12	110	4	1.5 × 0.23 × 0.18	1.8	60	48
	3	8	70	4	1.5 × 0.23 × 0.18	0.75	75	96

Table 8: Details of mechanically loaded pull-out fire tests

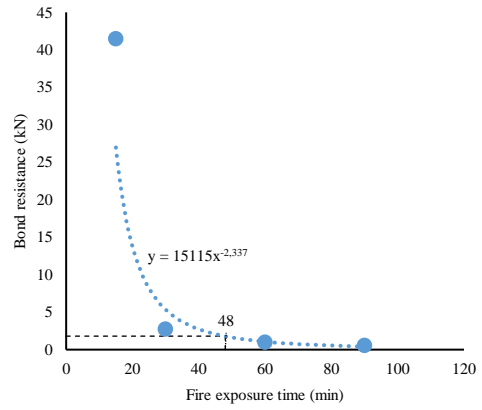
Three fire tests were performed with one loaded and one unloaded anchor per beam to validate this method. Tests were conducted on beams with 180 mm of thickness. The 1st test was loaded at 8.7% of the load-bearing capacity at ambient temperature and reached failure at 29 min while the estimated failure time using the resistance integration method was 28 min. The 2nd test was loaded at 1.7% of the load-bearing capacity at ambient temperature and reached failure after 60 min while the estimated failure time was 48 min. The 3rd test was loaded at 1.7% of the load-bearing capacity at ambient temperature as well, and reached failure after 75 min while the estimated failure time was 96 min (Fig. 54).

These load levels were chosen in order to compare the precision of failure prediction of bonded anchors under high and low load levels. Fig. 52 shows the bond stress vs. temperature relationship of the adopted adhesive resin.

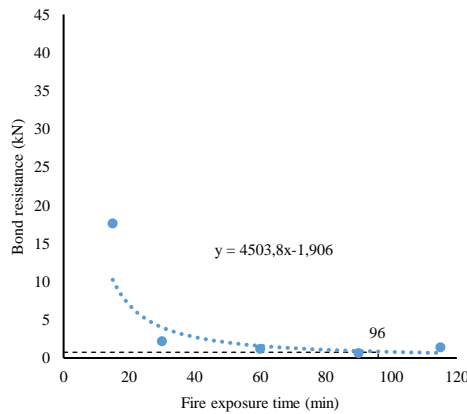
According to this relationship, failure temperature for low load levels presenting a bond stress below 6% of the load-bearing capacity at ambient temperature may vary significantly for a very minimal increase in bond stress. Thus, the 1st anchor was loaded under a bond stress larger than 1.5 MPa, and the remaining two loaded tests were conducted for bond stress below 6% of the load-bearing capacity at ambient temperature. Only one test was conducted per series. The repeatability of these tests could not be shown. The presented results and predictions are only indicative of the adopted experimental protocols and research practices detailed in this study.



Bond resistance vs. Time for the first case with a load of 9 kN and a failure time of 28 min



Bond resistance vs. Time for the second case with a load of 1.8 kN and a failure time of 48 min



Bond resistance vs. Time for the third case with a load of 0.75 kN and a failure time of 96 min

Fig. 54: Bond resistance vs. Time relationship for the loaded tests

Fig. 55 shows an illustration of pull-out failure of loaded bonded anchors after fire tests. The pull-out of the anchor clearly manifested at the steel/adhesive interface.



Fig. 55: Illustration of pull-out failure at the steel/resin interface of loaded bonded anchors under fire

It is concluded that for high load levels, the predicted time has a higher accuracy than for low load levels ($\leq 6\%$ of the reference bond stress at ambient temperature). A comparison between average temperatures of anchors shows that failure at low load levels is reached for a temperature at which the adhesive resin doesn't resist or has minimal resistance due to the degradation of its mechanical properties. It is supposed that large differences obtained for low load levels are due to the poor knowledge of temperature profiles. The hypothesis that temperature profiles of unloaded anchors are similar to those of loaded anchors in (Fig. 50) gives uncertain results for failure time prediction. This requires further investigation in order to determine the influence of the loading system on thermal distribution and the precision of the prediction method.

3. Thermal influence of different parameters of pull-out fire tests

Studies on other types of anchors in concrete at high temperatures have shown that anchor geometry and thermal boundary conditions of test setup have a significant influence on the prediction of the anchor's resistance [29]. Concrete beams in which the anchors were installed were subjected only to their weight and to thermal loading due to fire exposure. Each test was composed of two concrete beams on top of the furnace. In each beam, two bonded anchors were installed. The configuration of these anchors varies from one test to another according to the tested parameter. During these parametric thermal tests, bonded anchors were not subjected to pull-out loads. Thermal data obtained from temperature profiles along the embedment depth of anchors served to determine the bond resistance vs. fire exposure time by using the resistance integration design method presented earlier.

In order to assess the thermal influence of test configurations described in TR 020 [7], additional tests were conducted without mechanical loading. Tested bonded anchors were instrumented with 4 thermocouples per rod (Fig. 51).

Table 9 describes the positioning of thermocouples in the tested specimens.

TC n°	TC position
1 to 4	Embedment depth of the anchor
5 - 6	Bolt tightening the fixture
7 - 8	Exposed surface of the concrete beam
9 - 10	Flange of the fixture at mid-height
11	Unexposed surface of the beam

Table 9: Positioning of thermocouples

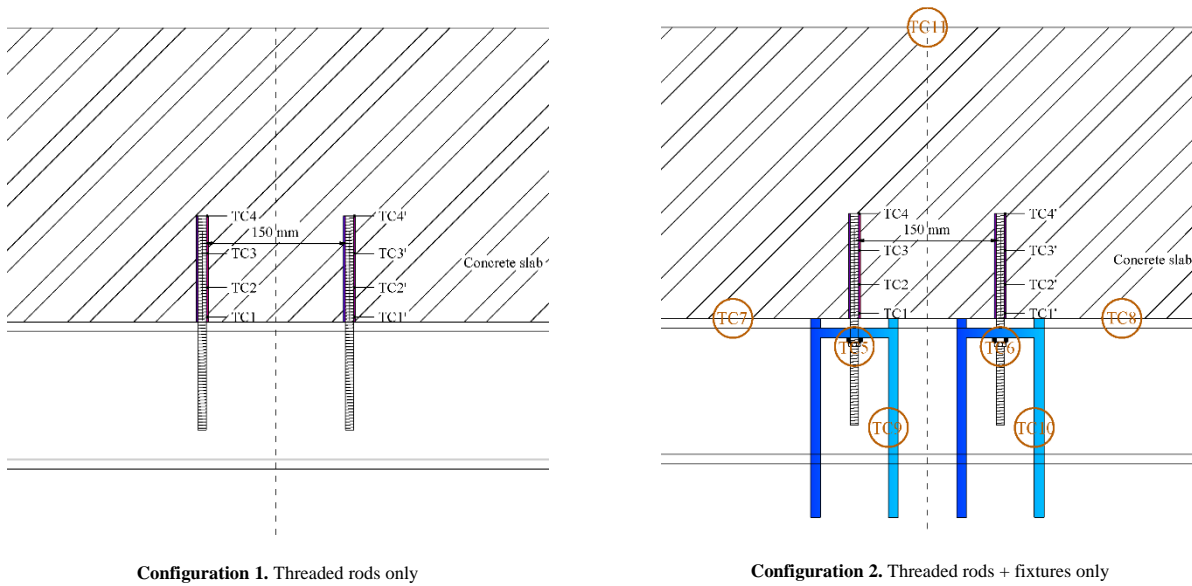
Temperatures of fixtures at mid-height, bolt tightening the fixture on the threaded rod, and applied ISO 834 fire were recorded in order to ensure the same testing conditions for compared anchors. Thermocouples from TC5 to TC11 were protected with a thin, small layer of insulation at the measuring head of the thermocouple in order to measure the surface temperature instead of that of the radiation of the furnace or of surrounding ambient gaz.

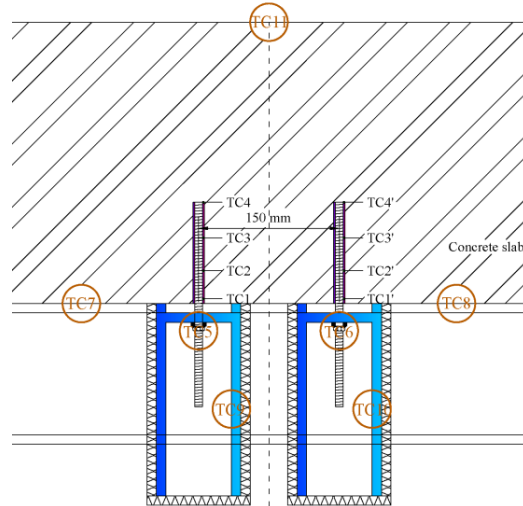
EOTA TR 020 [7] provides very little information on how to perform these tests. The application of the existing method of performing pull-out fire tests requires the study of its influence and limitations on thermal distribution. The limitation of the existing method is that in a real fire case scenario, the load may be applied on the bonded anchor without any insulation or fixtures (Configuration 1 in Fig. 56). Furthermore, the influence of different configurations on the precision of the method is linked to the difference between temperature profiles due to the presence of the parts of loading system that consist of fixtures (Configuration 2 in Fig. 56) and insulation around fixtures (Configuration 3 in Fig. 56).

Conducted thermal investigation tests are summarized in Table 10. Some tests were conducted several times for repeatability purposes. Details are presented in the following sections.

Fire type	Test n°	Test configuration	Anchor geometry		Concrete element dimensions (m)
			\varnothing (mm)	h_{ef} (mm)	Length \times width \times thickness
ISO 834	4	1	8	60	1.2 \times 0.45 \times 0.10
	5	1	12	60	1.2 \times 0.45 \times 0.10
	6	1	16	60	1.2 \times 0.45 \times 0.10
	7	2	8	70	1.5 \times 0.23 \times 0.15
	8	2	8	70	1.5 \times 0.23 \times 0.18
	9	2	8	70	1.5 \times 0.23 \times 0.30
	10	2	12	110	1.5 \times 0.23 \times 0.18
	11	2	12	110	1.5 \times 0.23 \times 0.18
	12	3	12	110	1.5 \times 0.23 \times 0.30

Table 10: Details of thermal investigation fire tests





Configuration 3. Threaded rods + fixtures + insulation

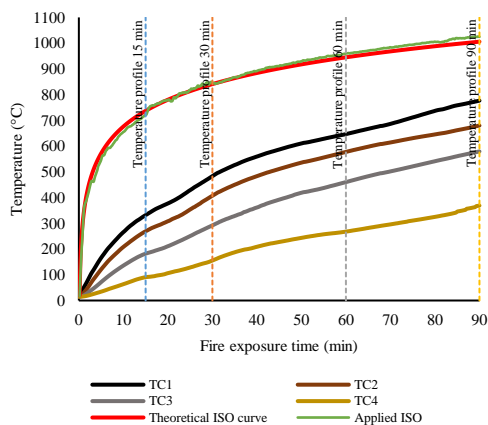
Fig. 56: Positioning of thermocouples in different configurations of unloaded fire tests.

3.1. Influence of anchor diameter and adoption of steel/concrete temperature in the resistance integration method

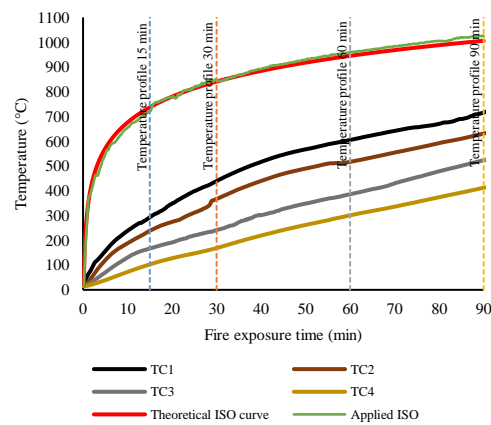
In order to determine the influence of anchor diameter on thermal distribution, three anchors with different diameters (8 mm, 12 mm and 16 mm) were installed with 60 mm embedment depth in a slab with the following dimensions: 1.2 m × 0.45 m × 100 mm. The anchors had the same configuration as presented in Configuration 1 in Fig. 56. The anchors were directly exposed to fire without any insulation or fixtures. Cast-in coax thermocouples were positioned along the thickness of the slab. These thermocouples were placed on a steel wire tightened in place on its upper and lower sides with wooden boards before pouring the concrete.

Fig. 57 shows the temperature of thermocouples vs. fire exposure time for each rod. For the M16 rod, thermocouples were positioned at 5, 19, 29 and 60 mm of the embedment depth. For the M12 rod, thermocouples were positioned at 7, 17, 31 and 55 mm of the embedment depth. For the M8 rod, thermocouples were positioned at 5, 12, 28 and 59 mm of the embedment depth. Afterwards, data from Fig. 57 were used to plot temperature profiles for specific exposure times (i.e. 15, 30, 60 and 90 min). A reduction of the temperature of thermocouples was noticed from TC1 to TC4 in all cases. This is due to the increase of distance between the thermocouple and the fire exposed surface. Indeed, as shown in Fig. 51, TC1 is the closest to the fire exposed surface and TC4 is the furthest. Sudden fluctuations in Fig. 57 are due to the movement of insulation around the beams during fire tests. A rapid homogenization of furnace temperature is noticed.

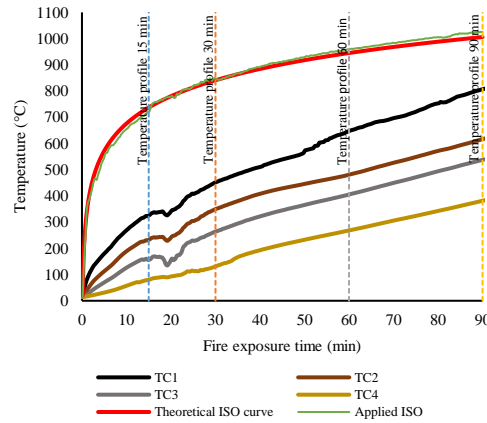
The relationship between temperature profiles vs. the embedment depth is then obtained in Fig. 58.



Temperature of thermocouples vs. exposure time for the M16 rod



Temperature of thermocouples vs. exposure time for the M12 rod



Temperature of thermocouples vs. exposure time for the M8 rod

Fig. 57: Temperature of thermocouples vs. exposure time for three different diameters of threaded rods

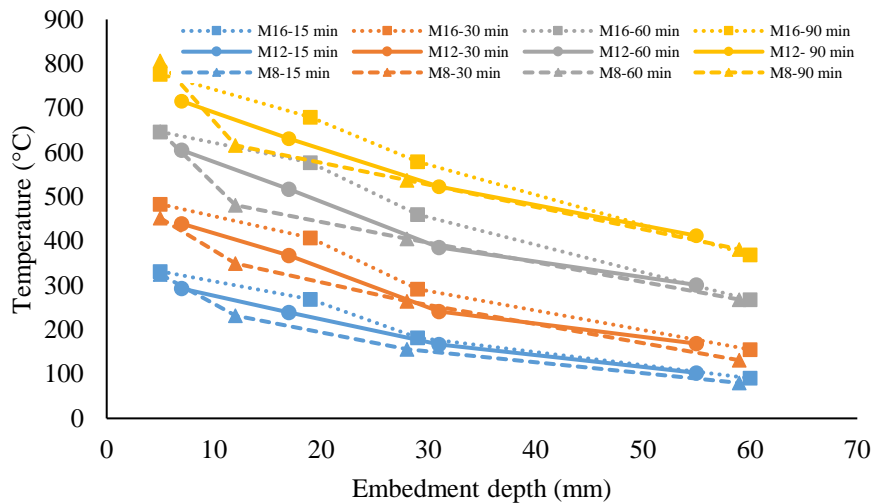


Fig. 58: Comparison of thermal profiles along the anchor for three different anchor diameters (Configuration 1 in Fig. 56)

The comparison in Fig. 58 shows that a bigger diameter gives a slightly higher temperature at the same point of observation. The difference of temperature between the smallest and the biggest diameter is 9% after 90 min of fire exposure and only near the exposed area (10 to 20 mm from the exposed surface). This difference of temperature profiles between different diameters increases with fire duration. It also decreases towards the bottom of the embedment length.

The temperature profiles plotted in Fig. 58 show that the bigger the diameter of the rod is, the higher the temperature is, especially near the exposed surface. Only points in the figure (thermocouples at four different depths) were measured. Temperature profiles are plotted by connecting the points using straight lines. This could be explained by the fact that for anchors with bigger diameters, steel quantity is larger, which increases the effect of heat transfer through the steel rod.

In order to quantify the influence of this parameter, the resistance integration method was applied to the three cases. For a stress of 0.43 MPa (same as loaded anchor n°2 and 3) applied to the three cases, the predicted failure times were 51 min for the M8 rod, 64 min for the M12 rod, and 43 min for the M16 rod. This does not necessarily mean that a larger diameter leads to a faster failure, because a larger diameter increases the bond surface around the rod. This could mean that for a given stress, there is an optimal diameter/embedment depth ratio leading to the best resistance vs. time curve.

The previous fire test, with cast-in thermocouples along the thickness aimed also to compare the temperature along the concrete thickness and the steel of the anchor. The anchor with a diameter of 12 mm was considered for comparison. The comparison was studied along the first 60 mm of the test.

Fig. 59 shows that the temperature profile measured at the steel-resin interface gives higher temperatures than the temperature of concrete for the first 15-20 min, except for the part of the rod near the exposed surface. The steel of the anchor tends to homogenize the temperature along the embedment depth. This explains why steel temperature is higher than concrete temperature in the deep part of the anchor after 15-20 minutes. Steel at the beginning of the fire test is hotter than concrete near the exposed side then the curves of temperature vs. depth for both materials cross at a certain moment. This point of crossing advances towards the unexposed side with fire exposure. This is due to the fact that steel behaves as a temperature vector compared to concrete.

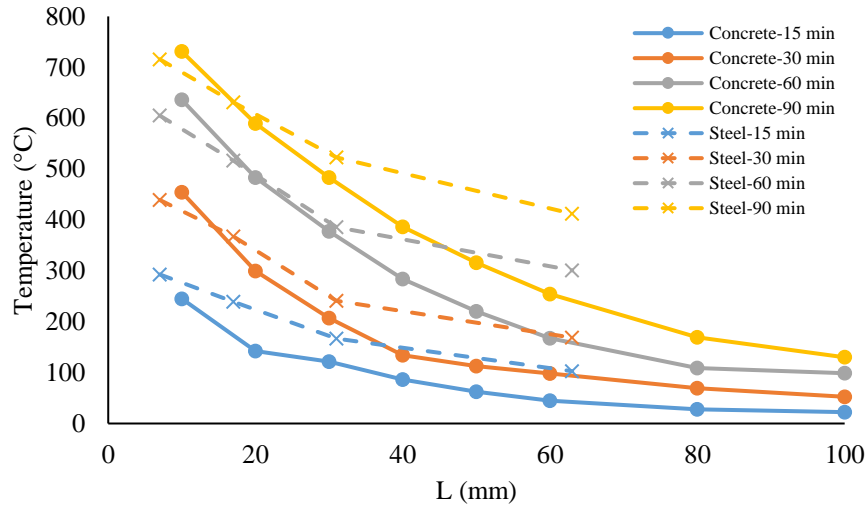


Fig. 59: Comparison between the thermal gradient of the beam and the temperature profile of the anchor (Configuration 1 in Fig. 56)

The resistance integration method was applied to the first 60 mm of concrete and steel of Fig. 59 to calculate the bond resistance of the anchor vs. fire exposure time, for a bond stress of 0.43 MPa (same as loaded anchor n°2 and 3) for example presented in Fig. 60.

In the work of Pinoteau [21] and Lahouar [30] on rebars in concrete, the effect of steel was not taken into account to calculate thermal profiles along the bond. Concrete temperature in the same position was adopted instead. This may be valid for steel cast in concrete because the thermal diffusion occurs via concrete. In the case of an anchor directly exposed to fire, the thermal attack occurs via the steel of the anchor and the concrete of the beam simultaneously.

In the results presented in Fig. 60, there is a 27% difference in the ratio between the resistance calculated based on concrete temperature and the resistance calculated based on steel temperature for low load levels ($\leq 6\%$ of the load-bearing capacity at ambient temperature) for bond stress. This difference is not negligible. The dependence on concrete temperature instead of steel temperature in the resistance integration method for bonded anchors directly exposed to fire may lead to a false estimation of failure for both low and high load levels.

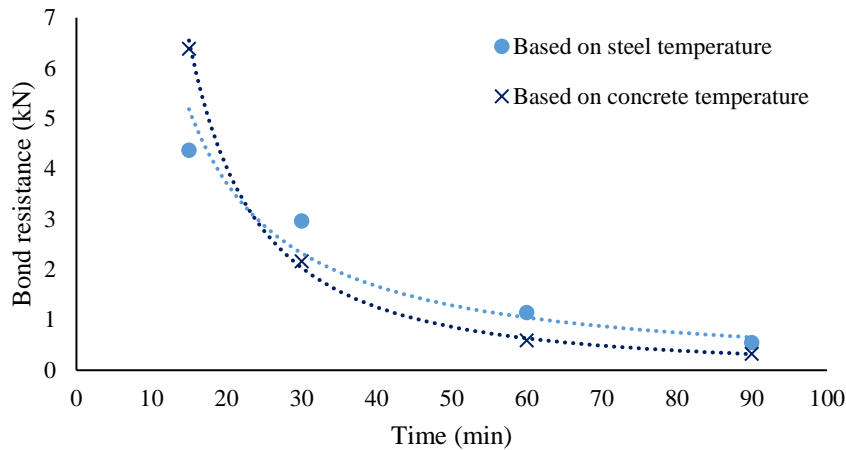


Fig. 60: Comparison between resistance integration based on concrete/steel temperature

3.2. Influence of concrete element thickness

The thickness of the tested concrete beam plays a role in influencing the temperature profiles. In order to assess this influence of the change in boundary conditions for the unexposed surface, three different beam thicknesses were tested: 150 mm, 180 mm and 300 mm. The temperature of the unexposed surface was recorded using copper disks thermocouples. Fig. 61 shows that the temperature of the unexposed surface is inversely proportional to the thickness of the beam. This result can be explained by the fact that thinner beams have higher temperature gradients along a shorter thickness and hence they homogenize temperature along the thickness faster than thicker beams.

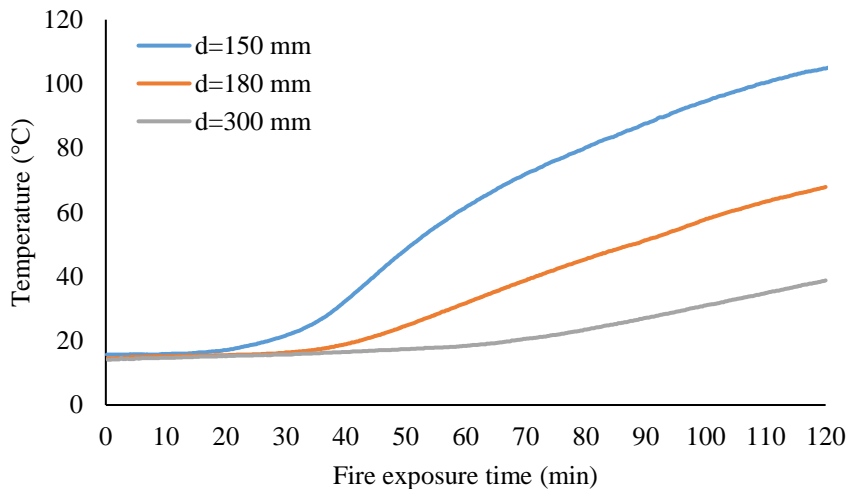


Fig. 61: Comparison between the temperatures of the unexposed surface vs. Fire exposure time for different beam thicknesses

The same comparison was done for temperature profiles for two threaded rods with a diameter of 8 mm and an embedment depth of 70 mm in two different beams with a thickness of 180 and 300 mm. The anchors had the same configuration as that presented in Configuration 1 in Fig. 56. For the rod installed in a 180 mm beam, thermocouples were positioned at 5, 25, 40 and 70 mm of the embedment depth with a margin up to ± 3 mm. For the rod installed in a 300 mm beam, thermocouples were positioned at the same distances of the embedment depth with a margin up to ± 2 mm. Fig. 62 shows a comparison between temperature profiles vs. embedment depth for both cases. A thinner beam shows a higher temperature profile for the same diameter and the same embedment depth, but the differences are rather small. However, this slight difference seems to decrease towards the foot of the anchor.

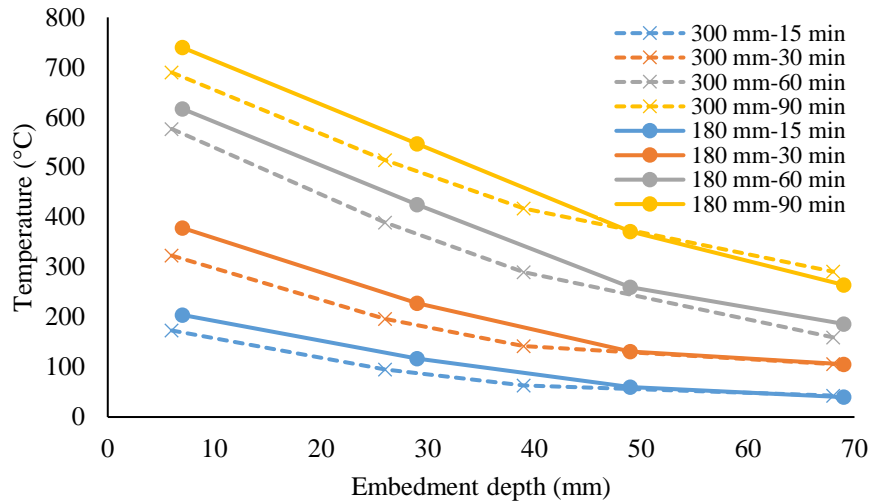


Fig. 62: Comparison between temperature profiles vs. Embedment depth for two anchors in different beam thicknesses (Configuration 1 in Fig. 56)

In order to quantify the influence of this parameter, the resistance integration method was applied on both cases. For a stress of 0.43 MPa (same as loaded anchor n°2) applied on both cases, the predicted failure times were 75 min for the anchor installed in a 180 mm beam, and 71 min for the anchor installed in a 300 mm beam. This means that thicker slabs result in a slightly faster failure for low load levels. For this small difference, the influence of beam thickness is most likely negligible for both low and high load levels.

3.3. Influence of fixtures

In EOTA TR 020 [7] only fixtures are represented with details. Due to the absence of requirements, inside a building an anchor may be exposed to fire without having steel plates attached to it, leading to a thermal transfer via the rod directly. Anchors with and without the existence of fixtures were tested.

Fig. 63 shows temperature profiles vs. the embedment depth for two anchors with a diameter of 12 mm in beams with a thickness of 300 mm, with and without fixtures (Configurations 1 and 2 in Fig. 56). The anchor without fixture had 8 thermocouples whereas the anchor with fixture had 4 thermocouples along the embedment depth. A slight difference is observed between the two cases. The difference decreases after 90 min of fire exposure. This could be caused by the homogenization of fixture temperature with furnace temperature. The existence of fixtures interferes with the thermal transfer mode and limits it to conduction. In the absence of fixtures, thermal transfer is mostly done by radiation. Fig. 63 shows that the temperature difference between the profiles of configurations 1 and 2 decrease with time, which is linked to the kinetics of the heating inside the furnace.

Fig. 64 shows temperature evolution of thermocouples vs. fire exposure time for both cases with and without fixture.

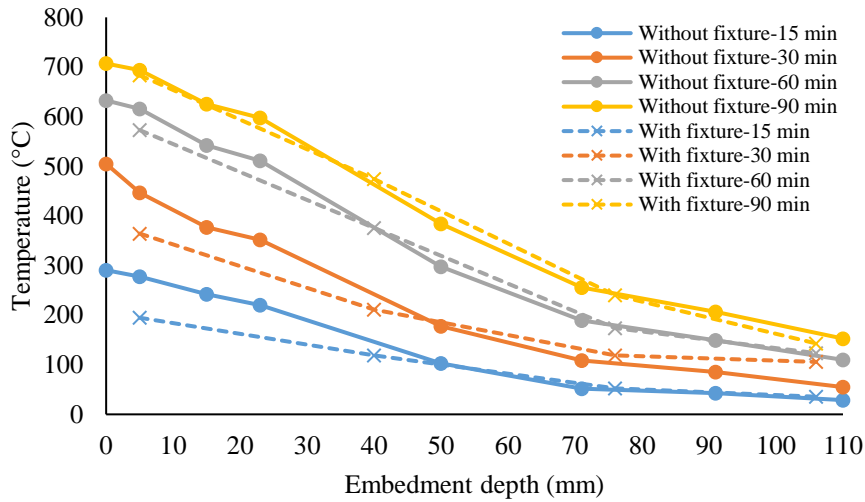


Fig. 63: Comparison between temperature profiles vs. Embedment depth for anchors with/without fixture (Configurations 1 and 2 in Fig. 56)

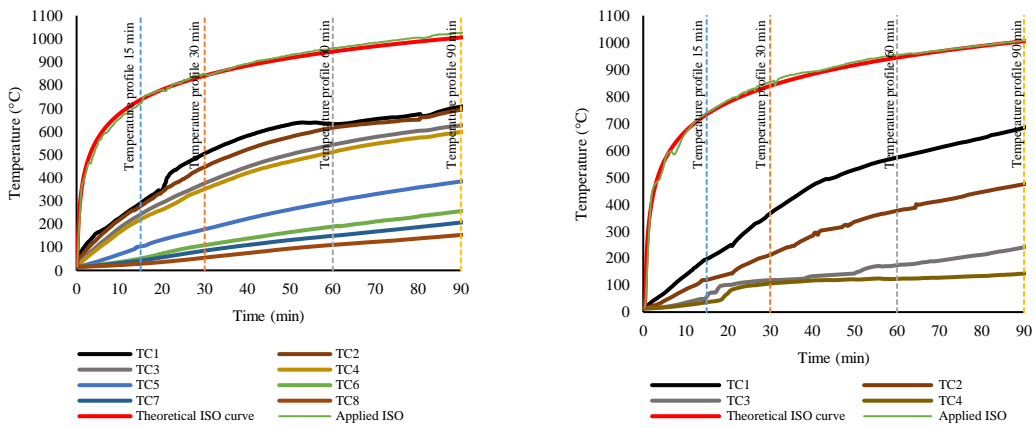


Fig. 64: Temperature evolution of thermocouples for test configurations 1 (left) and 2 (right) of Fig. 56

In order to quantify the influence of this parameter, the resistance integration method was applied on both cases. For a stress of 0.43 MPa (same as loaded anchor n^o2) applied on both cases, the predicted failure times were 74 min for the rod without fixture, and 80 min for the rod with fixture. This means that the existence of the fixture delays failure for low load levels. However, for a stress of 2.17 MPa (same as loaded anchor n^o1), the predicted failure times were 27 min for the rod without fixture, and 28 min for the rod with fixture.

Fig. 65 shows that the existence of fixtures has a slight influence on failure time prediction for high load levels. The difference between the precision of results for low and high load levels, despite of its negligence, could be attributed to the fact that for high load levels, the fitting curve of the bond stress vs. time relationship varies very little on the abscissa (time axis) during the first 30 min due to its slope. However, for low load levels, even the slightest difference between the fitting points (in this case at 30 min) can cause a significant change of slope at the end of the curve causing a noticeable difference of failure time between the two cases.

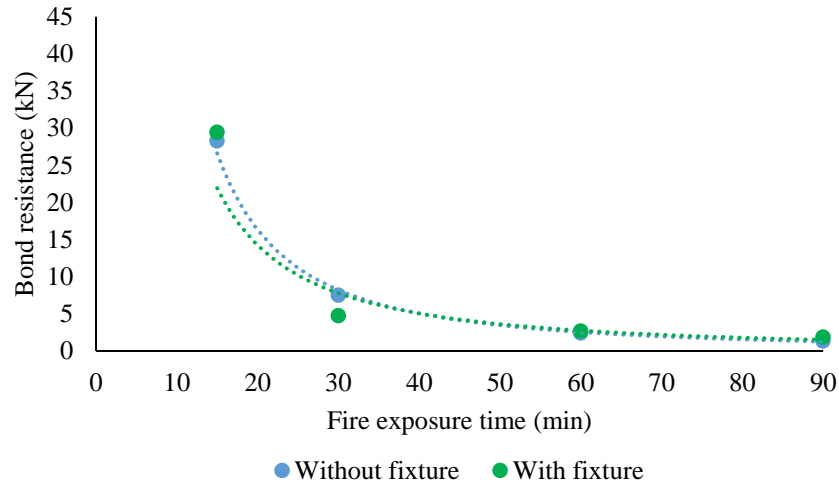


Fig. 65: Bond resistance vs. Time relationship for anchors with/without fixture

3.4. Influence of insulation

Insulation of the steel parts is required to perform pull-out tests in EOTA TR 020 [7]. It was also necessary to prevent the steel parts of fixtures from reaching failure before the anchor. In order to assess the influence of insulation around fixtures, four beams with a thickness of 300 mm were tested. Each beam had 2 bonded anchors, with a diameter of 12 mm (Configuration 3 in Fig. 56). Fig. 66 shows insulation around fixtures with 50 mm of glass wool before testing.

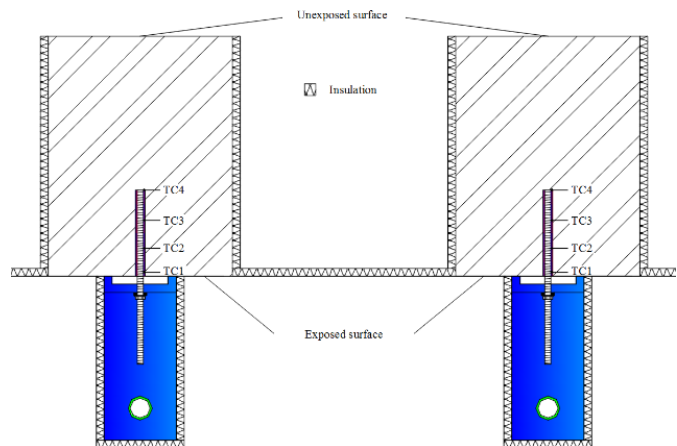


Fig. 66: Insulation of the fixtures and the lateral sides of beams (view B defined in Fig. 50)

Results presented in Fig. 67 show a significant reduction in temperature profiles for the insulated case, compared to the non-insulated case (Configurations 2 and 3 in Fig. 56). Fig. 68 shows that insulation also affects parts located inside the fixture. For example: the temperature of the bolt ensuring the connection between the fixture and the anchor is reduced by almost 500°C after one hour of heating in the insulated case. Temperature at mid-height of the fixture's flange is also reduced by almost 400°C after the same time of heating. This confirms that the thermal diffusion is reduced significantly due to insulation around fixtures

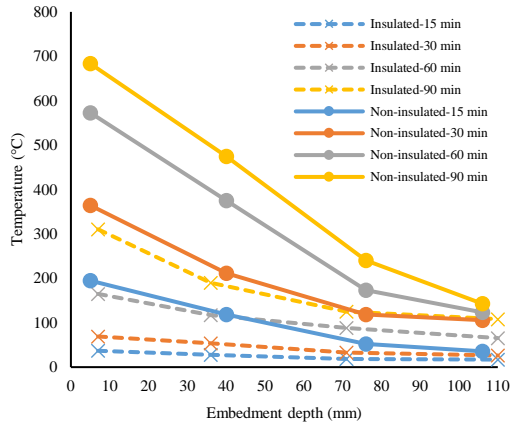


Fig. 67: Comparison between temperature profiles vs Embedment depth for insulated/non-insulated anchors (Configurations 2 and 3 in Fig. 56)

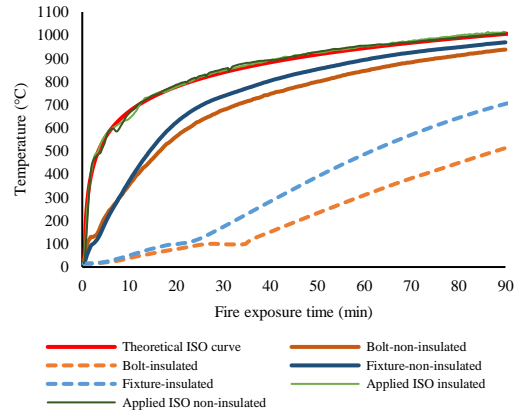


Fig. 68: Comparison between bolt temperature (TC5-TC6) and fixture temperatures (TC9-TC10) for insulated/non-insulated anchors

Fig. 69 shows temperature evolution of thermocouples vs. fire exposure time for insulated and non-insulated fixtures.

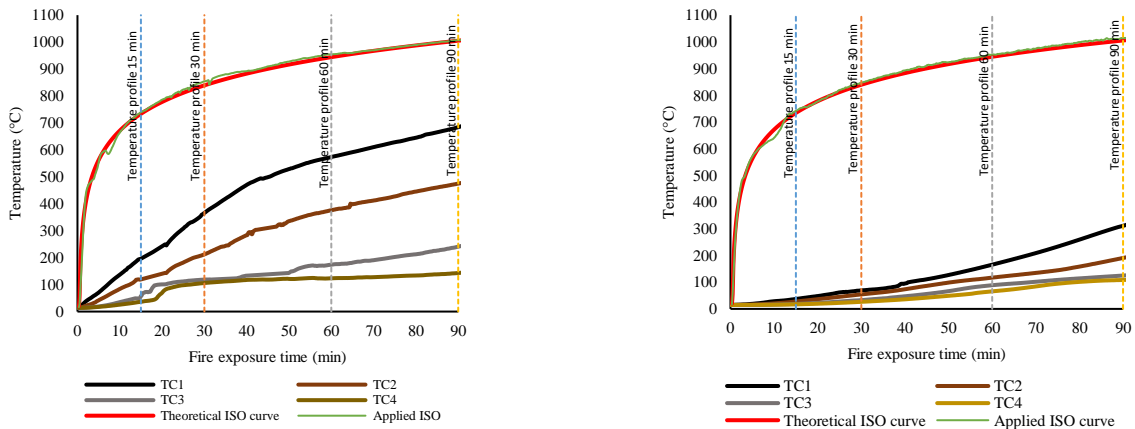


Fig. 69: Temperature evolution of thermocouples for test configurations 2 (left) and 3 (right)

In order to quantify the influence of this parameter, the resistance integration method was applied on both cases. For a stress of 0.43 MPa (same as loaded anchor n°2) applied on both cases, the predicted failure times were 80 min for the case without insulation, and 160 min for the case with insulation. For a stress of 2.17 MPa (same as loaded anchor n°1), the predicted failure times were 28 min for the case without insulation around the fixture, and 69 min for the case where the fixture was insulated with glass wool. This means that insulation delays predicted failure significantly for both low and high-load levels.

Table 11 summarizes all the results for unloaded thermal investigation tests on bonded anchors in concrete under fire.

Tested parameter	Test configuration	Anchor geometry		Concrete element dimensions	Supposed applied stress	Estimated failure time
		\varnothing (mm)	h_{ef} (mm)	(mm)	(MPa)	(min)
Anchor diameter	1	8	60	$1.2 \times 0.45 \times 0.10$	0.43	51
		12	60			64
		16	60			43
Concrete element thickness	2	8	70	$1.5 \times 0.23 \times 0.18$	0.43	75
				$1.5 \times 0.23 \times 0.30$		71
Fixture existence	1	12	110	$1.5 \times 0.23 \times 0.30$	0.43	80
					2.17	28
	2				0.43	74
					2.17	27
Insulation around fixtures	1	12	110	$1.5 \times 0.23 \times 0.30$	0.43	80
					2.17	28
	3	12	110		0.43	160
					2.17	69

Table 11: Summary of results for unloaded thermal investigation tests

4. Conclusion

This paper aimed to study and highlight the influence of testing conditions described in the existing guidelines for evaluating anchors in concrete under fire on the evaluation of pull-out strength of bonded anchors. Thanks to the strong bond between concrete and steel, mechanical anchors are lightly influenced by these test conditions. However, for bonded anchors, pull-out is more likely to occur at high temperatures. This is due to the rapid degradation of the mechanical properties of the bond. Thus, the variation of temperature profiles has a significant influence on the resistance of bonded anchors. In order to assess the mechanical behavior of bonded anchors, pull-out tests under ISO 834 fire were performed in this study. These tests were conducted on concrete beams with two bonded anchors in each: one loaded until pull-out and another unloaded but instrumented with thermocouples along the embedment depth to measure the same temperature profiles as the loaded one (Fig. 50). The unloaded anchor was not insulated and was left directly exposed to fire. Measured temperature profiles were used later to predict pull-out failure with the help of the resistance integration method. The predicted bond resistance vs. fire exposure time curves gave a reasonably precise accurate failure time for high load levels (> 6% of the load-bearing capacity at ambient temperature) at 28 minutes for the predicted failure and 29 min for the experimental failure (97% precision). However, for low load levels (\leq 6% of the load-bearing capacity at ambient temperature) the prediction was not accurate and needed further investigation of the influence of each parameter separately on the precision of this prediction.

In order to study the influence of these parameters, thermal investigation fire tests were conducted on different configurations (Fig. 56). The investigated parameters were: anchor diameter, replacement of steel temperature with concrete temperature for the prediction in the resistance integration method, beam thickness, fixture existence and insulation of the loading system. Testing derived the following conclusions:

- The diameter of larger anchors results in higher temperature profiles but not necessarily to faster failure time because of the increase of the bond area around the rod.
- The use of concrete temperature instead of steel temperature, for bonded anchors directly exposed to fire, in the resistance integration method may result in a non-conservative estimation of bond resistance and failure time consequently.
- The thickness of the concrete beam has low influence on the predicted bond resistance and failure time.
- The existence of the fixture has low influence on the predicted bond resistance and failure time.
- The insulation around fixtures significantly influences thermal distribution. Insulation decreases temperature profiles along the embedment depth of the anchor. This delays the decay of the mechanical properties of the bond hence the failure time by 30-60 min for load levels below 6% of the load-bearing capacity at ambient temperature MPa for bond stress.
- When designing bonded anchors directly exposed to fire, boundary conditions must take into account whether the metallic fixture transferring the load from the loading system to the rod is insulated or directly exposed to fire. This is associated to the intended configuration for the anchor inside the building.

The experimental work in this paper focused on two load ratios: 1.7% and 8.7% of the load-bearing capacity at ambient temperature. Since load ratio is one of the parameters most affecting the structural performance of bonded anchors under fire, other load ratios are advised to be undertaken in other studies to assess the influence of the studied parameters on the precision of failure prediction.

The current design method for bonded anchors under fire based on the resistance integration method was adopted in this paper. The predicted bond resistance and failure time for bonded anchors directly exposed to fire are influenced by insulation around the loading system. In order to precisely evaluate pull-out strength under fire of chemically bonded anchors, a second bonded anchor may be installed in the same concrete element as the loaded rod which is being tested. Furthermore, this anchor must be instrumented along the embedment depth of the anchor and must replicate the same testing conditions as the loaded one. Finally, more detailed guidelines are needed for performing pull-out tests on bonded anchors directly exposed to fire.

Acknowledgements

The experimental research presented in this paper was conducted at the fire-resistance laboratory at CSTB (Centre Scientifique et Technique du Bâtiment). The authors would like to acknowledge Dr. Mhd Amine Lahouar, Dr. Duc Toan Pham and Eng. Paul Lardet, Mr. Romuald Avenel, Mr. Stéphane Charuel, Mr. Luntala Diafunana, Mr. Jean-François Moller, Mr. Paulo Pangia Ngani and Mr. Florian Demoulin at CSTB for their contribution to this work.

References

- [1] Cook R. Behavior of chemically bonded anchors. *J Struct Eng* 1993;119(9):2744–62.
- [2] Reis J. Effect of temperature on the mechanical properties of polymer mortars. *Mater Res* 2012;15(4):645–9.
- [3] Rodrigues J., Laím L. Experimental investigation on the structural response of T, T-block and T-Perfobond shear connectors at elevated temperatures. *Engineering Structures* 2014; 75: 299–314.
- [4] Adams R, Coppendale J, Mallick V, Al-hamdani H. The effect of temperature on the strength of adhesive joints. *Int J Adhes Adhes* 1992;12(3):185–90.
- [5] M.C.S. Ribeiro, P.J.R.O. Nóvoa, A.J.M. Ferreira, A.T. Marques. Flexural performance of polyester and epoxy polymer mortars under severe thermal conditions. *Cem Compos*; 2004; (26): p. 803-9.
- [6] Frigione, M., Aiello, M. & Naddeo, C. Water effects on the bond strength of concrete/concrete adhesive joints. *Construction and building materials*. 2006; 20; p. 957-70.
- [7] EOTA TR 020. Evaluation of Anchorages in Concrete concerning Resistance to Fire. European Organization for Technical Approvals Technical report no. 20; May 2005.
- [8] Reichert M, Thiele C. Qualification of bonded anchors in case of fire. In: Proceedings of the 3rd international symposium on Connections between Steel and Concrete. Stuttgart, Germany, September 2017; p. 1191-9.
- [9] EOTA, EAD 330087-00-0601, Systems for post-installed rebar connections with mortar. no. EOTA14-33-0087-06.01; July 2015.
- [10] Pinoteau N, Heck J. V, Rivillon Ph, Avenel R, Pimienta P, Guillet T, Rémond S. Prediction of failure of a cantilever-wall connection using post-installed rebars under thermal loading. *Eng Struct J* 2013; 56: p. 1607-19.
- [11] Lahouar M A, Pinoteau N, Caron J-F, Forêt G, Mège R. A nonlinear shear-lag model applied to chemical anchors subjected to a temperature distribution. *Int J Adhes Adhes* 2018; 84: 438-50.
- [12] Lahouar M A, Pinoteau N, Caron J-F, Forêt G, Guillet T, Mège R. Chemically-bonded post-installed steel rebars in a full scale slab-wall connection subjected to the standard fire (ISO 834-1). In: Proceedings of the 3rd international symposium on Connections between Steel and Concrete. Stuttgart, Germany, September 2017; p. 1119-30.
- [13] Lakhani H, Hofmann J. A numerical method to evaluate the pull-out strength of bonded anchors under fire. In: Proceedings of the 3rd international symposium on Connections between Steel and Concrete. Stuttgart, Germany, September 2017; p. 1179-90.
- [14] Bouzaoui L, Li A. Analysis of steel/concrete interfacial shear stress by means of pull out test. *Int J Adhes Adhes* April 2008; 28(3):101–8.
- [15] Lahouar MA, Caron J-F, Pinoteau N, Forêt G, Benzarti K. Mechanical behavior of adhesive anchors under high temperature exposure: Experimental investigation. *International Journal of Adhesion and Adhesives* 2017; 78: 200–211.
- [16] Spieth H, Ozbolt J, Eligehausen A, Appl J. Numerical and experimental analysis of post-installed rebars spliced with cast-in-place rebars. *International symposium on connections between steel and concrete*, vol. 889, RILEM Publications, Stuttgart; 2001.
- [17] Eligehausen R, Mallée R, Silva J. F. *Anchorage in Concrete Construction*. Ernst & Sohn. 2006.
- [18] Pinoteau N, Rémond S, Pimienta P, Guillet T, Rivillon P. Post-installed rebars in concrete under fire. In: Proceedings of session 5-5 *fib* symposium on composites and hybrid. Czech, Prague 2011; p. 1197-200.
- [19] ISO 834-1 International Standard, Fire-resistance tests – Elements of building construction – Part 1: General requirements. First edition, 15 September 1999.
- [20] Paterson WS. I Indicative fire tests on fixings. Technical Note 92. London: Construction industry research and information association; 1978.
- [21] Pinoteau N [Ph.D thesis]: Behavior of post-installed rebars in concrete under fire, Lille: University of Lille (France). <https://ori-nuxeo.univ-lille1.fr/nuxeo/site/esupversions/de94303f-5d72-4f61-9183-515ff08b490b>; 2013.
- [22] Lahouar M A, Caron J-F, Pinoteau N, Forêt G, Benzarti K. Mechanical behavior of adhesive anchors under high temperature exposure: Experimental investigation. *Int J Adhes Adhes* 2017; 78: p. 200-11.
- [23] Van Gemart D. Force transfer in epoxy bonded steel/concrete joints. *Int J Adhes Adhes* October 1980; 1(2): p. 67–72.
- [24] Çolak A. Parametric study of factors affecting the pull-out strength of steel rods bonded into precast concrete panels. *Int J Adhes Adhes* 2001; 21(6): p. 487–93.

- [25] Çolak A. Estimation of ultimate tension load of methylmethacrylate bonded steel rods into concrete. *Int J Adhes Adhes* December 2007;27(8):653–60.
- [26] EN 1992-1-2: Eurocode 2: Design of concrete structures – Part 1-2: General rules – Structural fire design. July 2008.
- [27] EN 1363-1: 1999-10, Fire resistance tests Part 1: General requirements. 2012.
- [28] Lahouar M A, Pinoteau N, Caron J-F, Forêt, Rivillon Ph. Fire design of post-installed rebars: Full-scale validation test on a $2.94 \times 2 \times 0.15$ m³ concrete slab subjected to ISO 834-1 fire. *Eng Struct* J 2018; 174: p. 81-94.
- [29] Tian K., Ožbolt J., Periškić G., Hofmann J. Concrete edge failure of single headed stud anchors exposed to fire and loaded in shear: Experimental and numerical study. *Fire Safety Journal* 2018; 100: 32–44.
- [30] Lahouar M A [Ph.D thesis]: Fire resistance of chemical anchors in wood and concrete, Paris: University of Paris-Est (France). <https://pastel.archives-ouvertes.fr/tel-01738712/document>; 2018.

Discussion and analysis

Prior to the study conducted in this paper, a review of the literature was done to assess the influence of adopting tests on PIRs as entry data for design of bonded anchors under fire. Reichert and Thiele (2017) piloted a research project on the behavior of bonded anchors under fire at the university of Kaiserslautern. This project addressed the question in hand by means of tests according to EAD 330087-00-0601 (2018) on PIRs and bonded anchors using the same product for both applications. A nominal diameter of 12 mm was used as required in the EAD. There were two differences in installation parameters between PIRs and bonded anchors: 1) for PIRs, ribbed bars with a relative rib area of 0.076 were used whereas threaded rods were used for bonded anchors, 2) diameter of drilled hole was 16 mm (2 mm clearance between the rebar and the hole) for PIRs whereas it was 14 mm (1 mm clearance between the rod and the hole). Results indicated that a negligible difference was observed between both curves, where bonded anchors showed a slightly higher bond strength compared to PIRs (Fig. 70). The same tests were repeated using GEWI (high yield screwable steel with rolled on threads on both sides) rebars compared to PIRs (Fig. 71) with a slight advantage for the bond strength vs. temperature relationship of GEWI rebars. Therefore, it was concluded that adopting tests on PIRs for design of bonded anchors has a negligible influence. Should this influence be considered, the results would be on the conservative side due to the lower values of bond strength obtained from PIRs.

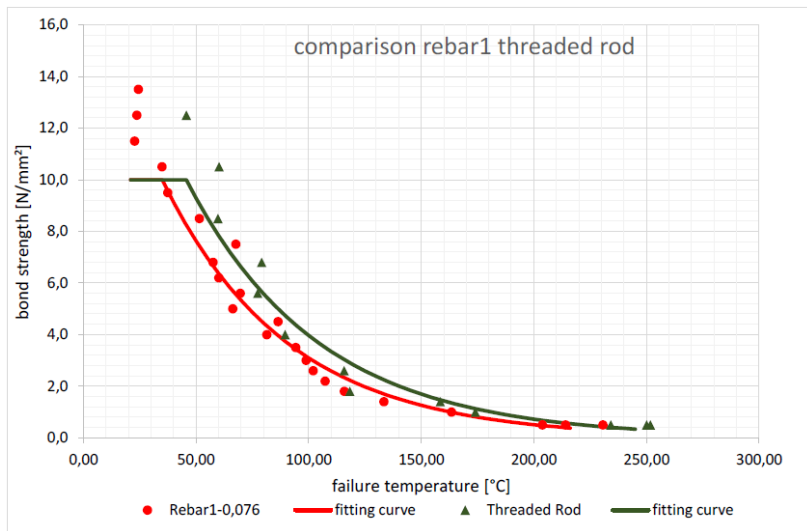


Fig. 70: Comparison of the bond strength vs. temperature relationship between PIRs and bonded anchors according (tests acc. EAD 330087-00-0601 using the same adhesive) Reichert and Thiele (2017)

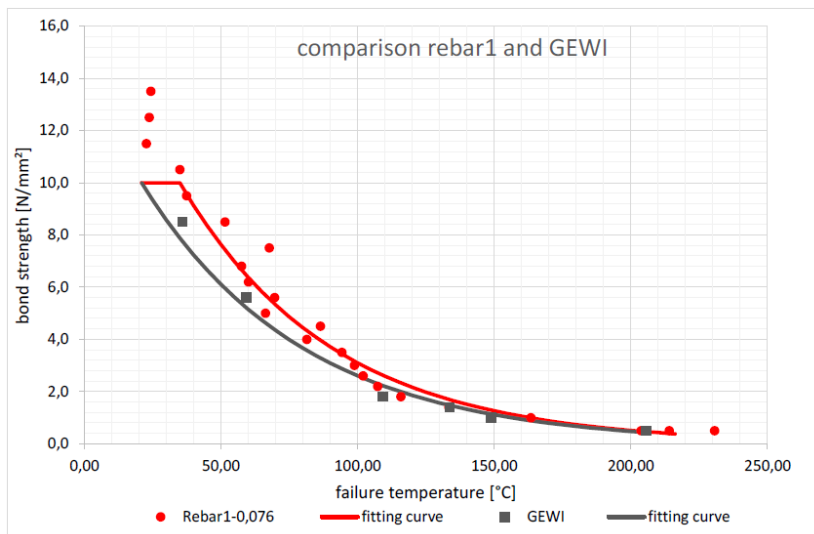


Fig. 71: Comparison of the bond strength vs. temperature relationship between PIRs and GEWI bonded anchors according (tests acc. EAD 330087-00-0601 using the same adhesive) Reichert and Thiele (2017)

The study conducted in the paper allows to conclude which test configuration is more suitable for fire tests of bonded anchors. If the objective is a product evaluation of the anchor, Configuration 1 in Fig. 72 is recommended to solely assess the fire resistance of the anchor. Nonetheless, it was shown that Configuration 2 in Fig. 72 can be very beneficial in terms of delaying the fire degradation of the bond due to the presence of the insulating material. Therefore, if a system qualification is the objective (anchor + fixture + insulation), it is recommended to precise the installation instructions of the insulating material in addition to the regular installation instructions of the anchor. Indeed, the behavior under fire may vary depending on the applied type of insulation, its thermal properties and its thickness. In addition, it is recommended to insulate all extended parts of the anchor rod and steel fixture to maximize insulation and minimize the effect of high diffusivity of steel. Additional insulation can be applied on the concrete surface near the anchor but as a second measure as the insulation of steel parts is more effective. Finally, it is clear that the current text stated in the TR 020 leaves the door open for several interpretations of the fire test configuration. Therefore, any future guidelines should be clear enough to avoid this type of controllable difference.

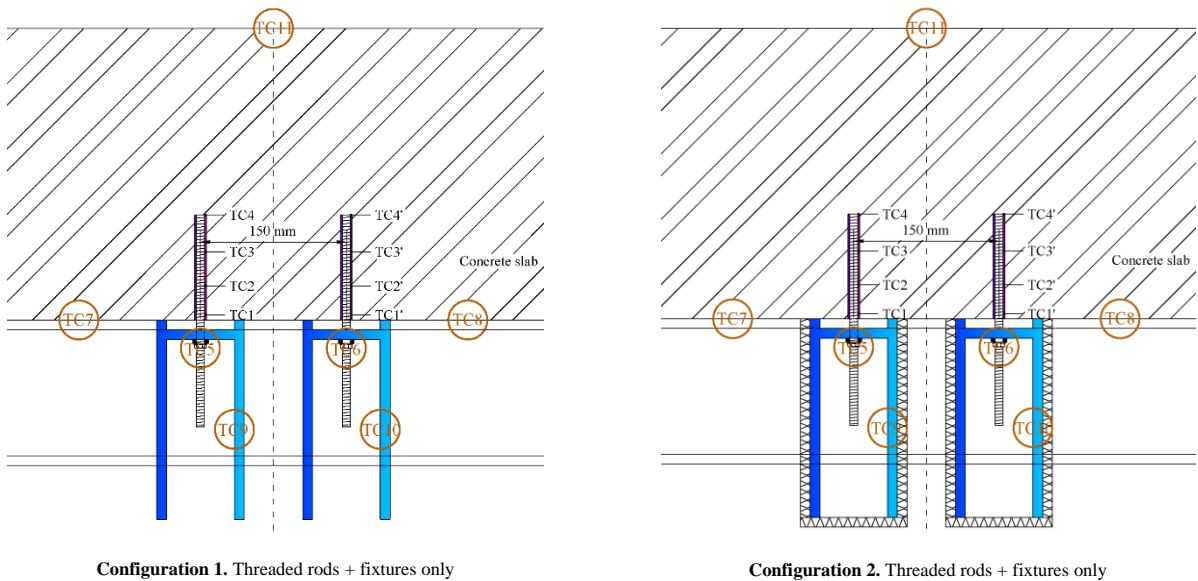


Fig. 72: Different configurations for fire tests on bonded anchors

Chapter III: Development of a 3D numerical model for the design of bonded anchors in uncracked concrete under ISO 834 fire

Chapter III resumes the paper entitled “**Numerical investigation of parameters influencing fire evaluation tests of chemically bonded anchors in uncracked concrete**” published on January 27, 2020 in the Journal of Engineering Structures. This paper focuses on the development of a numerical model first for the design of bonded anchors under fire, then after validation, for numerical investigation of parameters influencing fire tests.

Objectives

After considering the right configuration of the bonded anchor to be tested according to the previously presented results in Chapter II, the testing method can be applied on fire evaluation tests on bonded anchors. The obtained fire resistance from standard fire tests can be considered as a reference for validating any design method. Therefore, this chapter proposes a design method based on the existing knowledge on the testing configuration and the numerical modelling approach for the design of PIRs under fire (i.e. thermal calculations coupled with Pinoteau’s method). First, the design method should provide representative temperature profiles along the embedment depth of the bonded anchors compared to fire test measurements. Only then, these temperature profiles can be used as entry data for Pinoteau’s method (Resistance Integration Method). Indeed, stress profiles are obtained based on previous characterization of the adhesive at high temperatures. Therefore, any uncertainty or unconservativeness on temperature profiles can be reflected in the calculated stress profiles, hence the fire resistance.

This chapter has two main objectives:

1. Propose a model for the design of bonded anchors under fire using thermal calculations (FE simulations) used as entry data for Pinoteau’s method (Resistance Integration Method):
This paper presents different approaches for thermal modelling of anchors. In the literature, 2D plane modelling is very common but was never validated. The validation can be conducted through comparison of temperature profiles measured along the embedment depth of anchors in fire tests to those calculated by FE simulations. It was found that 2D plane modelling is not in agreement with experimental measurements. 3D modelling is proposed as a more representative solution. Both 2D plane and 3D approaches were coupled with Pinoteau’s method to calculate the fire resistance of bonded anchors for the 2 main test configurations evoked in the previous chapter. 3D modelling was found better representative of temperature profiles and yielded less conservative fire resistance than 2D plane modelling.
2. Investigate additional parameters influencing fire tests of bonded anchors:
Some parameters were left uninvestigated in the previous chapter. Therefore, a parametric study was conducted after validation of the 3D model on the remaining untested parameters.

Paper reference:

Al-Mansouri O, Mège R, Pinoteau N, Guillet T, Piccinin R, McBride K, Rémond S. Numerical investigation of parameters influencing fire evaluation tests of chemically bonded anchors in uncracked concrete. Eng Struct J 2020;209:110297.

NUMERICAL INVESTIGATION OF PARAMETERS INFLUENCING FIRE EVALUATION TESTS OF CHEMICALLY BONDED ANCHORS IN UNCRACKED CONCRETE

Omar Al-Mansouri^{a,b}, Romain Mège^a, Nicolas Pinoteau^a, Thierry Guillet^a, Roberto Piccinin^c, Kenton McBride^c, Sébastien Rémond^d

^a Université Paris-Est, Centre Scientifique et Technique du Bâtiment (CSTB), 84 avenue Jean Jaurès, Champs-sur-Marne, 77447 Marne-la-Vallée Cedex 2, France

^b IMT Lille-Douai, Univ. Lille, EA 4515 – LGCgE, Département Génie Civil & Environnemental, F-59000 Lille, France.

^c Hilti Corp., Schaan, Principality of Lichtenstein.

^d Univ Orléans, Univ Tours, INSA CVL, LaMÉ, EA 7494, France.

Corresponding author's e-mail: omar.almansouri@cstb.fr

Abstract

European guidelines for fire performance evaluation of post-installed anchoring systems are limited to mechanical (e.g. expansive, undercut) mechanisms of load transfer and the steel failure mode, whereas the adhesive bond mechanism remains unaccounted for in chemically bonded anchors. Furthermore, current evaluation methods do not account for the influence of practical testing conditions on temperature profiles along the bonded depth. This paper presents 3D finite element thermal simulations of chemically bonded anchors in uncracked concrete exposed to ISO 834 fire conditions with comparisons to experimental specimens. Five parameters representing application and testing conditions are investigated to assess their influence on temperature profiles along the embedment depth of bonded anchors. A numerical model is proposed based on the results of the numerical simulations to determine thermal data necessary for predicting the load-bearing capacities of bonded anchors using the Resistance Integration Method. The model adopts Eurocode material properties for concrete and steel, with 3D analysis yielding conservative capacity prediction compared to physical fire tests. 3D and 2D simulation results are compared, demonstrating that modelling using 2D heat transfer analysis yields inaccurate temperature profiles compared to 3D modelling. After experimental validation of the proposed model, additional parameters are explored in a numerical parametric study: embedded depth, external length of the anchor element, insulation of the anchor element, and insulation of the concrete element. Results show that the embedded depth has a significant influence on temperature profiles along the bond. Moreover, the external length of the anchor influences temperature profiles, but not beyond 20 mm from the concrete surface.

Keywords: adhesive resin, bonded anchor, fire tests, thermal distribution, numerical model, Resistance Integration Method.

1. Introduction

Post-installed anchoring systems may be split into two categories: (1) mechanical and bonded anchors used to transfer the combination of tensile and shear loads from a steel fixture to a concrete substrate and (2) post-installed reinforcement (PIR) used to connect new reinforced concrete elements to existing concrete. Post-installed chemically bonded anchoring systems are used in new and existing reinforced concrete structures as an alternative to cast-in-place solutions and where an anchoring location is unplanned or requires remediation. The bonding material may consist of combinations of polymeric resin, cement, other admixtures, and filling materials. Resins used in post-installed bonded anchors include polyester, vinylester, and epoxy resins [1]. Load is transferred to concrete through adhesive bond and friction, producing bond stresses that are nearly uniformly distributed along the bonded embedment depth, in contrast to headed and post-installed mechanical anchors where load introduction into concrete is concentrated at the end of the anchorage [2]. Resins used in bonded anchors are viscoelastic and therefore demonstrate creep deformation under sustained loads [3].

Studies have demonstrated that the mechanical behavior of bonded anchors is influenced by many factors including geometry, material properties, installation procedure, and environmental factors such as moisture and temperature [4-7]. The mechanical properties of adhesive resins are particularly temperature dependent [8]. In fire conditions, structural members are exposed to rapid temperature increases, producing temperature gradients along the

embedment of the bonded anchors. Elevated temperatures degrade material properties of steel [9], concrete [10, 11], and resin [12], thus reducing the load-bearing capacity of the connection.

Different resin types exhibit varying sensitivities to increases in temperature. Investigations have shown, for example, that epoxy resins are more sensitive to temperature than polyester mortars [13]. In general, the effect of temperature on polymeric materials can be quantified by the glass transition temperature (T_g) [14], beyond which a reduction in stiffness and ultimate capacity are observed [15]. Studies on bonded PIR (post-installed reinforcement) showed that temperature increases to values below the glass transition temperature lead to an enhancement of the material properties of the resin. This is linked to the accelerated curing of the resin. When the glass transition temperature is exceeded in a loaded anchor, changes in physical state and viscosity occur, leading to a different stress distribution along the bonded embedment [16, 17]. Another investigation focused on the effect of heating rates [18], where it was found that high heating rates can lead to an initial thermal gradient along the steel member and therefore to a redistribution of bond stress.

Presently, the guidelines in EOTA TR 020 [19] address fire evaluation of mechanical anchors for all failure modes, but bonded anchors are only evaluated for the steel failure mode. Design failure modes for bonded anchors under tensile loading are concrete cone failure, steel failure, pull-out failure of the anchor, splitting failure of concrete and combined cone/pull-out failure [20]. Research studies [21, 22] showed that under fire conditions, pull-out may occur more frequently than other failure modes for common ranges of bonded anchor diameter and embedment. Researchers have established that there is a need for an accurate evaluation and design method for bonded anchors to complete the existing guidelines in EOTA TR 020 [19]. In these guidelines, it is permitted to insulate the steel fixture that transfers loads to anchors preventing the fixture from failing before the anchor. In a previous experimental work [24] the current authors presented three possible configurations of an anchor inside a building: direct exposure to fire, presence of a metallic fixture, and presence of insulation around the fixture. It was shown that, under ISO 834 fire conditions [23], the insulated configuration may produce an unconservative estimation of bond strength compared to the configuration where the anchor was directly exposed to fire.

Prediction of the load-bearing capacity of bonded anchors has been investigated in multiple research studies. Thiele and Reichert [21] investigated different configurations of bonded anchors under fire conditions, also concluding that the current guidelines in EOTA TR 020 should be extended [19]. Lakhani and Hofmann [22] used finite element simulations to study the behavior of bonded anchors at high temperatures with a 2D model. This study recommended the Resistance Integration Method, which demonstrated promising results in the experimental work of Pinoteau et al. [18] and Lahouar et al. [25, 26]. Lakhani and Hofmann [22] concluded that the thermal distribution depends on the fire scenario under consideration (e.g. the ISO 834 fire and a cooling phase vs Hydrocarbon fire).

Lakhani and Hofmann [22,27] proposed a model to determine the load-bearing capacity of bonded anchoring systems (bonded anchors and PIR) under fire conditions. Their numerical results were compared to the experimental work of Muciaccia et al. [28] and Lahouar et al. [29]. The proposed model by Lakhani and Hofmann is based on the resolution of transient heat transfer using an implicit finite element scheme and an iterative solver. Only the concrete bearing element and the steel of the anchor were modelled and the adhesive resin was ignored, although [21] demonstrated that when the resin acts as an insulating material (having higher insulating properties than the insulating properties of concrete), it results in conservative calculations when it is not modelled. Their work highlighted the influence of different configurations of bonded anchors on thermal diffusion (e.g. direct exposure to fire, presence of an insulated fixture) and showed that the common modelling assumption of ignoring the reinforcing steel during heat transfer analysis may not be realistic due to the difference of thermal properties between steel and concrete.

Lakhani and Hofmann [27] performed 2D analysis with Cartesian coordinates on the failure of a post-installed cantilever floor modeling the test conducted by Lahouar et al. [29]. The experimental test failed at 117 min, whereas the predicted failure time by [27] was 80 min. For this example, temperature profiles calculated using 2D analysis modelling both concrete and the steel of the PIR (model A) for early exposure periods (e.g. 15 min) produce lower temperatures than 2D analysis accounting only for concrete and neglecting the modelling of steel (model B). This could be attributed to the fact that 2D analysis implies an infinite length of steel in the unmodelled 3rd dimension, whereas 2D analysis accounting only for concrete assumes that PIR has the same temperature as concrete at the same distance from the fire exposed surface. Furthermore, the model A did not account for the extended part of the anchor outside the concrete (see §2.1.).

Given the absence of generalized data and methodologies for fire-resistive design of anchoring systems, practical studies have been oriented toward providing solutions. Tian et al. [30] conducted an experimental study to enhance understanding of the behavior of mechanical anchors loaded in shear close to an edge under fire conditions. Bosnjak et al. [31] proposed a 3D model for the resistance of post-installed reinforcement in concrete after exposure to fire for one-sided and three-sided fire exposure. Halvička and Lublůy [32] proposed a design method for concrete cone failure of bonded anchors in thermally damaged concrete. Nevertheless, a general assessment and design concept for fire-resistance of bonded anchoring systems remains absent from guideline documents.

This paper presents a numerical study of the temperature profiles of bonded anchors exposed to ISO 834 fire conditions [23] for use in predicting the load-bearing capacity. A heat transfer analysis was conducted using ANSYS 3D finite element analysis to obtain the temporal and spatial distribution of temperature [Eq. (1)]. Using the output data of temperature profiles with the existing bond stress vs. temperature relationship of the adhesive resin, the load-bearing capacity of the anchor was computed by numerically integrating the temperature-dependent bond stress capacity along the embedment depth of the anchor. The results of this model were compared to test results from pull-out fire tests on bonded anchors with different configurations studied in [24]. After the validation of the model, a parametric study was conducted to investigate the influence of other parameters on the precision of evaluation tests of bonded anchors under fire conditions. The results of this 3D model were compared to a commonly used 2D Cartesian coordinate system without modelling the part of the anchor extending above the concrete surface.

Capacity prediction using the Resistance Integration Method depends on accurate knowledge of temperature profiles along the bonded embedment. Testing under ISO 834 fire conditions [23] is influenced by many parameters including fixture configuration and modelling assumptions. The 3D model was validated against empirical results for the following configurations:

- Direct exposure of the anchorage to fire.
- Insulation of fixtures.

The model was then used for the investigation of additional parameters that may influence temperature profiles along the embedment depth of the anchor under ISO 834 fire [23] exposure:

- Extended length of the anchor above the concrete surface.
- Embedded length of the anchor inside concrete.
- Concrete element insulation.

2. 3D model using ANSYS

This section describes the model used for the determination of the load-bearing capacity under ISO 834 fire conditions [23] for bonded anchors in uncracked concrete. Temperature profiles from this model are coupled with the Resistance Integration Method (see §2.2) for the determination of bond strength.

2.1. Description of the 3D model

The model consists of solving 3D transient heat transfer equations to obtain temperature distribution at any given time of fire exposure. Concrete and steel components are modeled, but the resin is conservatively ignored because the thermal properties are product dependent. Because polymer materials possess insulating properties, a model that takes only into account steel and concrete and ignores the resin yields higher temperature profiles. Material properties of concrete and steel are obtained from Eurocode 2 [10]. The fire exposed surface is subjected to both radiative and convective fluxes of the ISO 834 fire [23].

The numerical model presented in this paper observes the following characteristics

- The bonded anchor resin is not modeled.
- Steel threads are not modeled.
- The concrete remains uncracked.
- Concrete spalling is ignored.
- The fire exposed surface of all elements is subjected to convective and radiative fluxes of ISO 834 fire temperatures [23] on all sides.

- The unexposed fire surface of concrete beams is subjected to convective and radiative fluxes of ambient air at 20°C.
- Slip of anchors is ignored.

During a fire, heat transfer occurs between fire and exposed elements at the boundaries via convection and radiation. The heat propagates inside the members via conduction. ANSYS solves the governing differential equation for 3D transient heat conduction using implicit scheme and iterative solver [Eq. 8].

$$\rho c \frac{\partial T}{\partial t} = k \left(\frac{\partial^2 T}{\partial x^2} + \frac{\partial^2 T}{\partial y^2} + \frac{\partial^2 T}{\partial z^2} \right) \dots \text{ [Eq. 8]}$$

The 3D model represents the anchor as a cylinder inside a concrete beam with modelling of the extended and embedded length of the steel anchor element (Fig. 73).

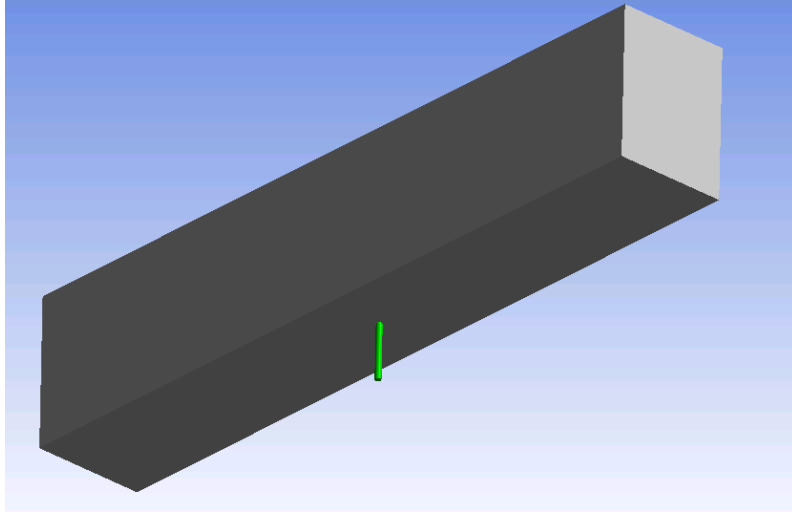


Fig. 73: Anchors directly exposed to fire using 3D modelling in ANSYS

Eq. 9 describes the Neumann boundary condition satisfied at the fire-exposed surface:

$$-k \frac{\partial T}{\partial n} = h_{\text{fire}} \cdot (T_s - T_{\text{fire}}) + \varepsilon \cdot \sigma \cdot (T_s^4 - T_{\text{fire}}^4) \dots \text{ [Eq. 9]}$$

Eq. 10 describes the Neumann boundary condition satisfied at insulated surfaces:

$$-k \frac{\partial T}{\partial n} = 0 \dots \text{ [Eq. 10]}$$

Eq. 11 describes the Neumann boundary condition satisfied at the upper surface of the beam exposed to ambient air at 20°C:

$$\dot{q}_{\text{total}} = h_{\text{air}} \cdot (T_s - T_{\text{air}}) + \varepsilon \cdot \sigma \cdot (T_s^4 - T_{\text{air}}^4) \dots \text{ [Eq. 11]}$$

Where:

- \dot{q}_{total} is the total heat flux applied to the surface.
- k is the thermal conductivity (W/m.K).
- ρ is the mass density (kg/m³).
- c is the specific heat (J/kg.K).
- h_{fire} is the convective heat transfer coefficient for the fire exposed surface (25 W/m².K).
- h_{air} is the convective heat transfer coefficient for the surface exposed to air at 20°C (4 W/m².K).
- ε is surface emissivity (0.7).
- σ is the Boltzmann constant (5.667×10⁻⁸ W/m².K⁴).
- T_s is the solid surface temperature (K).
- T_{fire} is gas temperature inside the furnace as a function of time (K).
- T_{air} is ambient air temperature (293 K).
- t is time.

Boundary conditions are represented in a profile view of the 3D model in Fig. 74.

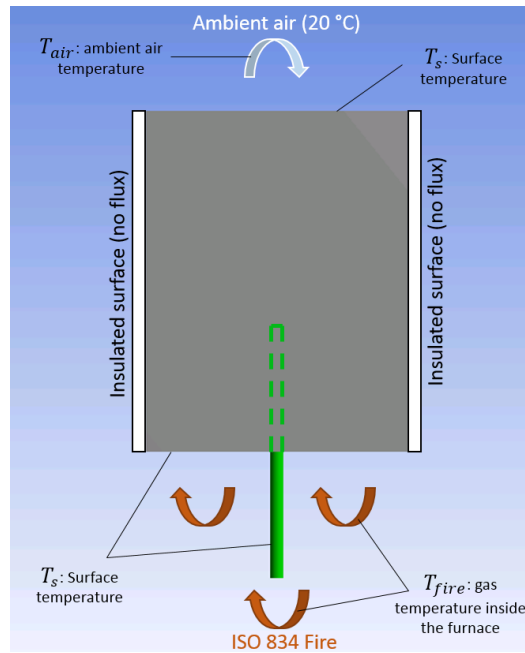


Fig. 74: Boundary conditions applied in the 3D heat transfer analysis for anchors directly exposed to fire.

Numerical studies of bonded anchors commonly model transient heat transfer in 2D using Cartesian coordinates and neglect the portion of the anchor outside the concrete surface. Eq. 12 is the governing equation solved to obtain the spatial and temporal temperature distribution in 2D.

$$\rho c \frac{\partial T}{\partial t} = k \left(\frac{\partial^2 T}{\partial x^2} + \frac{\partial^2 T}{\partial y^2} \right) \dots \text{ [Eq. 12]}$$

The 2D model implies that the anchor is a long plate inside the concrete beam as illustrated in Fig. 75, which overrepresents the quantity of steel in the concrete member.

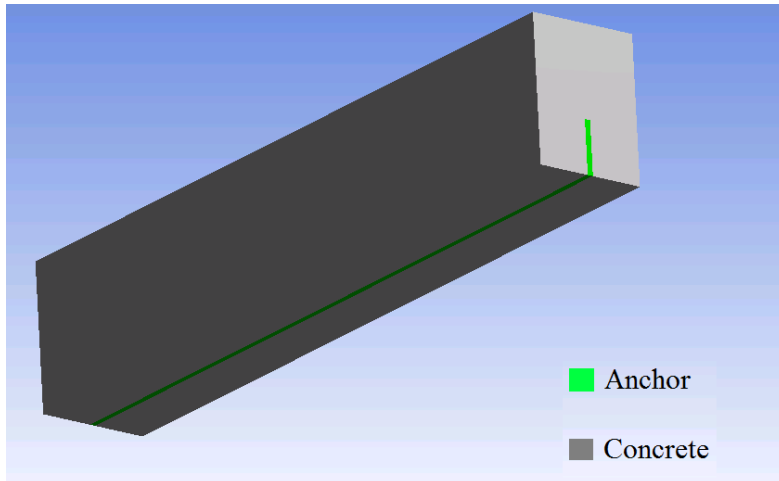


Fig. 75: Anchor directly exposed to fire using 2D modelling in ANSYS with Cartesian coordinates

Boundary conditions are represented in a profile view of the 3D model in Fig. 76.

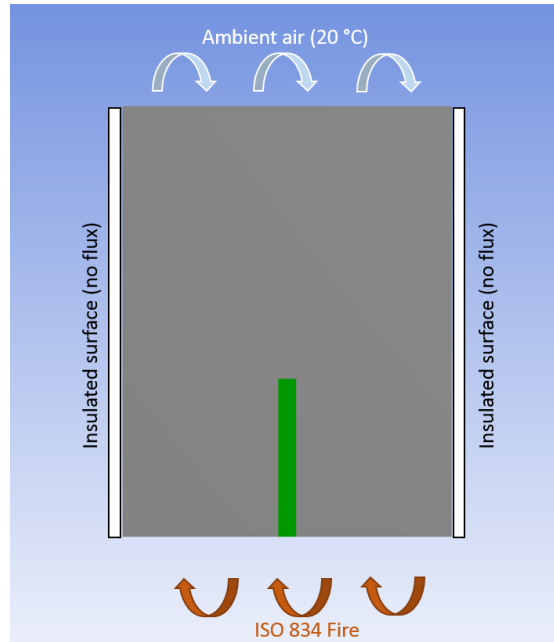
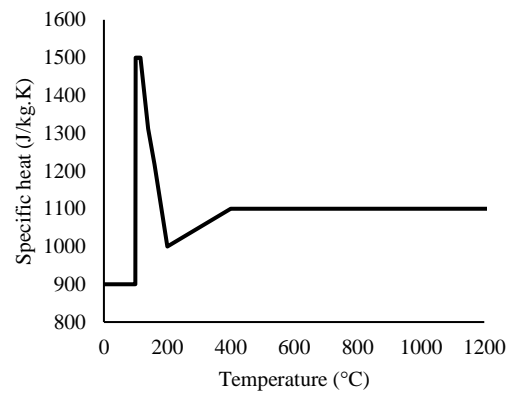
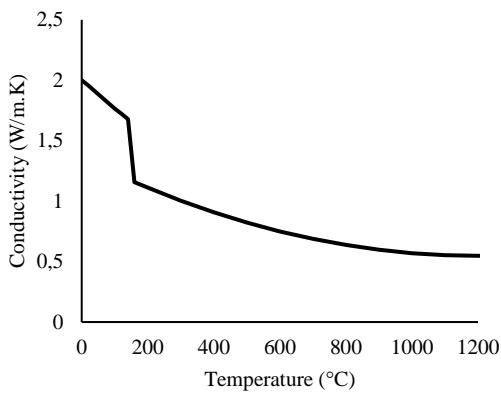
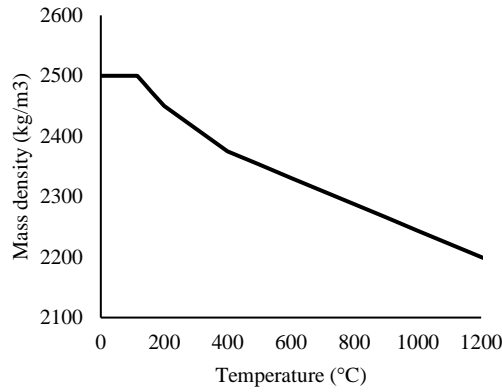


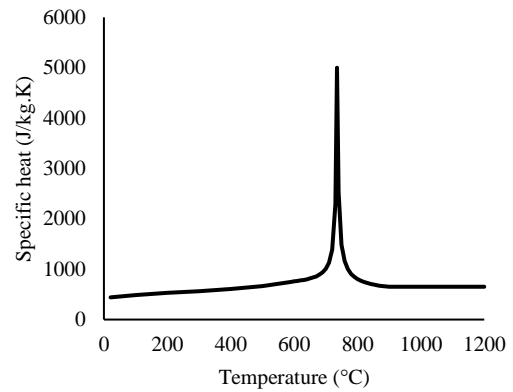
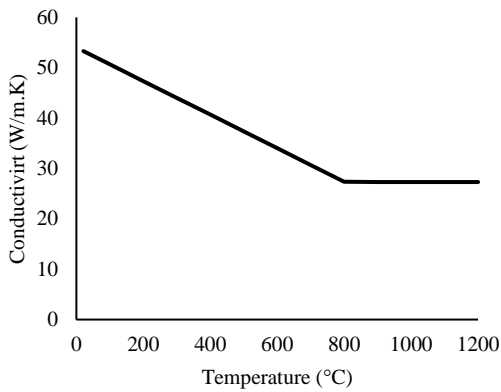
Fig. 76: Boundary conditions applied in the 2D heat transfer analysis for anchors directly exposed to fire.

Concrete and steel were modelled as solids in ANSYS. A bonded interface was chosen for the connection between steel and concrete. The bonded option in ANSYS allows no sliding or separation between faces or edges, resulting in perfect contact between the inner surface of the hole/concrete and the outer surface of the anchor/steel. No gaps are allowed with this option and the nodes of the mesh at the interface are superimposed from both concrete and steel surfaces. Thermal properties of concrete and carbon steel (conductivity, specific heat and mass density) are a function of temperature. The properties according to the French national annex in Eurocode 2 [10] for both materials were adopted in this study (Fig. 77). The mass density of the steel (7850 kg/m³) [9] is considered constant with respect to temperature.





(a) Concrete



(b) Carbon steel

Fig. 77: Variation of thermal properties of concrete and steel according to NF EN 1992-1-2 [10]

2.2. Prediction of the load-bearing capacity using the Resistance Integration Method

The transient heat transfer analysis conducted in the previous step produces the temperature profiles used by the Resistance Integration Method. In both 2D and 3D models, threads are ignored, and the nominal diameter is used. The bonded length is divided into 5-mm segments, where each segment is assigned a uniform temperature. The second input needed for the calculation of bond stress inside each segment of the anchor is the variation of bond stress capacity vs. temperature according to EAD 330087-00-0601 [33], for which bond stress capacities of the bonded anchor system are determined as a function of temperature. Each segment is therefore attributed an individual bond stress capacity based on the temperature associated with the segment. Numerical integration of the temperature-dependent bond stress capacity of all segments yields the predicted load-bearing capacity at any given moment of fire exposure.

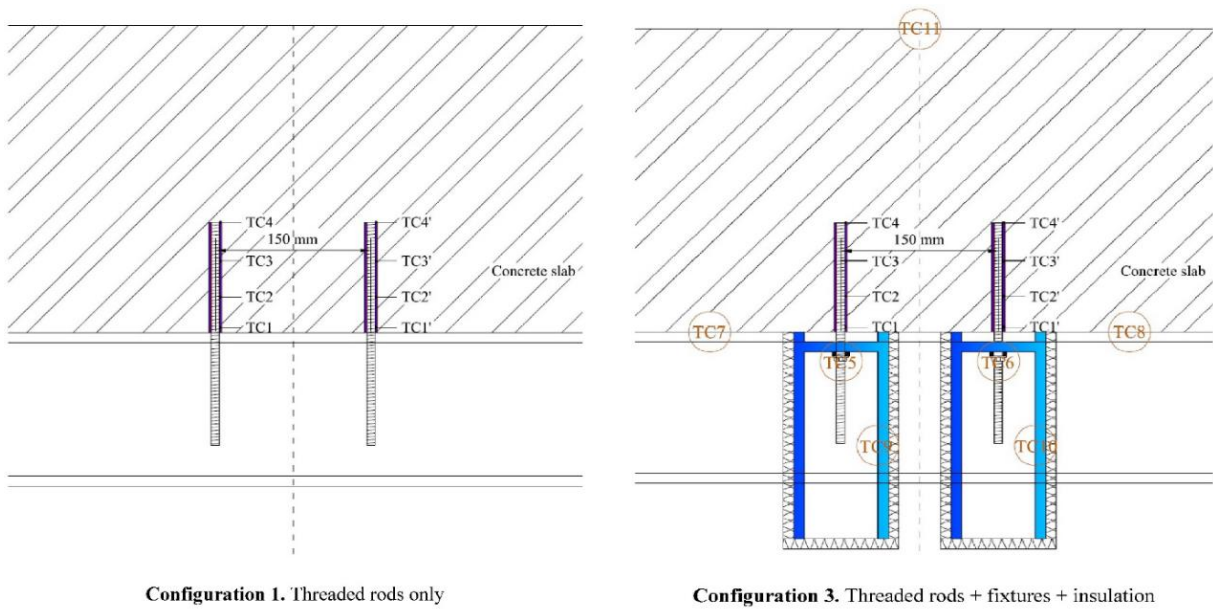


Fig. 78: Configurations of tested specimens in Al-Mansouri et al. [24]

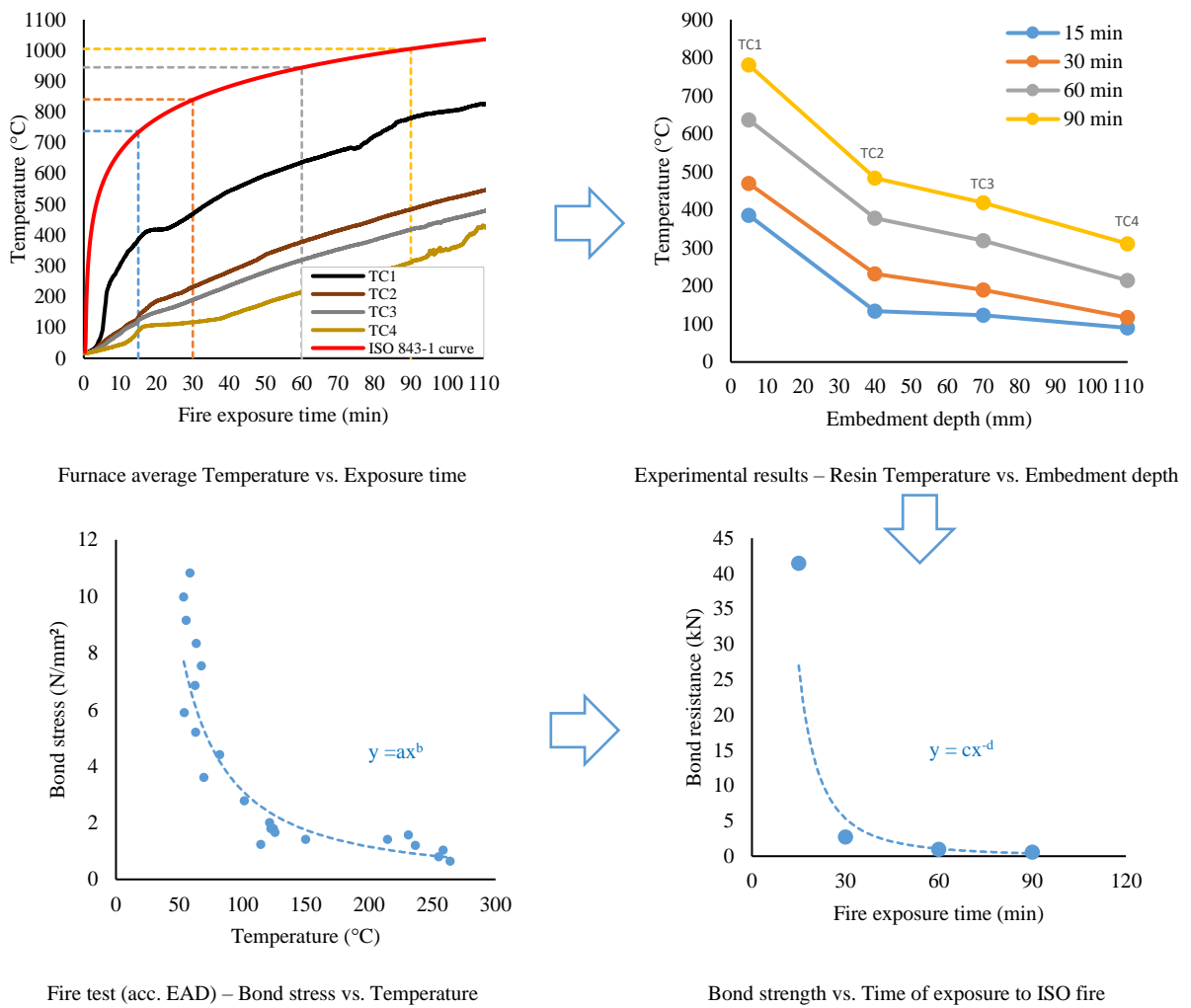


Fig. 79: Steps of the Resistance Integration Method

The bond capacity of the anchor at any given time is calculated according to Eq. 13:

$$N_{Rd,fire} = \pi \cdot d \cdot \int_0^{h_{ef}} f_{bd,0} \cdot k(\theta(x)) \cdot dx \dots \text{ [Eq. 13]}$$

Where: $N_{Rd,fire}$ is the capacity under fire conditions (N).

d is the diameter of the anchor (mm).

$f_{bd,0}$ is the design bond resistance at ambient temperature (N/mm²).

$k(\theta)$ is a reduction factor that depends on temperature.

$\theta(x)$ is the temperature distribution along the embedment depth of the anchor.

h_{ef} is the embedment depth of the anchor (mm).

3. Validation of the model

To validate the numerical model, experiments on loaded and unloaded specimens from [24] were selected. The experimental specimens consisted of post-installed bonded anchors with M12 threaded rods and a commercial resin in C20/25 uncracked concrete beams with 230 mm width, 1500 mm length and 300 mm beam depth. The experimental configurations were 1) anchors directly exposed to fire, 2) metallic fixtures attached to anchors, and 3) insulated fixtures (metallic fixtures filled and surrounded by 50 mm insulating material). Because fixtures without insulation demonstrated no significant influence on temperature profiles and the resulting predicted load-bearing capacity, only configurations 1) and 3) were used for the validation of the model.

For validating load-prediction using thermal results from 3D modelling, the Resistance Integration Method was applied on temperature profiles obtained from experimental pull-out tests under fire conditions in accordance with EOTA TR 020 [19]. Fig. 78 shows a side view of the studied configurations and Fig. 79 shows the steps of the bond Resistance Integration Method based on temperature profiles of the experimental tests adopted for validating the model. Fig. 80 shows the bond stress capacity vs. temperature relationship for the epoxy chemical resin obtained for the bonded anchor product used in the experimental specimens.

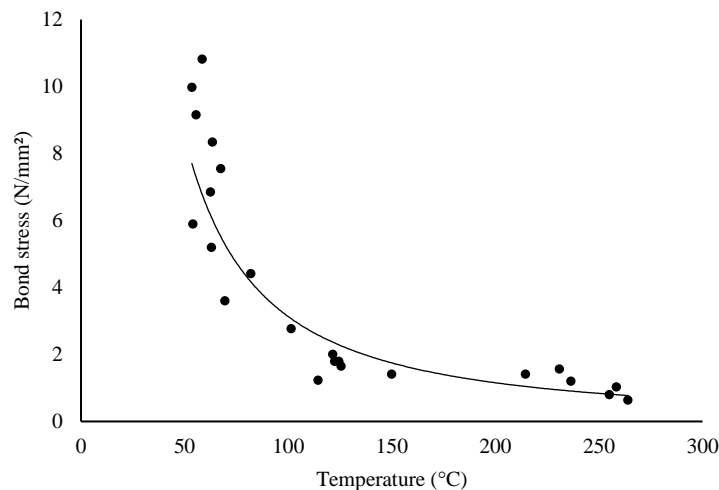


Fig. 80: Bond stress vs. temperature relationship for the bonded anchor product according to EAD 330087-00-0601 [33]

3.1. Anchors directly exposed to fire

For Configuration 1 in Fig. 78, M12 anchors directly exposed to fire were modelled with 110 mm embedment depth and 40 mm extended length outside the concrete surface. The numerical 3D model presented in Fig. 73 and Fig. 74 and the numerical 2D model presented in Fig. 75 and Fig. 76 represent configuration 1 in Fig. 78.

Fig. 81 shows a comparison between numerical (2D and 3D analysis) and experimental temperature profiles for anchors directly exposed to ISO 834 fire conditions [23]. Temperature profiles obtained numerically by 3D analysis are in agreement with experimental results. Numerical results of the 3D model produced higher temperatures due to several factors. The numerical model accounts for Eurocode conservative fire conditions which are represented at a homogeneous close distance from the exposed surface. In case of a real fire test, temperature measurement at concrete surface gives lower values than the numerical 3D model (1st thermocouple in experimental values in Fig. 81). The difference near the exposed surface of the anchor between numerical and experimental values is linked to the overestimation of temperature profiles in this area by the numerical model. In

addition, this difference could be explained by the absence of resin, which may serve as an insulator, in the model. Temperature measured at the deeper segments of the embedment, where fire conditions applied on the exposed surface and heat transfer occurs via conduction only, are in better agreement with the 3D model.

Simulation using 2D transient heat analysis yielded more homogeneous temperatures along the steel component compared to 3D analysis (Fig. 81). Compared to experimental results, this resulted in lower temperatures near the exposed surface and higher temperatures at the deeper parts of the anchor. The temperature inaccuracies are attributable to the inability of the geometry of 2D analysis to model the cylindrical anchor.

Comparison between the load-bearing capacity vs. fire exposure time relationships obtained numerically (both 2D and 3D analysis) and experimentally are plotted in Fig. 82. Four points were used to plot the bond strength vs. fire exposure time relationship, after which a power trend curve was fitted to the data. The numerically obtained curve based on 3D analysis yielded conservative results compared to the experimentally obtained curve. For example: for an applied load of 9 kN on M12 bonded anchor, the experimental result reached pull-out failure under ISO 834 fire conditions [23] at 29 min. The Resistance Integration Method predicted a failure time of 28 min using experimentally derived temperature profiles, 25 min using temperature profiles derived from 3D numerical analysis, and 19 min. using temperature profiles derived from 2D numerical analysis.

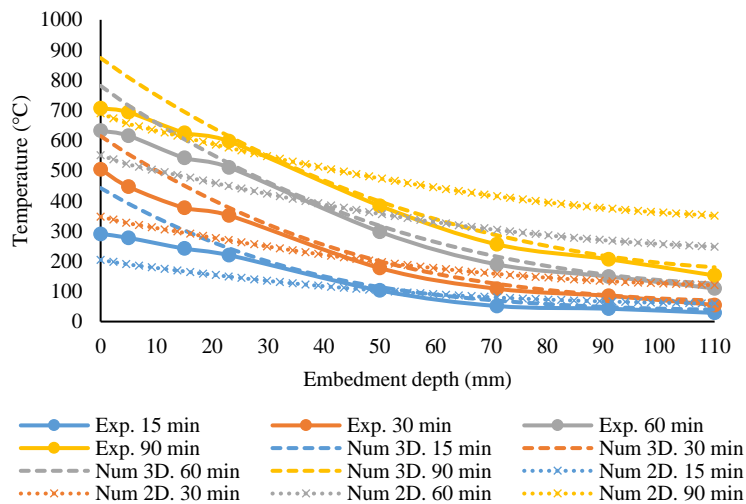


Fig. 81: Comparison between experimental and numerical (2D and 3D analysis) temperature profiles for M12 anchor directly exposed to fire

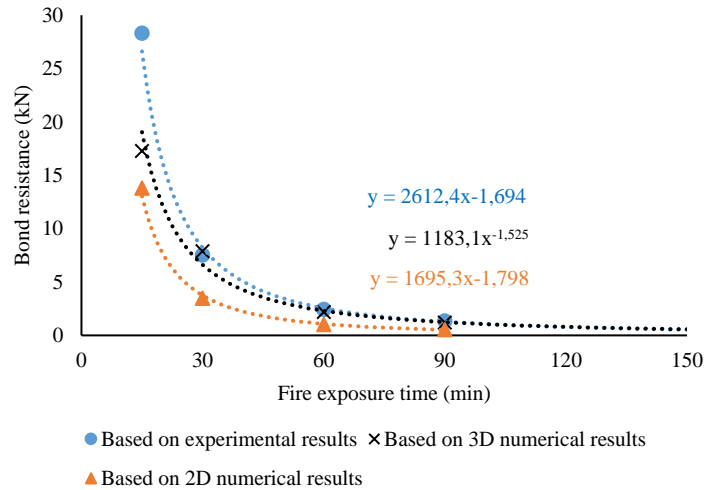


Fig. 82: Comparison between experimentally and numerically (2D and 3D analysis) predicted bond strength vs. fire exposure time relationships for anchors directly exposed to fire

3.2 Anchors with insulated fixtures

For Configuration 3 in Fig. 78 (anchors with insulated fixtures), the insulating material consisted of glass wool with a thickness of 50 mm. Thermal properties of the insulating material are plotted in Fig. 83. The M12 anchor was modelled with an embedment depth of 110 mm and extended length of 40 mm.

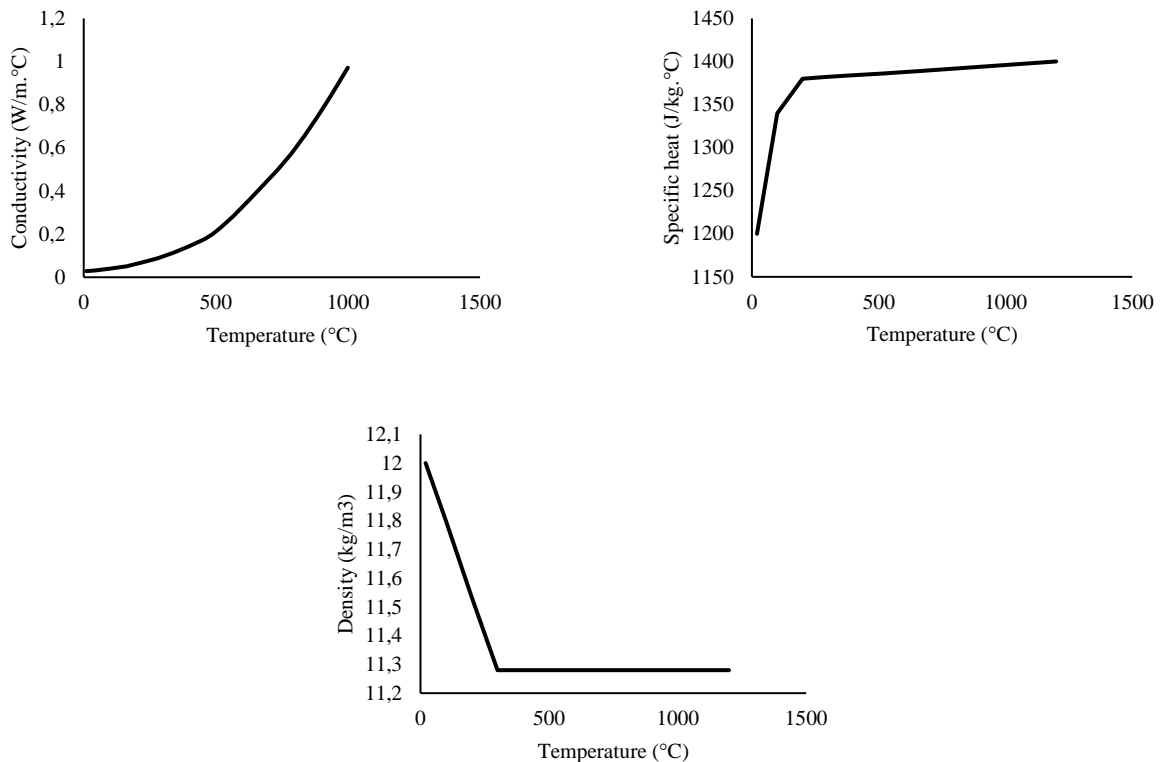


Fig. 83: Variation of thermal properties of the used insulating material

Fig. 84 shows a comparison between numerical and experimental temperature profiles for anchors with insulated fixtures. The Resistance Integration Method was applied to calculate the predicted load-bearing capacity vs. fire exposure time relationships. Comparison between load-bearing capacity vs. fire exposure time relationships obtained numerically (2D and 3D analysis) and experimentally are plotted in Fig. 84. The numerically obtained curve from 3D analysis is conservatively in agreement with the experimentally obtained curve. The small

difference observed between numerical (3D modelling) and experimental temperature profiles is due to conservative Eurocode material properties as described earlier in this section.

The presence of insulated fixtures is represented using 2D heat transfer analysis based on Cartesian coordinates by the same geometric configuration in Fig. 75. The difference between the two cases is that boundary conditions are only applied on the concrete surface beyond the insulated fixture and the fixture is not explicitly modelled. Therefore, Eq. 10 is applied on the surface where the insulated fixture is supposed to be. Fig. 85 represents boundary conditions applied in the 2D heat transfer analysis for anchors with insulated fixtures.

The presented model was used to study the case of anchors along with insulated fixtures based on the previous assumptions. Temperature profiles derived from 2D analysis produced lower temperatures than experimental results, which results in an unconservative prediction of the load-bearing capacity vs. fire exposure time using the Resistance Integration Method. The calculation of temperature profiles using 3D analysis modelling, both with fixture directly exposed to fire and with insulation, yields more accurate results (Fig. 86).

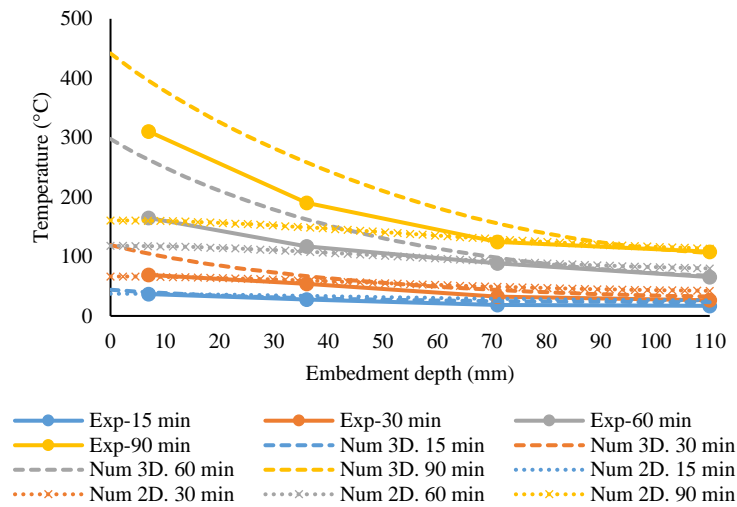


Fig. 84: Comparison between experimental and numerical (2D and 3D analysis) temperature profiles for M12 anchor with insulated fixtures

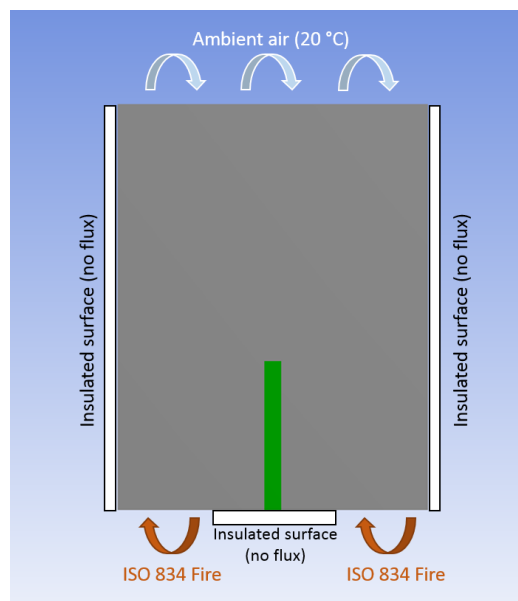


Fig. 85: Boundary conditions applied in the 2D heat transfer analysis for anchors with insulated fixtures

Comparisons between the load-bearing capacity vs. fire exposure time relationships obtained numerically (2D and 3D analyses) and experimentally are plotted in Fig. 86. The numerically obtained curve based on 3D analysis gave

safe results compared to the experimentally obtained curve. This may be attributed to the fact that the numerical model only takes into account steel and concrete, but in physical tests, the bonding material has an insulating effect on temperature profiles and reduces the thermal exchange between concrete and steel. Load prediction based on 2D analysis yielded unconservative results compared to experimental results.

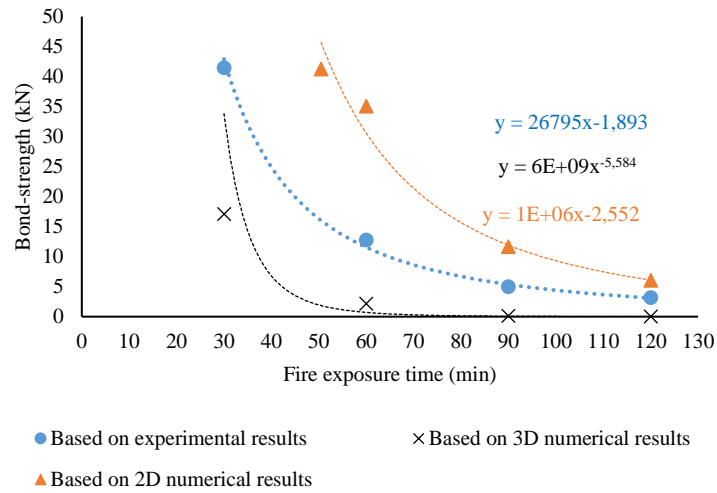


Fig. 86: Comparison between experimentally and numerically (2D and 3D analysis) predicted bond strength vs. fire exposure time relationships for M12 anchor with insulated fixtures

4. Parametric study

After validation of the proposed model, an expanded parametric study was conducted to investigate the effect of other parameters that may influence temperature profiles along the embedment depth of the anchor under ISO 834 fire [23] conditions. For the parametric study, material properties and specimen dimensions were identical to those used for the validation. For maximum influence of the boundary conditions of the ISO 834 fire, all studied parameters were conducted on anchors with configuration 1 in Fig. 78.

4.1 Extended part of the anchor

To assess the influence of the extended length of the anchor outside the concrete on the temperature distribution of bonded anchors under ISO 834 fire conditions [23], the proposed model was used to conduct simulations for multiple extended lengths (from no extended length to 15 diameters of extended length from concrete surface) for M8 and M12 diameters.

First, a series of simulations was conducted on an embedment depth of $h_{ef} = 10d$. Radiative and convective fluxes were applied on all the surfaces of the extended length. Results are shown in Fig. 87 for M8 and M12 diameters. The extended length of the anchor demonstrated a significant influence on temperature profiles from 0 mm (no extended length modelled, i.e. the steel of the anchor is flush with the concrete surface) to 20 mm for both diameters, then negligible influence beyond 20 mm. When modelling the steel of the anchor flush with the concrete surface, a reduction in temperature profiles was obtained, especially near the exposed part of the at the concrete surface. This could be attributed to the fact that the deeper embedded parts of the anchor are subjected to conduction with concrete, whereas embedded segments near the exposed surface are influenced by the absence of the extended length, which is subjected to radiation and convection from the ISO 834 fire [23].

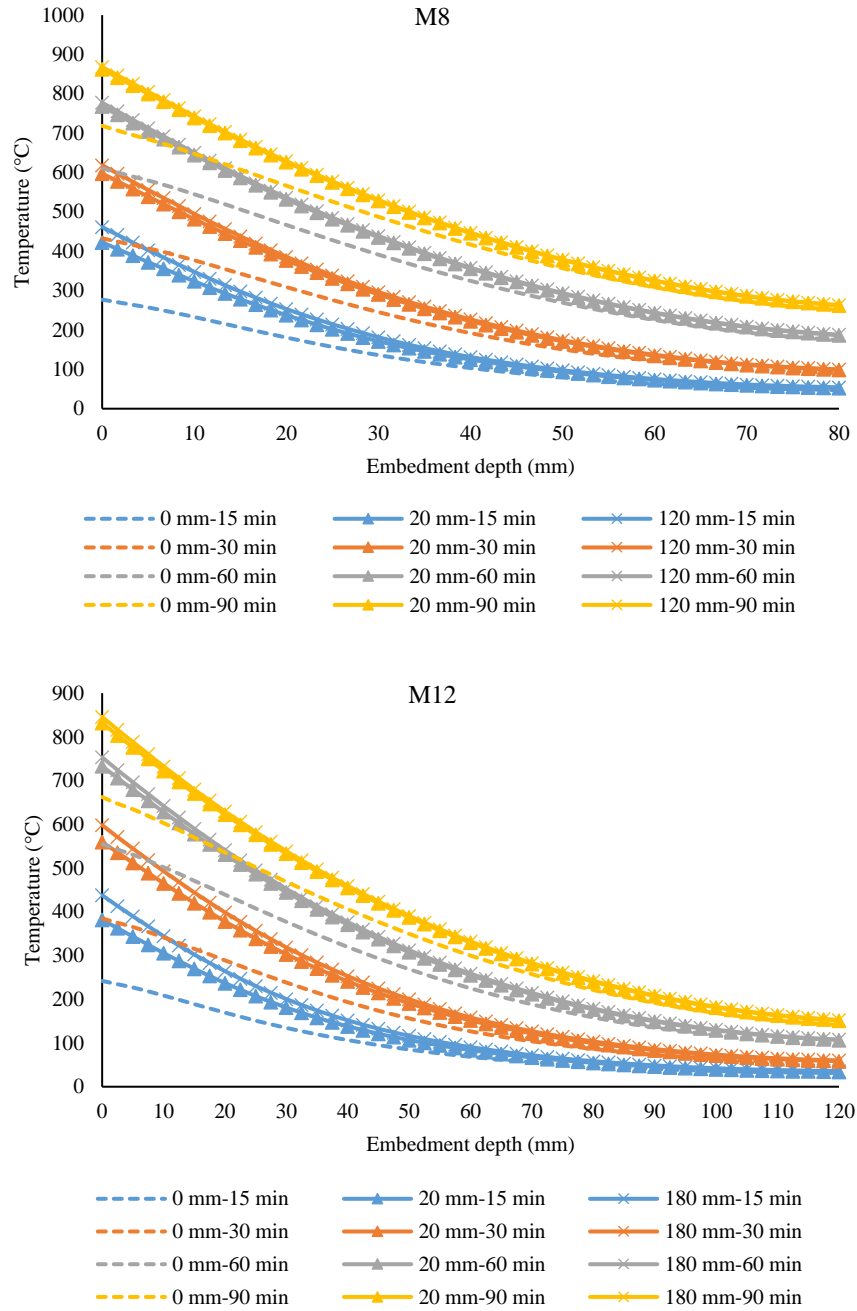


Fig. 87: Temperature profiles for M8 and M12 anchors with $h_{ef} = 10d$ for different extended lengths

4.2 Embedded depth of anchors (h_{ef})

To assess the influence of the embedment depth on the temperature profiles, simulations on anchors with embedment depths of $4d$, $10d$, and $20d$ were conducted for M8 and M12 anchor diameters. An extended length outside the concrete of $10d$ was chosen for both diameters. Dimensions for the concrete beam were the same as used for the validation. Fig. 88 shows temperature profiles for M8 and M12 anchors, respectively, for the studied embedment depths. At any given time of observation, temperatures near the exposed surface of the anchor were consistent between the three different embedment depths. However, significant temperature differences were observed between the $4d$ specimen and deeper specimens at the same location inside the concrete, with the maximum difference at the end of the $4d$ embedment. Higher temperatures were observed for shorter embedment depths within the concrete. For embedment depths between $10d$ and $20d$, difference in temperature were insignificant at the same measurement locations. The significant differences between $4d$ and deeper embedments at the same location within concrete may be attributed to the lower quantity of steel, where smaller thermal bridges are created and heat transfer between steel and concrete is lower. In addition, for shorter anchors there is a smaller

exchange surface between steel and concrete, leading to less thermal interaction between both materials and, therefore, higher temperatures.

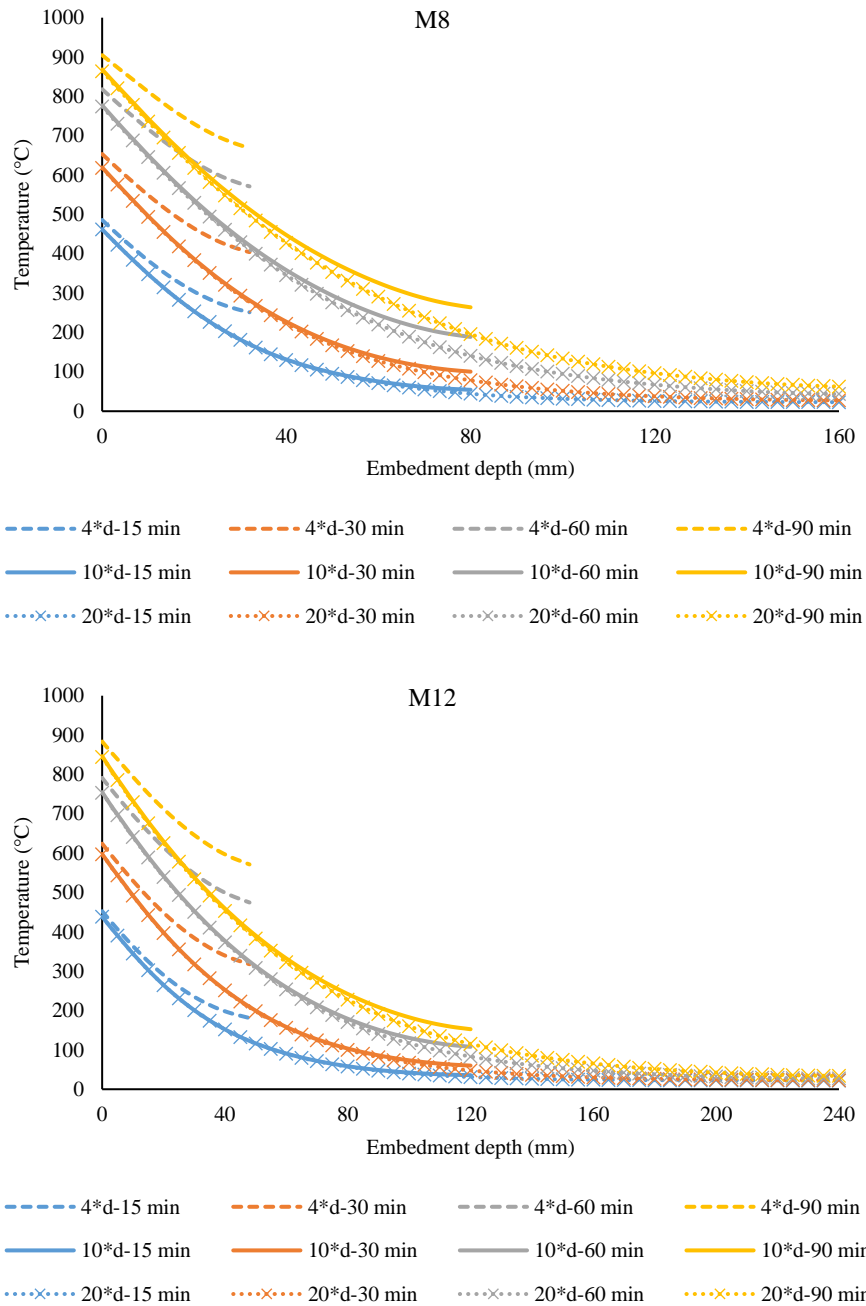


Fig. 88: Temperature profiles for M8 and M12 anchors with extended length of 10d for different embedment depths

4.3 Concrete element insulation

To assess the influence of insulating the side surfaces of the concrete element, simulations on beams exposed to a radiative and convective flux of ambient air (20°C) on lateral sides were conducted. Results were compared to anchors in beams insulated on the lateral sides. Studied anchors are M8 and M12 anchors with embedded and extended lengths of 10d. As with all other experiments, beam dimensions were 1500 mm length by 300 mm depth, but the width was reduced to 90 mm, resulting in approximately 40 mm cover on both sides for stronger influence. Fig. 89 shows that temperature profiles for insulated beams vs. exposed beams were nearly identical up to 30 min. Beyond 60 min, small differences were observed with the same initial conditions, wider beams will be less influenced by the existence/absence of insulation on the lateral sides of the beam.

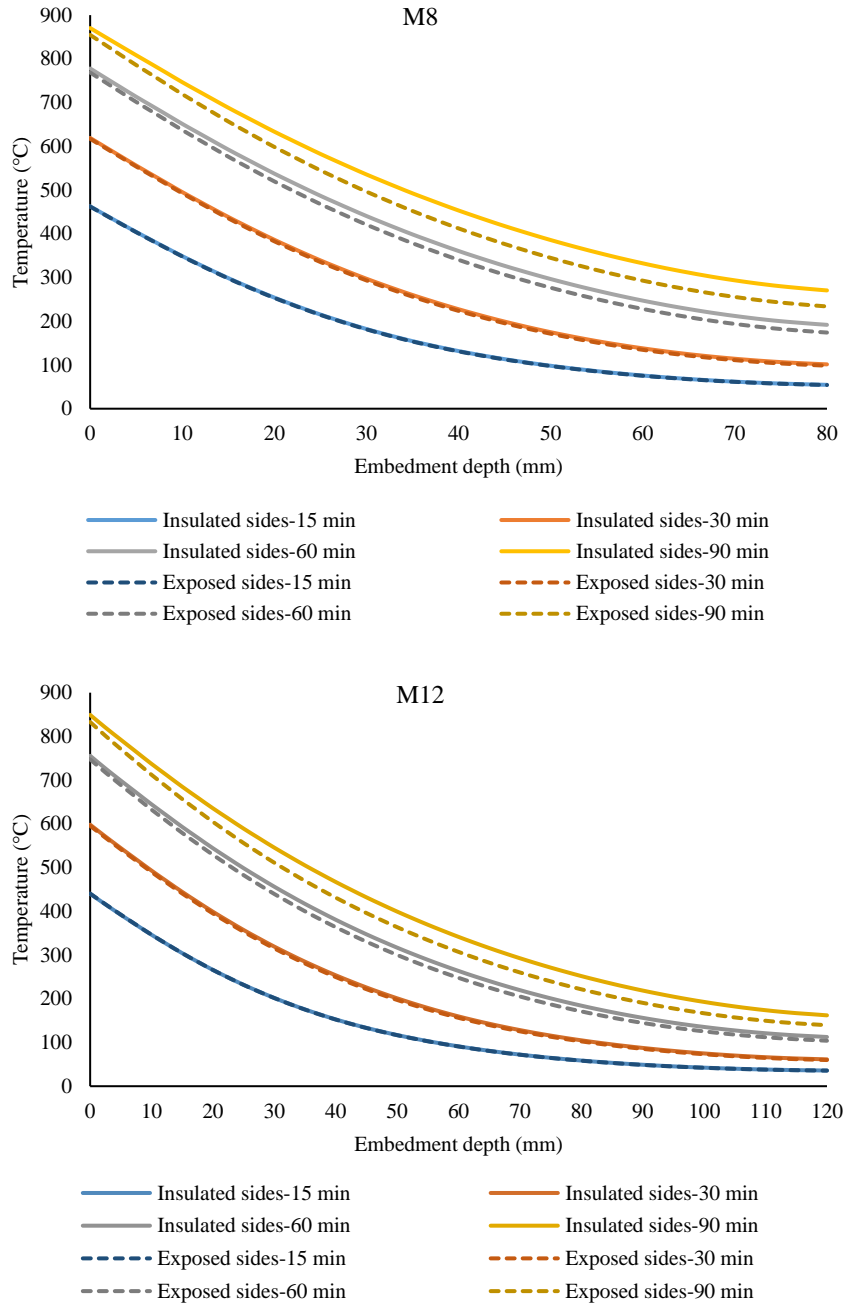


Fig. 89: Temperature profiles for M8 and M12 anchors in insulated beams and beams exposed to ambient air on all sides

5. Conclusions

This paper presents validation and parametric study of a numerical model for calculating the load-bearing capacity of bonded anchors in uncracked concrete under ISO 834 fire conditions [23]. The model employs 3D transient heat transfer equations to obtain temperature profiles along the embedment depth of anchors without considering the properties of the bonding material. The temperature profiles then serve as input for the bond Resistance Integration Method, in which bond strength contributions of discrete segments along the embedment depth of anchors is computed during fire exposure. In this study, the model was validated with experimental results obtained in a previous experimental study [24] resulting in conservative calculations of load-bearing capacities at various fire exposure times compared to experimental results.

Results of common assumptions for the modelling and design of bonded anchors with 2D transient heat transfer analysis based on Cartesian coordinates were compared with the proposed 3D model. 3D heat transfer analysis demonstrated better agreement with experimental results than 2D analysis results, resulting in the following conclusions:

- 2D analysis yields a rather a large margin of safety for the load-bearing capacity of anchors directly exposed to fire.
- 2D analysis may yield unsafe predictions for anchors with insulated fixtures.
- 2D analysis does not account for the extended part of the anchor in the modelling procedure (with applied radiation and convection on the extended part). This can lead to a significant reduction in temperature profiles near the fire exposed surface.

A parametric study was also presented after experimental validation of the model. This study investigated variables that may influence thermal evaluation of bonded anchors under fire conditions to produce temperature profiles, resulting in the following conclusions:

- Insulated fixtures significantly reduce the temperature profile of anchors exposed to fire conditions compared to uninsulated fixtures, which may lead to misrepresentations of product capacity assessed in accordance with TR 020.
- The length of the anchor extended outside the concrete surface has a significant influence on temperature profiles between no extended length and 20 mm of extended length. Beyond 20 mm, the influence is insignificant.
- The embedded depth of the anchor has an influence on temperature profiles up to $h_{ef} = 10d$. Beyond $h_{ef} = 10d$ of embedment depth the influence is insignificant.
- The insulation of the concrete bearing element's lateral sides has no significant influence on load prediction.

This parametric study establishes a basis for variables to be considered in guidelines for the evaluation of bonded anchors under fire conditions. Additional physical and analytical experimentation are recommended for further validation of the proposed method.

Acknowledgements

The research presented in this paper was conducted at CSTB (Centre Scientifique et Technique du Bâtiment). The authors would like to acknowledge the funding provided by Hilti corporation. The authors would also like to acknowledge Eng. Paul Lardet, Dr. Yahia Msaad, Dr. Seddik Sakji, Dr. Mhd Amine Lahouar, Dr. El Mehdi Koutaiba and the staff of the fire resistance laboratory of Mr. Romuald Avenel and Mr. Stéphane Charuel at CSTB for their contribution to this work.

References

- [1] Cook R. Behavior of chemically bonded anchors. *J Struct Eng.* 1993;119(9):2744–62.
- [2] Kumar S. Analysis of tabular adhesive joints with a functionnally modulus graded bondline subjected to axial loads. *Int J Adhes Adhes* 2009;29:785–95.
- [3] ACI Committee 318, " Building Code Requirements for Structural Concrete (ACI 318-11) and Commentary, " American Concrete Institute, Farmington Hills, MI, 2011, 503 pp. 2.
- [4] Eligehausen R, Werner F. Recent developments and open problems in fastening technique. In: 2nd international symposium on connections between steel and concrete, Stuttgart, *fib*, Germany; 2007.
- [5] Petit J, Nassiet V, Baziard YH-RB. Etude de la durabilité des assemblages collés. *Techniques de l'ingénieur*; 2005. p. COR160.
- [6] Zhang Y, Lou G, Chen K, Li G. Residual strength of organic anchorage adhesive for post-installed rebar at elevated temperatures and after heating. *Fire Technol J* 2016;52:877–95.
- [7] Muciaccia, G., Navarrete, D.D., Pinoteau, N., Mege, R. Effects of different test apparati and heating procedures on the bond properties of post-installed rebar connections under elevated temperatures. *Mater Struct* (2019) 52: 47.
- [8] Reis J. Effect of temperature on the mechanical properties of polymer mortars. *Mater Res* 2012;15(4):645–9.
- [9] EN 1993-1-2. Eurocode 3: Design of steel structures – Part 1-2: General rules – Structural fire design. November 2005.
- [10] EN 1992-1-2. Eurocode 2: Design of concrete structures – Part 1-2: General rules – Structural fire design. July 2008.
- [11] ACI 318-14, "Building code requirements for reinforced concrete" Detroit, Michigan: American Concrete Institute, 2014.
- [12] Sorathia U, Lyon R, Gann R, Gritz L. Materials and fire threat. *Fire Technol J* 1997;33(3):260–75.
- [13] Ribeiro MCS, Nóvoa PJRO, Ferreira AJM, Marques AT. Flexural performance of polyester and epoxy polymer mortars under severe thermal conditions. *Cem Compos* 2004;26:803–9.
- [14] Frigione M, Aiello M, Naddeo C. Water effects on the bond strength of concrete/ concrete adhesive joints. *Constr Build Mater* 2006;20:957–70.
- [15] Pinoteau N, Pimienta P, Guillet T, Rivillon R, Remond S. Effect of heat on the adhesion between post-installed bars and concrete using polymeric mortars. In Cairns JW, Metelli G, Plizzari GA, editors. *Bond in Concrete 2012 - Bond in New Materials and under Severe Conditions*; 2012; Brescia. Italy. p. 573-580.
- [16] Lahouar MA, Caron J-F, Pinoteau N, Forêt G, Benzarti K. Mechanical behavior of adhesive anchors under high temperature exposure: experimental investigation. *Int J Adhes Adhes* 2017;78:200–11.
- [17] Adams R, Coppendale J, Mallick V, Al-hamdan H. The effect of temperature on the strength of adhesive joints. *Int J Adhes Adhes* 1992;12(3):185–90.
- [18] Pinoteau N, Heck J, Avenel R, Pimienta P, Guillet T, Remond S. Prediction of failure of a cantilever-wall connection using post-installed rebars under thermal loading. *Eng Struct* 2013;56:1607–19.
- [19] EOTA TR 020. Evaluation of anchorages in concrete concerning resistance to fire. European Organization for Technical Approvals Technical report no. 20. May 2005.
- [20] Eligehausen R, Mallée R, Silva JF. Anchorage in concrete construction. Ernst & Sohn; 2006.
- [21] Reichert M, Thiele C. Qualification of bonded anchors in case of fire. Proceedings of the 3rd international symposium on connections between steel and concrete. Stuttgart, Germany. September 2017. p. 1191–9.
- [22] Lakhani H, Hofmann J. A numerical method to evaluate the pull-out strength of bonded anchors under fire. Proceedings of the 3rd international symposium on Connections between Steel and Concrete. Stuttgart, Germany. September 2017. p. 1179–90.
- [23] ISO 834-1 International Standard. Fire-resistance tests – Elements of building construction – Part 1: General requirements. First edition, 15 September 1999.
- [24] Al-Mansouri O, Mege R, Pinoteau N, Guillet T, Rémond S. Influence of testing conditions on thermal distribution and resulting load-bearing capacity of bonded anchors under fire. *Eng Struct J* 2019;192:190-204.
- [25] Lahouar MA, Pinoteau N, Caron J-F, Forêt G, Mège R. A nonlinear shear-lag model applied to chemical anchors subjected to a temperature distribution. *Int J Adhe Adhes* 2018;84:438–50.

- [26] Lahouar MA, Pinoteau N, Caron J-F, Forêt, Rivillon Ph. Fire design of post-installed rebars: full-scale validation test on a $2.94 \times 2 \times 0.15$ m³ concrete slab subjected to ISO 834-1 fire. *Eng Struct J* 2018;174:81-94.
- [27] Lakhani H, Hofmann J. On the pull-out capacity of post-installed bonded anchors and rebars during fire. *Proceedings of the 10th International Conference on Structures in Fire*. Belfast, UK. June 2018. p. 165-71.
- [28] Muciaccia, G., Consiglio, A., & Rosati, G. (2016). Behavior and design of post installed rebar connections under temperature. *Key Engineering Materials*, 711, 783-790.
- [29] Lahouar MA, Pinoteau N, Caron J-F, Forêt G, Guillet T, Mège R. Chemically-bonded post-installed steel rebars in a full scale slab-wall connection subjected to the standard fire (ISO 834-1). *Proceedings of the 3rd international symposium on connections between steel and concrete*. Stuttgart, Germany. September 2017. p. 1119-30.
- [30] Tian K, Ožbolt J, Sharma A, Hofmann J. Experimental study on concrete edge failure of single headed stud anchors after fire exposure. *Fire Safety J* 2018;96:176-88.
- [31] Bosnjak J, Sharma A, Ožbolt J. Modelling bond between reinforcement and concrete after exposure to fire. In: *5th International Conference on Computational Modeling of Fracture and Failure of Materials and Structures*. Nantes, France.
- [32] Halvička V, Lublój É. Concrete cone failure of bonded anchors in thermally damaged concrete. *Construction Build. Mater. J* 2018;171:588-97.
- [33] EOTA. EAD 330087-00-0601. Systems for post-installed rebar connections with mortar. no. EOTA14-33-0087-06.01. July 2015.

Analysis and discussion

Influence of modelling the adhesive resin

Prior to the study conducted in this paper, the effect of not modelling the adhesive layer in the 3D thermal model was investigated. The adhesive resin has different thermal properties (diffusivity) compared to those of concrete, therefore, neglecting the existence of the adhesive resin in the model should be proven to be conservative. Furthermore, the thermal properties of adhesive resin materials vary from one product to another. Therefore, a numerical investigation focused on the influence of modelling the adhesive resin and variation of its thermal properties was performed.

Thermal properties consist of conductivity, heat capacity and density. In the heat equation they can be regrouped in one term “diffusivity”. Concrete is considered as the reference material to which the adhesive resin’s thermal properties should be compared. Indeed, the anchor is embedded in concrete and heat flows from the anchor towards the concrete colder parts. The adhesive layer around the anchor was modelled for the case of an M12 with an embedment length of 110 mm (similar to the previous study). The diffusivity of the adhesive resin was varied from 0.1 to 10 times the diffusivity of concrete. The presented and analyzed results herebelow show that a thin bond layer around the anchor rod does not affect the calculation of temperature profiles significantly and can therefore be neglected when modelling bonded anchors exposed to fire.

Advantages of thermal 3D modelling

In this chapter, the proposed model requires 3D FE simulations to calculate temperature profiles along the embedment depth of anchors. Usually, 3D FE mechanical models are heavy in terms of calculation time and consumed energy to build the model. However, thermal modelling is not the case. Using 3D instead of 2D plane simulations requires slightly more calculation time and gives a better representativity of the problem. Moreover, it does not reach the complexity and weight of 3D mechanical models. Indeed, the model solves the heat equation numerically and the calculation time should not exceed a few minutes. For simplifications purposes, if the problem is symmetrical, only ¼ of it can be considered. Also, axisymmetrical modelling yields the same outcome as 3D modelling and can be considered to alleviate the size of the model. Using different numerical approaches (e.g. finite differences) should not change the outcome of the thermal model as long as the boundary conditions and material properties are the same.

1. Reference model without adhesive resin

This first model does not take into account the presence of the adhesive resin and places the steel of the anchor in direct contact with concrete. Hence, the temperature profile is measured at the steel/concrete interface. It assumes constant thermal and physical properties for concrete and steel at high temperatures. The same properties at ambient temperature were adopted.

Table 12 summarizes concrete properties:

Conductivity [W/m.K]	Density [kg/m ³]	Specific heat [J/kg.K]	h_{fire} [W/m ² .K]	h_{air} [W/m ² .K]	Emissivity [-]
1.958	2500	900	25	4	0.7

Table 12: Constant thermal and physical properties of concrete at ambient temperature

Table 13 summarizes steel properties:

Conductivity [W/m.K]	Density [kg/m ³]	Specific heat [J/kg.K]	h_{fire} [W/m ² .K]	Emissivity [-]
53.301	7850	440.51	25	0.7

Table 13: Constant thermal and physical properties of carbon steel at ambient temperature

2. Model with adhesive resin assumed having 0.1 times concrete diffusivity

This model takes into account the presence of a 1 mm adhesive resin thickness around the M12 anchor. It assumes that the adhesive resin has 0.1 times concrete diffusivity. This assumption is represented by varying the thermal conductivity in the heat equation at 0.1 times concrete conductivity. The remaining properties (density and specific heat remain unchanged). Concrete and steel properties remain the same as before.

Table 14 summarizes the adopted thermal properties for the adhesive resin:

Conductivity [W/m.K]	Density [kg/m ³]	Specific heat [J/kg.K]	h_{fire} [W/m ² .K]	h_{air} [W/m ² .K]	Emissivity [-]
0.1958	2500	900	25	4	0.7

Table 14: Constant thermal and physical properties of adhesive resin having 0.1 concrete diffusivity

3. Model with adhesive resin assumed having 10 times concrete diffusivity

This model assumes that the adhesive resin has 10 times concrete diffusivity. This assumption is represented by varying the thermal conductivity in the heat equation at 10 times concrete conductivity. The remaining properties (density and specific heat remain unchanged). Concrete and steel properties remain the same as before.

Table 15 summarizes the adopted thermal properties for the adhesive resin:

Conductivity [W/m.K]	Density [kg/m ³]	Specific heat [J/kg.K]	h_{fire} [W/m ² .K]	h_{air} [W/m ² .K]	Emissivity [-]
19.58	2500	900	25	4	0.7

Table 15: Constant thermal and physical properties of adhesive resin having $10 \times$ concrete diffusivity

The comparison of temperature profiles of the three cases in Fig. 90 shows that when the adhesive resin has an equal or greater thermal diffusivity than concrete, taking into account the adhesive resin in the model does not change the outcome of the calculation. Indeed, the same temperature profiles are observed for both cases with 1 and 10 times the concrete diffusivity considered for the adhesive resin. However, in the case where the adhesive resin has a lower thermal diffusivity than concrete, slightly higher temperature profiles are observed. This difference is on the further conservative side compared to the fire resistance vs. fire exposure time curve (Fig. 82) obtained without modelling the presence of the adhesive. Therefore, neglecting the presence of the adhesive resin remains conservative compared to fire test results.

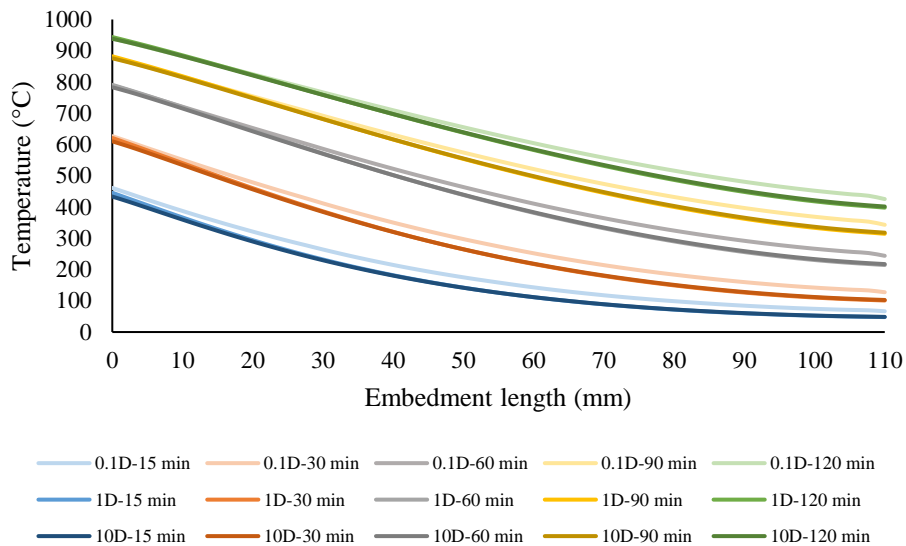


Fig. 90: Comparison of temperature profiles along the embedment depth of an M12 anchor using numerical modelling taking into account different thermal diffusivity of the adhesive resin compared to concrete

In the framework of the research conducted in this thesis, two different adhesive resins used for bonded anchor applications (epoxy and cementitious/acrylate) were characterized in a lateral flux test to determine their thermophysical properties.

The first adhesive resin is polymer based. Fig. 91 shows its thermophysical properties. The temperature conductivity decreases up to 400°C. The thermal conductivity decreases to 100°C and then rises again slightly. Because of the strong decomposition effects and shape change (shrinkage) of the sample, the measurement at higher temperatures was not possible. Table 16 shows the values of the specified thermophysical properties. The determined density values and the extrapolated cp values are used to calculate the thermal conductivity.

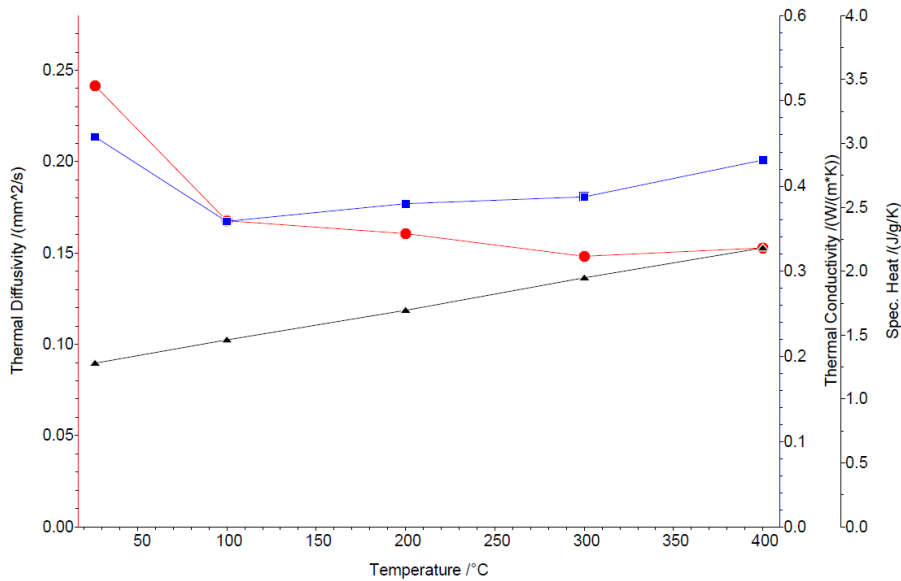


Fig. 91: Thermophysical properties of an epoxy based adhesive resin used for bonded anchor applications

Temperature [°C]	Conductivity [W/m·K]	Specific heat [J/kg·K]	Density at 20°C [kg/m³]	Diffusivity [m²/s]
26	0.458	1281	1483	2.4108810^{-7}
100	0.359	1463		1.6546610^{-7}
200	0.379	1694		1.5086410^{-7}
300	0.387	1949		1.3389310^{-7}
400	0.430	2182		1.3288410^{-7}

Table 16: Thermophysical properties of an epoxy-based adhesive resin used for bonded anchor applications

The second adhesive resin is a cementitious/acrylate-based mortar. Fig. 92 shows its thermophysical properties. The thermal conductivity decreases to 500°C and then rises continuously to 900°C. The slightly stronger drop up to 100°C is probably due to the water vapour flow (steam evacuation). Above 500°C, the radiation energy transport within the porous structure of the cement sample presumably increases, as a result of which the temperature conductivity increases again. The thermal conductivity shows two distinct levels at 100°C and 400°C, which refer to the water vapour flow (steam evacuation) and can be attributed to the decomposition. Table 17 shows the values for the thermophysical properties.

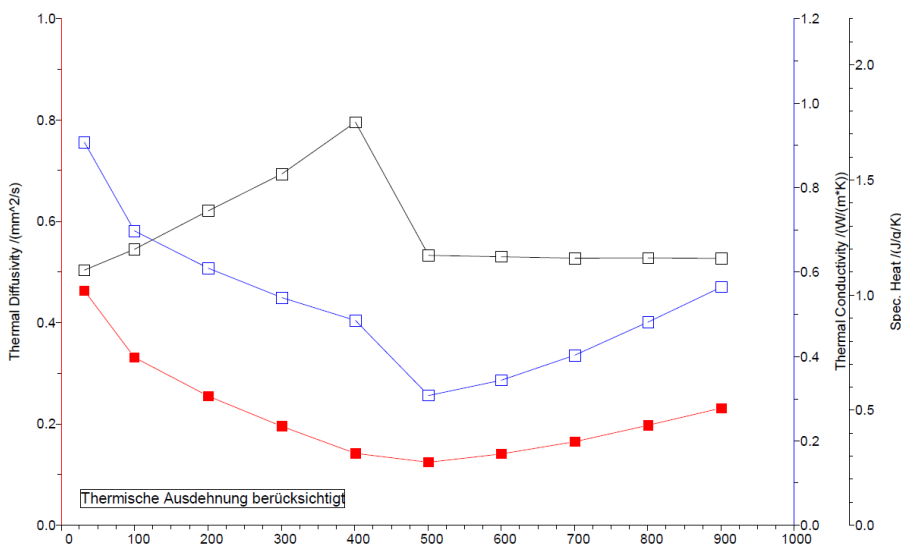


Fig. 92: Thermophysical properties of a cementitious/acrylate based adhesive resin used for bonded anchor applications

Temperature [°C]	Conductivity [W/m·K]	Specific heat [J/kg·K]	Density at 20°C [kg/m ³]	Diffusivity [m ² /s]
32	0.908	1108	1770	4.62991×10^{-7}
100	0.692	1199		3.26072×10^{-7}
200	0.601	1366		2.48571×10^{-7}
301	0.514	1526		1.90298×10^{-7}
401	0.411	1752		1.32536×10^{-7}
501	0.218	1172		1.05089×10^{-7}
601	0.240	1167		1.1619×10^{-7}
701	0.280	1160		1.36372×10^{-7}
800	0.335	1161		1.63019×10^{-7}
901	0.393	1158		1.91739×10^{-7}

Table 17: Thermophysical properties of a cementitious/acrylate based adhesive resin used for bonded anchor applications

The previous characterization of the diffusivity of two different adhesive resins used for bonded anchor applications allows a comparison with the diffusivity of concrete according to Eurocode 2 – French national annex (2008). Table 18 summarizes the thermophysical properties of concrete.

Temperature [°C]	Conductivity [W/m·K]	Specific heat [J/kg·K]	Density [kg/m ³]	Diffusivity [m ² /s]
20	1.958	900	2500	8.70222×10^{-7}
99	1.77	900	2500	7.86667×10^{-7}
100	1.7656	1500	2500	4.70827×10^{-7}
115	1.735	1500	2500	4.62667×10^{-7}
140	1.678	1312	2485.3	5.14611×10^{-7}
160	1.1576	1217	2473.5	3.84553×10^{-7}
200	1.1108	1000	2450	4.53388×10^{-7}
300	1.0033	1050	2412.5	3.96072×10^{-7}
400	0.9072	1100	2375.1	3.47239×10^{-7}
500	0.8225	1100	2353.1	3.17763×10^{-7}
600	0.7492	1100	2331.2	2.92163×10^{-7}
700	0.6873	1100	2309.4	2.70554×10^{-7}
800	0.6368	1100	2287.5	2.53075×10^{-7}
900	0.5977	1100	2265.6	2.39832×10^{-7}
1000	0.57	1100	2243.8	2.30939×10^{-7}
1100	0.5537	1100	2221.9	2.26546×10^{-7}
1200	0.5488	1100	2200	2.26777×10^{-7}
1500	0.5439	1100	2134.4	2.3166×10^{-7}

Table 18: Thermophysical properties of concrete according to Eurocode 2 – French national Annexe (2008)

Fig. 93 plots a comparison between the diffusivities of both adhesive resins, as well as concrete diffusivity with temperature. This comparison shows that the adhesive resins taken as example possess a lower diffusivity than concrete. Indeed, the ratio between the mortar diffusivity and concrete diffusivity is higher than 0.1 for both cases (Fig. 94).

Finally, this parametric study leads to conclude that the studied adhesive resins (used for bonded anchor products) have a slight insulating effect. Indeed, the adhesive resins are less diffusive compared to the thermal properties of concrete. This yields slightly higher temperature profiles compared to the case where the steel of the anchor in the embedded length is modelled in direct contact with concrete.

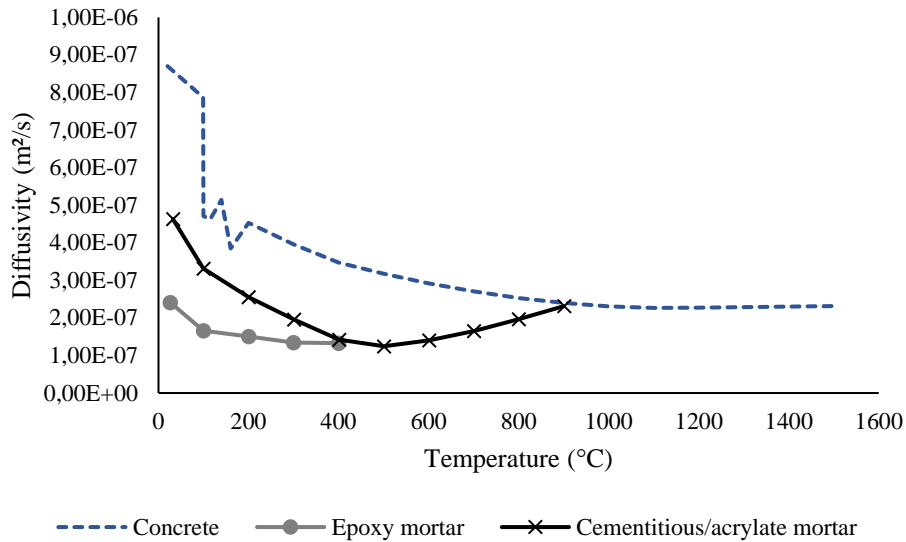


Fig. 93: Comparison between diffusivities of two adhesive resins used for bonded anchor application and concrete at high temperatures

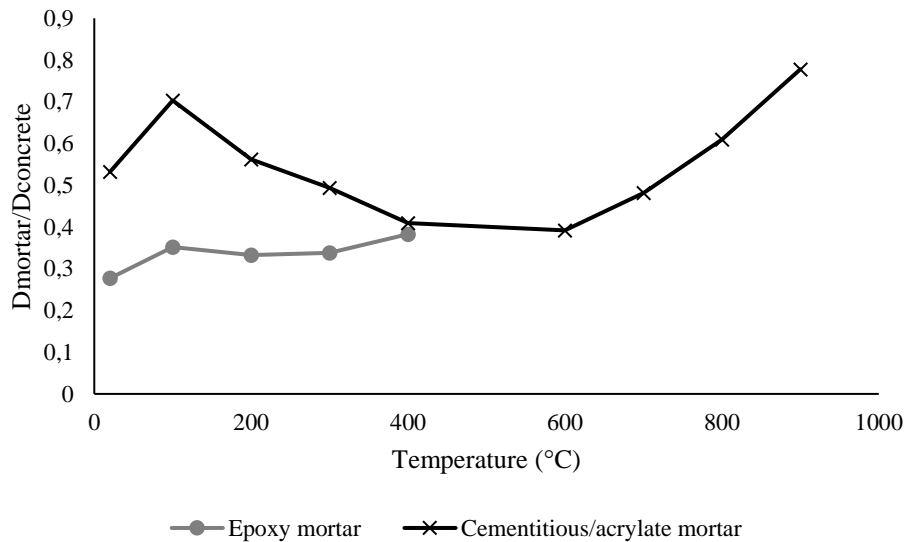


Fig. 94: ratio between mortar diffusivity and concrete diffusivity at high temperature for examples of the studied epoxy and cementitious/acrylate adhesive resins

Conclusion:

The effect of neglecting the presence of the bonding material for a thin layer (1 to 2 mm of bond thickness) has a negligible influence on the outcome of the calculation results (temperature profiles along the embedment depth of the anchor). Therefore, for thin layers of bond around the anchor, the problem of bonded anchors exposed to fire can be modelled without taking into account the existence and the thermal properties of the bonding material. However, the evaluation guidelines do not set a limit for the thickness of the bonding material around the steel insert. It is up to the manufacturer to specify the installation instructions (e.g. diameter of the hole). It is recommended that such a parametric study as the one presented in this work be conducted on a case by case basis to assess the influence of the bonding material on the calculated temperature profiles (by FE simulations) compared to measured temperature profiles (in fire tests).

Furthermore, the proposed 3D FE model in this work was only validated for an M12 anchor size on one adhesive resin. In order to extend the validity of Pinoteau’s method (Resistance Integration Method) for all anchor sizes, more tests and calculations should be conducted on a larger population of anchor sizes with different embedment depths. Indeed, Pinoteau’s method can be used for all rebar sizes following two full scale tests on a column-wall

connection conducted at CSTB (*Pinoteau, 2013*). In order to have a validation of Pinoteau's method, fire tests should also provide the experimental data to be compared to calculation results. The next chapter in the thesis concentrates on extending the validation of Pinoteau's method for all anchor sizes from M8 to M30 for different embedment depths and several adhesive resins.

Chapter IV: Validation of Pinoteau's method (Resistance Integration Method) for the evaluation and design of bonded anchors in uncracked concrete under ISO 834 fire

Chapter IV resumes the paper entitiled “**Recommendations for design of bonded anchors under fire using Pinoteau's method (Resistance Integration Method)**” submitted on February 2, 2021 in the Fire Safety Journal. This paper attempts to validate the Resistance Integration Method for the design of bonded anchors on a wide range of anchor sizes (diameter \times embedment depth) of three different adhesive resins.

Objectives

Following the proposal of a design method in the previous chapter, which was validated on one anchor size (M12) with a single embedment (110 mm) using an epoxy based adhesive resin. The design method should prove to be applicable on all bonded anchor sizes/embedments for pull-out failure mode under fire. This chapter proposes to extend the validation of the design method by validating test results (i.e. calculated pull-out resistance under fire) for different anchor sizes and different adhesive resins. Therefore, tests conducted at CSTB in addition to tests in the literature were identified as reference for this validation. A thorough study was conducted on the level of conservativeness of Pinoteau's method (initially proposed for design of PIRs under fire) and how it can be enhanced to allow more realistic design values (closer to fire test results), while remaining on the conservative side.

This chapter has two main objectives:

1. Validate the Pinoteau's Method (Resistance Integration Method) on a wide range of anchor sizes under fire. Indeed, the previous studies in this thesis focused only on small anchor sizes (M8 and M12). This study enlarges the scope of the method from anchor size M8 to anchor size M30, and embedments from 50 to 120 mm, for pull-out failure mode under fire.
2. Recommend lowering the level of conservativeness of Pinoteau's method when used to design bonded anchors under fire. Indeed, the current approach according to EAD 330087-00-0601 (2018) allows characterization of the bond strength up to a temperature limit of around 300°C. Also, no extrapolation is allowed beyond this limit, yielding zero bond strength resistances for the design method at higher temperatures. Fire tests for long duration exposures showed that bonded anchors can retain a certain level of resistance, when the design method predicted zero pull-out resistance under fire. This recommendation allows to design bonded anchors for conservative fire resistance values closer to fire test results without penalizing the product by assuming no resistance under fire.

DESIGN RECOMMENDATIONS FOR BONDED ANCHORS UNDER FIRE CONDITIONS USING THE RESISTANCE INTEGRATION METHOD

Omar Al-Mansouri^{a,b}, Romain Mège^a, Nicolas Pinoteau^a, Thierry Guillet^a, Roberto Piccinin^c, Kenton McBride^c, Marco Abate^c, Sébastien Rémond^d

^a Centre Scientifique et Technique du Bâtiment (CSTB), 84 avenue Jean Jaurès, Champs-sur-Marne, 77447 Marne-la-Vallée Cedex 2, France

^b IMT Lille-Douai, Univ. Lille, EA 4515 – LGCgE, Département Génie Civil & Environnemental, F-59000 Lille, France.

^c Hilti Corp., Schaan, Principality of Liechtenstein

^d Univ Orléans, Univ Tours, INSA CVL, LaMé, EA 7494, France.

Corresponding author's e-mail: omar.almansouri@cstb.fr

Abstract

Fire design of cast-in place and post-installed anchors in concrete under fire is covered by EN 1992-4, Annex D [1], allowing to calculate steel and concrete related failure modes of anchors, under tension or shear loading. This informative annex of EN 1992-4 is limited to cast-in place or mechanical (e.g. expansive, undercut) anchors, whereas post-installed adhesive anchors remain out of its scope. This is due to the high probability of pull-out failure of post-installed adhesive anchors under fire conditions. Furthermore, the fire design method provided in EN 1992-4 is empirical, based on specific fire ratings (30, 60, 90 and 120 min) and is not temperature based (i.e. by performing thermal and mechanical calculations). This paper presents a study of the applicability of the more flexible Resistance Integration Method (RIM), proposed originally for the design of the pull-out resistance of Post-Installed Reinforcement (PIR) by Pinoteau, on bonded anchors in uncracked concrete. This method is validated from a comparison of test results obtained from two research projects conducted at CSTB and TU Kaiserslautern on bonded anchors in uncracked concrete under ISO 834-1 fire conditions. The data considered include tests conducted on anchor sizes from M8 to M30 using three different adhesives (two epoxy adhesives and one cementitious mortar). Design of the pull-out resistance under fire using RIM requires numerical calculation of temperature profiles considering models of concrete and steel elements; different assumptions about modeling these elements can produce vastly different end results. The influence of these assumptions on the outcome of the method is also presented. Finally, recommendations for assessment procedures for bonded anchors under fire conditions are provided as entry data for design.

Keywords: adhesive resin, bonded anchor, fire tests, thermal distribution, numerical model.

1. Introduction

Post-installed bonded anchors are commonly used for steel to concrete connections and offer flexibility compared to other anchor types due to their range of embedment depths and relatively smaller required edge distances and spacings. Bonded anchors transfer tensile load to concrete through adhesive bond and friction, exhibiting the following possible tensile failure modes: concrete cone, steel, anchor pull-out (bond), and concrete splitting [1,2]. Many bonded anchors can be designed to similar or higher strengths than most post-installed mechanical anchors at ambient temperature. However, bonded anchors are sensitive to several environmental factors [3-6]. To address these sensitivities, the assessment of bonded anchors in European [7] and American guidelines [8] requires tests on different anchor geometries accounting for dry and wet concrete, minimum curing time, freeze/thaw conditions, high alkalinity, sulphurous atmosphere, installation in insufficiently clean holes, installation in freezing conditions, and in-service temperatures. Accidents involving bonded anchors [9,10] have underscored the importance of proper testing, assessment, design, and installation protocols for these systems. The mechanical properties of adhesive resins are particularly temperature dependent [11]. Under fire conditions, research studies [12,13] have shown that bond failure occurs more frequently than other failure modes for common ranges of bonded anchor diameter and embedment due to exceedance of glass transition temperatures and material softening. As with other sensitivities, use of bonded anchors in cases where fire ratings are required must be accompanied by proper assessment and design procedures.

Current assessment and design guidelines do not offer evaluation and design methods for bonded anchors under fire conditions [7,14]. Existing guidelines in European Assessment Document (EAD) 330087 [15] for post-installed reinforcement (PIR), however, provide criteria to produce bond stress vs. temperature curves for adhesives at high temperature expected during fire events. In these guidelines, a temperature response curve is obtained by a minimum of 20 tests on 12 mm diameter reinforcing bars installed with 120 mm embedment depths in confined concrete cylinders. After curing of the adhesive, tests are subjected to different magnitudes of constant load and increasing temperature until failure. The resulting curve allows design of PIR under fire conditions using Pinoteau's bond strength Resistance Integration Method (RIM) [16]. The load-bearing capacity of the PIR connection is calculated using temperature profiles along the embedment depth for fire design, which is normally determined through numerical calculations. Using the bond stress vs. temperature curve of the adhesive, resistance contributions associated with the temperatures along the length of the connection can be integrated into an overall connection resistance specific to temperature profiles. For standard fire conditions where the required capacity and temperature distributions during fire exposure are known, the time to failure of the connection can be calculated.

The steps of the Resistance Integration Method were established first by Pinoteau et al. [16] and validated on a large scale test at the fire resistance laboratory at CSTB on cantilever-wall connection using PIRs under ISO 843-1 fire conditions [17]. Another large scale validation was performed at CSTB on a slab-wall connection under ISO 843-1 fire conditions by Lahouar et al [18]. Lahouar et al. [19] also proposed a non-linear shear-lag model taking into account the displacement compatibility of PIR at high temperature (unaccounted for in RIM). Both approaches yielded accurate predictions of fire resistance durations of cantilever connections. Reichert and Thiele [20] also attempted to adapt the method for bonded anchors under fire conditions using axisymmetric thermal modelling of the anchors, yielding conservative design values compared to fire tests. Lakhani and Hofmann [16, 21] presented RIM results based on 2D thermal modelling of anchors, yielding higher design capacities than fire tests in some cases (e.g. bonded anchors with insulated fixtures). Al-Mansouri et al. [22] validated RIM for the design of bonded anchors by investigating the parameters influencing fire tests on bonded anchors (fixtures, insulation conditions, concrete member thicknesses). The case of an anchor directly exposed to fire (i.e. using a metallic fixture and without insulating material) was identified as the most conservative testing condition [23]. Al-Mansouri et al. based the RIM on 3D thermal modelling and the example of M12 rods with 110 mm embedment depth yielding conservative design values compared to fire tests.

In Reichert and Thiele [20], ISO 834-1 fire tests were conducted on bonded anchors in uncracked concrete using two adhesives (one epoxy and one cementitious) and a large combination of configurations for anchor sizes from M10 to M30. Their design calculations, based on 2D axisymmetric transient heat transfer, yielded conservative results for most of the cases, but for some cases the calculation yielded higher resistances compared to fire tests. At CSTB, a study was conducted on the thermal influence of testing conditions on the resulting load-bearing capacity of bonded anchors (one epoxy adhesive) under fire conditions. This study is completed on the same adhesive in this paper with loaded fire tests on two different anchor geometries (M8 and M12). Both testing campaigns were performed according to the general requirements of fire tests according to [24]. This standard gives a heating curve to be applied inside the furnace (i.e. measured temperature of hot gas inside the furnace during heating). The heating curve is derived from the ISO 834-1 standard [17].

The objective of this paper is to regroup the data from Al-Mansouri et al [22, 23] and Reichert and Thiele [20] to reevaluate the calculation method (based on 3D transient heat transfer and Eurocode material properties for steel [25] and concrete [26, 27]) to test its sensitivity to the bond stress vs. temperature relationship adopted in the RIM process. The aim is to extend the validity of RIM method for the design of bonded anchors under fire conditions for all anchor sizes and propose recommendations for the evaluation method consistent with Eurocode design requirements. The same methodology for determining bond stress vs. temperature curves for PIR in EAD 330087 is applied to bonded anchors using threaded rods. Unlike PIR, however, bonded anchors are not protected by a concrete cover and are directly exposed to fire, resulting in significantly higher temperatures transmitted through the steel element. The modified evaluation method is therefore assessed in this paper for bond stress vs. temperature curves with the expectation of higher temperatures. The extension of the curve should be based only on test results up to a maximum temperature respecting the 3 hour and 5°C/min heating rate (imposed on the exterior of the specimen) in EAD 330087. To assess the beneficial effect (increase of calculated pull-out resistance of the bonded anchor) of accounting for this extension of the bond stress vs. temperature curve, a study was conducted based on the presented calculations in this paper.

2. Description of test campaigns and properties of the materials

The testing campaigns in Al-Mansouri et al [22,23] and Reichert and Thiele [20] were conducted at *Technical Universität Kaiserslautern* (TU Kaiserslautern) in Kaiserslautern, Germany and *Centre Scientifique et Technique du Bâtiment* (CSTB) in Paris, France, respectively. This section describes the configuration of fire tests on bonded anchors adopted by TU Kaiserslautern and CSTB. In addition, relevant material properties are presented.

2.1. Description of fire tests

Fire tests were conducted at TU Kaiserslautern and CSTB according to the specifications of EOTA TR 020 [14]. Bonded anchors were installed according to manufacturers' instructions and loaded with varying degrees of constant tensile load at ambient temperatures. The fire scenario applied in the furnace on test specimens was ISO 834-1 [17] until anchor failure. For each test, a fire resistance in terms of load and failure time were reported for the failed anchor.

Testing conditions in both campaigns were similar, with slight differences in the load transfer system and concrete bearing elements. The TU Kaiserslautern approach consisted of loading the anchors (installed in slabs) by dead load or hydraulic jacks at the bottom (exterior) of the furnace, connected to the anchor with the help of a steel arm and a metallic fixture (Fig. 95). The CSTB approach consisted of loading the anchors (installed in beams) using a metallic frame connected to the fixture of the anchor inside the furnace and to a hydraulic jack outside the furnace (Fig. 96).



Fig. 95: TU Kaiserslautern's furnace and loading system for fire tests on bonded anchors [20]

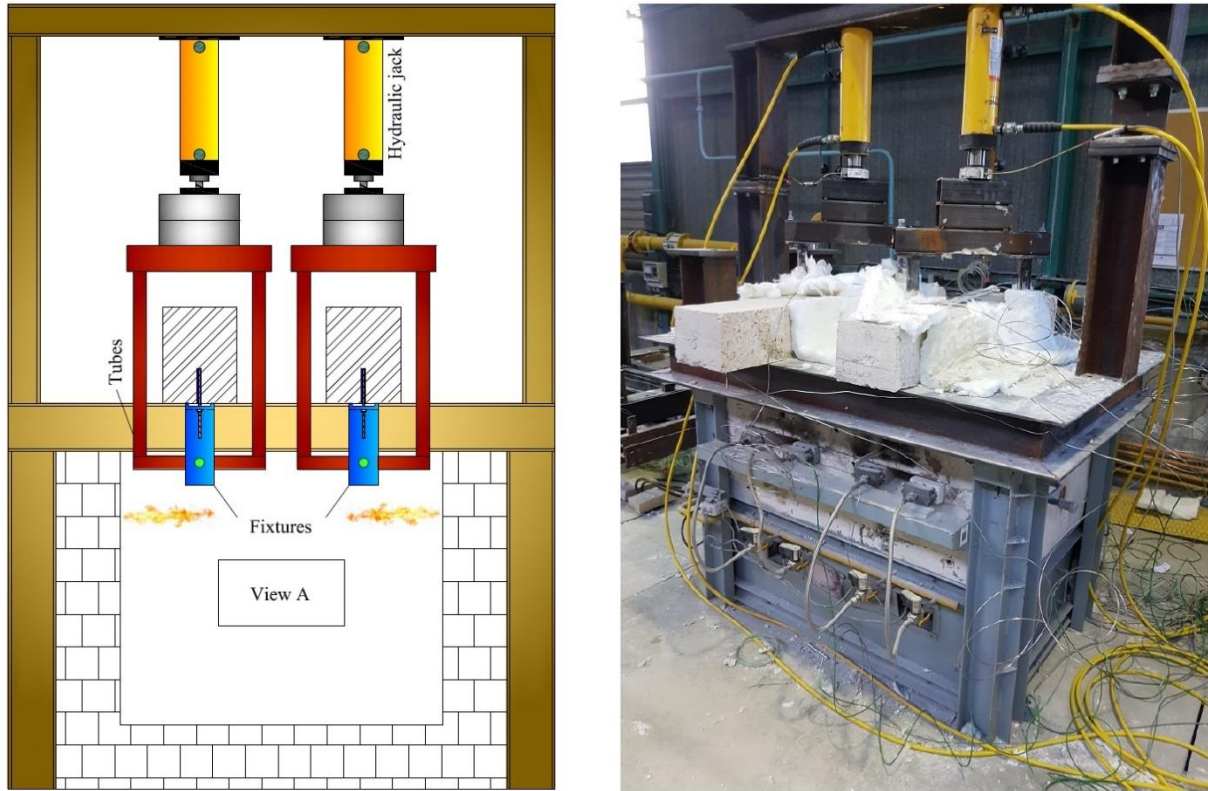


Fig. 96: CSTB's furnace and loading system for fire tests on bonded anchors [23]

In a previous experimental work [23] the current authors investigated the influence of the loading system on temperature profiles and resulting load-bearing capacity of bonded anchors and found it negligible. Details of load-transfer fixtures were adopted from EOTA TR 020 [14] depending on the applied load of the anchor.

2.2 Summary of tested materials and test results

TU Kaiserslautern's test campaign contained tests on two adhesives. The first adhesive was an epoxy resin (named mortar B in their report and referred to as Adhesive-1 henceforth), and the second adhesive was a cementitious mortar (called mortar C in their report and referred to as Adhesive-2 henceforth). CSTB's test campaign was on one epoxy resin (referred to as Adhesive-3 henceforth).

2.3. Prediction of the load-bearing capacity using Pinoteau's Resistance Integration Method The numerical model [22] is based on the following analytical procedures:

- The bonded anchor adhesive is not modeled,
- Steel threads are not modeled (i.e. cylindrical geometry for the anchor rod),
- The concrete remains uncracked,
- Concrete spalling is ignored,
- The fire exposed surface of all elements is subjected to convective and radiative fluxes of ISO 834-1 fire temperatures [17] on all sides,
- The unexposed fire surface of concrete beams is subjected to convective and radiative fluxes of ambient air at 20°C, and
- Slip of anchors is ignored.

During a fire test, heat transfer from hot gas inside the furnace to the exposed elements occurs via convection and radiation. Inside the members, conduction transfers the heat from the fire exposed surface inside the elements towards the unexposed surface. This problem can be solved by finite element modelling using ANSYS with the governing differential equation for 3D transient heat conduction using implicit scheme and iterative solver expressed in Eq. 14:

$$\rho c \frac{\partial T}{\partial t} = k \left(\frac{\partial^2 T}{\partial x^2} + \frac{\partial^2 T}{\partial y^2} + \frac{\partial^2 T}{\partial z^2} \right) \dots \text{ [Eq. 14]}$$

The 3D model represents the anchor as a cylinder inside of a concrete bearing element with modelling of the extended and embedded length of the steel anchor element (Fig. 73).

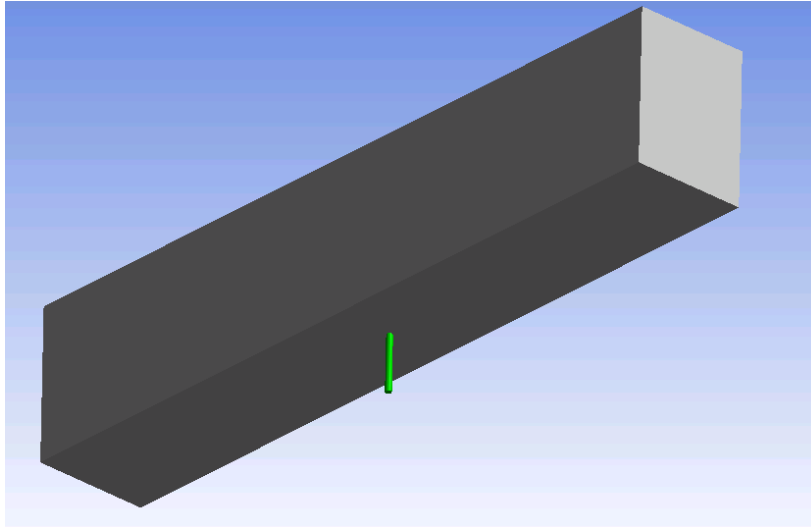


Fig. 97: Anchors directly exposed to fire using 3D modelling in ANSYS

Eq. 15 describes the Neumann boundary condition satisfied at the fire-exposed surface:

$$-k \frac{\partial T}{\partial n} = h_{\text{fire}} \cdot (T_s - T_{\text{fire}}) + \varepsilon \cdot \sigma \cdot (T_s^4 - T_{\text{fire}}^4) \dots [\text{Eq. 15}]$$

Eq. 16 describes the Neumann boundary condition satisfied at insulated surfaces:

$$-k \frac{\partial T}{\partial n} = 0 \dots [\text{Eq. 16}]$$

Eq. 17 describes the Neumann boundary condition satisfied at the upper surface of the beam exposed to ambient air at 20°C:

$$\dot{q}_{\text{total}} = h_{\text{air}} \cdot (T_s - T_{\text{air}}) + \varepsilon \cdot \sigma \cdot (T_s^4 - T_{\text{air}}^4) \dots [\text{Eq. 17}]$$

Where:

- \dot{q}_{total} is the total heat flux applied to the surface.
- k is the thermal conductivity (W/m·K).
- ρ is the mass density (kg/m³).
- c is the specific heat (J/kg·K).
- h_{fire} is the convective heat transfer coefficient for the fire exposed surface (25 W/m²·K).
- h_{air} is the convective heat transfer coefficient for the surface exposed to air at 20°C (4 W/m²·K).
- σ is the Boltzmann constant (5.667×10⁻⁸ W/m²·K⁴).
- ε is surface emissivity (0.7).
- T_s is the solid surface temperature (K).
- T_{fire} is gas temperature inside the furnace as a function of time (K).
- T_{air} is ambient air temperature (293 K).
- t is time.

Boundary conditions are represented in a profile view of the 3D model in Fig. 98.

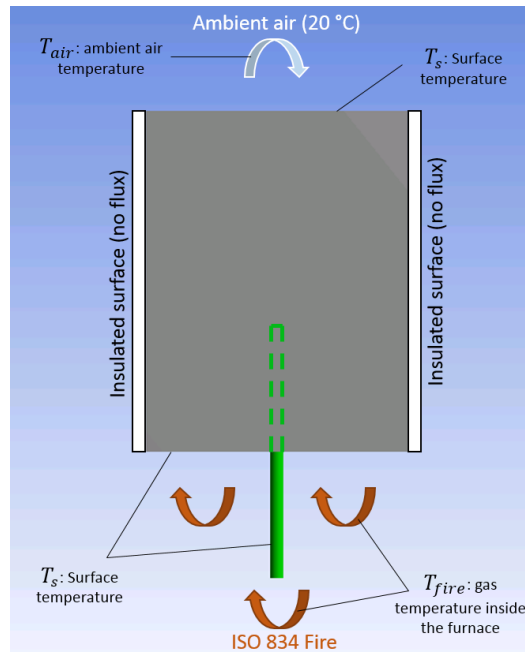
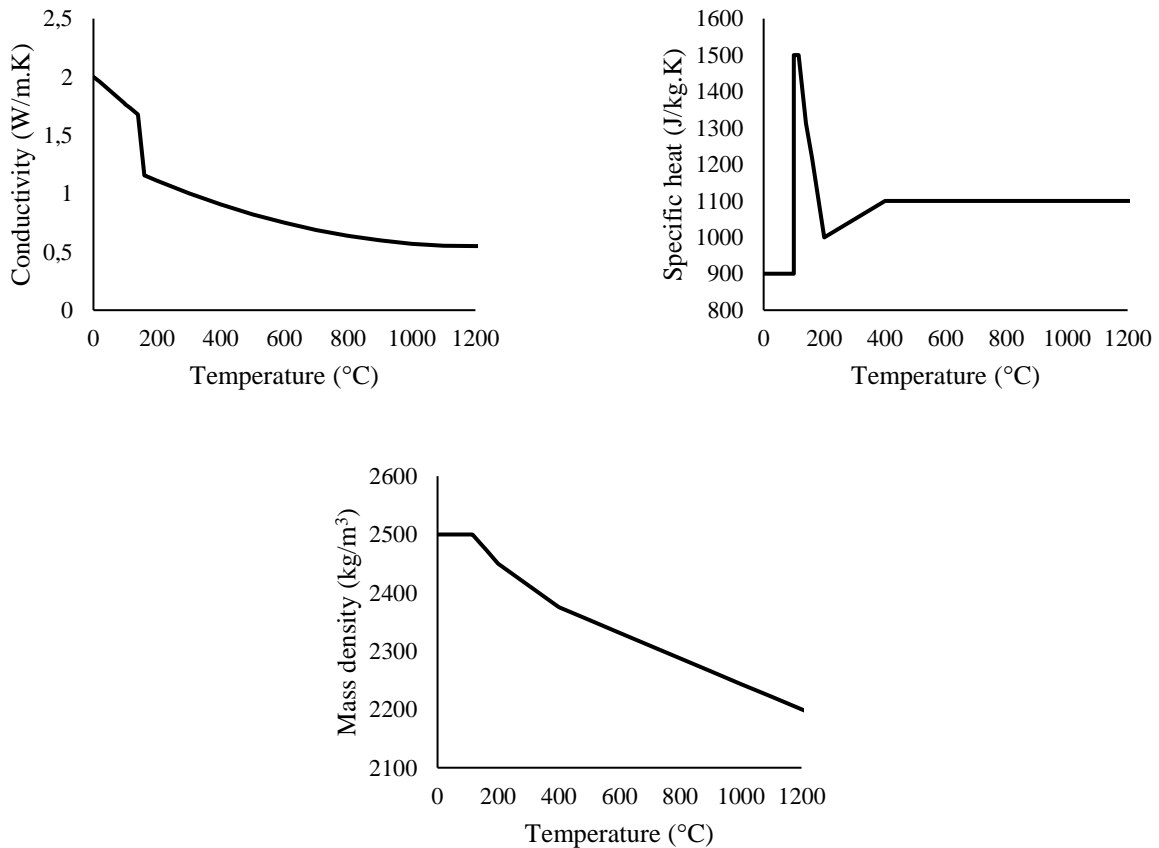
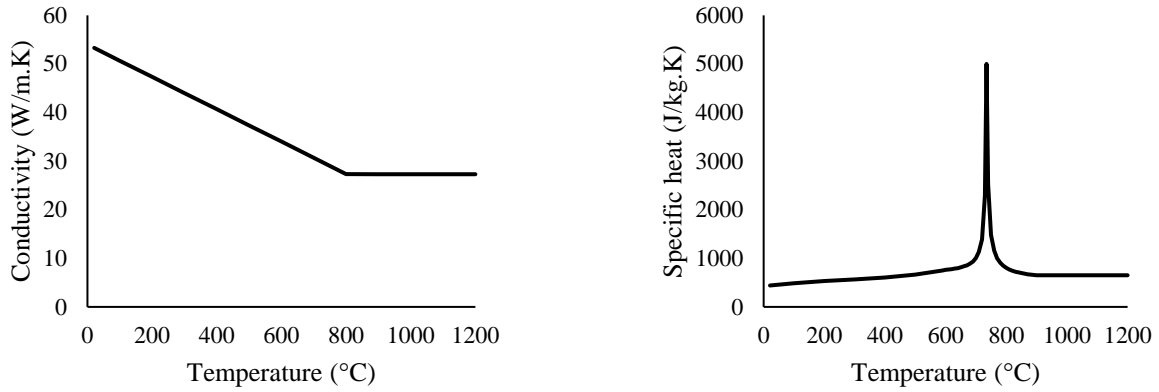


Fig. 98: Boundary conditions applied in the 3D heat transfer analysis for anchors directly exposed to fire

Thermal properties of concrete and carbon steel (conductivity, specific heat and mass density) are a function of temperature. The properties according to the French national annex in Eurocode 2 [26] for both materials are adopted in this study (Fig. 77). The mass density of the steel (7850 kg/m³) [25] is considered constant with respect to temperature.



(a) concrete



(b) Carbon steel

Fig. 99: Variation of thermal properties of concrete and steel according to NF EN 1992-1-2 [26]

Knowing the thermal distribution along the anchor at each moment of heating, it is possible to associate a resistance to each temperature using the resistance-temperature relationship. Pinoteau [16] illustrated schematically how the resistance at a depth x_i is determined at a time t_i based on the thermal distribution (Fig. 100).

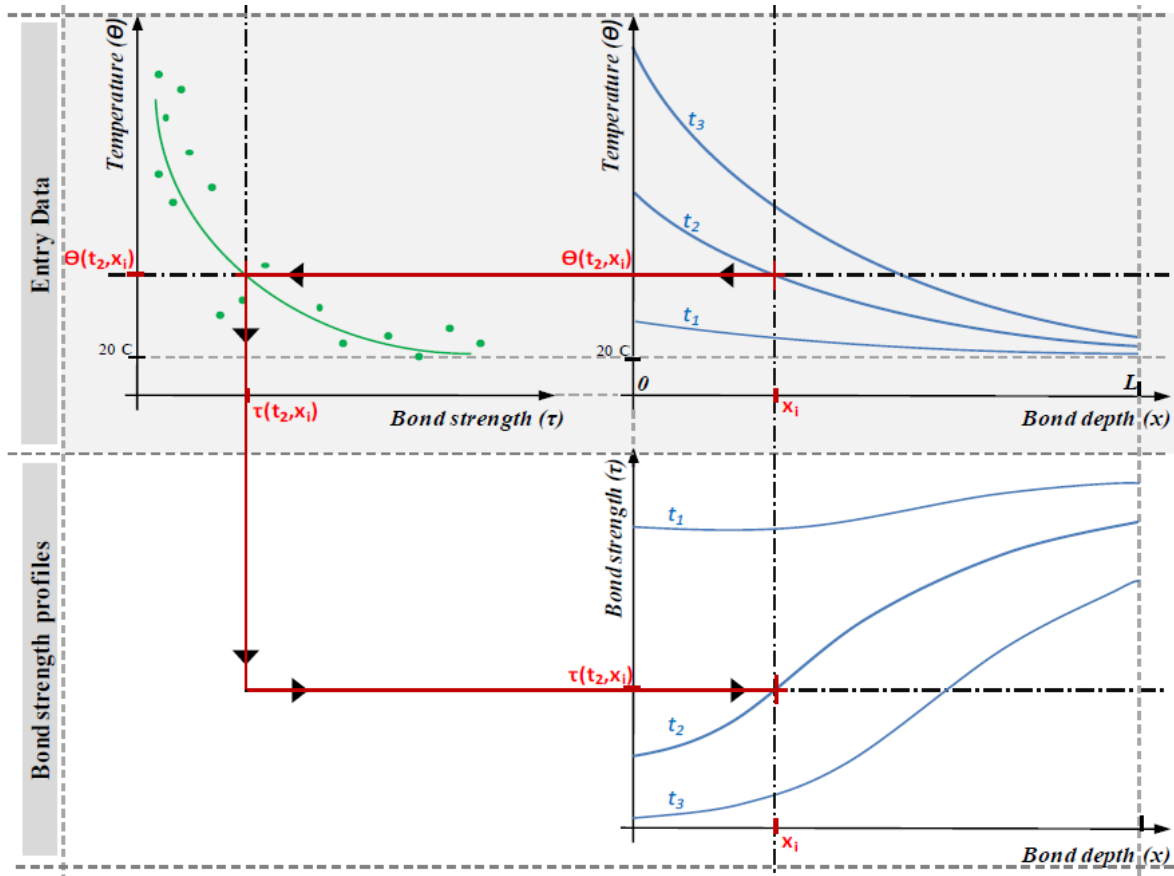


Fig. 100: Schematic representation of Pinoteau's method to obtain resistance profiles of bonded anchors at high temperatures [16]

This method allows to determine the evolution of the load-bearing capacity of the bonded anchor during heating. Knowing the applied mechanical force on the anchor during heating, failure time under fire conditions can be determined.

The bond capacity of the anchor at any given time is calculated according to Eq. 18:

$$N_{Rd,fire} = \pi \cdot d \cdot \int_0^{h_{ef}} f_{bd,0} \cdot k(\theta(x)) \cdot dx \dots [\text{Eq. 18}]$$

Where: $N_{Rd,fire}$ is the load bearing capacity under fire conditions (N).

d is the diameter of the anchor (mm).

$f_{bd,fire}$ is the design bond resistance at ambient temperature (N/mm²).

$k(\theta)$ is a reduction factor that depends on temperature.

$\theta(x)$ is the temperature distribution along the embedment depth of the anchor.

h_{ef} is the embedment depth of the anchor (mm).

By integrating the resistances, this method does not take into account the stress distribution along the anchor. When a tensile force is applied on the anchor, a distribution of bond stresses occurs in a phenomenon called “shear-lag”. This stress profile is equal or lower than the resistance profile. When temperature increases under a constant mechanical load, the sum (integration) of the stress profile decreases until it reaches a maximum bond stress value at a certain depth. The saturation of bond stresses at certain depths leads to a redistribution of these stresses towards the deeper parts of the anchor where the stress is still less than the resistance. The area under the stress profile remains unchanged in a way to ensure the integrity of the anchor. Pull-out failure occurs when all the stresses along the anchor saturate, in this case the stress profile is equal to the resistance profile. Therefore, this justifies the determination of the load-bearing capacity by only considering the resistances (Eq. 18).

Fig. 101 illustrates the evolution of temperature and bond stress profiles at three different times during heating t_1 , t_2 and t_3 . Stress profiles are represented for a constant load applied at $x = 0$ (head of the anchor), and temperature profiles are represented for a non-uniform heating applied near $x = 0$. At t_1 (low temperatures), the stress profile is lower than the resistance profile because the temperature profile is still at low temperatures. At t_2 (higher temperatures), heating at the head of the anchor decreases the resistance profile and leads to a saturation of stresses. At t_3 (near failure point), all the stresses along the embedment depth have saturated and pull-out occurs if the temperature continues to increase.

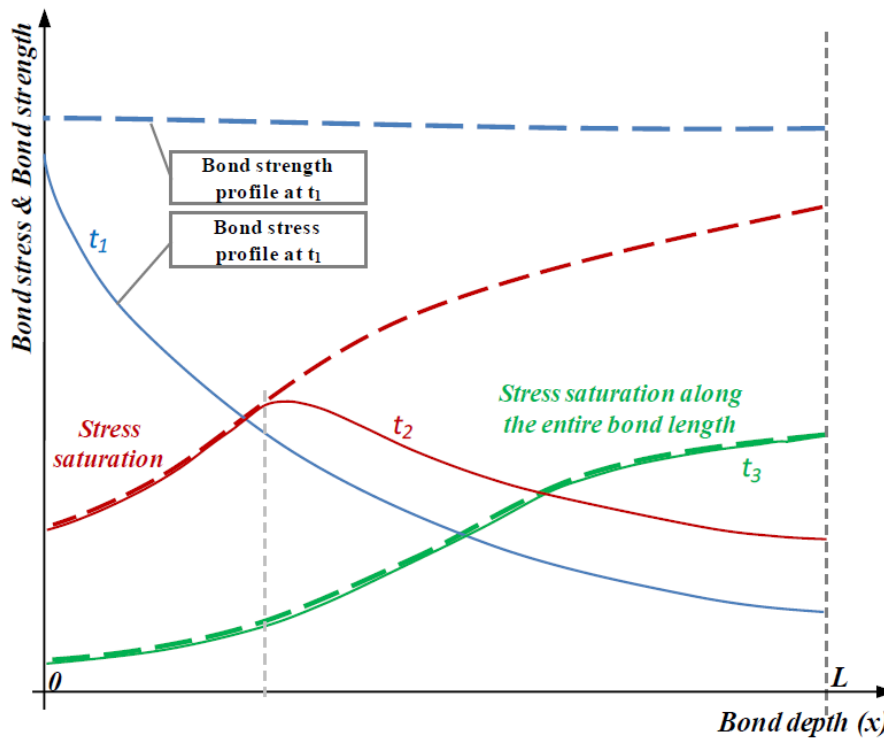


Fig. 101: Representation of stress distribution along the anchor at different times during heating [16]

2.4. Bond stress capacity vs. temperature relationship

The bond stress capacity vs. temperature relationship was obtained from tests according to EAD 330087-00-0601 [15]. Fig. 102-Fig. 104 show test results for the three adhesives used in this study. It should be noted that the evaluations of Adhesive-1 and Adhesive-3 have a large gap between test 150 and 200-250°C. This gap does not

respect the maximum distance between neighboring points given in the guidelines of EAD 330087-00-0601 (50°C). However, the other criteria for maximum distance of 1 N/mm² is respected. The curves were therefore considered beyond this gap for better representability of the adhesive's behavior at high temperature. Placing an additional data point would fill the gap and have a negligible statistical weight on the fitting curve.

Furthermore, the criterion for maximum bond stress corresponding to 10 N/mm² for C20/25 concrete was not adopted in this study. The 10 N/mm² criterion is set by EAD 330087-00-0601 for the design of PIRs, where a post-installed rebar is designed for the ultimate bond stress of a cast-in bar at ambient temperature. Bonded anchors are not governed by this criterion and the limit should be set therefore for their ultimate bond strength at ambient temperature. In this study, the upper limit of the bond stress vs. temperature curves was set to the reference tests at 20°C for Adhesives 1 and 3, and the highest bond strength obtained at the beginning of the curve for Adhesive 2, due to the lack of reference tests (Fig. 102-Fig. 104).

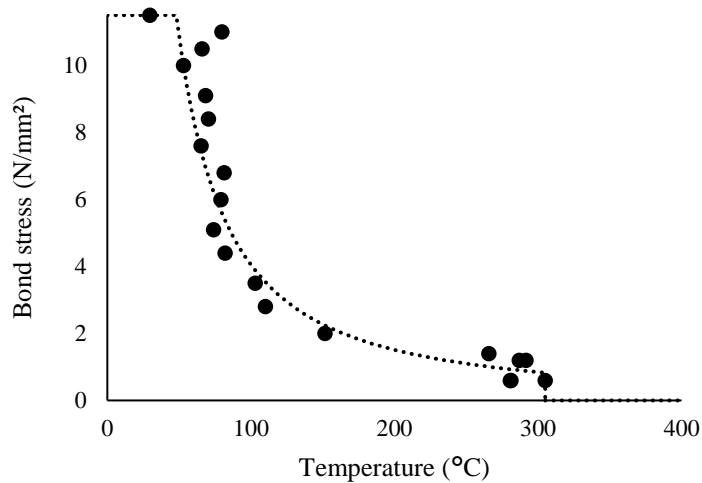


Fig. 102: Bond stress vs. temperature relationship for Adhesive-1 according to EAD 330087-00-0601 [15]

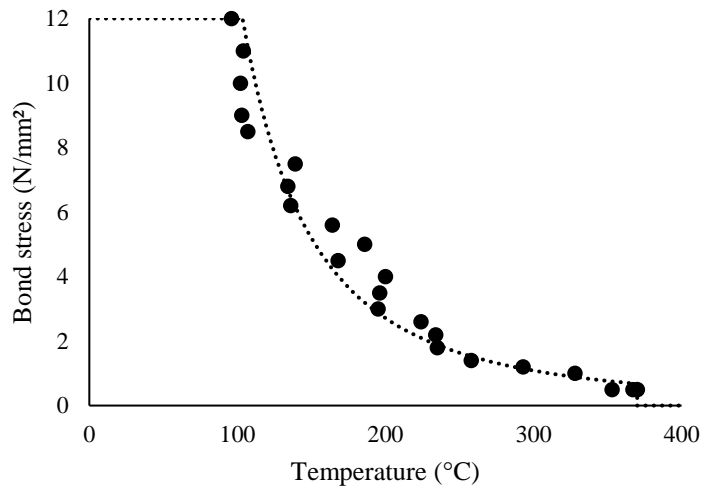


Fig. 103: Bond stress vs. temperature relationship for Adhesive-2 according to EAD 330087-00-0601 [15]

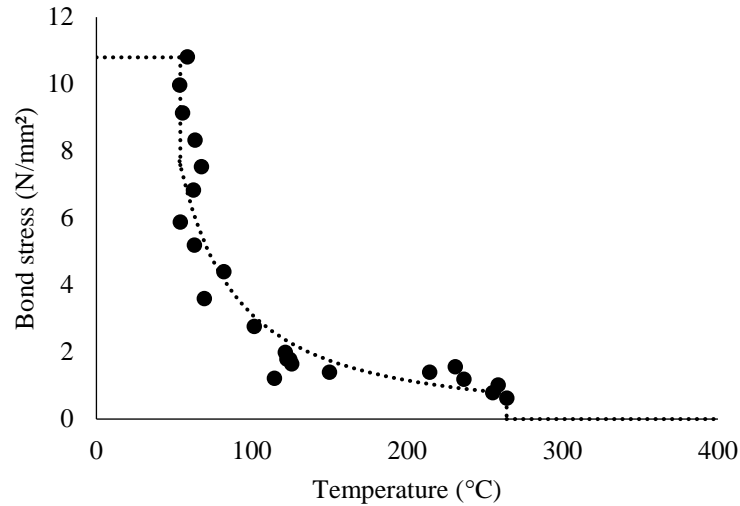


Fig. 104: Bond stress vs. temperature relationship for Adhesive-3 according to EAD 330087-00-0601 [15]

3. Validation of Pinoteau’s Resistance Integration Method (RIM) for fire design of bonded anchors

To investigate the validity of Pinoteau’s RIM, pull-out fire tests were selected from two projects (Table 19). Fig. 105-Fig. 107 show a comparison between fire tests and the outcome of Pinoteau’s method for one example of each of the three adhesives used in this study. The figures show calculated resistances using Pinoteau’s method (Resistance Integration) at 15, 30, 60, 90, 120, 180 and 240 minutes of ISO 834-1 fire exposure in addition to the times where pull-out failure in fire tests occurred.

M10×50 Adhesive-1

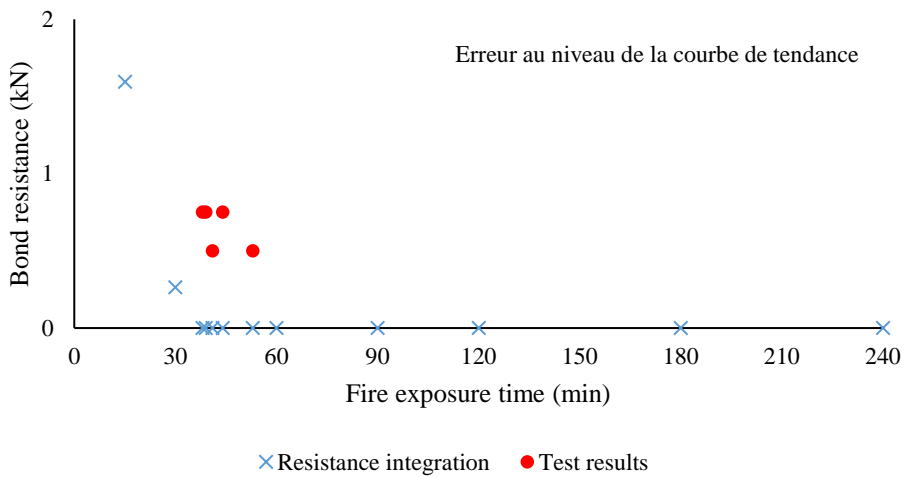


Fig. 105: Fire resistance of M10×50 bonded anchor using Adhesive-1

M12×70 Adhesive-2

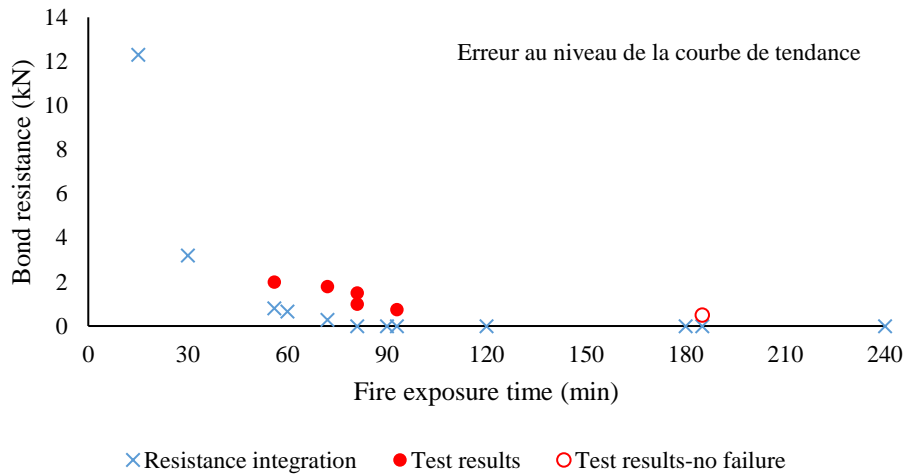


Fig. 106: Fire resistance of M12×70 bonded anchor using Adhesive-2

M8x70 Adhesive-3

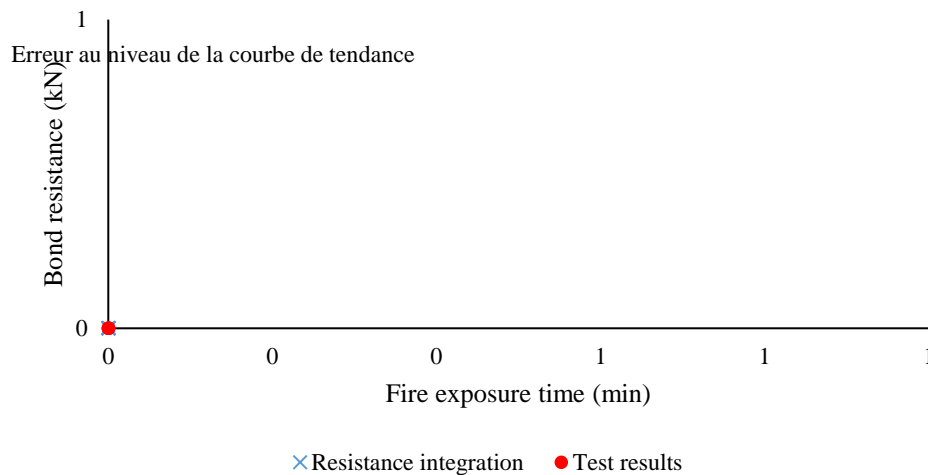


Fig. 107: Fire resistance of M8×70 bonded anchor using Adhesive-3

From the previous results it can be concluded that Pinoteau’s method (Resistance Integration) can be used for the design of bonded anchors under fire conditions. Pinoteau’s method yields conservative design values compared to fire tests. However, some calculated resistances are too conservative where the design method shows that the anchor possesses no resistance under fire conditions. This is due to the fact that Resistance Integration is based on the bond stress vs. temperature curve. So far, this curve was only assessed through the approach in EAD 330087-00-0601 up to a maximum temperature T_{max} for a maximum test duration of less than 3 hours, beyond which no extrapolation is allowed. Therefore, in the Resistance Integration process, when the temperature of the anchor (in a segment or over the whole embedment depth) exceeds the maximum temperature of the bond stress vs. temperature curve, the segment is attributed zero bond stress, hence no contribution to the fire resistance. It should be noted that for an anchor exposed directly to fire conditions, temperature profiles reach and exceed the maximum tested temperatures in Fig. 102, Fig. 103 and Fig. 104 (usually chosen for fire evaluation of Post-Installed Rebars) along the embedment depth very rapidly. This explains the difference between calculated resistances and fire test results, where in reality the anchor still shows a certain resistance at these high temperatures (mostly by friction).

In order to minimize the difference between calculated resistances (Pinoteau’s RIM) and fire test results, a parametric study was conducted to assess the influence of considering the remaining bond stress beyond T_{max} in the Resistance Integration Method. This study is only informative and is only based on test data points up to T_{max}

around 300°C. The curve is extrapolated beyond T_{max} . For design of anchors in reality, this extension of the bond stress vs. temperature curve should be based on test data and not extrapolation. A study was conducted to assess the effects of extending the bond stress vs. temperature curve up to 450°C on the design values of the studied adhesives.

Fig. 108-Fig. 110 show an example for each of the three adhesives on the beneficial influence of considering the bond stress beyond T_{max} in the design method, on the calculated design values (fire resistance of the anchor).

M10×50 Adhesive-1

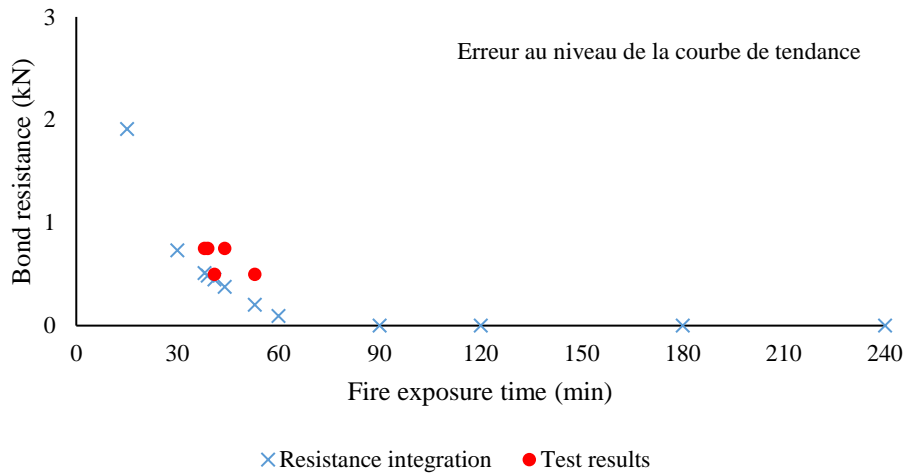


Fig. 108: Fire resistance of M10×50 bonded anchor using Adhesive-1 after consideration of bond stress beyond T_{max}

M12×70 Adhesive-2

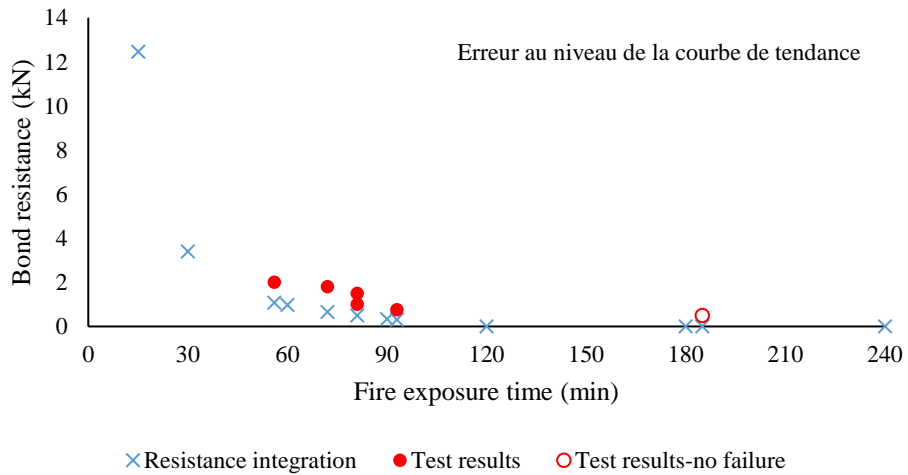


Fig. 109: Fire resistance of M12×70 bonded anchor using Adhesive-2 after consideration of bond stress beyond T_{max}

M8x70 Adhesive-3

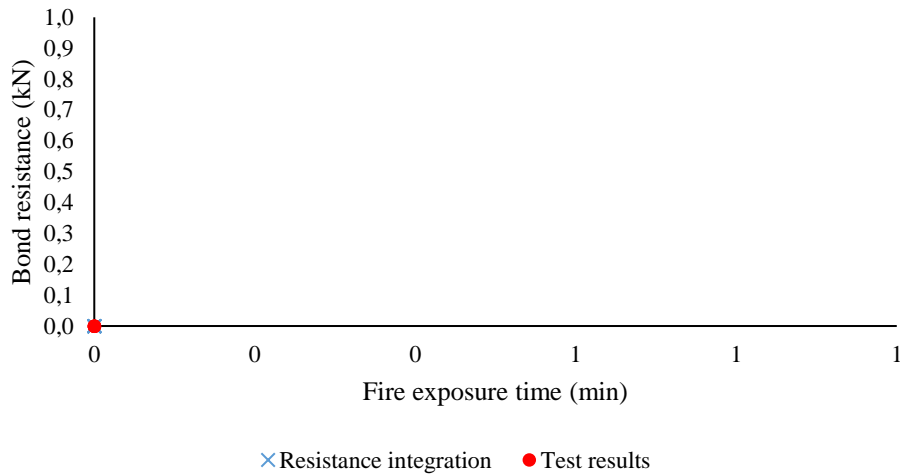


Fig. 110: Fire resistance of M8×70 bonded anchor using Adhesive-3 after consideration of bond stress beyond T_{max}

It should be noted that Pinoteau's RIM does not count as a predictive method for the fire resistance of bonded anchors. It contains several safety factors:

- The method is based on evaluation of PIRs according to [15]. The resulting bond stress vs. temperature curve is slightly conservative compared to tests on bonded anchors (threaded rod inserts). Adopting a curve based on tests with rods could have a beneficial impact on the calculated design values while still preserving the inherent conservatism of the method.
- The bond stress vs. temperature curve is obtained for a constant load and increased temperature applied on the anchor until failure. Failure temperature is obtained by the weighted average of measurements of two thermocouples (head and bottom of the anchor) = 1/3 of the higher measured temperature and 2/3 of the lower measured temperature, yielding a conservative failure temperature value.
- The stress (resistance) profiles are obtained based on temperature profiles calculated according to Eurocode thermophysical properties of concrete and steel using numerical modelling. These material properties are design properties. Calculation based on these properties yield conservative design values and not physically representative values.

Table 19 summarizes the data of this study: fire test data (applied load and pull-out failure time under fire conditions), Pinoteau's RIM results considering the bond stress vs. temperature curve with/without considering temperatures beyond T_{max} .

Adhesive	Anchor geometry (size × embedment [mm])	Applied load [kN]	Pull-out failure time under fire conditions [min]	Pull-out resistance acc. Pinoteau's RIM results (cut at T_{max}) [kN]	Pull-out resistance acc. Pinoteau's RIM results (extended to 450°C) [kN]
Adhesive-1 (epoxy)	M10 × 50	0.50	41	0	0.45
		0.50	53	0	0.20
		0.75	38	0	0.51
		0.75	39	0	0.49
		0.75	44	0	0.38
	M10 × 60	1.00	38	0.50	0.95
	M12 × 55	1.00	45	0	0.50
		1.00	56	0	0.27
	M16 × 70	0.75	61	0	0.74
	M16 × 80	1.00	82	0	0.75
		2.50	52	0.68	1.71
		2.50	67	0	1.15
		2.50	82	0	0.75
	M24 × 95	2.00	75	0	1.77
M30 × 120	9.00	83	0	3.79	
Adhesive-2 (cementitious)	M10 × 60	0.50	185 (no failure)	0	0
		1.00	66	0	0.38
		1.50	60	0.20	0.49
	M10 × 85	0.50	180 (no failure)	0	0
	M12 × 70	0.50	185 (no failure)	0	0
		0.75	93	0	0.30
		1.00	81	0	0.49
		1.50	81	0	0.49
		1.80	72	0.28	0.65
		2.00	56	0.81	1.08
	M12 × 90	1.00	158	0	0.36
	M16 × 80	1.00	101	0	0.32
		1.50	82	0	0.76
		3.00	73	0.49	1.04
	M16 × 100	1.00	180 (no failure)	0	0.34
		2.50	118	0.64	1.27
	M20 × 90	3.50	75	0.80	1.57
	M20 × 110	2.50	137	0.20	1.32
M24 × 96	2.00	106	0	0.64	
	5.50	72	1.17	2.18	
	6.50	52	3.32	4.06	
M24 × 120	2.50	142	0.13	1.70	
Adhesive-3 (epoxy)	M8 × 70	0.60	80	0	0.17
		0.70	69	0	0.23
		0.75	112	0	0.08
		0.75	75	0	0.20
		0.90	100	0	0.11
	M12 × 110	1.50	146	0	0.46
		1.80	115	0.31	0.69
		1.80	60	1.80	1.80
		2.40	55	2.12	2.40
		2.90	68	1.42	1.69
	9.0	29	6.57	6.78	

Table 19: Summary of the data of the study (fire tests and simulation results)

Results in Table 19 show that there is a beneficial effect of accounting for the remaining bond stress at high temperatures in the design calculations. This benefit remains nonetheless on the conservative side as the design values do not exceed test results. Several factors could bring the design calculations closer to test results (reality). In this work, as a continuity of what the authors initiated in previous publications, the work focuses on minimizing the differences between reality and calculations (i.e. more realistic thermal calculations, better bond stress temperature curve to be used as entry data). The discrepancy between design and test results can be linked to a number of factors; of which the following can be noted:

1. The applied ISO curve inside the furnace (allowing a certain tolerance of $\pm 100^{\circ}\text{C}$ during the test). The allowance of such tolerance has an impact on temperature profiles. In addition, there are other factors in play, the objective of the authors was to remain on the conservative side.
2. The applied load on anchors (using dead loads or hydraulic jacks): using dead loads has proven to be more accurate since using hydraulic jacks has shown that it is hard to compensate the loss in applied load due to creep during the test (sometimes occurring very rapidly).
3. The population of the bond stress temperature curve obtained from EAD as entry data on PIRs, and its representability of the curve obtained using rods (curve based on rods was shown to have a similar or better behavior than curve on PIRs).
4. The lower limit imposed on the bond stress temperature curve (proposed to be increased to 450°C in this paper): a residual resistance can still be found above this temperatures showing discrepancies for long exposures to fire conditions (i.e. high temperatures along the embedment depth) between calculations and fire tests.

4. Conclusions

This paper presents validation and parametric study of Pinoteau's Resistance Integration Method (RIM) for calculating the load-bearing capacity of bonded anchors in uncracked concrete under ISO 834-1 fire conditions [17]. The method employs 3D transient heat transfer equations to obtain temperature profiles along the embedment depth of anchors. The temperature profiles then serve as input for the RIM, in which bond strength contributions of discrete segments along the embedment depth of anchors is computed during fire exposure. In this study, the method was validated with experimental results obtained in two previous experimental studies [22, 23] on three different adhesives (two epoxy based mortars and one cementitious based mortar) resulting in conservative calculations of load-bearing capacities at various fire exposure times compared to experimental results for various configurations and sizes of bonded anchors (sizes from M8 to M30, embedment depths from 50 to 120 mm).

A study was also presented after experimental validation of Pinoteau's method. This study investigated the influence of considering the bond stress vs. temperature curve beyond the maximum temperature allowed for the assessment of post-installed reinforcement (PIR) in EAD 330087-00-0601, resulting in the following conclusion: Extending the curve up to a temperature of 450°C yielded more advantageous and conservative design values (less conservative than stopping the curve at $\sim 300^{\circ}\text{C}$) for bonded anchors under fire conditions for the investigated adhesives.

The authors therefore recommend adoption of Pinoteau's Resistance Integration Method in assessment and qualification documents for bonded anchors under fire conditions. Furthermore, the extension of the bond stress vs. temperature curve by means of testing to benefit from the residual bond stress of the bonded anchor at very high temperatures is recommended. Since bonded anchors are directly exposed to fire through the steel element, they reach much higher temperatures in a short period of fire exposure time compared to post-installed reinforcement. The extension of the curve can be achieved by increasing the heat rate imposed on the characterization tests according to existing EAD 330087-00-0601 procedures while respecting the 3 hour and $5^{\circ}\text{C}/\text{min}$ heating rate conditions. Another method to achieve this goal can also be by conducting bond strength at increased temperature tests according to EAD 330087-00-0601 procedures using stabilized temperature and increased displacement at the desired moment of characterization [15].

References

- [1] EN 1992-4. Eurocode 2 – Design of concrete structures – Part 4 : Design of fastenings for use in concrete. September 2018.
- [2] Eligehausen R, Mallée R, Silva JF. Anchorage in concrete construction. Ernst & Sohn; 2006.
- [3] Eligehausen R, Werner F. Recent developments and open problems in fastening technique. In: 2nd international symposium on connections between steel and concrete, Stuttgart, *fib*, Germany; 2007.
- [4] Petit J, Nassiet V, Baziard YH-RB. Etude de la durabilité des assemblages collés. *Techniques de l'ingénieur*; 2005. p. COR160.
- [5] Zhang Y, Lou G, Chen K, Li G. Residual strength of organic anchorage adhesive for post-installed rebar at elevated temperatures and after heating. *Fire Technol J* 2016;52:877–95.
- [6] Muciaccia, G., Navarrete, D.D., Pinoteau, N., Mege, R. Effects of different test apparatus and heating procedures on the bond properties of post-installed rebar connections under elevated temperatures. *Mater Struct* (2019) 52: 47.
- [7] EOTA. EAD 330499-01-0601. Bonded fasteners for use in concrete. June 2019.
- [8] ICC-ES. AC308. Acceptance criteria for post-installed adhesive anchors in concrete elements. October 2017.
- [9] National Transportation Safety Board, 2006. Ceiling Collapse in the Interstate 90 Connector Tunnel Boston, Massachusetts.
- [10] Georgia Department of Transportation, 2012. 17th Street Bridge Canopy Failure Investigation, s.l.: WJE.
- [11] Reis J. Effect of temperature on the mechanical properties of polymer mortars. *Mater Res* 2012;15(4):645–9.
- [12] Reichert M, Thiele C. Qualification of bonded anchors in case of fire. Proceedings of the 3rd international symposium on connections between steel and concrete. Stuttgart, Germany. September 2017. p. 1191–9.
- [13] Lakhani H, Hofmann J. A numerical method to evaluate the pull-out strength of bonded anchors under fire. Proceedings of the 3rd international symposium on Connections between Steel and Concrete. Stuttgart, Germany. September 2017. p. 1179–90.
- [14] EOTA TR 020. Evaluation of anchorages in concrete concerning resistance to fire. European Organization for Technical Approvals Technical report no. 20. May 2005.
- [15] EOTA. EAD 330087-00-0601. Systems for post-installed rebar connections with mortar. May 2018.
- [16] Pinoteau N [Ph.D thesis]: Behavior of post-installed rebars in concrete under fire, Lille: University of Lille (France). <https://ori-nuxeo.univ-lille1.fr/nuxeo/site/esupversions/de94303f-5d72-4f61-9183-515ff08b490b>; 2013.
- [17] ISO 834-1 International Standard. Fire-resistance tests – Elements of building construction – Part 1: General requirements. First edition, 15 September 1999.
- [18] Lahouar MA, Pinoteau N, Caron J-F, Forêt, Rivillon Ph. Fire design of post-installed rebars: full-scale validation test on a $2.94 \times 2 \times 0.15$ m³ concrete slab subjected to ISO 834–1 fire. *Eng Struct J* 2018;174:81–94.
- [19] Lahouar MA, Pinoteau N, Caron J-F, Forêt G, Mège R. A nonlinear shear-lag model applied to chemical anchors subjected to a temperature distribution. *Int J Adhe Adhes* 2018;84:438–50.
- [20] Reichert, M, Thiele, C, 2017. Verbunddübel im Brandfall-DIBt. Kaiserslautern, University of Kaiserslautern.
- [21] Lakhani H, Hofmann J. On the pull-out capacity of post-installed bonded anchors and rebars during fire. Proceedings of the 10th International Conference on Structures in Fire. Belfast, UK. June 2018. p. 165-71.
- [22] Al-Mansouri O, Mège R, Pinoteau N, Guillet T, Piccinin R, McBride K, Rémond S. Numerical investigation of parameters influencing fire evaluation tests of chemically bonded anchors in uncracked concrete. *Eng Struct J* 2020;209:110297.
- [23] Al-Mansouri O, Mege R, Pinoteau N, Guillet T, Rémond S. Influence of testing conditions on thermal distribution and resulting load-bearing capacity of bonded anchors under fire. *Eng Struct J* 2019;192:190-204.
- [24] EN 1363-1. Fire resistance tests Part 1: General requirements. February 2020.
- [25] EN 1993-1-2. Eurocode 3: Design of steel structures – Part 1-2: General rules – Structural fire design. November 2005.
- [26] EN 1992-1-2. Eurocode 2: Design of concrete structures – Part 1-2: General rules – Structural fire design. July 2008.
- [27] ACI 318-14, "Building code requirements for reinforced concrete" Detroit, Michigan: American Concrete Institute, 2014.

Analysis and discussion

Applicability of Pinoteau's method for the design of bonded anchors under fire:

The results presented in the previous paper provide an experimental proof that Pinoteau's method is applicable for the design of pull-out failure of bonded anchors under fire in uncracked concrete. These results show that for a variety of anchor sizes from M8 to M30 with embedment depths from 50 to 120 mm, the calculation of the pull-out resistance under fire using Pinoteau's method yielded conservative values compared to fire tests.

In any future extension of the current guidelines to cover the evaluation of bonded anchors under fire, fire tests should provide the experimental proof that Pinoteau's method (the current experience) still applies and yields conservative design values. Therefore, a minimum embedment depth shall be specified (usually by the manufacturer) to induce the pull-out failure under fire in the fire tests. It is recommended that such a program be limited to a few fire tests on a medium size and fewer on a small and large size. *Reichert and Thiele (2017)* have proposed such a testing program for bonded anchors under fire. It is also recommended that such tests be used for the validation of the applicability of Pinoteau's method for the design of bonded anchors with variable embedment depth. In other words, a reduced test program should be required to assess the pull-out resistance on a bonded anchor configuration resulting in pull-out failure under fire. Following the validation of conservativeness of Pinoteau's method on the tested adhesive resin, the design should be allowed for deeper embedment depths (higher than the tested embedment). Indeed, the goal for any designer would be to get the maximum resistance of the product, which in the case of bonded anchors under fire is the minimum of all resistances of all failure modes. By increasing the embedment depth, the designers can increase the bond resistance of the anchor until it exceeds another resistance for other failure modes (e.g. steel or concrete cone failure modes).

Repeatability and correction of fire test results

The (*EN 1363-1, 2020*) referenced in the European guidelines allows to conduct fire tests according to the ISO 834 standard curve. Fire tests on anchors in the literature and in this work were conducted in special gas furnaces allowing to apply the thermal conditions (i.e. hot gas temperature) following the standard ISO 834 heating curve (Fig. 4). Inside the furnace, the applied heating curve shall not deviate from the theoretical curve by $\pm 100^\circ\text{C}$ at any time starting from 10 min from the beginning of the test (beginning of fire exposure). In practice, the applied heating curve is measured by different plate thermometers inside the furnace (Fig. 36) and its value is calculated as the mean value of all measured temperature by plate thermometers inside the furnace. Such heating configuration inside the furnace can result in local differences between different plate thermometers inside the furnace within the \pm tolerance interval of the measurement of the furnace temperature (using plate thermometers, see Fig. 36), but the whole test can still qualify for fire resistance. This leads to a mean measurement of the furnace temperature following the theoretical standard curve but can also lead to a local difference (at the position where the anchor is installed in the concrete element) with $+ \text{ or } - 100^\circ\text{C}$ from the standard curve. Fig. 111 shows an example of furnace operating of a fire test on bonded anchors. According to the requirements of *NF EN 1363-1 (2020)* and the *ISO 834-1 (1999)* standard, the test respects the requirements for the determination of fire resistance. Although the temperature of the furnace (measured by the mean value of plate thermometers: TC no. 01F and TC no. 02F) follows the standard curve, anchors installed in the concrete element and positioned in front of these plate thermometers are subjected to different heating. For example in Fig. 111, anchors positioned in front of TC no. 01F are subjected to a heating curve very similar to the standard curve up to almost 70 min of fire exposure. Beyond 70 min, these anchors can experiment a failure earlier than expected compared to the standard curve due to excessive heating. On the other hand, for anchors positioned in front of TC no. 02F are subjected to a heating curve very similar to the standard curve up to almost 35 min of fire exposure. Beyond 35 min, these anchors can experiment a delay of failure time than expected compared to the standard curve due to insufficient heating.

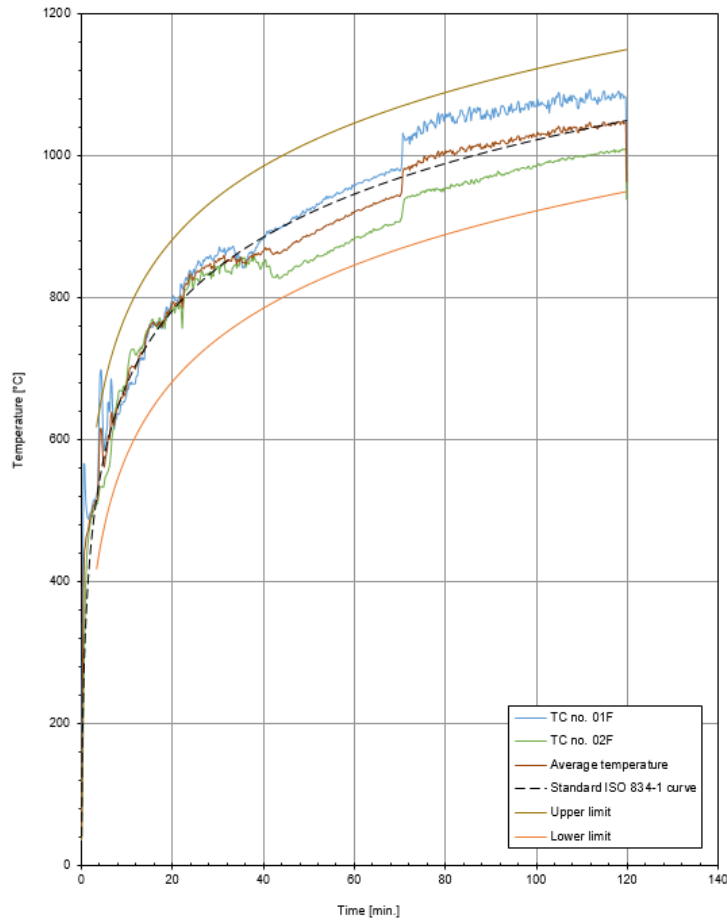


Fig. 111: Example of furnace operating of fire tests on anchors

These local differences between different locations inside the furnace can dissipate if the tested element is a concrete beam or slab and the goal is to characterize the concrete element or a concrete-concrete connection (e.g. testing a structural connection of post-installed rebars embedded in a concrete element). Indeed, the concrete surface and the thermal resistance of concrete contribute to distributing the heat equally on the surface and minimizing the effect of heating differences inside the furnace. However, such local differences can yield a significant impact if the tested element is a small anchor embedded in a specific position in the slab exposed to a different local temperature evolution inside the furnace during the fire test compared to the standard curve. Therefore, the obtained test results (i.e. fire resistance vs. fire exposure time) correspond only to the applied heating at the position of the anchor that can sometimes be different from the standard ISO 834 curve by $\pm 100^{\circ}\text{C}$. This could lead to false reporting of test results by means of fire resistance as a function of a fire exposure duration. Therefore, fire test results on anchors should be corrected using a correlation factor allowing by assessing the amount of heating energy applied on the anchor compared to the theoretical amount of energy that should have been applied on the anchor if the standard curve was applied all along the fire test.

The ISO 834-1 (1999) standard does not allow such a correction. However, the American standard (ASTM E119, 2020) allows a correction factor taking into account such an effect: “When the indicated resistance period is 30 min or over, a correction factor shall be applied for variation of the furnace exposure from that prescribed (i.e. standardizes curve), where it will affect the classification, by multiplying the indicated period by two thirds of the difference in area between the curve for the first three fourths of the time period and dividing the product by the area between the standard curve and a base line of 20°C for the same part of the indicated period, the latter area increased by $30^{\circ}\text{C}\cdot\text{h}$ or $1800^{\circ}\text{C}\cdot\text{min}$ to compensate for the thermal lag of the furnace thermocouples during the first part of the test. For fire exposure in the test higher than the standard, the indicated resistance period shall be increased by the amount of the correction and be similarly decreased for fire exposure below standard”. The correction can follow the following [Eq. 19]:

$$C = 2I/(A - A_s)/3(A_s + L) \dots [\text{Eq. 19}]$$

With: C is the correction in the same unit as I , I is the indicated fire resistance, A is the area under the curve of indicated average furnace temperature for the first three fourths of the indicated period, A_s is the area under the standard furnace curve for the same part of the indicated period and L is the lag correlation in the same unit as A and A_s ($30^\circ\text{C}\cdot\text{h}$ or $1800^\circ\text{C}\cdot\text{min}$).

It should be noted that the ASTM E119 standard provides the requirements for fire tests in North America. The standard curve is very similar to the ISO 834 curve. However, it is not measured by the same type of thermometers. In the ISO 834 curve, plate thermometers are used allowing to measure directly the hot gas temperature with negligible thermal lag. However, in the ASTM E119 curve the thermocouples are inclosed in protection tubes of such materials and dimensions that the time constant of the protected thermocouple assembly lies within the range from 5.0 to 7.2 min. Therefore, the correction proposed for fire tests in ASTM E119 can be used for correcting fire test results on anchors in general (or bonded anchors specifically), by replacing the value of the term A in Eq. 19 by the area under the curve of the measured temperature by the closest plate thermometers or the mean measured value of temperature by the surrounding closest plate thermometers. In addition, the thermal lag is expected to be negligible in ISO 834 fire tests. Hence, the coefficient L should be dropped out of the equation.

This correction was not taken into account in this work but is proposed for any future guidelines dealing with the evaluation of fire tests on anchors.

In this thesis, all the presented data and fire tests on bonded anchors followed the standard curve very closely and very small local deviations from the standard curve temperature during the fire test were observed in the measurements. Therefore, no correction of test results was needed. Fig. 112 shows an example of furnace operating following the standard heating curve with negligible tolerances between different plate thermometers inside the furnace.

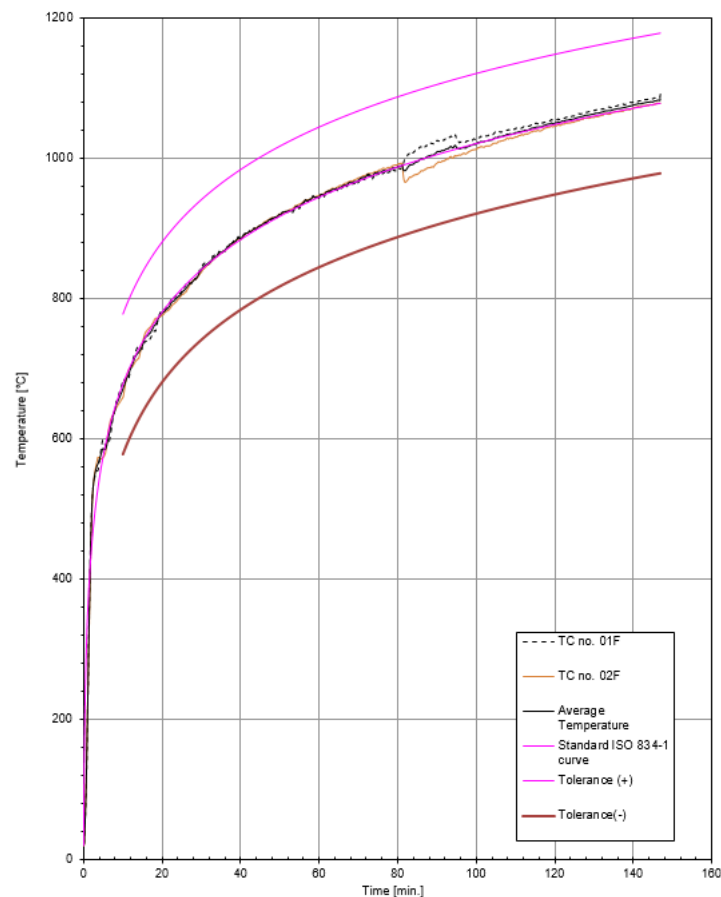


Fig. 112: Example of furnace operating for conducted fire tests in this thesis

Accounting for cracked concrete:

Fire design of anchors in general under fire should be conducted accounting for cracked concrete. It is supposed that cracks in the concrete element might appear due to the tensile loads or thermal cracks might be created during a fire event. These cracks are logically supposed to pass by the weakest path in the concrete element, where concrete was removed of the section to create a local stress concentration area where the anchor is installed.

So far, the work in this thesis concentrated on the validation of the existing methods for the evaluation of bonded anchors (based on the existing method for mechanical anchors) and design of bonded anchors (adapting Pinoteau's method that was initially developed for post-installed rebars). However, the influence of cracked concrete is still unaccounted for. Cracks running through the embedment depth of bonded anchors have a significant mechanical effect on the load-carrying capacity. Also, during heating crack width might change due to the thermal expansion of the concrete element. Such influence should be assessed in order to provide a full view on the evaluation of bonded anchors under fire by:

- 1- Starting by the characterization tests to determine the bond strength vs. temperature relationship according to EAD 330087-00-0601 (2018).
- 2- Conducting fire tests in uncracked concrete on a reduced number of samples with minimum embedment depth to provoke pull-out failure. The results of these tests are used to validate the calculations based on Pinoteau's method to prove its applicability on the tested adhesive.
- 3- Assessing the influence of cracked concrete (the next chapter in this thesis) to provide a load-carrying capacity reduction factor due to crack existence (reduction factor = pull-out resistance in cracked concrete/pull-out resistance in uncracked concrete).

Chapter V: Behavior of bonded anchors in cracked concrete at high temperature using electrical heating

Chapter V resumes the conference paper entitiled “**Behavior of bonded anchors in cracked concrete at high temperatures**” published on November 23, 2020 in the 2020 *fib* symposium in Shanghai. This paper focuses on the influence of cracked concrete on the bond strength of bonded anchors at high temperatures.

Objectives

Following the adaptation of the testing method and the validation of the design method for pull-out failure mode of bonded anchors under fire on a wide range of anchor sizes/embedments, the question of bonded anchors in cracked concrete at high temperature should be addressed to fully cover the evaluation of its performance in reinforced concrete elements. This chapter focuses on the influence of crack existence on the load-bearing behavior of bonded anchors at high temperatures in comparison with its influence at ambient temperature. Indeed, the current state of the art and evaluation standards allow proper evaluation of bonded anchors in cracked concrete at ambient temperature.

Such influence should be studied at high temperatures to assess if it is expected to vary with increased heating. Indeed, it could cause more degradation of the bond due to a direct exposure to temperature at various embedment depth along the crack, or the crack might close due to the thermal expansion of the concrete element where probably no influence of cracking can be noticed. Both thermal and mechanical aspects of crack existence at high temperatures should be regarded as well. Therefore, a new testing method was developed at CSTB to test a large number of anchor sizes in relatively small size slabs at high temperatures. This allows to increase the population of test series to allow a more pronounced conclusion on the obtained test results (i.e. in order to reach a minimum level of repeatability in the test results). Finally, the conclusions of this study open a window towards the evaluation of bonded anchors in cracked concrete under fire without the actual testing under ISO834 fire. Nonetheless, the developed testing method allows to assess if crack existence might or might not have a more severe influence at high temperature than at ambient temperature (i.e. more reduction on the load-bearing capacity compared to the case without fire).

This chapter has two main objectives:

1. Assess crack influence on bonded anchors at high temperatures and its evolution with increased heating: the reduction of the bond strength due to the existence of the crack is assessed for different heating scenarios (heating duration by radiant panels). The influence of crack existence without heating (i.e. at ambient temperature) is taken as the reference reduction ratio.
2. Propose a new testing method allowing to test bonded anchors in cracked concrete with controlled heating and more repeatability tests: conducting ISO 834 fire tests offers less repeatability and controllability of the applied fire inside the furnace (compared to the standard curve). The proposed approach using electrical heating by radiant panels offers a more controllable heating scenario allowing more repeatability. The obtained reduction of the bond strength due to crack existence at high temperature from such tests is therefore more reliable than the one obtained by standard fire tests.

BEHAVIOR OF BONDED ANCHORS IN CRACKED CONCRETE AT HIGH TEMPERATURES

Omar AL-MANSOURI^{1,2}, Romain MEGE¹, Nicolas PINOTEAU¹, Thierry GUILLET¹, Roberto PICCININ³, Kenton MCBRIDE³, Sébastien REMOND⁴

¹ Université Paris-Est, Centre Scientifique et Technique du Bâtiment (CSTB), Champs-sur-Marne, France

² IMT Lille-Douai, Univ. Lille, EA 4515 – LGCgE, Département Génie Civil & Environnemental, Lille, France

³ Hilti Corp., Schaan, Principality of Liechtenstein

⁴ Univ Orléans, Univ Tours, INSA CVL, LaMé, EA 7494, France

Corresponding author's email: omar.almansouri@cstb.fr

Abstract

Post-installed bonded anchors are commonly used in steel-to-concrete connections that demand high load-carrying capacities and flexible and/or unplanned anchoring locations. While formulations of polymer-based bonded anchors have continued to advance in their temperature-resistant properties, all polymers possess an inherent sensitivity in load-carrying capacity to temperatures near and above glass transition.

Protocols for determining fire performance of post-installed bonded fastening products are described in EOTA TR 020 for bonded anchors and EAD 330087 (2018) for post-installed reinforcement (PIR). No fire criteria are currently provided in EAD 330499 (2019) for bonded fasteners or in any American anchor assessment documents. Beyond the limitation that TR 020 (2005) cannot be used as the basis for a European Technical Assessment, descriptions in TR 020 permit a degree of interpretation that can significantly influence the evaluated performance of bonded anchors under fire conditions. Therefore, there is a need to improve the fire assessment of bonded anchors in uncracked and cracked concrete by recommending clearer and more specific criteria that can be placed into anchor assessment documents.

This paper presents an experimental study on bonded anchors using an epoxy resin in cracked concrete exposed to high temperature. Reference confined pull-out tests were conducted on bonded anchors in cracked (0.3 mm crack width) and uncracked concrete at ambient temperatures in accordance with existing European guidelines. Tests were then conducted on bonded anchors in cracked and uncracked concrete exposed to high temperature with an electrical heating system. The results were analysed to understand the thermal and mechanical influence of a crack running along the embedment depth of the anchors at ambient and elevated temperatures. This experimental study provides a database for future development of testing and assessment requirements for bonded anchors exposed to high-temperature fire conditions.

Keywords: *Bond, anchor, anchor, crack, fire, resin, adhesive, thermal distribution.*

Literature review

Over the years, many types of anchorage systems have been developed and tested. Post-installed anchors are increasingly used in the field of construction thanks to their easy and rapid installation in pre-existing structural and non-structural elements for retrofitting as well as strengthening of existing structures (ACI 318-11, 2011). Post-installed bonded anchors transfer loads to the concrete bearing element by chemical bond and friction, producing bond stresses that are nearly uniformly distributed along the embedment depth (Kumar, 2009).

The behaviour of bonded anchors is influenced by many factors (e.g. geometry, installation procedure, moisture, material properties of the adhesive and the adherent and temperature...) (Petit et al., 2005), (Eligehausen et al., 2007), (Zhang et al., 2016), (Muciaccia et al., 2019). The mechanical properties of adhesive resins are particularly temperature-dependant (Reis, 2012). When exposed to fire, structural members are subjected to heavy thermal loading inducing thermal gradients in a short period of time. The increase of temperature degrades the material properties of concrete (EN 1992-1-2, 2008), (ACI 318-14, 2014), steel (EN 1993-1-2, 2005) and resin (Sorathia et al., 1997), reducing the load-bearing capacity of the connection.

Studies have shown that different types of adhesive resins exhibit varying levels of sensitivity to temperature increase. Epoxy resins in particular are more sensitive to temperature than polyester mortars (Ribeiro et al., 2004). The glass transition temperature (T_g) of the polymer quantifies the temperature effect on polymeric materials. The adhesive bond shows a reduction in stiffness and ultimate capacity when its temperature exceeds T_g (Pinoteau et al., 2013). Temperature increases to values below the glass transition temperature enhance the mechanical properties of the resin due to the continuation of the cross-linking reaction between the mother resin and the hardener. Studies on Post-installed reinforcement (PIR) showed that when bond temperature of loaded anchors exceeds T_g , changes of physical state occur leading to a stress redistribution along the embedment length of the anchors (Lahouar et al., 2017). Other studies on PIR showed that the heating rate of the adhesive bond is of importance (Pinoteau et al., 2013), where they demonstrated that high heating rates lead to thermal gradients along the steel member and therefore to a stress redistribution of bond stress.

Anchors may fail in different failure modes at ambient temperatures (Eligehausen et al., 2006), (EN 1992-4, 2018). Under fire, the pull-out failure mode may occur more frequently than other failure modes due to the high sensitivity of the adhesive to temperature increase and rapid degradation of its mechanical properties. Therefore, it is most interesting to evaluate the bond capacity of bonded anchors in accidental situations such as fire exposure.

The guidelines in EOTA TR 020 (2005) for determining fire performance of anchors were integrated in the European Assessment Document EAD 330232 (2019) for mechanical anchors. Their integration in the European Assessment Document 330499 (2019) for bonded fasteners is still in progress. However, no American assessment document provides protocols for this particular problem. Furthermore, the limitations of the EOTA TR 020 (2005) for the case of bonded anchors were investigated by several authors (Reichert and Thiele, 2017) and (Al-Mansouri et al., 2019). The existing assessment protocol prescribes a steel fixture for load transfer to anchors. The steel fixture is directly exposed to fire for the assessment of anchors in uncracked concrete. The allowance of insulating material to protect the fixture from direct exposure to fire in the case of anchors in cracked concrete raises questions. Indeed, (Reichert and Thiele) signalled that tests on bonded anchors in cracked concrete according to EOTA TR 020 (2005) using insulating material around the fixture should be avoided and Al-Mansouri et al (2019) showed that insulating material around the fixture protects the fixture and the bonded anchors from fire leading sometimes to twice the resistance compared to the case with no insulation around the fixture.

The existing assessment documents for anchors in concrete at ambient temperature give clear guidelines for determining the ratio of the load-bearing capacity between anchors in cracked concrete and anchors in uncracked concrete for concrete classes between C20/25 to C50/60. In general, for common size bonded anchors with small and medium size anchors, the ratio of bond strength for anchors in cracked concrete to uncracked concrete is around 70%.

This paper presents an experimental study to investigate the bond behaviour of bonded anchors at high temperature in cracked concrete. First, reference tests were conducted in uncracked and cracked concrete (0.3 mm crack width) at ambient temperature (20°C) using the European Assessment Document for bonded fasteners (EAD 330499, 2019). Then, tests on bonded anchors in uncracked and cracked concrete were conducted at high temperature to capture the reduction of pull-out strength due to crack existence. Heating was done using radiant panels capable of radiating at a surface temperature up to (400°C) at the surface of the panels. The anchors were directly exposed to heating up to a certain thermal gradient along the embedment depth of the anchor with no load applied on anchors. Then, the heating system was removed, and a confined tension test was immediately conducted on the anchor to determine the pull-out capacity of the anchor. The results of different series of tests with different heating durations (2 hours, 3 hours and 4 hours) were assessed and the ratio of bond resistance in cracked concrete to uncracked concrete was determined from the mean value of bond strength.

Experimental procedure

This section describes the testing procedure using radiant panels as a heating system and the ratio of the pull-out capacity for bonded anchors in cracked concrete to uncracked concrete. Test results at ambient and high temperature allowed to determine if the reduction due to crack existence at ambient temperature changes due to temperature increase. Indeed, the current guidelines in EOTA TR 020 (2005) consider that the values of fire tests on anchors in uncracked concrete can be taken without reduction for use in cracked concrete.

The goal of this work was to check if the reduction from uncracked to cracked changes at high temperature (Fig. 113). Reichert (2017) investigated the reduction of strength of bonded anchors loaded in tension under fire due to

crack existence compared to uncracked concrete. This work, although done on a limited number of tests, proves that there is a reduction due to crack existence under fire and that the current status of the guidelines allowing adoption of the values of fire tests in uncracked concrete for the case of cracked concrete should be revoked. However, this work did not investigate the evolution of this reduction with temperature increase, and the ratio of bond strength between uncracked and cracked concrete is calculated from power trend tendency curves based on a limited number of fire tests.

The principle of the research done in this paper (as summarized in Fig. 113) is the following: the reduction of bond strength at ambient temperature from uncracked to cracked concrete α can be found by conducting a series of tests according to the EAD 330499 (2019) for bonded fasteners. At high temperature, such as in the case of fire (or any high temperature short term heating scenario), a reduction of bond strength β in uncracked concrete can be found from ambient to high temperature. The question arising is whether the reduction of bond strength at high temperature from uncracked to cracked concrete γ is different from α . If this is the case, then the reduction factor δ for bond strength in cracked concrete from ambient to high temperature is different from β . If not, then the reduction γ does not change at high temperature and the reduction α can be taken from tests at ambient temperature for the reduction from uncracked to cracked concrete at high temperature.

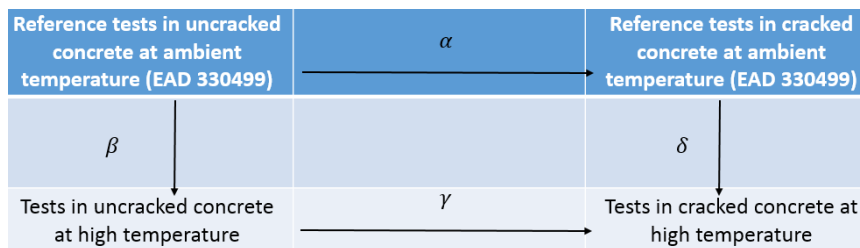


Fig. 113: Reduction factors of bond strength from uncracked to cracked concrete at ambient and high temperatures

Reference tests at ambient temperatures

Series of 5 confined tension tests were conducted on bonded anchors in uncracked and cracked concrete ($\Delta w = 0.3$ mm) using an adhesive epoxy resin (Hilti HIT-RE 500 V3) according to the European Assessment Document for bonded fasteners (EAD 330499, 2019).

The concrete slabs had a reinforcement degree of approximately 0.8%. Slab dimensions were (1.5 m length \times 0.5 m width \times 0.2 m thickness). Fig. 114 shows a cross section (0.5 \times 0.2 m) in the slab with the bonded anchor installed at $4d$ for reference tests. A concrete class of C20/25 was used for the slabs. The compressive strength of concrete was tested on a series of 3 cubes (15 \times 15 \times 15 cm) and 3 cylinders (ϕ 16 cm – L32 cm) at 28 and 256 days (date of testing). The concrete compressive strengths were $f_{c,28} = 35.5$ MPa, $f_{ck} = 32.1$, $f_{c,256} = 38$ MPa and $f_{ck,256} = 35.7$ MPa.

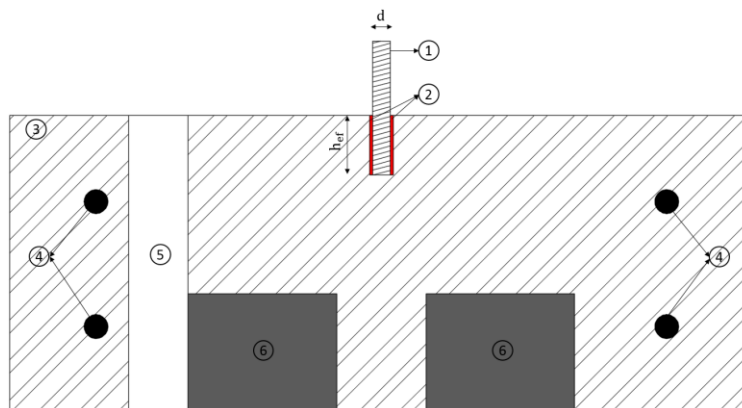


Fig. 114: Cross section of the slab with: (1) threaded rod, (2) adhesive resin, (3) concrete slab, (4) HA16 reinforcement bars, (5) hole for wedges and (6) thin steel plates for crack orientation.

The diameter of the threaded rods used for tests was $d = 12$ mm (M12 rods) made of carbon steel with a steel grade of 10.9. An embedment length of approximately $h_{ef} = 4d$ was adopted for the reference tests. This length was chosen to avoid steel failure of the rod and obtain pull-out failure of the anchor because the study focuses on the behaviour of the bond. An adhesive layer around the rod of 2 mm thickness was adopted. Anchors were installed in cracked concrete after creation of cracks. The hole cleaning procedure in the MPII (Manufacturer's Product Installation Instructions) using compressed air and a specific brush was adopted. The anchors were left to cure at the curing time defined by the manufacturer.

Hairline cracks were initiated prior to installation of anchors using wedges (Fig. 115). Wedges were installed inside the concrete slab and crossed the entire section of the slab. The diameter of the wedge before expansion is 40 mm. The advantage of using wedges is that they ensure a homogeneous crack along the section of the concrete slab (around the cross section). Crack width was measured using displacement sensors placed on the upper side of the slab prior to cracking. Crack displacement sensors were placed on one side of the anchor and measured the displacement of a metallic ring placed around the anchor with the anchor in its centre. The crack displacement sensor was fixed on one side of the crack and the metallic ring was fixed on the other side of the crack (Fig. 116).

Wedges were expanded by applying a pressure that leads to the required opening of cracks. The crack displacement sensor measured the displacement of the slab on one side of the crack to the other which corresponds to the width of the crack (Δw). Special measures were taken to ensure vertical-straight-like cracks along the section. These measures consisted in placing (prior to casting of concrete) adhesive tape around the reinforcement bars at the area where the cracks have to be created and the use of steel plates at the bottom of the slab to orient the cracks in a favourable path.



Fig. 115: Wedges used for cracking concrete with: (1) lower side of the slab, (2) thin steel plate, (3) wedges and (4) hairline crack.

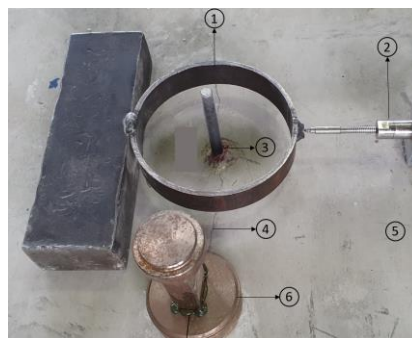


Fig. 116: Crack width measurement with: (1) metallic ring, (2) displacement sensor, (3) bonded anchor, (4) crack, (5) upper side of the slab and (6) wedges.

Each slab had a total of 3 cracks with approximately 350 mm spacing between the cracks. In each crack one M12 bonded anchor was installed at an embedment depth of $h_{ef} = 100$ mm $\approx 8.33d$ with an adhesive layer of 2 mm around the rod (Fig. 117). Other anchors were installed in uncracked concrete at the same embedment depth with enough spacing to prevent mechanical and thermal interaction between neighbouring anchors.

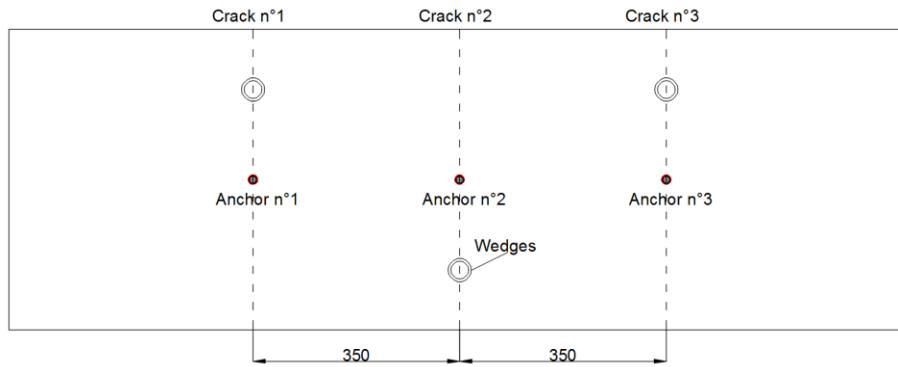


Fig. 117: View of the test slab with the position of anchors in cracked concrete

The results of confined tension tests at ambient temperature on bonded anchors are given in details in Fig. 118. The ratio of bond strength between bonded anchors in cracked concrete and uncracked concrete is 68%. This ratio is close to the usual ratio of 70%.

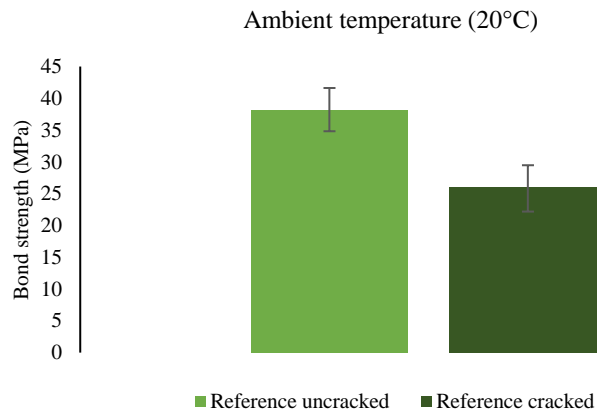


Fig. 118: Results of pull-out tests on bonded anchors in uncracked and cracked concrete

Tests at high temperatures

In order to assess if the ratio of bond strength between cracked and uncracked concrete changes at high temperatures, tests in cracked and uncracked concrete on bonded anchors were conducted using electrical heating. The heating system consisted of radiant panels capable of radiating at a surface temperature (surface of the panels) of approximately 400°C. This device was developed internally in CSTB to conduct tests on concrete elements with a relatively slow heating rate compared to a standard ISO fire. Heating is applied on the exposed surface of the slab by radiation only without convection. The heating system is capable of covering a slab of the same dimensions as used for the reference tests (1.5 × 0.5 × 0.2). The panels are situated on the upper side of the heating system. They consist of small radiant units distributed homogeneously around the surface of the heating system (Fig. 119). Fig. 120 shows a photo of the heating system on top of a test slab. The sides of the heating system were insulated with a rock wool-based material to provide optimal heating inside and limit energy loss.

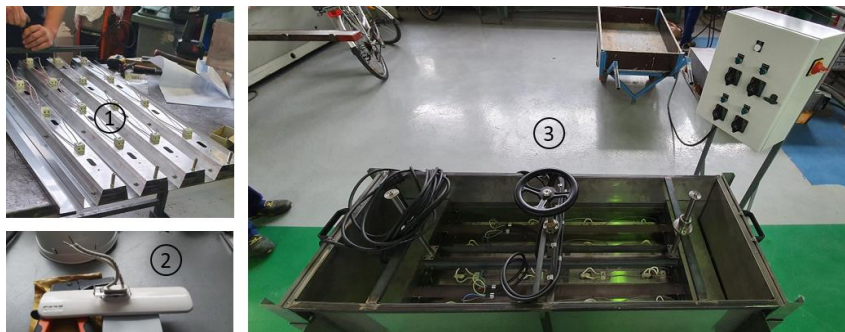


Fig. 119: Electrical heating system with: (1) radiant panels, (2) radiant units and (3) complete heating system.



Fig. 120: Heating system on top of a test slab in the fire resistance laboratory at CSTB.

The cracks were opened at 0.3 mm width prior to thermal heating. No crack measurement was ensured during heating. The slab along with the anchors on the upper side were heated up during 2, 3, and 4 hours. Multiple series of confined tension tests were done for each heating time.

The results of confined tension tests on bonded anchors at high temperatures in uncracked and cracked concrete are given in details in Fig. 121. The values represent the average of a series of tests. Tests were conducted at 2h, 3h and 4h of heating to ensure that all the embedment depth of the anchor has exceeded the glass transition temperature of 15 to 20°C of the adhesive to avoid the post-cure phenomenon due to the slow heating rate.

Test results in Fig. 121 show that a reduction of bond strength from uncracked to cracked concrete is maintained at high temperature. The ratio of bond strength from uncracked to cracked concrete was found to be 69% for 2 hours of heating, 66% for 3 hours of heating and 71% for 4 hours of heating. At 2 hours of heating, 13 tests were conducted in uncracked concrete and 6 in cracked concrete. Test results at 3 hours of heating had a higher standard deviation because the series of tests consisted of 4 tests in uncracked and 4 tests in cracked concrete. At 4 hours of heating, 17 tests were conducted in uncracked concrete and 6 in cracked concrete. The standard deviation for 4 hours of heating is slightly elevated due to the fact that a large area of the embedment length was tested at a temperature close to the glass transition temperature of the adhesive $T_g = 66.7^\circ\text{C}$.

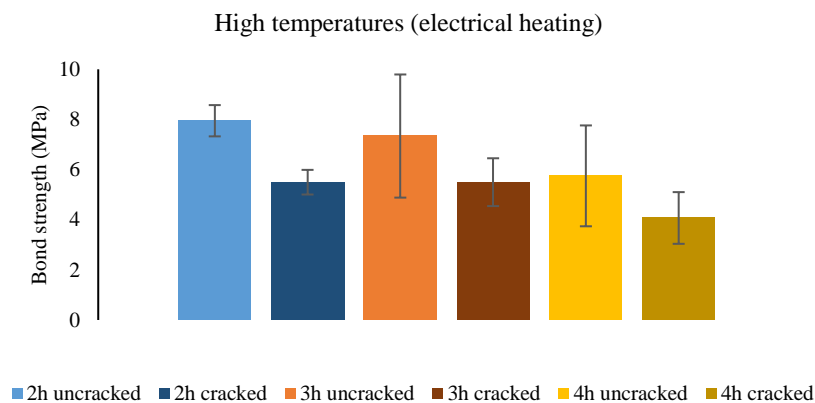


Fig. 121: Results of pull-out tests on bonded anchors in uncracked and cracked concrete at high temperatures

Conclusion

This paper presented an experimental investigation of the pull-out behavior of bonded anchors (epoxy resin) in uncracked and cracked concrete at high temperature (using electrical heating). First, reference tests were done at ambient temperature to find the ratio of bond strength between cracked and uncracked concrete (generally around 70%). Then, tests at high temperature were conducted to assess if this reduction changes with temperature increase. Tests were conducted for different heating times (2 hours, 3 hours and 4 hours). The results at high temperature show that the same ratio is also found at high temperature. This result confirms that the current state of the guidelines for fire tests on bonded anchors in cracked concrete must be revised. The reduction due to crack existence at high temperature should be considered and fire test results on bonded anchors in uncracked concrete should not be used for cracked concrete. The reduction can also be taken from reference tests at ambient temperatures.

The results of this experimental work can establish the basis for a new assessment method of bonded anchors in cracked concrete under fire. The behavior under constant load might vary from the behavior with the testing method used in this work (heating followed with pull-out test) due to the creep phenomenon and the slow heating rate compared to standardized fires. Also, The phenomena occurring in concrete under fire might vary from those occurring under slow rate radiative electrical heating. Therefore, the authors will pursue this research in the future by means of fire tests on bonded anchors in cracked concrete under sustained load on several types of adhesives to confirm the findings of this paper.

References

- ACI 318-14, "Building code requirements for reinforced concrete" Detroit, Michigan: American Concrete Institute, 2014.
- ACI Committee 318, " Building Code Requirements for Structural Concrete (ACI 318-11) and Commentary, " American Concrete Institute, Farmington Hills, MI, 2011, 503 pp. 2.
- EOTA. EAD 330087-00-0601. Systems for post-installed rebar connections with mortar. May 2018.
- EOTA. EAD 330232-01-0601. Mechanical fasteners for use in concrete. December 2019.
- EOTA. EAD 330499-00-0601. Bonded fasteners for use in concrete. July 2017.
- EN 1992-1-2. Eurocode 2: Design of concrete structures – Part 1-2: General rules – Structural fire design. July 2008.
- EN 1992-4. Eurocode 2: Design of concrete structures – Part 4: Design of fastenings for use in concrete. September 2018.
- EN 1993-1-2. Eurocode 3: Design of steel structures – Part 1-2: General rules – Structural fire design. November 2005.
- EOTA TR 020. Evaluation of anchorages in concrete concerning resistance to fire. European Organization for Technical Approvals Technical report no. 20. May 2005.
- Eligehausen R, Mallée R, Silva JF. Anchorage in concrete construction. Ernst & Sohn; 2006.
- Eligehausen R, Werner F. Recent developments and open problems in fastening technique. In: 2nd international symposium on connections between steel and concrete, Stuttgart, *fib*, Germany; 2007.
- Kumar S. Analysis of tabular adhesive joints with a functionally modulus graded bondline subjected to axial loads. *Int J Adhes Adhes* 2009;29:785–95.
- Lahouar MA. Fire resistance of chemical anchors in wood and concrete PhD thesis Paris: University of Paris-Est (France); 2018.
- Muciaccia, G., Consiglio, A., & Rosati, G. (2016). Behavior and design of post installed rebar connections under temperature. *Key Engineering Materials*, 711, 783-790.
- Pinoteau N. Behavior of post-installed rebars in concrete under fire PhD thesis Lille: University of Lille (France); 2013.
- Petit J, Nassiet V. Baziard YH-RB. Etude de la durabilité des assemblages collés. *Techniques de l'ingénieur* 2005:COR160.
- Reichert M. Projekt: Verbunddübel im Brandfall PhD thesis: TU Kaiserslautern (Germany), 2017.
- Reichert M, Thiele C. Qualification of bonded anchors in case of fire. Proceedings of the 3rd international symposium on connections between steel and concrete. Stuttgart, Germany. September 2017. p. 1191–9.
- Reis J. Effect of temperature on the mechanical properties of polymer mortars. *Mater Res* 2012;15(4):645–9.
- Ribeiro MCS, Nóvoa PJRO, Ferreira AJM, Marques AT. Flexural performance of polyester and epoxy polymer mortars under severe thermal conditions. *Cem Compos* 2004;26:803–9.
- Sorathia U, Lyon R, Gann R, Gritz L. Materials and fire threat. *Fire Technol J* 1997;33(3):260–75.
- Zhang Y, Lou G, Chen K, Li G. Residual strength of organic anchorage adhesive for post-installed rebar at elevated temperatures and after heating. *Fire Technol J* 2016;52:877–95.

Analysis and discussion

The presented work investigated the mechanical influence of cracks in concrete on the bond strength of bonded anchors at high temperature. The experimental investigation conducted in this work was done using electrical heating instead of heating in a gas furnace (standard fire tests) for several reasons:

- 1- Electrical heating allows a better control over the applied heating scenario and thermal boundary conditions, allowing therefore a better comparability between different tests.
- 2- The repeatability of the applied thermal boundary conditions using radiant panels from one test to another allow to conduct a large number of tests and increase the population of test results yielding therefore more confidence in the test results.
- 3- Economical and time gain: electrical heating using radiant panels allows to test several anchors in the same slab with little energy and time consumed compared to gas heating in a standard furnace. The time gain can be observed on the preparation and conduction of tests at high temperature giving more flexibility for the lab (no special loading system to be installed. Only a hydraulic jack for a confined test setup is needed like reference tension tests).

Although electrical heating provides the previous advantages, fire tests cannot be omitted and need to be conducted to confirm the findings of this study. Indeed, there are major differences between electrical heating by radiant panels and fire tests:

- 1- Fire tests apply a much higher heating rate on the thermal boundary conditions reaching higher temperatures than the used electrical heating in this study in a shorter period of time. The higher heating rate leads to different phenomena occurring inside the concrete and along the embedment length (e.g. water migration inside the concrete and through the crack, higher thermal gradient between the top and bottom of the anchor...etc.).
- 2- Fire tests apply a pressure inside the furnace to push the hot gas against the fire exposed surface. Such pressure can allow the hot gas to enter inside the crack, especially at the beginning of the fire where the thermal expansion of concrete is still taking place and has not closed the crack due to the expansion of both sides of the crack plane.
- 3- Fire tests allow to apply a sustained load on the anchor during fire exposure. Whereas, the electrical heating apparatus used in this study does not allow this option yet. The effect of sustained load on the creep of the adhesive resin was neglected in this study because the bond strength was characterized for temperatures beyond glass transition of the tested adhesive resin (irreversible damage and transformation of the adhesive resin assumed).

The previous study in the chapter allows to develop further research on the topic of bonded anchors in cracked concrete at high temperature. The following perspectives are identified:

- 1- Product differentiation: the previous study was conducted on one epoxy adhesive resin. More research will be done in the future to confirm the findings of this study (stability of the reduction on bond strength at high temperature taken as equal to the one at ambient temperature). Another type of organic adhesive resins (metacrylate adhesive resin) and an inorganic adhesive resin are identified for the perspectives of this work, as well as cast-in place threaded rods as a reference sample (without adhesive resin) to only assess the degradation at the steel/concrete interface.
- 2- Validation with fire tests in uncracked and cracked concrete: the findings of this study will be confirmed with pull-out fire tests in both uncracked and cracked concrete to eliminate the factor of different heating methods (electrical vs. fire heating).

Conclusion:

The previous chapter opens a window to the world of bonded anchors in cracked concrete under fire by a preliminary investigation using electrical heating at high temperature. The proposed methodology for the assessment of crack influence at high temperature can be validated further in the future allowing to amend tests under fire for bonded anchors in cracked concrete if the same findings in this study are obtained for other products and for fire tests.

General conclusion and perspectives

The research presented in this dissertation was conducted on the behavior of bonded anchors under fire. The thermal and mechanical behavior of bonded anchors was studied at high temperature to investigate the phenomena that occur when an anchor is exposed to fire. The existing design method for post-installed rebars (Pinoteau's method) allowing to calculate the pull-out fire resistance vs. fire exposure time was studied; and its applicability on the case of bonded anchors was investigated.

1. Scientific contribution

This study highlights certain characteristics of the behavior of bonded anchors under fire on three scales:

At the testing procedure scale, the testing method of anchors under fire existing in the literature and developed for mechanical anchors almost two decades ago was reviewed. The influence of different testing configurations and the loading system (when made of steel) on the temperature profiles along the embedment depth of bonded anchors was assessed by fire tests (see Chapter 2). The loading system did not seem to influence the thermal distribution due to the high diffusivity of its steel components and its limited geometry inside the furnace (not acting as a protective screen against fire exposure at the anchor location). The thickness of the concrete bearing element also had very little influence on the thermal distribution. However, parameters like anchor diameters and the existence of thermal insulation around the fixture have a significant influence on thermal diffusion and the resulting load-bearing capacity. It is then recommended that the thermal insulation must be taken into account in the revision of the existing testing method as well as new test method to be developed for bonded anchors. However, in order to assess the performance of the anchor separately from the insulation material, it is recommended to adopt a configuration where the anchor is directly exposed to fire without any thermal protection.

At the design procedure scale, the design method based on numerical calculations coupled with the Pinoteau's Method (Resistance Integration Method) can be influenced by several factors. Using 2D plane modelling to represent the case of anchors in fire proved to be unrepresentative of temperature profiles obtained along the anchors in fire tests. Therefore, the results of Pinoteau's method based on such models can fall on the overly-conservative (in the case of anchors directly exposed to fire) or non-conservative (in the case of anchors with insulated fixtures) side of the fire resistance-duration design. Using 3D modelling with correct representation of the geometry of the anchor yielded much more accurate temperature profiles with a limited computational time and proved to be on the conservative side of the fire resistance prediction (see Chapter 3).

Another focus was attributed to the entry data for Pinoteau's method consisting of the characterization of the bond strength at high temperature on small scale tests (see Chapter 4). The current approach for PIRs (acc. EAD 330087-00-0601) stops the characterization at 3 hours of electrical heating, meaning that the bond strength vs. temperature curve is usually stopped at around 300°C and zero bond strength is assumed for higher temperatures. Accounting for the residual bond strength at higher temperatures was proven to be of beneficial effect on the calculated design values using Pinoteau's method, all while remaining on the conservative side compared to fire test results. This exercise was conducted on a large number of fire tests on 3 different bonded anchor products with sizes going from M8 to M30. The design results were always found to be conservative compared to ISO 834 fire tests.

The development of an evaluation standard for bonded anchors under fire should take into account that pull-out fire tests shall be conducted on the minimum embedment depth specified by the manufacturer in order to induce the pull-out failure. Otherwise, other failure modes may occur (possibly steel or concrete cone failure). As a next step, the verification of the applicability of Pinoteau's method (Resistance Integration method) should be conducted on a case by case basis for each product. Indeed, it is not possible to confirm based on the results in this work or in the literature that this method is applicable for all products on the market. The current experience proves that Pinoteau's method provides calculated pull-out fire resistances lower than fire test results. However, each adhesive resin has a different chemical content and different performances compared to other adhesive resins on the market. Once Pinoteau's method is validated on the shortest embedment depth, the anchor can be designed for a variable embedment depth (higher than the shortest one tested for validation) and the obtained pull-out resistance can be compared to other failure modes under fire to design according to the smallest resistance among all failure modes.

At the scale of bonded anchors in uncracked/cracked concrete comparison at high temperature, the design of PIRs bonded anchors in the literature focused so far on the uncracked concrete case. Indeed, specifications were given for bonded anchors to account for the major differences between a rebar embedded in concrete and exposed

to fire through the concrete cover, compared to an anchor directly exposed to fire. However, very little data exists on bonded anchors in cracked concrete at high temperatures. Generally, in fire situations (acc. Eurocode 2-4) and when anchors are installed on the tension side of concrete elements, cracked concrete is assumed at ambient temperature. Therefore, it is required to assess this issue under fire conditions.

The effect of cracks on the bond strength at high temperatures was studied in this work (Chapter 5). A testing approach was developed to test a large number of bonded anchors at high temperatures in cracked and uncracked concrete. The obtained bond strength reduction from uncracked to cracked concrete was compared to the reduction obtained at ambient temperature for different heating times (using electrical heating by radiant panels). The presented results showed that the reduction coefficient cracked versus uncracked concrete remains the same at high temperatures compared to ambient temperatures. Although this study opens a window into the world of bonded anchors in cracked concrete under fire, it needs to be extended with large scale ISO 834 fire tests on bonded anchors in cracked and uncracked concrete to confirm these findings. Product differentiation (testing other adhesive resin types) is also recommended.

Using standard fire tests (e.g. ISO 834) to compare the pull-out resistance in cracked concrete to that in uncracked concrete can result in false comparisons. Standard fire tests are conducted in special gaz furnaces with specific requirements on the mean heating curve applied in the furnace (measure by plate thermometers) to follow the theoretical standard curve with a certain tolerance (i.e. $\pm 100^{\circ}\text{C}$ for the ISO 834 fire curve). Such requirements have a small influence on full scale tests on post-installed rebars because the rebar is embedded in a concrete member and the variation of the applied thermal heating (i.e. radiation and convection) is minimized by the thermal resistance of the concrete member. In the case of anchors where the extended part outside of concrete is directly exposed to fire, such a tolerance can yield huge differences in test results and no repeatability from one test to another. Therefore, the obtained fire test results can sometimes provide higher resistances for anchors in cracked concrete (heated with a lower tolerance of the standard ISO 834 curve of $- 100^{\circ}\text{C}$) compared to anchors in uncracked concrete (heated with an upper tolerance of the standard curve of $+ 100^{\circ}\text{C}$). The proposed testing approach in this work using electrical heating with radiant panels provides more certainty and repeatability for the comparison of test results in cracked concrete to uncracked concrete.

2. Perspectives

This study focused on the bond failure (pull-out) of bonded anchors under fire. Other failure modes may occur based on the configuration of the anchor (steel failure, concrete cone, concrete breakout, ...etc). These failure modes are covered by the provisions of Eurocode 2-4. However, they are based on fire ratings (a given resistance as a function of a duration of the standard ISO 834-1 fire curve) and very limited experimental data in the literature using only one fire scenario. The current empirical models in the Eurocode are also very conservative compared to fire tests for concrete cone and steel failure modes. The design for these failure modes could be optimized by developing temperature-based models for the calculation of the corresponding fire resistance in order to design anchors under fire for any given configuration and possible failure modes while yielding less conservative but safe design values.

In addition, the displacement compatibility was not verified for the design approach of bonded anchors under fire. The Pinoteau's method (Resistance Integration Method) integrates temperature-associated bond stresses along the embedment depth at any time during the fire based on temperature distribution. However, it assumes that failure occurs for the same displacement for all segments. The current experience with the tested adhesive resins in this work and in the literature shows that this assumption is conservative and the results of Pinoteau's method can be used safely for the design of bonded anchors. However, this assumption is only valid in the case of small displacements. If an adhesive resin shows large displacements (high creep behavior) under fire or if this work is used to model and study long term temperature effect, this assumption could be revoked and a more advanced shear-lag including creep model should be developed to account for the displacement compatibility between the design method and fire tests. The prediction of the bond strength of bonded anchors under fire can be calculated using the shear-lag model taking into account the creep behavior at different temperatures. This can be done by characterizing the long-term behavior of the bond (example shown in Fig. 24) based on creep tests on small samples of the adhesive resin at different temperatures.

Furthermore, this study also focused on tension loads under fire. Anchors can also be loaded in shear or combined shear-tension. In direct shear load situations, the failure mode is not expected to change compared to mechanical

anchors, therefore the current provisions in Eurocode 2-4 can be reasonably applied. However, in combined shear-tension situations, a pull-out failure/combined pull-out steel with lever arm failure can occur.

An additional point would be to account for the anchor-structure interaction during fire. This work only focused on anchor behavior from an evaluation point of view (product only). Therefore, all calculations were compared to fire tests on free slabs (no mechanical boundary conditions applied on the reinforced concrete bearing element). It would be of interest to study the conventional case of fixed slabs/fixed beams and verify that the assumptions adopted in this work remain applicable for such a case.

The behavior of groups of anchors can also be expected to change significantly under fire. From a thermal point of view, the required spacing between anchors at ambient temperature is expected to be of negligible influence on the temperature profiles. However, regarding the load distribution/redistribution of the group, the influence of an anchor failing first before the whole group, edge distance, different anchor sizes and embedment depths...etc. are expected to be of significant influence. In addition, it is expected that an anchor designed to sustain a significant load in tension under fire will need to be embedded at a very large embedment depth. Therefore, the spacing to the embedment ratio will be small and interactions event for a relatively large spacing could happen.

The post-fire performance of bonded anchors (and post-installed rebars) is still uninvestigated. In a fire event, the fire can occur for a short period of time resulting in no failure but in a degradation of the material properties of the anchor assembly (concrete, steel and bond). The post-fire assessment of the bond is required to validate any rehabilitation provisions to ensure that the connection can still withstand the applied loads. Therefore, structural tests at the scale 1 should be conducted to assess the residual capacity after fire exposure in order to verify any evaluation or design method.

Finally, the studied case of bonded anchors at high temperatures in this work was based on medium size anchors (M12). The crack effect on the bond strength of bonded anchors varies from one anchor size to another. Large anchor sizes (above M24) are less influenced by crack existence at ambient temperature (anchor diameter \gg crack width). At high temperatures, it would be interesting to investigate if crack influence still decreases/vanishes for a certain anchor size.

Annex A: Principles of fire safety engineering

Under fire conditions, the thermal diffusion between the hot gazes of the fire and the exposed element occurs via radiation and convection at the exposed surface and via conduction inside the element. The methods allowing to measure the radiative and convective heat flux are numerous and their use in a particular situation is not guaranteed. Indeed, the use of different measurement methods can result in different outcomes giving different results for the same problem. The concept of *Adiabatic surface temperature* is introduced as a practical mean to express the thermal exposure of a surface. This concept can be used successfully when exposure conditions are issued from modelling or measured directly from fire tests. In the latter case, temperature gauges of the type plate thermometers, defined in the guides of fire resistance tests (*ISO 834-1, 1999*) and (*NF EN 1363-1, 2020*), can be employed. This implicitly signifies that the temperature of structural elements tested according to these guides can be predicted using measures from plate thermometers which are designed to follow specific time-temperature curves. The plate thermometer (*ISO 834-1, 1999*) or also named thermoplate (*NF EN 1363-1, 2020*) is detailed in the following sections of this study (see section 3.3).

A *fire model* in this context is every calculation method whose principal objective is to predict the temperature and species concentrations of the fire-driven flow (*Wikström, 2007*). Such a model allows to calculate temperature evolving at the surfaces of the solid tested elements but does not necessarily include a detailed description of these objects. Even a model that takes into account fluid dynamics can only approximate a bounding solid as an infinitely thick slab to estimate its surface temperature.

A *structural fire model* allows to study the resistance of the structure as a function of the temperature of hot gases inside the furnace applied on its boundary conditions. It allows to determine the requirements for the fire resistance of the structure.

After the collapse of the World Trade Center in 2001, the subject of interfacing between fire models and thermal mechanical models became of great importance to understand the response of structures (*Gann, R., et al., 2005*). Fire models and thermal structural models are conducted at variable scales for time and dimensions, and with different hypotheses concerning the respect of boundary conditions (thermal, chemical, force or displacement boundary conditions). In order to study precisely the response of a structure subjected to fire, a fire model has to be developed and its output must be communicated to a thermal structural model to serve as thermal boundary conditions. Fire models predict typically the heat flux for a relatively simple solid material. As for thermal structural models, they suppose a global gas temperature surrounding a relatively simple geometry such as a column or a beam.

Basic theory:

Heat is transferred from flames and hot gases to the exposed surfaces of the solid material by radiation and convection (*Wiktröm, 2004*). Both contributions make the *net* total heat flux:

$$\dot{q}_{tot}'' = \dot{q}_{rad}'' + \dot{q}_{con}'' \dots [\text{Eq. 20}]$$

Where: \dot{q}_{tot}'' is the total heat flux applied to the fire exposed surface, \dot{q}_{rad}'' is the radiative heat flux and \dot{q}_{con}'' is the convective heat flux. The radiation term \dot{q}_{rad}'' in Eq. 20 is the difference between the incident radiation and the radiation emitted from the surface. The incident heat flux is what can be measured by any heat flux meter in practice and is independent of the target body surface temperature and properties. However, so-called heat fluxes frequently used in fire engineering respond to heat transfer to a water-cooled surface. In these instruments a temperature difference is created depending on how much heat is transferred to the sensing surface by radiation and convection. Therefore, they are called ‘total heat transfer’ meters. However, since they can be calibrated in difference they can never directly measure ‘net heat transfer’ or ‘total heat transfer’ to an arbitrary surface, only to the cooled sensing surface of the meter.

In Eq. 20 the heat transmitted through the surface is neglected and no consideration is made for the influence of various wavelengths. Thus, as the absorptivity and emissivity are equal, the net heat received by the surface can be written as:

$$\dot{q}_{rad}'' = \varepsilon \cdot (\dot{q}_{inc}'' - \sigma \cdot T_s^4) \dots [\text{Eq. 21}]$$

Where: \dot{q}_{inc}'' is the incident flux, σ is the Stephan Boltzman constant and T_s is surface temperature. The emissivity ε is a material property of the surface. It can be measured but in most cases of structures exposed to fire it can be taken equal to 0.7 or 0.8 except for shiny steel where it is lower. Fire is characterized by non-homogeneous thermal distribution. Thus, the incident heat flux should include contributions from nearby flames, hot gases and surfaces. In this case, the incident heat flux can be written as the sum of all radiative sources:

$$\dot{q}_{inc}'' = \sum_i \varepsilon_i \cdot F_i \cdot \sigma \cdot T_i^4 \dots \text{ [Eq. 22]}$$

Where, ε_i is the emissivity of the i^{th} flame or surface, F_i and T_i are the corresponding view factor (the proportion of the radiation leaving a heating surface A that is received by a heated surface B, also known as shape factor, form factor, configuration factor or angle factor) and temperature, respectively. It is generally very complicated to obtain incident heat flux from Eq. 22 by manual calculation, but current generation fire models have algorithms capable of calculating it.

The convective heat flux depends on the difference between surrounding gas temperature and surface temperature. It is often taken proportional to this difference and can be written as:

$$\dot{q}_{con}'' = h \cdot (T_{gas} - T_s) \dots \text{ [Eq. 23]}$$

Where: h is the heat transfer coefficient and T_{gas} is gas temperature adjacent to the exposed surface.

Adiabatic surface temperature:

The total net heat flux can be written from the previous discussion as:

$$\dot{q}_{tot}'' = \varepsilon \cdot (\dot{q}_{inc}'' - \sigma \cdot T_s^4) + h \cdot (T_{gas} - T_s) \dots \text{ [Eq. 24]}$$

Consider the surface of a perfect insulating material exposed to the same heating conditions as the real surface. Its temperature is referred to as “*Adiabatic surface temperature*” (AST). By definition, the total net heat flux to this ideal surface is zero, thus:

$$\varepsilon \cdot (\dot{q}_{inc}'' - \sigma \cdot T_{AST}^4) + h \cdot (T_{gas} - T_{AST}) = 0 \dots \text{ [Eq. 25]}$$

The adiabatic surface temperature can be obtained as an output from a fire model. It can also be measured from real fire tests or in experiments using an instrument like the plate thermometer. Adiabatic surface temperature is what is measured by an ideal plate thermometer. Indeed, the plate thermometer is used in fire tests (*ISO 834-1, 1999*) and (*NF EN 1363-1, 2020*) to control furnace temperature. It harmonizes tests in different furnaces and allows to harmonize testing and theory. The measured quantity by the plate thermometer is precisely what is needed to calculate the temperature of a structural element exposed to fire (*Wickström, 1994*) and (*Wickström and Hermodsson, 1996*). It also represents hot gas temperature in Eq. 25. With this hypothesis, T_{AST} becomes the only unknown in Eq. 25. The error of such a calculation is relatively small. Indeed, the plate thermometer with a diameter of 0.7 mm is generally placed at 10 cm of the fire exposed surface to measure hot gas temperature inside the furnace. In the theory of basic heat transfer, objects smaller than a few millimeters have a large heat transfer coefficient h and thus they reach temperatures close to surrounding gas temperature T_{gas} rapidly.

Numerical consideration:

Numerically, adiabatic surface temperature is a very useful quantity because it provides the natural interface between fire models and thermal structural models. So, if fire model results have to be exploited for a more detailed heat transfer calculation in a tested solid object, an interface is required to transfer the information to the gas-solid interface. The most obvious quantity to do so is heat flux.

First, the net heat flux applied on a surface depends on the calculated surface temperature by a given fire model. Depending on the used model, surface temperature may vary with the entry parameters introduced by the user. Secondly, it is common in several structural heat transfer softwares (in solid phase) to enter a heat flux value as a function of surrounding gas temperature and surface temperature [Eq. 28] instead of defining heat flux directly. The communicational problem between a fire model and a thermal structural model is then linked to the two different methods for introducing heat flux as a boundary condition. The solution is to use adiabatic surface temperature T_{AST} as an intermediate (interface) between the fire model and the thermal structural model.

The interface can be constructed simply. For any surface point at which the fire model (FM) calculates the incident radiation heat flux $\dot{q}_{inc,FM}''$ and a corresponding gas temperature adjacent to the surface $T_{gas,FM}$, it is trivial to solve the implicit equation to calculate T_{AST} by supposing that the emissivity and the heat transfer coefficient are constants. The following equation can be solved by using an analytical solution given by (Malendowski, 2017):

$$\varepsilon \cdot (\dot{q}_{inc,FM}'' - \sigma \cdot T_{AST}^4) + h \cdot (T_{gas,FM} - T_{AST}) = 0 \dots [\text{Eq. 26}]$$

A fire model does not need any hypothesis to calculate the incident radiation heat flux. Eq. 21 only defines adiabatic surface temperature and does not signify that the fire model calculates heat flux using a specific method. It does not signify either that the fire model uses a fixed heat transfer coefficient h . The value that should be taken for h is the energy intensity exchanged by a unit of surface and a unit of time as a function of the temperature difference between both sides of the exposed surface. Since this difference varies with time, the value of h is variable and must be recalculated at every time interval by the model. These values are provided for common materials (such as concrete and structural steel) in the Eurocodes. Practically, the values of T_{AST} are stored in a file according to a user-specified time interval and length increment appropriate for the application.

For thermal structural models (TSM), heat flux is calculated based on the boundary conditions calculated by the fire model. Surface temperature calculated by the thermal structural model can be written as:

$$\dot{q}_{tot,TSM}'' = \varepsilon \cdot (\dot{q}_{inc}'' - \sigma \cdot T_{s,TSM}^4) + h \cdot (T_{gas,FM} - T_{s,TSM}) \dots [\text{Eq. 27}]$$

By subtracting Eq. [27] from Eq. [28], the total net heat flux at the surface can be written as:

$$\dot{q}_{tot,TSM}'' = \varepsilon \cdot \sigma \cdot (T_{AST}^4 - T_{s,TSM}^4) + h \cdot (T_{AST} - T_{s,TSM}) \dots [\text{Eq. 28}]$$

Note that the adiabatic surface temperature is interpreted by the thermal structural model as a *black body radiation* temperature for the purpose of calculating the incident radiant heat flux, to which is added a *gas* temperature for the purpose of calculating the convective heat flux. They can also be interpreted as a single fictitious temperature, commonly used to calculate both radiative and convective heat transfer.

Black body radiation is the radiation emitted by an opaque and non-reflective body, maintained at a constant and uniform temperature. The radiation has a specific spectrum and intensity that depends only on the body temperature (Loudon, 2000), (Mandel et Wolf, 1995), (Kondepudi et Prigogine, 1998) and (Landsberg, 1990).

The use of adiabatic surface temperature allows to transfer only one quantity between the fire model and the thermal structural model instead of transferring heat flux, surface temperature and the convective heat transfer coefficient. Another advantage is that the model does not need to be reconfigured to accept heat flux as a boundary condition. It only needs to be modified to accept a temporal and spatial variation of the hot gas temperature considered in the calculation of the heat flux. The model can then give the calculated surface temperature and finally the mechanical response of the studied object. An additional advantage is that the use of AST reduces the size of datasets and simplifies the execution of large-scale models such as the analysis of structures under fire.

References

- ACI Committee 503, 1973. Use of epoxy compounds with concrete.
- Apicella, A., Nicolais, L. & Cataldis, C., 1985. Adv. Polymers 66: 189-207.
- Aref-Azar, A., Arnoux, F., Biddlestone, F. & Hay, J. H., 1996. Physical aging in amorphous and crystalline polymers. Part 2. Polyethylene terephthalate. *Thermochimica Acta* 273, pp 217-29.
- ASTM E119, 2020. Standard test methods for fire tests for building construction and materials.
- Bardonnet, P., 1992a. Résines époxydes (EP) - Composants et propriétés. *Traité plastiques et composites*, éditions T.I. (Techniques de l'ingénieur).
- Barrère, C. & Dal Maso, F., 1997. Résine époxy réticulées par des polyamines : Structure et propriétés. *Revue de l'institut français du pétrole*, Volume 52, pp. 317-35.
- Bazant, Z. & Kaplan, M., 1996. *Concrete at High Temperatures: Material properties and Mathematical Models*. s.l.: Pearson Education.
- Berthumeyrie S., Colin, A., Esparcieux, C., Baba, M., Catalina, F., Bussiere, P. O. & Therias, S., 2013. Photodegradation of tetramethylpolycarbonate (TMPC) 98, pp 2081-88.
- Candlot, E., 1906. *Ciments et chaux hydrauliques. Fabrication. Propriétés. Emploi*, troisième édition. Paris et Liège.
- Canopy Failure Investigation, 2011. 17th street Bridge, Atlanta, Georgia.
- Chin, J. et al., 2010. Thermoviscoelastic Analysis and Creep Testing of Ambient Temperature Cure Epoxies Used in Adhesive Anchor Applications. *Journal of Materials in Civil Engineering*, pp. 1039-46.
- Coppendale, J., 1977. *The stress and failure analysis of structural adhesive joints (Ph.D. Thesis)*. Bristol, University of Bristol.
- Debauve, A., 1886. *Procédés et matériaux de construction*, Chez Ch. Dunod et P. Vicq. Paris, t. III.
- Dessertenne, E., 2012. *Matériaux solide conducteur thermodurcissable : Application aux plaques bipolaires pour piles à combustible (thèse de doctorat)*. Lyon, INSA de Lyon.
- Diederichs U., Jumppanen U.M., Penttala V., Behaviour of high strength concrete at high temperature, Espoo: Helsinki University of Technology, Report 92, 1989.
- DTU 13.2, 1992. *Travaux de bâtiment - Fondations profondes - Partie 1 : éléments relatifs à l'exécution - Cahier des clauses techniques types*.
- Durand-Claye, C. L., 1885. *Chimie appliquée à l'art de l'ingénieur. Encyclopédie des travaux publics*, librairie polytechnique, Éditions Baudry et C^{ie}, Paris.
- Eligehausen, R., Mallee, R., Silva, J. F., 2006. *Anchorage in concrete constructions*. Wilhem Ernest & Sohn, Berlin.
- EN 1992-4, 2018. Eurocode 2 – Design of concrete structures – Part 4: Design of fastenings for use in concrete.
- EOTA EAD 330087-00-0601, 2018. Systems for post-installed rebar connections with mortar. July. Issue EOTA 14-33-0087-06.01.
- EAD 330232-01-0601, 2019. Mechanical fasteners for use in concrete. December.
- EAD 330499-01-0601, 2019. Bonded fasteners for use in concrete. July.
- EOTA TR23, 2009. ETAG N°001, Part 5- Guideline for European Technical Approval of Metal Anchors for Use in Concrete, Part 5: Bonded Anchors. Technical report for Post-Installed Rebar Connections.

- EOTA, 2001. ETAG 2001: European Techniques of Anchor Guideline.
- ETAG 001 Part 1 Metal Anchors for use in concrete, amended version April 2013.
- François, D., 1984. Essais mécaniques des métaux. Traité matériaux métalliques M 120, vol. M1 I, 4-1984, Techniques de l'ingénieur.
- Fritsch, J., 1911. Fabrication du ciment, Paris, Self édition. Paris.
- Gann, R., Hamins, A., McGrattan, K. & Mulholland, G., 2005. Reconstruction of the Fires in the World Trade Center Towers. Federal Building and Fire Safety Investigation of the World Trade Center Disaster, NIST NCSTAR 1-5, National Institute of Standards and Technology. USA.
- Gernet, J. & Légendre, B., 2010. Analyse calorimétrique différentielle à balayage (DSC). Traité techniques d'analyses, éditions T.I. (Techniques de l'ingénieur).
- Hager, G. I., 2004. Comportement à haute température des bétons à hautes performances - évolution des principales propriétés mécaniques (*thèse de doctorat*). École Nationale des Ponts et Chaussées et l'École Polytechnique de Cracovie.
- Heinfling, G., 1998. Contribution à la modélisation numérique du comportement du béton et des structures en béton armé sous sollicitations thermo-mécaniques à hautes températures (*thèse de doctorat*). Lyon, INSA de Lyon. N 98 ISAL 0002.
- Hunston, D.L., Carter, W.T., Rushford, J.L., 1981. Linear Viscoelastic Properties of Solid Polymers as Modelled by a Simple Epoxy.
- Jansson, R. & Bostrom, L., 2013. Fire spalling in concrete – The moisture effect, part II, concrete spalling due to fire exposure. In: Proceedings of the 3rd international workshop, Paris, France, September 25-27.
- Kanema, M., 2007. Influence des paramètres de formulation sur le comportement à haute température des bétons (*thèse de doctorat*). Université de Cergy-Pontoise.
- Khoury, G. A., 1992. Compressive strength of concrete at high temperatures: a reassessment. Magazine of Concrete Research, Vol 44, N° 161, pp 291-309.
- Khoury, G. A., 2000. Effect of fire on concrete and concrete structures. Prog. Struct. Engng Mater., Volume 2, pp. 429-47.
- Kondepudi, D. et Prigogine, I., 1998. Modern Thermodynamics. From Heat Engines to Dissipative Structures, John Wiley & Sons. ISBN 0-471-97393-9.
- Lahouar, M A, 2018. Tenue au feu des goujons collés dans le bois et dans le béton (*thèse de doctorat*). Paris : Université Paris-Est.
- Lahouar M A, Caron J-F, Pinoteau N, Forêt G, Benzarti K. Mechanical behavior of adhesive anchors under high temperature exposure: Experimental investigation. Int J Adhes Adhes 2017; 78: p. 200-11.
- Lahouar M A, Pinoteau N, Caron J-F, Forêt G, Mège R. A nonlinear shear-lag model applied to chemical anchors subjected to a temperature distribution. Int J Adhe Adhes 2018; 84: 438-50.
- Lahouar M A, Pinoteau N, Caron J-F, Forêt G, Rivillon Ph. Fire design of post-installed rebars: Full-scale validation test on a $2.94 \times 2 \times 0.15$ m³ concrete slab subjected to ISO 834-1 fire. Eng Struct J 2018; 174: p. 81-94.
- Lankard, D. R., Brikimer, D. L., Fondriest, F. F. & Synder, M. J., 1971. Effects of moisture content on the structural properties of Portland cement concrete exposed to temperature up to 500 F. 21st ACI Fall Meeting, Memphis, Tennessee, USA.
- Landsberg, P. T., 1990. Thermodynamics and statistical mechanics, Courier Dover Publications. ISBN 0-486-66493-7.

- Larché, J. F., Bussière, P. O. & Gradette, J. L., 2011. Photo-oxidation of acrylic-urethane thermoset networks. Relating material properties to changes of chemical structure. *Polymer degradation and stability* 96, pp 1438-44.
- Leduc, E., 1902. *Chaux et ciments*, Librairie JB Baillière et Fils. Paris.
- Loudon, R., 2000. *The Quantum Theory of Light*, Cambridge University Press (1re éd. 1973). ISBN 0-19-850177-3.
- M. Allenbach Patrick, 2014. La résine époxy. [En ligne] disponible à : <http://www.sol-industriel.net/resine-et-finition/resine-epoxy>
- Malendowski, M., 2017. Analytical Solution for Adiabatic Surface Temperature (AST). *Fire Technology*, 53:413–20.
- Mallick, V., 1989. Stress analysis of metal/CFRP adhesive joints subjected to the effects of thermal stresses (*Ph.D. Thesis*). Bristol, University of Bristol.
- Mandel, L. et Wolf, E., 1995. *Optical Coherence and Quantum Optics*, Cambridge University Press. ISBN 0-521-41711-2.
- Marques, E. A. S. & Lucas F. M. da Silva, 2014. Adhesive joints for low and high temperatures use: an overview. *The journal of Adhesion* 91:7, pp 556-85.
- Meszaros, J. & Eligehausen, R., 1998. Einfluss der Bohrlochereinigung und vo feuchtem Beton auf das Tragverhalten von ijektions düblen (Influence of hole cleaning and of humid concrete on the load bearing behaviour of injection anchors), Universität Stuttgart : Institut für Werkstoffe im Bauwesen.
- Meszaros, J. (1999): *Tragverhalten von Verbunddübeln im ungerissenen und gerissenen Beton (Load-bearing behaviour of bonded anchors in uncracked and cracked concrete)*. Doctor thesis, Universität Stuttgart, 1999 (in German).
- Mindeguia, J. C., 2009. Contribution expérimentale à la compréhension des risques d'instabilité thermique des bétons (*thèse de doctorat*). Pau, Université de Pau et des Pays de l'Adour.
- Mindeguia, J. C., Carré, H., Pimienta, P. & La Borderie, C., 2014. Experimental discussion on the mechanisms behind the fire spalling of concrete. *Fire and Materials* 39:7, pp 619-35.
- Msaad, Y., 2005. Analyse des mécanismes d'écaillage du béton soumis à des températures élevées (*thèse de doctorat*). Paris, Ecole des Ponts ParisTech.
- National Transportation Safety Board, 2006. *Ceiling Collapse in the Interstate 90 Connector Tunnel Boston, Massachusetts*.
- NF EN 10269, 2013. Acier et alliage de nickel pour éléments de fixation utilisés à température élevée et/ou basse température.
- NF EN 10025, 2005. Produits laminés à chaud en acier de construction.
- NF EN 10080, 2005. Acier pour l'armature du béton.
- NF EN 1363-1, 2020. Essais de résistance au feu – Partie 1 : Exigences générales.
- NF EN 1992-1-1, 2005. Eurocode 2 : Calcul des structures en béton – Partie 1-1 : Règles générales et règles pour le bâtiment.
- NF EN 1992-4, 2018. Eurocode 2 – Partie 4 : Calcul des structures en béton – Partie 4 : Conception et calcul des éléments de fixation pour béton.
- NF EN 1993-1-2, 2005. Eurocode 3 – Partie 1-2 : Calcul des structures en acier – Partie 1-2 : Règles générales – Calcul du comportement au feu.
- NF EN 934, 2012. Adjuvants pour béton, mortier et coulis.
- NF EN ISO 225, 2010. Eléments de fixation – Vis, goujons et écrous.

- NF EN ISO 3506, 2010. Caractéristiques mécaniques des éléments de fixations en acier inoxydable résistant à la corrosion.
- NF EN ISO 6892-1, 2016. Matériaux métalliques – Essai de traction.
- NF EN ISO 834-1 : 1999. Norme Internationale. Essai de résistance au feu – Eléments de construction – Partie 1 : exigences générales.
- NF EN ISO 888, 2018: Fasteners, bolts, screws and studs – nominal lengths and thread lengths.
- NF EN ISO 898, 2013. Caractéristiques mécaniques des éléments de fixation en acier au carbone et en acier allié.
- Nguyen, T., Byrd, E., Bentz, D., Lint, C., 1996. In situ measurement of water at the organic coating/substrate interface. *Progress in Organic Coatings* 27, 181–93.
- Noumowé, A. N., 1995. Effet de hautes températures (20-600°C) sur le béton. Cas particulier du béton à hautes performances (*thèse de doctorat*). Institut National des Sciences Appliquées de Lyon.
- Noumowé, A. N., Clasters, P., Debicki, G. & Costaz, J. L., 1996. Thermal stresses and water vapor pressure of high performance concrete at high temperature. *Forth International Symposium on the utilization of high strength / high performance concrete*, Paris, pp 561-70.
- Pabiot, J., 1991. Essais thermomécaniques et rhéologiques à l'état solide. *Traité matériaux non métalliques*. A 3 510 et suivant, AM3, 5-1985 à 8-1991.
- Pandini, S., Pegoretti, A., 2008. Time, Temperature, and Strain Effects on Viscoelastic Poisson's Ratio of Epoxy Resins.
- Phan, L. T. & Carino, N. J., 2001. Mechanical Properties of High-Strength Concrete at Elevated Temperatures", Report NISTIR 6726, Building and Fire Research Laboratory, National Institute of Standards and Technology, Gaithersburg, Maryland.
- Pinoteau, N., 2013. Comportement des scellements chimiques rapportés pour béton en situation d'incendie (*thèse de doctorat*). Lille : Université Lille I.
- Pinoteau N, Heck J. V, Rivillon Ph, Avenel R, Pimienta P, Guillet T, Rémond S. Prediction of failure of a cantilever-wall connection using post-installed rebars under thermal loading. *Eng Struct* J 2013; 56: p. 1607-19.
- Pimienta, P., Alonso, M. C., McNamee, R. J. & Mindeguia, J. C., 2017. Behaviour of high-performance concrete at high temperatures: some highlights. *RILEM Technical Letters*. 2. 45. 10.21809/rilemtechlett.2017.53.
- Pimienta, P., Anton, O., Mindeguia, J. C., Avenel, R., Cuypers, H., & Cesmat, E., 2010. Fire protection of concrete structures exposed to fast fires. In: *Forth international symposium on tunnel safety and security*. Frankfurt, Germany.
- Pliya, P., 2010. Contribution des fibres de polypropylène et métalliques à l'amélioration du comportement du béton soumis à une température élevée (*thèse de doctorat*). Université de Cergy-Pontoise.
- R.F. Feldman and P.J. Serada. A model for hydrated portland cement paste as deduced from sorption-length change and mechanical properties. *Matériaux et constructions*, 1 :509–519, 1968.
- Reichert, M, Thiele, C, 2017. Verbunddübel im Brandfall-DIBt. Kaiserslautern, University of Kaiserslautern.
- Rekik Medhioub, H., 2009. Caractérisation structurale et suivi du vieillissement par diffusion X aux petits angles d'un polymère époxyde : Contribution à l'étude des propriétés électriques (*Thèse de doctorat*). Sfax, Faculté des Sciences de Sfax.
- Sato, H., Fujikake, K. & Mindess, S., 2004. Study on dynamic pullout strength of anchors based on failure modes. *13th World Conference on Earthquake Engineering*, 1-6 August. Volume 854.
- Shaw, J.D.N., 1985. Resins in construction. *International Journal of Cement Composites and Lightweight Concrete* 7, 217–223.

- Struik, L. C. E., 1978. Physical ageing in amorphous polymers and other materials. Elsevier, N.Y.
- Tamulevich, T.W., Moore, V.E., 1980. The significance of glass transition temperature on epoxy resins for fiber optic applications. Epoxy Technology, Inc., Billerica, Mass.
- Teyssède, G., Lacabanne, C., 1997. Caractérisation des polymères par analyse thermique. Traité plastiques et composites, éditions T.I. (Techniques de l'ingénieur).
- Theocaris, P.S., 1979. Influence of plasticizer on Poisson's ratio of epoxy polymers. Polymer 20, 1149–1154.
- Tsimbrovska, M., 2018. Dégradation des bétons à hautes performances soumis à des températures élevées. Evolution de la perméabilité en liaison avec la microstructure (*thèse de doctorat.*, Université Grenoble 1.
- Verdu, J., 2000. Action de l'eau sur les plastiques. Traité plastiques et composites, éditions T.I. (Techniques de l'ingénieur).
- Volkersen, O., 1938. Die Niekraftverteilung in Zugbeanspruchten mit Konstanten Laschenquerschnitten. Luftfahrtforschung, Volume 15, pp. 41-47.
- Wagner, R., Fischer, F. et Gautier, L., 1903. Traité de chimie industrielle, tome second. Paris.
- Wikström, U., 1994. The plate thermometer for calculating heat transfer and controlling fire resistance tests. Fire Technology, 30(2):195-208.
- Wikström, U. & Hermodsson, T., 1996. Comments on paper by Kay, Kirby and Preston on 'calculation of the heating rate of an unprotected steel member in a standard fire resistance test. Fire Safety Journal, 26(4):327-50.
- Wikström, U., 2004. Short communication: Heat transfer by radiation and convection in fire testing. In: Fire and Materials, 28(5):411-15.
- Wu, P., Siesler & H.W., 2003. Water diffusion into epoxy resin: a 2D correlation ATR-FTIR investigation. Chemical Physics Letters 374, 74–78.
- Xing, Z., 2011. Influence de la nature minéralogique des granulats sur leur comportement et celui du béton à haute température (*Thèse de Doctorat*). Université de Cergy-Pontoise.
- Xiao, J., et Falkner, H, 2006. "On residual strength of high performance concrete with and without polypropylene fibres at elevated temperatures", Fire Safety Journal, vol. 41, n°2, p. 115-121.
- Yu, H., 1999. Experimental determination of shrinkage, modulus and residual stresses in adhesives during the cure process (*Ph.D. Thesis*). Bristol, University of Bristol.